

1	<b>Table of Contents</b>
2	2.0 SITE CHARACTERIZATION.....2-6
3	2.1 Geology.....2-13
4	2.1.1 Data Sources .....2-14
5	2.1.2 Geologic History.....2-16
6	2.1.3 Stratigraphy and Lithology in the Vicinity of the WIPP Site .....2-19
7	2.1.3.1 General Stratigraphy and Lithology below the Bell Canyon ...2-23
8	2.1.3.2 The Bell Canyon.....2-24
9	2.1.3.3 The Castile.....2-26
10	2.1.3.4 The Salado .....
11	2.1.3.5 The Rustler .....
12	2.1.3.6 The Dewey Lake .....
13	2.1.3.7 The Santa Rosa.....2-53
14	2.1.3.8 The Gatuña .....
15	2.1.3.9 Mescalero Caliche .....
16	2.1.3.10 Surficial Sediments.....2-57
17	2.1.3.11 Summary .....
18	2.1.4 Physiography and Geomorphology.....2-58
19	2.1.4.1 Regional Physiography and Geomorphology.....2-59
20	2.1.4.2 Site Physiography and Geomorphology .....
21	2.1.5 Tectonic Setting and Site Structural Features.....2-62
22	2.1.5.1 Tectonics .....
23	2.1.5.2 Loading and Unloading .....
24	2.1.5.3 Faulting.....2-69
25	2.1.5.4 Igneous Activity .....
26	2.1.6 Nontectonic Processes and Features .....
27	2.1.6.1 Evaporite Deformation .....
28	2.1.6.2 Evaporite Dissolution .....
29	2.2 Surface Water and Groundwater Hydrology .....
30	2.2.1 Groundwater Hydrology .....
31	2.2.1.1 Conceptual Models of Groundwater Flow .....
32	2.2.1.2 Units Below the Salado .....
33	2.2.1.3 Hydrology of the Salado.....2-93
34	2.2.1.4 Units Above the Salado .....
35	2.2.1.5 Hydrology of Other Groundwater Zones of Regional 36 Importance.....2-122
37	2.2.2 Surface-Water Hydrology .....
38	2.3 Resources .....
39	2.3.1 Extractable Resources .....
40	2.3.1.1 Potash Resources at the WIPP Site .....
41	2.3.1.2 Hydrocarbon Resources at the WIPP Site .....
42	2.3.1.3 Other Resources .....
43	2.3.2 Cultural and Economic Resources .....
44	2.3.2.1 Demographics.....2-138
45	2.3.2.2 Land Use.....2-141
46	2.3.2.3 History and Archaeology.....2-142

1	2.4	Background Environmental Conditions.....	2-145
2	2.5	Climate and Meteorological Conditions .....	2-145
3	2.5.1	Historic Climatic Conditions .....	2-145
4	2.5.2	Recent Climatic Conditions .....	2-148
5	2.5.2.1	General Climatic Conditions .....	2-148
6	2.5.2.2	Temperature Summary .....	2-148
7	2.5.2.3	Precipitation Summary .....	2-149
8	2.5.2.4	Wind Speed and Wind Direction Summary .....	2-149
9	2.6.1	Seismic History.....	2-160
10	2.6.2	Seismic Risk.....	2-162
11	2.6.2.1	Acceleration Attenuation.....	2-162
12	2.6.2.2	Seismic Source Zones .....	2-163
13	2.6.2.3	Source Zone Recurrence Formulas and Maximum	
14		Magnitudes .....	2-163
15	2.6.2.4	Design Basis Earthquake.....	2-166
16	REFERENCES .....		2-168

17

## 18 List of Figures

19	Figure 2-1.	WIPP Site Location in Southeastern New Mexico .....	2-8
20	Figure 2-2.	WIPP Site and Vicinity Borehole Location Map (partial) .....	2-17
21	Figure 2-3.	Locations of Culebra Monitoring Wells Inside the WIPP Site Boundary .....	2-18
22	Figure 2-5.	Locations of Magenta Monitoring Wells .....	2-19
23	Figure 2-6.	Locations of Monitoring Wells Completed to Hydrostratigraphic Units Other 24 Than the Culebra and Magenta Dolomite Members (See also Figure 2-	
25		39). .....	2-20
26	Figure 2-7.	Major Geologic Events - Southeast New Mexico Region .....	2-21
27	Figure 2-8.	Partial Site Geologic Column.....	2-22
28	Figure 2-9.	Schematic Cross-Section from Delaware Basin (southeast) through Marginal 29 Reef Rocks to Back-Reef Facies (based on King 1948).....	2-25
30	Figure 2-10.	Structure Contour Map of Top of Bell Canyon .....	2-27
31	Figure 2-11.	Generalized Stratigraphic Cross Section above Bell Canyon Formation at 32 WIPP Site.....	2-28
33	Figure 2-12.	Salado Stratigraphy in the Vicinity of the WIPP Disposal Zone .....	2-32
34	Figure 2-13.	Dissolution Margin for the Upper Salado .....	2-36
35	Figure 2-14.	Rustler Stratigraphy .....	2-39
36	Figure 2-15.	Halite Margins for the Rustler Formation Members.....	2-41
37	Figure 2-16.	Isopach Map of the Entire Rustler .....	2-43
38	Figure 2-17.	Percentage of Natural Fractures in the Culebra Filled with Gypsum .....	2-46
39	Figure 2-18.	Log Character of the Rustler Emphasizing Mudstone-Halite Lateral 40 Relationships.....	2-49
41	Figure 2-19.	Isopach of the Dewey Lake.....	2-52
42	Figure 2-20.	Isopach of the Santa Rosa .....	2-54
43	Figure 2-21.	Isopach of the Gatun.....	2-56

1	Figure 2-22. Physiographic Provinces and Sections .....	2-60
2	Figure 2-23 Topographic Map of the Area Around the WIPP Site .....	2-61
3	Figure 2-24. Structural Provinces of the Permian Basin Region .....	2-64
4	Figure 2-25. Loading and Unloading History Estimated to the Base of the Culebra .....	2-67
5	Figure 2-26. Regional Structures .....	2-70
6	Figure 2-27. Igneous Dike in the Vicinity of the WIPP Site .....	2-72
7	Figure 2-28. Elevations of the Top of the Culebra Dolomite Member.....	2-75
8	Figure 2-29. Isopach from the Base of MB 103 to the Top of the Salado .....	2-79
9	Figure 2-30. Schematic West-East Cross Section through the North Delaware Basin .....	2-84
10	Figure 2-31. Schematic North-South Cross Section through the North Delaware Basin.....	2-85
11	Figure 2-33. Outline of the Groundwater Basin Model Domain on a Topographic Map .....	2-98
12	Figure 2-34. Transmissivities of the Culebra.....	2-104
13	Figure 2-35. Correlation Between Culebra Transmissivity ( $\log T$ ( $m^2/s$ )) and Overburden Thickness for Different Geologic Environments (after Holt and Yarbrough 2002).....	2-106
14	Figure 2-36. Water-level Trends in Nash Draw Wells and at P-14 (see Figure 2-2 for well locations).....	2-109
15	Figure 2-37. Hydraulic Heads in the Culebra .....	2-111
16	Figure 2-38. Hydraulic Heads in the Magenta (1980s).....	2-118
17	Figure 2-39. Site Map of WIPP Surface Structures Area Showing Location of Wells (e.g., C-2505) and Piezometers (e.g., PZ-1) (after INTERA 1997).....	2-123
18	Figure 2-40. Santa Rosa Potentiometric Surface Map.....	2-124
19	Figure 2-41. Brine Aquifer in the Nash Draw (Redrawn from CCA Appendix HYDRO, Figure 14).....	2-126
20	Figure 2-42. Measured Water Levels of the Los Medaños and Rustler-Salado Contact Zone (1980s) .....	2-128
21	Figure 2-43. Location of Reservoirs and Gauging Stations in the Pecos River Drainage Area.....	2-130
22	Figure 2-44. Known Potash Leases Within the Delaware Basin .....	2-135
23	Figure 2-45. Extent of Economically Mineable Reserves Inside the Site Boundary (Based on NMBMMR Report) .....	2-136
24	Figure 2-46. Delaware Basin Boundary.....	2-139
25	Figure 2-47. Distribution of Existing Petroleum Industry Boreholes Within Two Miles of the WIPP Site.....	2-140
26	Figure 2-48. Monthly Precipitation for the WIPP Site from 1990-2002 .....	2-151
27	Figure 2-49. 1995 Annual Wind Rose at 10-m (33-ft.) Height at WIPP Site.....	2-152
28	Figure 2-50. 1996 Annual Wind Rose at 10-m (33-ft.) Height at WIPP Site.....	2-153
29	Figure 2-51. 1997 Annual Wind Rose at 10-m (33-ft.) Height at WIPP Site.....	2-154
30	Figure 2-52. 1998 Annual Wind Rose at 10-m (33-ft.) Height at WIPP Site.....	2-155
31	Figure 2-53. 1999 Annual Wind Rose at 10-m (33-ft.) Height at WIPP Site.....	2-156
32	Figure 2-54. 2000 Annual Wind Rose at 10-m (33-ft.) Height at WIPP Site.....	2-157
33	Figure 2-55. 2001 Annual Wind Rose at 10-m (33-ft.) Height at WIPP Site.....	2-158
34	Figure 2-56. 2002 Annual Wind Rose at 10-m (33-ft.) Height at WIPP Site.....	2-159
35	Figure 2-57. Regional Earthquake Epicenters Occurring between 1961 and 2002 .....	2-161
36	Figure 2-58. Seismic Source Zones .....	2-164
37	Figure 2-59. Alternate Source Geometries .....	2-165

1	Figure 2-60. Total WIPP Facility Risk Curve Extrema.....	2-167
2		

### 3                   **List of Tables**

4	Table 2-1. Issues Related to the Natural Environment That Were Evaluated for the WIPP	
5	PA Scenario Screening .....	2-9
6	Table 2-2. Chemical Formulas, Distributions, and Relative Abundances of Minerals in the	
7	Castile, Salado, and Rustler Formations .....	2-33
8	Table 2-3. Culebra Thickness Data Sets .....	2-47
9	Table 2-4. Hydrologic Characteristics of the Rustler at the WIPP and in Nash Draw .....	2-86
10	Table 2-5. Depth Intervals of the Injection Zones of Six Salt-Water Injection Wells	
11	Located Near Well H-9 (after SNL 2003a).....	2-91
12	Table 2-6. WIPP Salado and Castile Brine Compositions.....	2-94
13	Table 2-7. Estimates of Culebra Transmissivity Model Coefficients.....	2-106
14	Table 2-8. Ninety-Five Percent Confidence Intervals for Culebra Water-Quality Baseline ..	2-108
15	Table 2-9. Ninety-Five Percent Confidence Intervals for Dewey Lake Water-Quality	
16	Baseline.....	2-120
17	Table 2-10. Capacities of Reservoirs in the Pecos River Drainage .....	2-131
18	Table 2-11. Current Estimates of Potash Resources at the WIPP Site .....	2-134
19	Table 2-12. In-Place Oil within Study Area .....	2-137
20	Table 2-13. In-Place Gas within Study Area .....	2-137
21	Table 2-14. Annual Average, Maximum, and Minimum Temperatures .....	2-149
22		

1

This page intentionally left blank

1                   **2.0 SITE CHARACTERIZATION**

2       The U.S. Department of Energy (DOE) uses the performance assessment (PA) methodology  
3       described in Chapter 6.0 to demonstrate that the Waste Isolation Pilot Plant (WIPP) disposal  
4       system will meet the environmental performance standards of Title 40 of the Code of Federal  
5       Regulations (CFR) Part 191 Subparts B and C. In order to effectively use PA, three inputs are  
6       necessary: What can happen to the disposal system? What are the chances of it happening? What  
7       are the consequences if it happens? The answers to these questions are derived from many  
8       sources, including field studies, laboratory evaluations, experiments, and, in the case of some  
9       features not amenable to direct characterization, professional judgment. The information used in  
10      PA is described in terms of features of the disposal system that can be used to describe its  
11      isolation capability, events that can affect the disposal system, and processes that are reasonably  
12      expected to act on the disposal system.

13      The DOE selected the Los Medaños region and present site for the WIPP based on certain  
14      defined siting criteria. The site selection process, which was focused on sites that contained  
15      certain favorable features while other unfavorable features were excluded, was applied by the  
16      DOE with the intent of finding the area that best met the siting criteria. The siting process is  
17      discussed in CCA Appendix GCR. Chapters 3.0, 4.0, and 6.0 and several appendices provide  
18      additional information supporting this chapter.

19      Conceptual models of the WIPP disposal system simulate the interaction between the natural  
20      environment (described in this chapter), the engineered structures (described in Chapter 3.0) and  
21      the waste (described in Chapter 4.0). One starting point in developing conceptual models of the  
22      WIPP disposal system is an understanding of the natural characteristics of the site and of the  
23      region around the site. Site characterization and model development is an interactive process  
24      that the DOE has used for many years. Basic site information leads to initial models. Initial  
25      model sensitivity studies indicate the need for more detailed information. More site  
26      characterization then leads to improved models. In addition, an assessment of the impacts of  
27      uncertainty inherent in the parameters used to numerically simulate geological features and  
28      processes has also led the DOE to conduct more in-depth investigations of the natural system.  
29      These investigations generally proceeded until uncertainty was sufficiently reduced or to the  
30      point where no further information could be reasonably obtained.

31      The discussion of conceptual models and initial and boundary conditions is in Section 6.4 and  
32      Appendix PA, Attachment MASS. Conceptual models implement scenarios about the future.  
33      Scenario development is discussed in Section 6.3. Scenario development requires as inputs  
34      information about the natural features, events, and processes (FEPs) that can reasonably be  
35      expected to act on the disposal system. While the list of possible FEPs is derived independently  
36      of the disposal system, their screening (in Section 6.2 and Appendix PA, Attachment SCR) is  
37      based on an understanding of the geology, hydrology, and climatology of the region and the site  
38      in particular. The screening methodology follows U.S. Environmental Protection Agency (EPA)  
39      criteria on the Scope of Performance Assessments (40 CFR § 191.32). This basic understanding  
40      is provided in this chapter and its associated appendices.

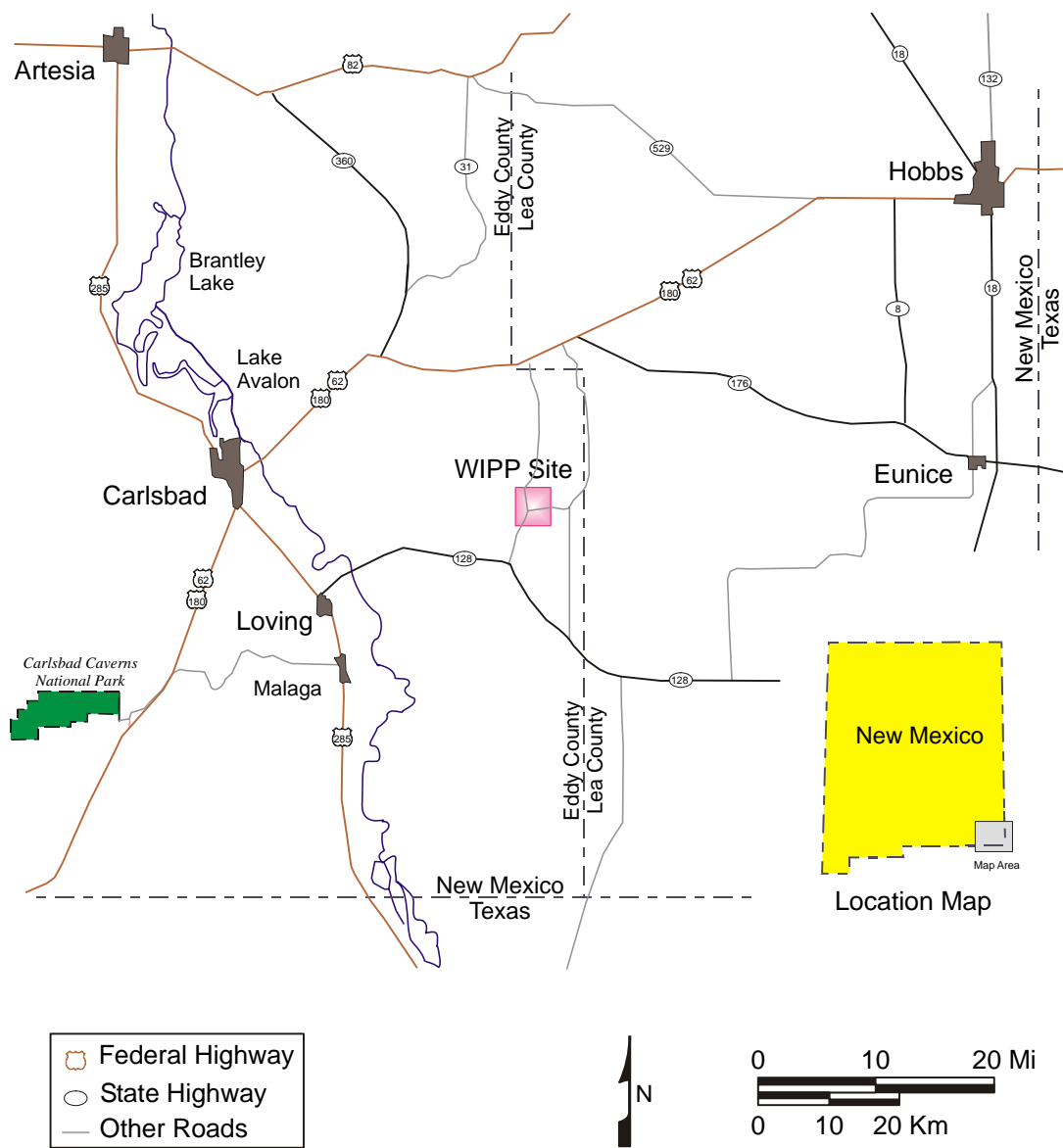
41      Table 2-1 shows the tie between the list of natural FEPs that were identified and screened for the  
42      WIPP and the sections of this chapter or Appendix PA, Attachment SCR. Those FEPs that have

1 been retained for inclusion in the modeling are shown in bold in Table 2-1. These generally  
2 receive a greater level of detail in the following discussions and are supported by additional  
3 discussion in Chapter 6.0, Appendix PA, Attachments MASS and SCR. In addition, parameter  
4 values that have been derived for these FEPs are included in Appendix PA, Attachment PAR.

5 In this chapter, the DOE describes the WIPP site geology, hydrology, climatology, air quality,  
6 ecology, and cultural and natural resources. This chapter's purpose is to (1) explain  
7 characteristics of the site, (2) describe background environmental quality, and (3) discuss  
8 features of the site that might be important for inclusion in a quantitative PA. The DOE has used  
9 this information to develop and screen FEPs and to develop conceptual, mathematical, and  
10 computational models to evaluate the efficacy of natural and engineered barriers in meeting  
11 environmental performance standards (Chapter 6.0). Results of these predictive models are used  
12 by the DOE to demonstrate that the DOE has a reasonable expectation that compliance with  
13 applicable regulations will be achieved. This chapter has been prepared to describe the site prior  
14 to excavating the repository. Excavation of the repository and its associated effects, such as the  
15 disturbed rock zone (DRZ), are discussed in Chapter 3.0.

16 The DOE located the WIPP site 42 km (26 mi) east of Carlsbad, New Mexico, in Eddy County  
17 (Figure 2-1). Additional details related to the location of the WIPP site can be found in Section  
18 2.1.4.2 and in Figure 3-1 (see Chapter 3.0). The latitude of the WIPP site center is 32°22' 11" N  
19 and the longitude is 103°47' 30" W. The region surrounding the WIPP site has been studied for  
20 many years, and exploration of both potash and hydrocarbon deposits has provided extensive  
21 knowledge of the geology of the region. Two exploratory holes were drilled by the federal  
22 government in 1974 at a location northeast of the present site; that location was abandoned in  
23 1975 as a possible repository site after U.S. Energy Research and Development Administration  
24 (ERDA) 6 borehole was drilled and unacceptable structure and pressurized brine were  
25 encountered. The results of these investigations are reported in Powers et al. (1978, 2 – 6;  
26 included in CCA Appendix GCR). During late 1975 and early 1976, the ERDA identified the  
27 current site, and an initial exploratory hole (ERDA-9) was drilled. By the time an initial phase of  
28 site characterization was completed in August 1978, 47 holes had been or were being drilled for  
29 various hydrologic and geologic purposes. Geophysical techniques were applied to augment  
30 data collected from boreholes. Since 1978, the DOE has drilled additional holes to support  
31 hydrologic studies, geologic studies, and facility design. Geophysical logs, cores, basic data  
32 reports, geochemical sampling and testing, and hydrological testing and analyses are reported by  
33 the DOE and its scientific advisor, Sandia National Laboratories (SNL), in numerous public  
34 documents. Many of those documents form the basis for the DOE's positions in this application.  
35 As necessary, specific references from these documents are cited to reinforce statements being  
36 made.

37 Biological studies of the site began in 1975 to gather information for the Environmental Impact  
38 Statement (DOE 1980). Meteorological studies began in 1976, and economic studies were  
39 initiated in 1977. Baseline environmental data were initially reported in 1977 and are now  
40 updated annually by the DOE.



1

CCA-021-2

2

**Figure 2-1. WIPP Site Location in Southeastern New Mexico**

1

**Table 2-1. Issues Related to the Natural Environment That Were Evaluated for the WIPP PA Scenario Screening**

<b>Features, Events, and Processes (FEPs)</b>	<b>EPA FEP No.</b>	<b>Discussion</b>
<b>NATURAL FEPs</b>		
Stratigraphy		
Stratigraphy	N1	Section 2.1.3
Brine reservoirs	N2	Section 2.2.1.2.2
Tectonics		
Changes in regional stress	N3	Section 2.1.5.1
Regional tectonics	N4	Section 2.1.5.1
Regional uplift and subsidence	N5	Section 2.1.5.1
Structural FEPs		
Deformation		
Salt deformation	N6	Section 2.1.6.1
Diapirism	N7	Appendix PA, Attachment SCR
Fracture development		
Formation of fractures	N8	Section 2.1.5
Changes in fracture properties	N9	Section 2.1.5
Fault movement		
Formation of new faults	N10	Section 2.1.5
Fault movement	N11	Section 2.1.5.3
Seismic activity		
Seismic activity	N12	Section 2.6
Crustal processes		
Igneous activity		

2

**Table 2-1. Issues Related to the Natural Environment That Were Evaluated for the WIPP PA Scenario Screening — Continued**

<b>Features, Events, and Processes (FEPs)</b>	<b>EPA FEP No.</b>	<b>Discussion</b>
Volcanic activity	N13	Section 2.1.5.4
Magmatic activity	N14	Appendix PA, Attachment SCR
Metamorphic activity		
Metamorphism	N15	Appendix PA, Attachment SCR
Geochemical FEPs		
Dissolution		
Shallow dissolution	N16	Section 2.1.6.2
Lateral dissolution	N17	Section 2.1.6.2
Deep dissolution	N18	Section 2.1.6.2
Solution chimneys	N19	Section 2.1.6.2
Breccia pipes	N20	Section 2.1.6.2
Collapse breccias	N21	Section 2.1.6.2
Mineralization		
Fracture infills	N22	Section 2.1.3.5.2
<b>SUBSURFACE HYDROLOGICAL FEPs</b>		
Groundwater characteristics		
Saturated groundwater flow	N23	Section 2.2.1
Unsaturated groundwater flow	N24	Section 2.2.1
Fracture flow	N25	Section 2.2.1
Density effects on groundwater flow	N26	Section 2.2.1
Effects of preferential pathways	N27	Section 2.2.1
Changes in groundwater flow		
Thermal effects on groundwater flow	N28	Appendix PA, Attachment SCR
Saline water intrusion	N29	Appendix PA, Attachment SCR
Freshwater intrusion	N30	Appendix PA, Attachment SCR
Hydrological effects of seismic activity	N31	Appendix PA, Attachment SCR
Natural gas intrusion	N32	Appendix PA, Attachment SCR
<b>SUBSURFACE GEOCHEMICAL FEPs</b>		
Groundwater geochemistry		
Groundwater geochemistry	N33	Section 2.2.1.4.1.2
Changes in groundwater geochemistry		
Saline water intrusion	N34	Appendix PA, Attachment SCR
Freshwater intrusion	N35	Appendix PA, Attachment SCR
Changes in groundwater Eh	N36	Appendix PA, Attachment SCR
Changes in groundwater pH	N37	Appendix PA, Attachment SCR

**Table 2-1. Issues Related to the Natural Environment That Were Evaluated for the WIPP PA Scenario Screening — Continued**

<b>Features, Events, and Processes (FEPs)</b>	<b>EPA FEP No.</b>	<b>Discussion</b>
Effects of dissolution	N38	Appendix PA, Attachment SCR
<b>GEOMORPHOLOGICAL FEPs</b>		
Physiography		
Physiography	N39	Section 2.1.4
Meteorite impact		
Impact of a large meteorite	N40	Appendix PA, Attachment SCR
Denudation		
Weathering		
Mechanical weathering	N41	Appendix PA, Attachment SCR
Chemical weathering	N42	Appendix PA, Attachment SCR
Erosion		
Eolian erosion	N43	Section 2.1.3.10
Fluvial erosion	N44	Section 2.1.3.6
Mass wasting	N45	Appendix PA, Attachment SCR
Sedimentation		
Eolian deposition	N46	Appendix PA, Attachment SCR
Fluvial deposition	N47	Appendix PA, Attachment SCR
Lacustrine deposition	N48	Appendix PA, Attachment SCR
Mass wasting (deposition)	N49	Appendix PA, Attachment SCR
Soil development		
Soil development	N50	Section 2.1.3.10
<b>SURFACE HYDROLOGICAL FEPs</b>		
Fluvial		
Stream and river flow	N51	Section 2.2.2
Lacustrine		
Surface water bodies	N52	Section 2.2.2
Groundwater recharge and discharge		
Groundwater discharge	N53	Section 2.2.1
Groundwater recharge	N54	Section 2.2.1
Infiltration	N55	Section 2.1.3 Section 2.2.1
Changes in surface hydrology		
Changes in groundwater recharge and discharge	N56	Section 2.2.1
Lake formation	N57	Section 2.2.2
River flooding	N58	Section 2.2.2

**Table 2-1. Issues Related to the Natural Environment That Were Evaluated for the WIPP PA Scenario Screening — Continued**

Features, Events, and Processes (FEPs)	EPA FEP No.	Discussion
<b>CLIMATIC FEPs</b>		
Climate		
Precipitation (for example, rainfall)	N59	Section 2.5.2.3
Temperature	N60	Section 2.5.2.2
Climate change		
Meteorological		
Climate change	N61	Section 2.5
Glaciation		
Glaciation	N62	Section 2.5.1
Permafrost	N63	Appendix PA, Attachment SCR
<b>MARINE FEPs</b>		
Seas		
Seas and oceans	N64	Appendix PA, Attachment SCR
Estuaries	N65	Appendix PA, Attachment SCR
Marine sedimentology		
Coastal erosion	N66	Appendix PA, Attachment SCR
Marine sediment transport and deposition	N67	Appendix PA, Attachment SCR
Sea level changes		
Sea level changes	N68	Appendix PA, Attachment SCR
<b>ECOLOGICAL FEPs</b>		
Flora and fauna		
Plants	N69	Section 2.4.1
Animals	N70	Section 2.4.1
Microbes	N71	Appendix PA, Attachment SCR
Changes in flora and fauna		
Natural ecological development	N72	Section 2.4.1

1 \*NOTE: Additional information for FEPs N1-N72 is located in Appendix PA, Attachment SCR.

2 The DOE located the WIPP disposal horizon within a rock salt deposit known as the Salado  
 3 Formation at a depth of 650 m (2,150 ft) below the ground surface. The Salado is regionally  
 4 extensive, includes continuous beds of salt without complicated structure, is deep with little  
 5 potential for dissolution in the immediate vicinity of the WIPP, and is near enough to the surface  
 6 to make access reasonable. Particular site selection criteria narrowed the choices when the  
 7 present site was located during 1975 and 1976, as is discussed in CCA Appendix GCR and  
 8 summarized by Weart (1983).

1    **2.1 Geology**

2    The DOE and its predecessor agencies determined at the outset of the geological disposal  
3    program that the geological characteristics of the disposal system are extremely important  
4    because the natural barriers provided by the geological units have a significant impact on the  
5    performance of the disposal system. Among the DOE's site selection criteria was the intent to  
6    maximize the beneficial impacts of the geology. This was accomplished when the DOE selected  
7    (1) a host formation that behaves plastically, thereby creeping closed to encapsulate buried  
8    waste, (2) a location where the effects of dissolution are minimal and predictable, (3) an area  
9    where deformation of the rocks is low, (4) an area where excavation is relatively easy, (5) an  
10   area where future resource development is predictable and minimal, and (6) a repository host  
11   rock that is relatively uncomplicated lithologically and structurally. Therefore, a thorough and  
12   accurate description of the WIPP facility's natural environmental setting is considered crucial by  
13   the DOE for a demonstration of compliance with the disposal standards and is an EPA  
14   certification criterion in 40 CFR § 191.14(a). The DOE is providing the detail necessary to  
15   assess the achievable degree of waste isolation. In this chapter, the DOE addresses  
16   environmental factors and long-term environmental changes that are important for assessing the  
17   waste isolation potential of the disposal system. The first of these environmental factors is  
18   geology.

19   Geological data have been collected from the WIPP site and surrounding area to evaluate the  
20   site's suitability as a radioactive waste repository. These data have been collected principally by  
21   the DOE, the DOE's predecessor agencies, the United States Geological Survey (USGS), the  
22   New Mexico Bureau of Mines and Mineral Resources (NMBMMR), and private organizations  
23   engaged in natural resource exploration and extraction. The DOE has analyzed the data and has  
24   determined that the data support the DOE's position that the WIPP site is suitable for the long-  
25   term isolation of radioactive waste.

26   Many issues have been discussed, investigated, and resolved in order for the DOE to conclude  
27   that the site is suitable. The DOE discusses these issues in the following sections. Most of the  
28   data collected have been reported or summarized in CCA Appendices GCR, SUM, HYDRO, and  
29   FAC. These appendices represent the majority of the site characterization results for the WIPP  
30   site which ended in 1988. A number of more focused geological and hydrological studies  
31   continued after this date. These latter studies provided detailed information needed to construct  
32   the conceptual models for disposal system performance that are discussed in Section 6.4. An  
33   example of these studies is the H-19 multiwell tracer test that was completed in early 1996.  
34   Results of this test were incorporated into the discussions in this chapter and into the conceptual  
35   models described in Section 6.4.6. Model parameters derived from the data are displayed in  
36   Appendix PA, Attachment PAR. A discussion of the data is included in CCA Appendix MASS;  
37   and Appendix PA, Attachment MASS.

38   Geological field studies designed to collect data pertinent to the WIPP PA continue. The Culebra  
39   Dolomite Member and Magenta Dolomite Members are the two carbonates in the Rustler  
40   Formation, the youngest evaporite-bearing formation in the Delaware Basin. Geologic data  
41   related to the Culebra and Magenta remain of particular interest, as these members are the most  
42   significant transmissive units at the WIPP site.

1 The EPA's December 19, 1996 letter (A-93-02, Docket II-I-01) made a request to the DOE for  
2 recent studies that had provided detailed information used in developing conceptual models for  
3 disposal system performance. In a response letter to EPA dated February 26, 1997 (Docket A-93-  
4 02, Item II-I-10), the DOE cited Holt (1997) for detailed information on the recent enhancement  
5 of the conceptual model for transport in the Culebra. Holt (1997) discusses interpretation and  
6 conceptual insights obtained from field and laboratory tracer tests and core studies that support  
7 the double-porosity conceptual model of the Culebra, in which Culebra porosity is divided into  
8 advective and diffusive components.

9 Geological data provide the basis for a different approach to estimating the transmissivity field  
10 for modeling fluid flow and transport in the Culebra (Beauheim 2002). Geological data correlate  
11 strongly with Culebra transmissivity (Holt and Yarbrough 2002), and they are available from  
12 many more locations, such as industry (oil, gas, potash) drillholes, than are transmissivity data.  
13 With this correlation, Culebra properties can be inferred over a wide area, leading to an  
14 improved computational model of the spatial distribution of Culebra transmissivity. Initial  
15 results from this computational model of the spatial distribution of Culebra transmissivity have  
16 been incorporated in the PA; they are discussed in more detail in Section 2.2.1.4.1.2, and are  
17 incorporated in Appendix PA, Attachment TFIELD. Additional data in support of this modeling  
18 are being collected through field activities, including drilling and testing of new wells, to  
19 improve understanding of the Culebra and to assess the causes(s) of rising water levels (see  
20 Section 2.2.1.4.1.2).

21 **2.1.1 Data Sources**

22 The geology of southeastern New Mexico has been of great interest for more than a century. The  
23 Guadalupe Mountains have become a common visiting and research point for geologists because  
24 of the spectacular exposures of Permian-age reef rocks and related facies (see Shumard 1858,  
25 Crandall 1929, Newell et al. 1953, and Dunham 1972 in the CCA bibliography). Because of  
26 intense interest in both hydrocarbon and potash resources in the region, a large volume of data  
27 exists as background information for the WIPP site, though some data are proprietary. Finally,  
28 there is the geological information developed directly and indirectly by studies sponsored by the  
29 DOE for the WIPP project; it ranges from raw data to interpretive reports.

30 Elements of the geology of southeastern New Mexico have been discussed or described in  
31 professional journals or technical documents from many different sources. These types of  
32 articles are an important source of information, and where there is consistency among the  
33 technical community, the information in these articles is referenced when subject material is  
34 relevant. Implicit rules of professional conduct for research and reporting have been assumed, as  
35 have journal and editorial review. Elements of the geology presented in such sources have been  
36 deemed critical to the WIPP and have been the subject of specific DOE-sponsored WIPP studies.

37 The geological data that the DOE has developed explicitly for the WIPP project have been  
38 produced over a 25-year period by different organizations and contractors using applicable  
39 national standards (Quality Assurance Program history is described in Section 5.1.2). During a  
40 rulemaking in 1988 related to the underground injection of hazardous wastes, the EPA addressed  
41 the use of older geological data in making a long-term demonstration of repository performance.  
42 In response to comments on a proposed rule regarding the permitting of underground injection

1 wells, the EPA concluded that “[e]xcluding historical data or information which might have been  
2 gathered off-site by methods not consistent with certain prescribed procedures may be  
3 counterproductive.” The EPA further stated that such data should be used as long as their  
4 limitations are accounted for. In the final rule, the EPA stipulated “that only measurements  
5 pertaining to the waste or that result from testing performed to gather data for the petition  
6 demonstration comply with prescribed procedures.” Further, the EPA stated that “the concerns  
7 about the accuracy of geologic data are addressed more appropriately by requiring that the  
8 demonstration identify and account for the limits on data quality rather than by excluding data  
9 from consideration” (EPA 1988).

10 As site characterization activities progressed, the DOE, along with independent review groups  
11 such as the National Academy of Sciences (NAS), the Environmental Evaluation Group (EEG),  
12 and the state of New Mexico acting through the Governor’s Radioactive Waste Consultation  
13 Task Force, identified natural FEPs that required additional detailed investigation. Because  
14 these investigations, in many cases, were to gather data that would either be used in developing  
15 conceptual models or in the prediction of disposal system performance, the quality assurance  
16 (QA) standards applied to these investigations were more stringent, thereby ensuring accuracy  
17 and repeatability to the extent possible for geologic investigations.

18 Geological data from site characterization have been developed by the DOE through a variety of  
19 WIPP-sponsored studies using drilling, mapping or other direct observation, geophysical  
20 techniques, and laboratory work. Most of the techniques and statistics of data acquisition will be  
21 incorporated by specific discussion. The processes used in deriving modeling parameters from  
22 field and laboratory data are discussed in records packages which support the conceptual models  
23 in Section 6.4 and the parameters in Appendix PA, Attachment PAR. Pointers to these records  
24 packages are provided principally in Appendix PA, Attachment PAR. Records packages are  
25 stored in the Sandia WIPP Records Center in Carlsbad. Access to review of these records  
26 packages can be obtained by contacting the person designated in Table 1-10. Borehole  
27 investigations are a major source of geological data for the WIPP and surrounding area.  
28 Borehole studies provide raw data (for example, depth measurements, amount of core,  
29 geophysical logs) that support point data and interpreted data sets. These data sets are used in  
30 developing other analysis tools such as structure maps for selected stratigraphic horizons or  
31 isopachs (thicknesses) of selected stratigraphic intervals.

32 The borehole data set that was used specifically for obtaining WIPP geologic information is  
33 included as reference information in CCA Appendix BH. A map of some borehole locations in  
34 the data set is provided in Figure 2-2. Figure 2-3 shows Culebra monitoring wells within the site  
35 boundary as of December 2002, including well C-2737, which was drilled and completed in  
36 2001 (Powers 2002c). Figure 2-4 shows Culebra monitoring wells outside the WIPP site as of  
37 December 2002; plugged and abandoned wells formerly monitored are not included in this  
38 figure. Figure 2-5 shows the locations of wells configured to monitor the Magenta, including  
39 well C-2737. Other hydrostratigraphic units are monitored in wells shown in Figure 2-6,  
40 including well C-2811, which was drilled and completed in 2001 to monitor a shallow saturated  
41 zone developed since the WIPP surface structures were constructed (Powers and Stensrud 2003).  
42 Other holes are not shown because they were not of sufficient depth, were not cored, or were not  
43 drilled for purposes of site characterization. A more comprehensive drillhole database of the

1 entire Delaware Basin is addressed in Section 2.3.1.2 and is presented in Appendix DATA. This  
2 database includes all drillholes used in evaluating human intrusion rates for the WIPP PA.

3 **2.1.2 Geologic History**

4 In this section, the DOE summarizes the more important points of the area's geologic history  
5 within about 320 km (200 mi) of the WIPP site, with emphasis on more recent or nearby events.  
6 Figure 2-7 shows the major elements of the area's geological history from the end of the  
7 Precambrian Period.

8 The geologic time scale that the DOE uses for WIPP is based on the compilation by Palmer  
9 (1983, pp. 503 – 504) for *The Decade of North American Geology* (DNAG). There are several  
10 compiled sources of chronologic data related to different reference sections or methods (see, for  
11 example, Harland et al. 1989 and Salvador 1985. Although most of these sources show generally  
12 similar ages for chronostratigraphic boundaries, there is no consensus on either reference  
13 boundaries or most-representative ages. The DNAG scale is accepted by the DOE as a standard  
14 that is useful and sufficient for WIPP purposes, as no known critical performance assessment  
15 parameters require more accurate or precise dates.

16 The geologic history in this region can be conveniently subdivided into three general phases:

- 17     • A Precambrian Period, represented by metamorphic and igneous rocks ranging in age  
18       from about 1.5 to 1.1 billion years;
- 19     • A period from about 1.1 to 0.6 billion years ago, from which no rocks are preserved.  
20       Erosion may have been the dominant process during much of this period; and
- 21     • An interval from 0.6 billion years ago to the present represented by a more complex set  
22       of mainly sedimentary rocks and shorter periods of erosion and dissolution.

23 This latter phase is the main subject of the DOE's detailed discussion in this text.

24 Only a few boreholes in the WIPP region have bored deep enough to penetrate Precambrian  
25 crystalline rocks, and, therefore, relatively little petrological information is available. Foster  
26 (1974, Figure 3) extrapolated the elevation of the Precambrian surface under the area of WIPP as  
27 being between 4.42 km (14,500 ft) and 4.57 km (15,000 ft) below sea level; the site surface at  
28 WIPP is about 1,036 m (3,400 ft) above sea level. Keesey (1976, Vol. II, Exhibit No. 2)  
29 projected a depth of about 5,545 m (18,200 ft) from the surface to the top of Precambrian rocks  
30 in the vicinity of the WIPP. The depth projection is based on the geology of the nearby borehole  
31 in Section 15, T22S, R31E.

32 Precambrian rocks of several types crop out in the following locations: the Sacramento  
33 Mountains northwest of WIPP; around the Sierra Diablo and Baylor Mountains near Van Horn,  
34 Texas; west of the Guadalupe Mountains at Pump Station Hills; and in the Franklin Mountains

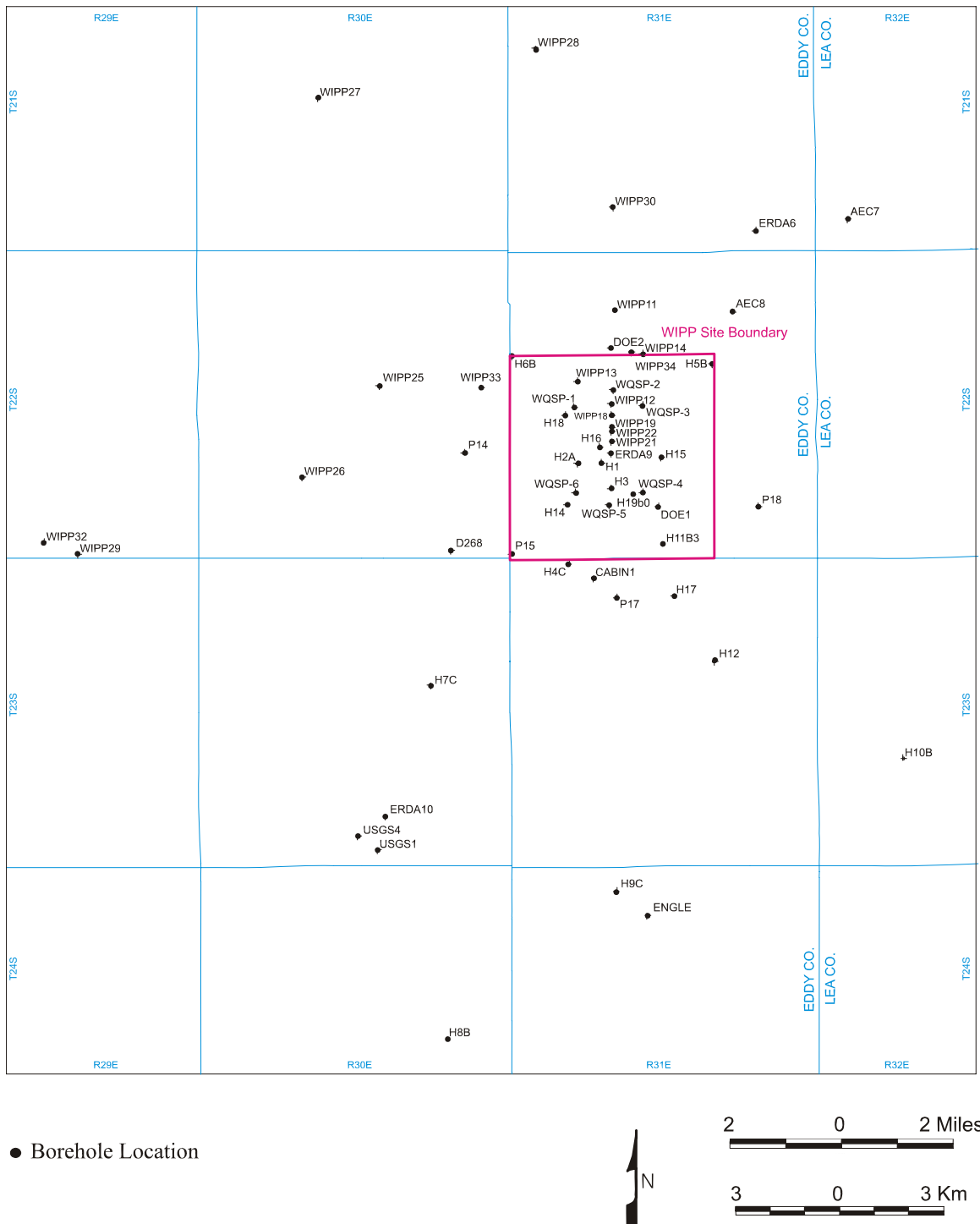
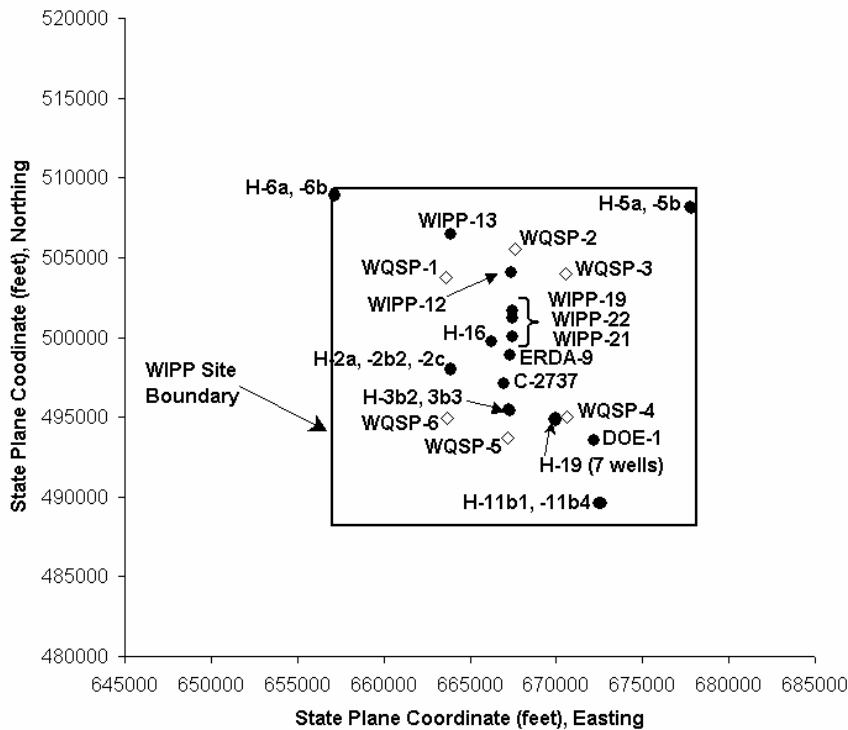
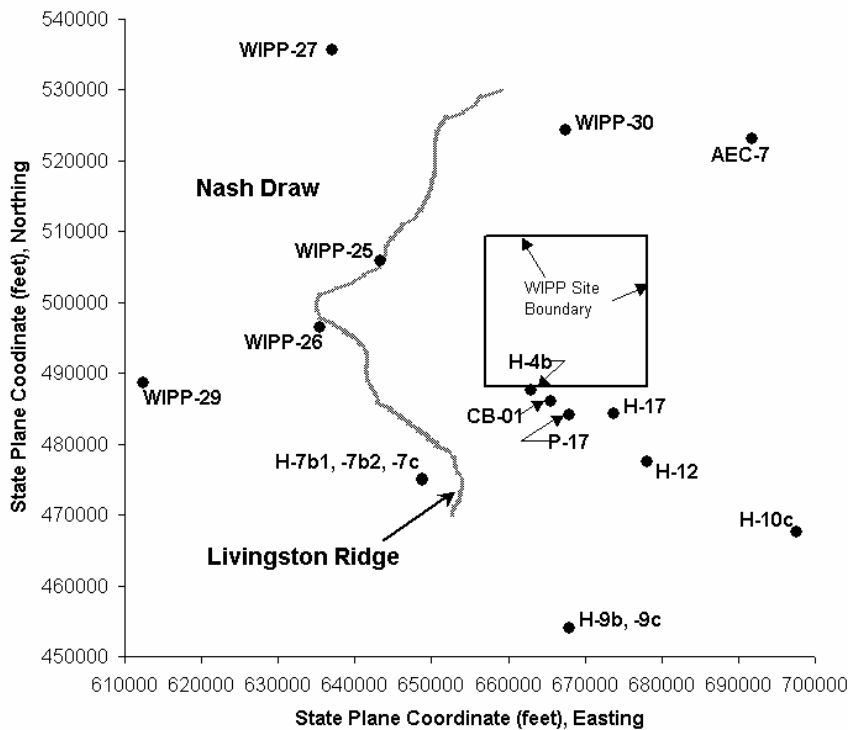


**Figure 2-2. WIPP Site and Vicinity Borehole Location Map (partial)**



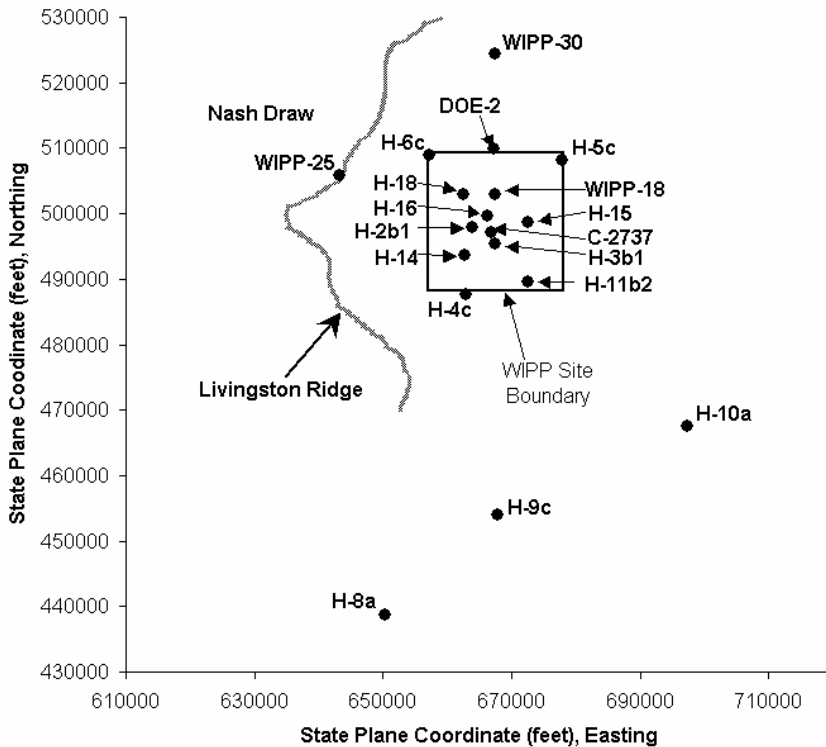
1

**Figure 2-3. Locations of Culebra Monitoring Wells Inside the WIPP Site Boundary**



3

**Figure 2-4. Locations of Culebra Monitoring Wells Located Outside the WIPP Site Boundary**



1

## 2      **Figure 2-5. Locations of Magenta Monitoring Wells**

3      near El Paso, Texas. East of the WIPP, a relatively large number of boreholes on the Central  
 4      Basin Platform have penetrated the top of the Precambrian (Foster 1974, Figure 3). As  
 5      summarized by Foster (1974, 10), Precambrian rocks in the area considered similar to those in  
 6      the vicinity of the site range in age from about 1.14 to 1.35 billion years.

7      For about 500 million years (1.1 to 0.6 billion years ago), there is no certain rock record in the  
 8      region around the WIPP. The most likely rock record for this period may be the Van Horn  
 9      sandstone (McGowan and Groat 1971), but there is no conclusive evidence that it represents part  
 10     of this time period (CCA Appendix GCR, Section 3.3.1). The region is generally thought to  
 11     have been subject to erosion for much of the period until the Bliss sandstone began to  
 12     accumulate during the Cambrian.

13     There is additional geologic history information contained in the EPA Technical Support  
 14     Document for Section 194.14: Content of Compliance Certification Application, Section IV  
 15     (Docket A-93-02, Item V-B-3).

### 16    ***2.1.3 Stratigraphy and Lithology in the Vicinity of the WIPP Site***

17     The conceptual model of the disposal system uses information about the geometry of the various  
 18     rock layers as a model input as described in Section 6.4.2.1. This means that stratigraphic  
 19     information (thickness and lateral extent) provided in the following sections are important inputs.

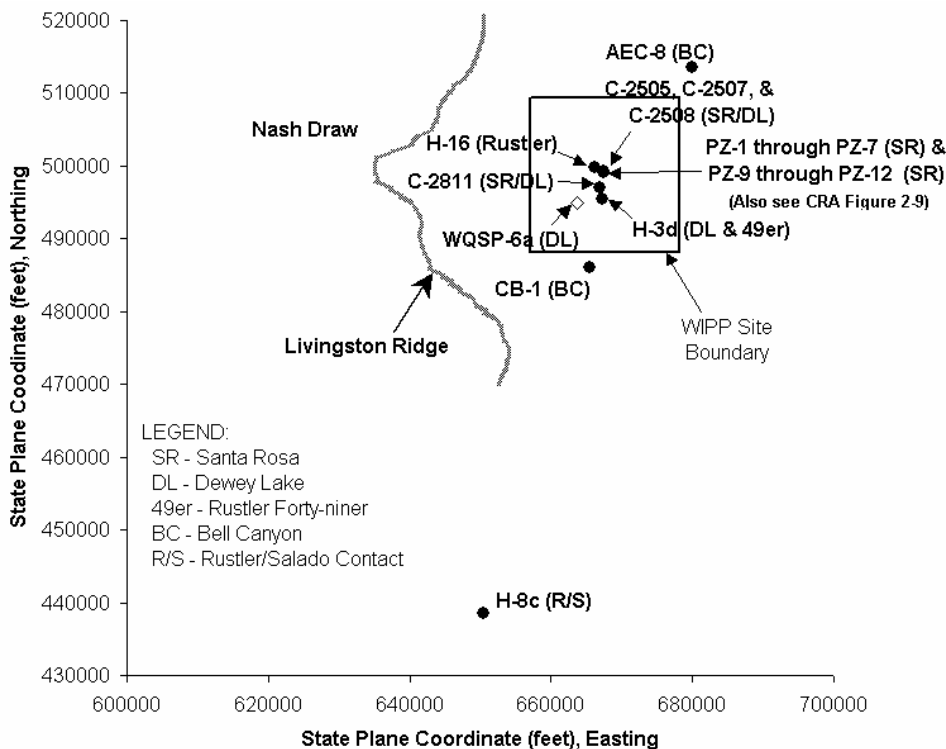


**Figure 2-6. Locations of Monitoring Wells Completed to Hydrostratigraphic Units Other Than the Culebra and Magenta Dolomite Members (See also Figure 2-39).**

In addition, less important features such as the lithology and the presence of geochemically significant minerals are provided to support screening arguments in Appendix PA, Attachment SCR. Consequently, this discussion has focused on the general properties of the various rock units as determined from field studies. Specific parameters used in the modeling described in Sections 6.4.5 and 6.4.6 are summarized in Appendix PA, Attachment PAR. Stratigraphy-related parameters are input as constants. Stratigraphic thicknesses of units considered in modeling are compiled in Appendix PA, Attachment PAR, Table PAR-49.

This section describes the stratigraphy and lithology of the Paleozoic and younger rocks underlying the WIPP site and vicinity (Figure 2-8), emphasizing the units nearer the surface. After briefly describing pre-Permian rocks, the section provides detailed information on the Permian (Guadalupian) Bell Canyon Formation (hereafter referred to as the Bell Canyon)—the upper unit of the Delaware Mountain Group—because this is the uppermost transmissive formation below the evaporites. The principal stratigraphic data are the chronologic sequence, age, and extent of rock units, including some of the nearby relevant facies changes. For deeper rocks, characteristics such as thickness and depth are summarized from published sources, and for shallower rocks, they are mainly based on data sets presented in CCA Appendix BH (above the Bell Canyon). The lithologies of upper formations and some formation members are described. A comprehensive discussion of stratigraphy in the WIPP area is presented in CCA Appendix GCR. Detailed referencing to original investigations by the USGS and others is included.

E R A	PERIOD	EPOCH	YEARS		MAJOR GEOLOGIC EVENTS - SOUTHEAST NEW MEXICO REGION
			DURATION	BEFORE PRESENT	
C E N O Z O I C	Quaternary	Holocene	10,000	1,600,000 66,400,000 144,000,000 208,000,000 245,000,000 286,000,000 320,000,000 360,000,000 408,000,000 438,000,000 505,000,000 570,000,000	Eolian and erosion/solution activity. Development of present landscape. Continued deposition of Gatuña sediments.
		Pleistocene	1,590,000		
	Tertiary	Pliocene	3,700,000		Deposition of Gatuña sediments. Formation of caliche caprock. Regional uplift and east-southeastward tilting; Basin-Range uplift of Sacramento and Guadalupe-Delaware Mountains.
		Miocene	18,400,000		
		Oligocene	12,900,000		Erosion dominant. No Early to Mid-Tertiary rocks present.
		Eocene	21,200,000		Laramide revolution. Uplift of Rocky Mountains. Mild tectonism and igneous activity to west and north.
		Paleocene	8,600,000		
		Cretaceous	77,600,000		Submergence. Intermittent shallow seas. Thin limestone and clastics deposited.
	Jurassic		64,000,000		Emergent conditions. Erosion, formation of rolling terrain.
	Triassic		37,000,000		Deposition of fluvial clastics. Erosion. Broad flood plain develops.
P A L E O Z O I C	Permian		41,000,000		Deposition of evaporite sequence followed by continental redbeds. Sedimentation continuous in Delaware, Midland, Val Verde basins and shelf areas.
	Pennsylvanian		34,000,000		Massive deposition of clastics. Shelf, margin, basin pattern of deposition develops.
	Mississippian		40,000,000		Regional tectonic activity accelerates, folding up Central Basin platform. Matador arch, ancestral Rockies. Regional erosion. Deep, broad basins to east and west of platform develop.
	Devonian		48,000,000		Renewed submergence. Shallow sea retreats from New Mexico; erosion.
	Silurian		30,000,000		Mild epeirogenic movements. Tobosa basin subsiding. Pedernal landmass and Texas Peninsula emergent until Middle Mississippian.
	Ordovician		67,000,000		Marathon-Quachita geosyncline, to south, begins subsiding. Deepening of Tobosa basin area; shelf deposition of clastics, derived partly from ancestral Central Basin platform and carbonates.
	Cambrian		65,000,000		Clastic sedimentation - Bliss sandstone.
	PRECAMBRIAN				Erosion to a nearly level plain. Mountain building, igneous activity, metamorphism, erosional cycles.

SYSTEM/ Series		Group	Formation	Members
PERMIAN	TERTIARY	Dockum	surficial deposits	
			Mescalero caliche	
			Gatuña	
			Santa Rosa	
			Dewey Lake	
			Rustler	<i>Forty-niner</i> <i>Magenta Dolomite</i> <i>Tamarisk</i> <i>Culebra Dolomite</i> <i>Los Medaños</i>
			Salado	<i>upper</i> <i>Vaca Triste Sandstone</i> <i>McNutt potash zone</i> <i>lower</i>
			Castile	
		Delaware Mountain	Bell Canyon	
			Cherry Canyon	
			Brushy Canyon	

1  
2

Figure 2-8. Partial Site Geologic Column

1    2.1.3.1 General Stratigraphy and Lithology below the Bell Canyon

2    As stated previously, the Precambrian basement near the site is projected to be about 5,545 m  
3    (18,200 ft) below the surface (Keesey 1976, Vol. II, Exhibit No. 2), consistent with information  
4    presented by Foster in 1974. Ages of similar rock suites in the region range from about 1.14 to  
5    1.35 billion years.

6    A detailed discussion of the distribution of Precambrian rocks in southeastern New Mexico and  
7    Texas can be found in CCA Appendix GCR. Figure 3.4-2 in CCA Appendix GCR provides a  
8    structure contour map of the Precambrian. The basal Paleozoic units overlying Precambrian  
9    rocks are clastic rocks commonly attributed either to the Cambrian Bliss sandstone or the  
10   Ellenberger Group (Foster 1974, p. 10), considered most likely to be Ordovician in age in this  
11   area. The Ordovician System comprises the Ellenberger, Simpson, and Montoya Groups in the  
12   northern Delaware Basin. Carbonates are predominant in these groups, with sandstones and  
13   shales common in the Simpson Group. Foster (1974, Figure 4) reported 297 m (975 ft) of  
14   Ordovician-age rocks north of the site area and extrapolated a thicker section of about 396 m  
15   (1,300 ft) at the present site (Foster 1974, Figure 5). Keesey (1976, Vol. II, Exhibit No. 2)  
16   projected a thickness of 366 m (1,200 ft) for the Ordovician System within the site boundaries.

17   Silurian-Devonian rocks in the Delaware Basin are not stratigraphically well defined, and there  
18   are various notions for extending nomenclature into the basin. Common drilling practice is not  
19   to differentiate, though the Upper Devonian Woodford shale at the top of the sequence is  
20   frequently distinguished from the underlying dolomite and limestone (Foster 1974, p. 18). Foster  
21   (1974, Figure 6) showed a reference thickness of 384 and 49 m (1,260 and 160 ft) for the  
22   carbonates and the Woodford shale, respectively; he estimated thickness of these units at the  
23   present WIPP site to be about 351 m (1,150 ft) (Foster 1974, Figure 7) and 52 m (170 ft) (Foster  
24   1974, Figure 8), respectively. Keesey (1976, Vol. II, Exhibit No. 2) projected 381 m (1,250 ft)  
25   of carbonate and showed 25 m (82 ft) of the Woodford shale.

26   The Mississippian System in the northern Delaware Basin is commonly attributed to  
27   Mississippian limestone and the overlying Barnett shale (Foster 1974, p. 24), but the  
28   nomenclature is not consistently used. At the reference well used by Foster (1974, 25), the  
29   limestone is 165 m (540 ft) thick and the shale is 24 m (80 ft); isopachs at the WIPP are 146 m  
30   (480 ft) (Foster 1974, Figure 10) and less than 61 m (200 ft). Keesey (1976, Vol. II, Exhibit No.  
31   2) indicates 156 m (511 ft) and 50 m (164 ft), respectively, within the site boundaries.

32   The nomenclature of the Pennsylvanian System applied within the Delaware Basin is both varied  
33   and commonly inconsistent with accepted stratigraphic rules. Chronostratigraphic, or time-  
34   stratigraphic, names are applied from base to top of these lithologic units: the Morrow, Atoka,  
35   and Strawn (Foster 1974, p. 31). Foster (1974, Figure 13) extrapolated thicknesses of about 671  
36   m (2,200 ft) for the Pennsylvanian at the WIPP site. Keesey (1976, Vol. II, Exhibit No. 2)  
37   reports 636 m (2,088 ft) for these units. The Pennsylvanian rocks in this area are mixed clastics  
38   and carbonates, with carbonates more abundant in the upper half of the sequence.

39   The Permian is the thickest system in the northern Delaware Basin, and it is divided into four  
40   series from the base to top: Wolfcampian, Leonardian, Guadalupian, and Ochoan. According to  
41   Keesey (1976, Vol. II, Exhibit No. 2), the three lower series total 2,647 m (8,684 ft) near the site.

1 Foster (1974, Figures 14, 16, and 18) indicates a total thickness for the lower three series of  
2 2,336 m (7,665 ft) for a reference well north of WIPP. Foster's isopach maps of these series  
3 (Foster 1974, Figures 15, 17, and 19) indicate about 2,591 m (8,500 ft) for the WIPP site area.  
4 The Ochoan Series at the top of the Permian is considered in more detail later because the  
5 formations host and surround the WIPP repository horizon. Its thickness at DOE-2, about 3.2  
6 km (2 mi) north of the site center, is 1,200 m (3,938 ft), according to Mercer et al. (1987, p. 23).

7 The Wolfcampian Series is also referred to as the Wolfcamp Formation (hereafter referred to as  
8 the Wolfcamp) in the Delaware Basin. In the site area, the lower part of the Wolfcamp is  
9 dominantly shale with carbonate and some sandstone, according to Foster (1974, Figure 14);  
10 carbonate increases to the north (Foster 1974, p. 36). Clastics increase to the east toward the  
11 margin of the Central Basin Platform. Keesey (1976, Vol. II, Exhibit No. 2) reports the  
12 Wolfcamp to be 455 m (1,493 ft) thick at a well near the WIPP site.

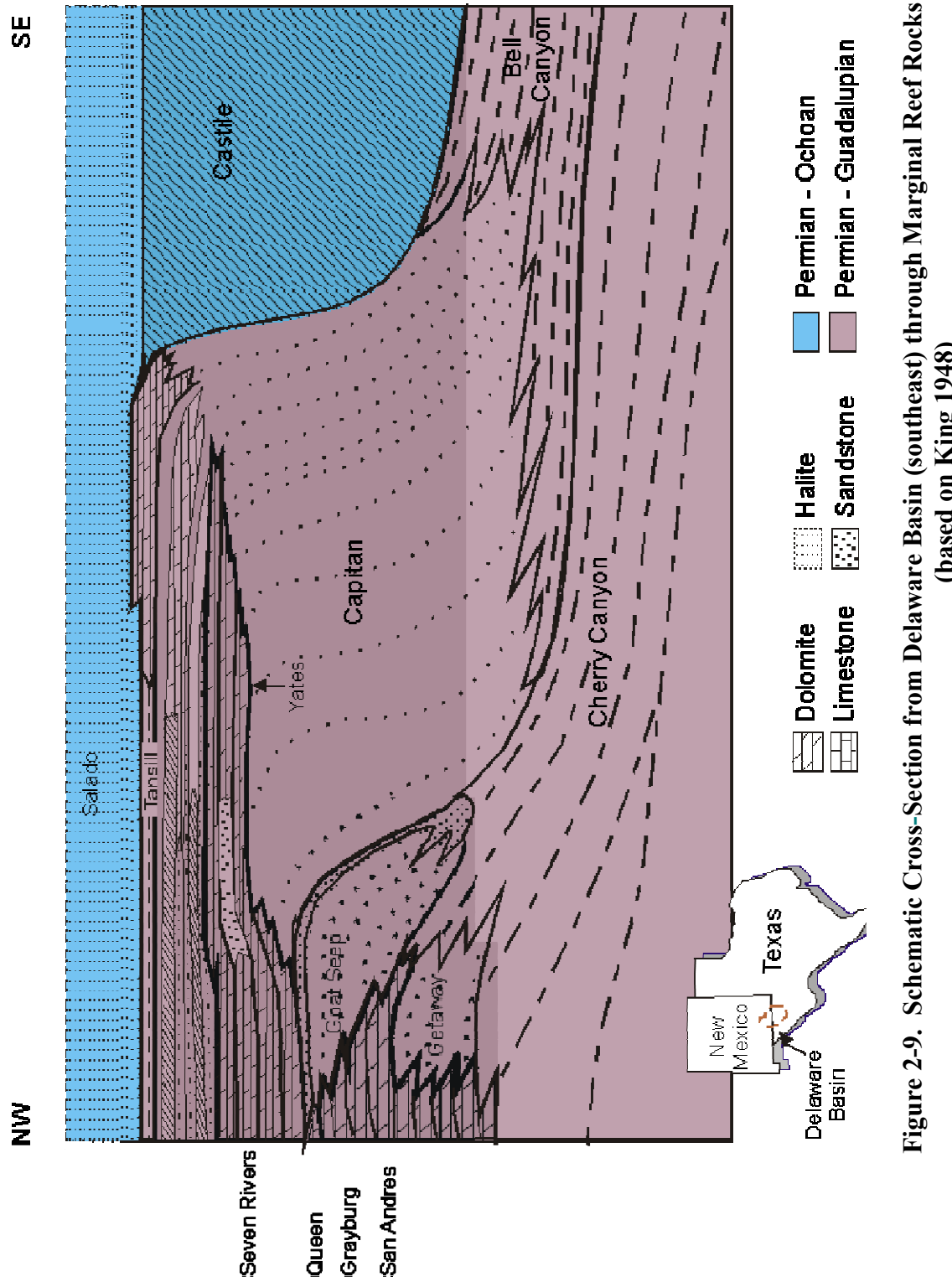
13 The Leonardian Series is represented by the Bone Spring Limestone or Formation (hereafter  
14 referred to as the Bone Spring). According to Foster (1974, pp. 35 - 36), the lower part of the  
15 formation is commonly interbedded carbonate, sandstone, and some shale, while the upper part is  
16 dominantly carbonate. Near the site the Bone Spring is 990 m (3,247 ft) thick, according to  
17 Keesey (1976, Vol. II, Exhibit No. 2).

18 The Guadalupian Series is represented in the general area of the site by a number of formations  
19 exhibiting complex facies relationships (Figure 2-9). The Guadalupian Series is known in  
20 considerable detail west of the site from outcrops in the Guadalupe Mountains, where numerous  
21 outcrops are present and subsurface studies have been undertaken. (See, for example, King  
22 1948, Newell et al. 1953, and Dunham 1972 in the CCA bibliography.)

23 Within the Delaware Basin, the Guadalupian Series, known as the Delaware Mountain Group,  
24 comprises three formations: Brushy Canyon, Cherry Canyon, and Bell Canyon, from base to  
25 top. These formations are dominated by submarine channel sandstones with interbedded  
26 limestone and some shale. The Lamar limestone generally tops the series, immediately  
27 underneath the Castile Formation (hereafter referred to as the Castile). Around the margin of the  
28 Delaware Basin, reefs developed when the Cherry Canyon and Bell Canyon were being  
29 deposited. These massive reef limestones, the Goat Seep and Capitan Limestones, are equivalent  
30 in time to the basin sandstone formations but were developed topographically much higher  
31 around the basin margin. A complex set of limestone-to-sandstone and evaporite beds was  
32 deposited further away from the basin, behind the reef limestones. The Capitan Reef and back-  
33 reef limestones are well known because numerous caves, including the Carlsbad Caverns, are  
34 partially developed in these rocks.

35 **2.1.3.2 The Bell Canyon**

36 As will be discussed in Section 2.1.3.3, the Castile is a 427-to-487m (1,400-to-1,600ft) thick  
37 layer of nearly impermeable anhydrites and halites that isolate the Salado from the



1 deeper water-bearing rocks. This notwithstanding, the DOE is interested in the Bell Canyon  
2 because it is the first laterally continuous transmissive unit below the WIPP repository. The  
3 significance of this unit is related to the FEP in Table 2-1 for deep dissolution. In evaluating this  
4 FEP, the DOE considers the potential for groundwater to migrate from the Bell Canyon or lower  
5 units into the repository and cause dissolution. The following discussion summarizes the basic  
6 understanding of the Bell Canyon lithology. Dissolution is discussed in Section 2.1.6. Bell  
7 Canyon hydrology is presented in Section 2.2.1.2. A thorough discussion of dissolution is in  
8 CCA Appendix DEF.

9 The Bell Canyon is known from outcrops on the west side of the Delaware Basin and from  
10 subsurface intercepts for oil and gas drilling. Several informal lithologic units are commonly  
11 named during such drilling. Mercer et al. (1987, p. 28) stated that DOE-2 penetrated the Lamar  
12 limestone, the Ramsey sand, the Ford shale, the Olds sand, and the Hays sand. This informal  
13 nomenclature is used for the Bell Canyon in some other WIPP reports.

14 The Clayton Williams Badger Federal borehole (Section 15, T22S, R31E) intercepted 961 feet  
15 (293 meters) of Bell Canyon, including the Lamar limestone, according to Keesey (1976, Vol. II,  
16 Exhibit No. 2). Reservoir sandstones of the Bell Canyon were deposited in channels that are  
17 straight to slightly sinuous. In their 1988 paper, Harms and Williamson proposed that density  
18 currents flowed from shelf regions, cutting channels and depositing the sands.

19 Within the basin, the Bell Canyon (Lamar limestone) Castile contact is distinctive on  
20 geophysical logs because of the contrast in low natural gamma of the basal Castile anhydrite  
21 compared to the underlying limestone. Density or acoustic logs are also distinctive because of  
22 the massive and uniform lithology of the anhydrite compared to the underlying beds. In cores,  
23 the transition is sharp, as described by Mercer et al. (1987, 312) for DOE-2. A structure contour  
24 map of the top of the Bell Canyon is shown in Figure 2-10. Also see CCA Appendix MASS,  
25 MASS Attachment 18-6, Figure 5.3-3. According to Powers et al. (1978) (CCA Appendix GCR,  
26 4-59), this structure does not reflect the structure of deeper formations, suggesting different  
27 deformation histories. The rootless character of at least some of the normal faulting in the lower  
28 Permian suggests these are shallow-seated features.

29 **2.1.3.3 The Castile**

30 The Castile is the lowermost lithostratigraphic unit of the Late Permian Ochoan Series (Figure 2-  
31 11) and is part of the thick layer of evaporites within the WIPP disposal system. It was  
32 originally named by Richardson (1904, p. 43) for outcrops in Culberson County, Texas.

33 The Castile crops out along a lengthy area of the western side of the Delaware Basin. The two  
34 distinctive lithologic sequences now known as the Castile and the Salado were separated into the  
35 Upper and Lower Castile by Cartwright (1930). Lang (1939) clarified the nomenclature by  
36 restricting the Castile to the lower unit and naming the upper unit the Salado. By defining an  
37 anhydrite resting on the marginal Capitan limestone as part of the Salado, Lang in 1939  
38 effectively restricted the Castile to the Delaware Basin inside the reef rocks.

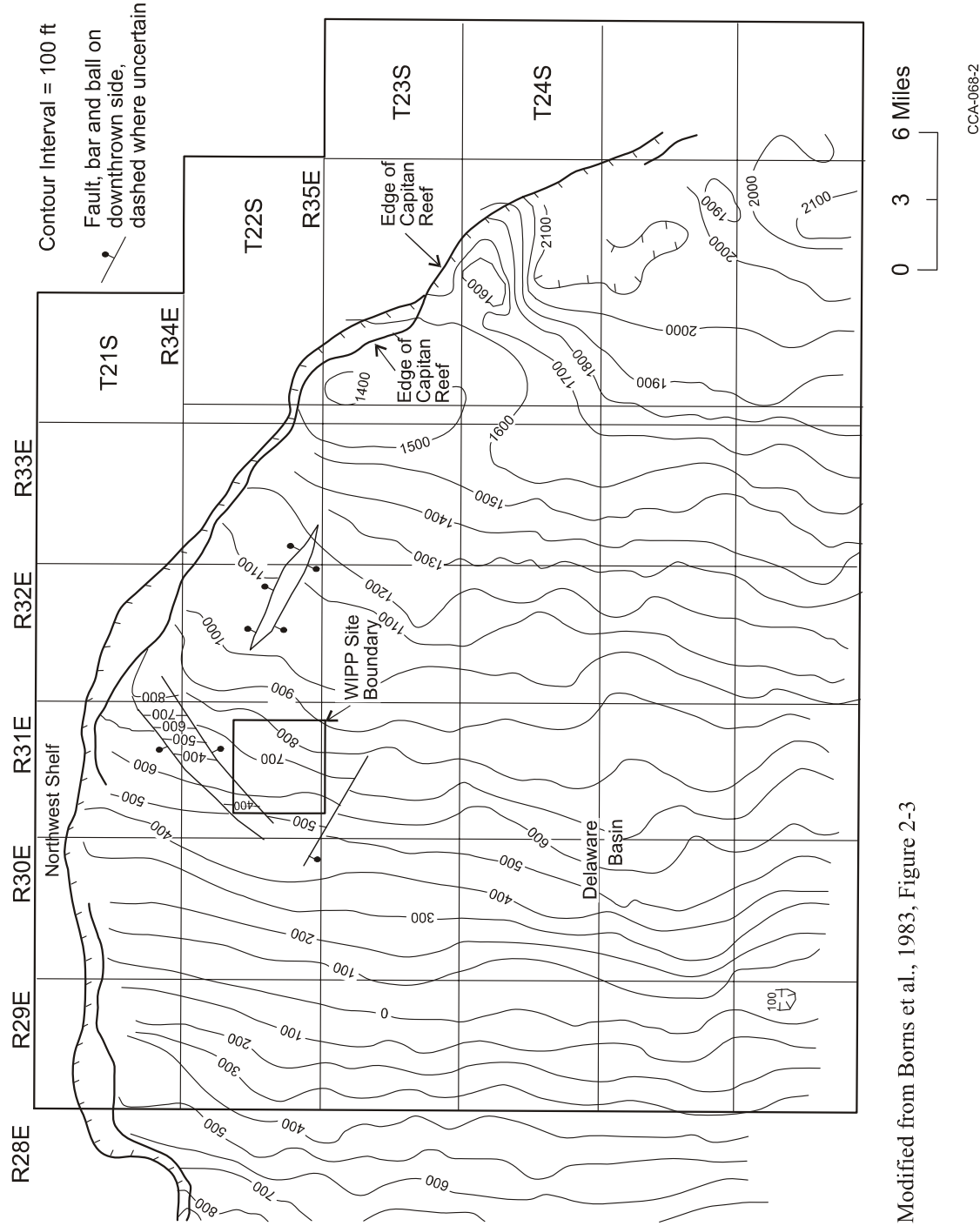
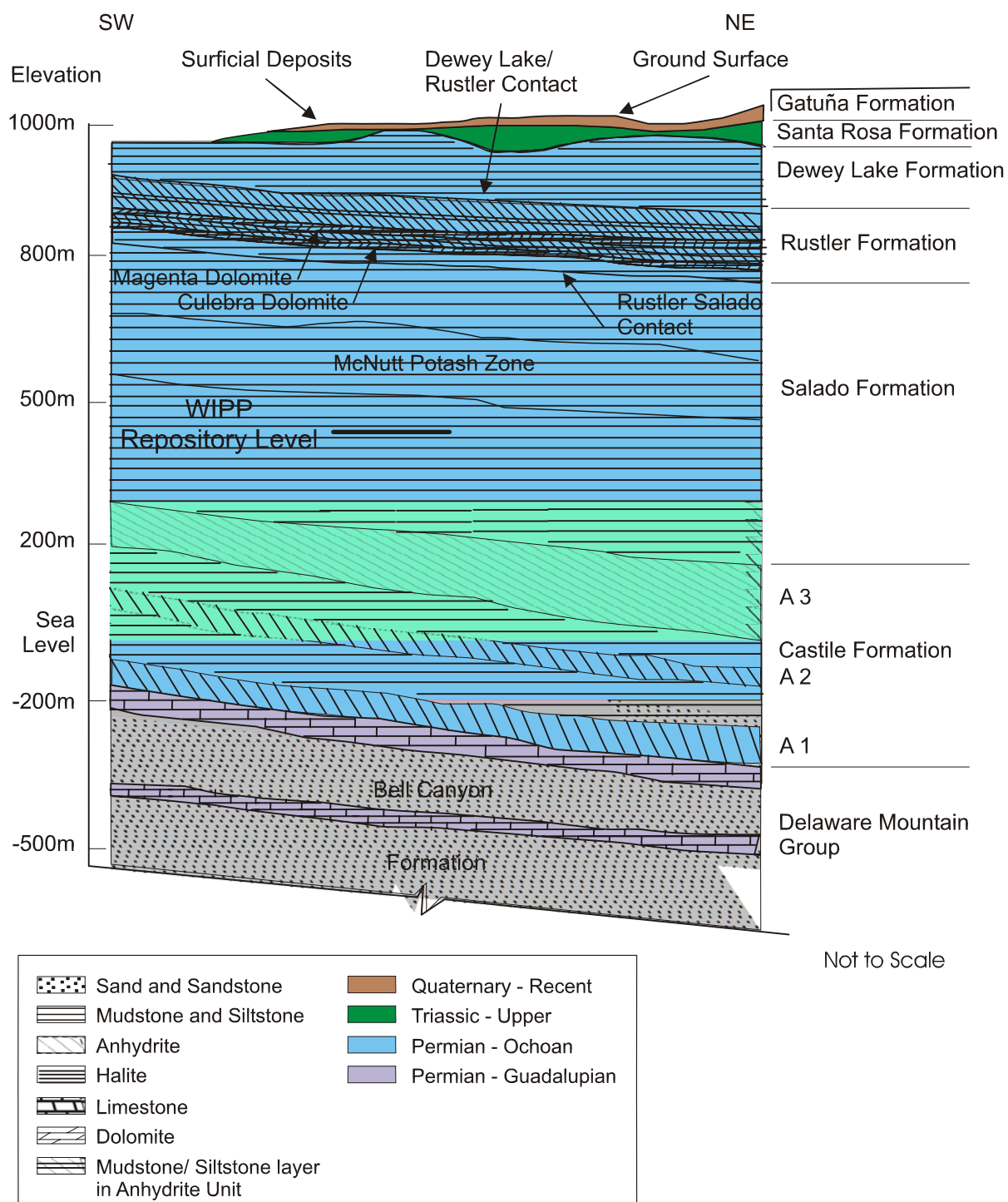


**Figure 2-10. Structure Contour Map of Top of Bell Canyon**

Modified from Borns et al., 1983, Figure 2-3

CCA-068-2



CCA-025-2

1

2      **Figure 2-11. Generalized Stratigraphic Cross Section above Bell Canyon Formation at**  
 3      **WIPP Site**

1 Through detailed studies of the Castile, Anderson et al. (1972) introduced an informal system of  
2 names that is widely used and included in many WIPP reports. The units are named from the  
3 base as anhydrite I (A1), halite I (H1), anhydrite II (A2), etc. The informal nomenclature varies  
4 through the basin from A3 up because of complexity of the depositional system. The Castile  
5 consists almost entirely of thick beds of two lithologies: (1) interlaminated carbonate and  
6 anhydrite, and (2) high-purity halite.

7 In the eastern part of the Delaware basin, the Castile thickness ranges from about 299 to 616 m  
8 (980 to 2,022 ft) (derived from Powers et al. 1996, Figure 5.3-1; see also Borns and Shaffer  
9 1985, Figures 9, 11, and 16 for an earlier range based on fewer drillholes). At DOE-2, the  
10 Castile is 301 m (989 ft) thick. The Castile is thinner in the western part of the Delaware Basin,  
11 and it lacks halite units.

12 Anderson et al. (1978) and Anderson (1978, Figures 1, 3, 4, and 5) correlated geophysical logs  
13 throughout the WIPP region, interpreting thin zones equivalent to halite units as dissolution  
14 residues. Anderson et al. (1972, p. 81) further attributed the lack of halite in the basin to its  
15 removal by dissolution. A structure contour map of the top of the Castile is reported in Figure  
16 4.4-6, CCA Appendix GCR based on seismic data gathered for site characterization. In addition,  
17 Borns et al. (1983) prepared a seismic time structure of the middle Castile for identifying  
18 deformation. This map is shown in Figure DEF-2.2 in CCA Appendix DEF. Powers et al.  
19 (1996; Figures 5.2-1, 5.2-2, and 5.2-3) provide comparative figures of the elevations of the top of  
20 the Bell Canyon, top of Anhydrite 2 (of the Castile), and top of Anhydrite 3 (of the Castile),  
21 respectively, based on geophysical log data from oil and gas wells.

22 For borehole DOE-2, a primary objective was to ascertain whether a series of depressions in the  
23 Salado 3.3 km (2 mi) north of the site center was from dissolution in the Castile and related  
24 processes, as proposed by Davies (1984, p. 175) in his doctoral thesis. Studies have suggested  
25 that these depressions were not from dissolution but from halokinesis in the Castile (see, for  
26 example, Borns 1987). Robinson and Powers (1987, pp. 22 and 78) interpreted one deformed  
27 zone in the Castile in the western part of the Delaware Basin as partly caused by synsedimentary,  
28 gravity-driven, clastic deposition and suggested that the extent of dissolution may have been  
29 overestimated by previous workers. No Castile dissolution is known to be present in the  
30 immediate vicinity of the WIPP site. The process of dissolution and the resulting features are  
31 discussed later in this chapter. See CCA Appendix DEF, Section DEF.3 for a more in-depth  
32 discussion of the study of dissolution in the Castile.

33 In Culberson County, Texas, the Castile hosts major native sulfur deposits. The outcrops of  
34 Castile on the Gypsum Plain south of White's City, New Mexico, have been explored for native  
35 sulfur without success, and there is no reported indication of native sulfur anywhere in the  
36 vicinity of the WIPP.

37 In part of the area around the WIPP, the Castile has been significantly deformed and there are  
38 pressurized brines associated with the deformed areas; borehole ERDA-6 encountered both  
39 deformation and pressurized brine. WIPP-12, 1.6 km (1 mi) north of the site center, revealed  
40 lesser Castile structure, but it also encountered a zone of pressurized brine within the Castile.  
41 Castile deformation is described and discussed in Section 2.1.5 and in CCA Appendix DEF,

1 which detail structural features. Pressurized brine is described in Section 2.2.1, which details the  
2 area's hydrology.

3 Where they exist, Castile brine reservoirs in the northern Delaware Basin are believed to be  
4 fractured systems, with high-angle fractures spaced widely enough that a borehole can penetrate  
5 through a volume of rock containing a brine reservoir without intersecting any fractures and  
6 therefore not produce brine. They occur in the upper portion of the Castile (Popielak et al.  
7 1983). Appreciable volumes of brine have been produced from several reservoirs in the  
8 Delaware Basin, but there is little direct information on the areal extent of the reservoirs or the  
9 interconnection between them. The presence of a pressurized brine pocket is treated in the  
10 conceptual model of WIPP as discussed in Section 6.4.8.

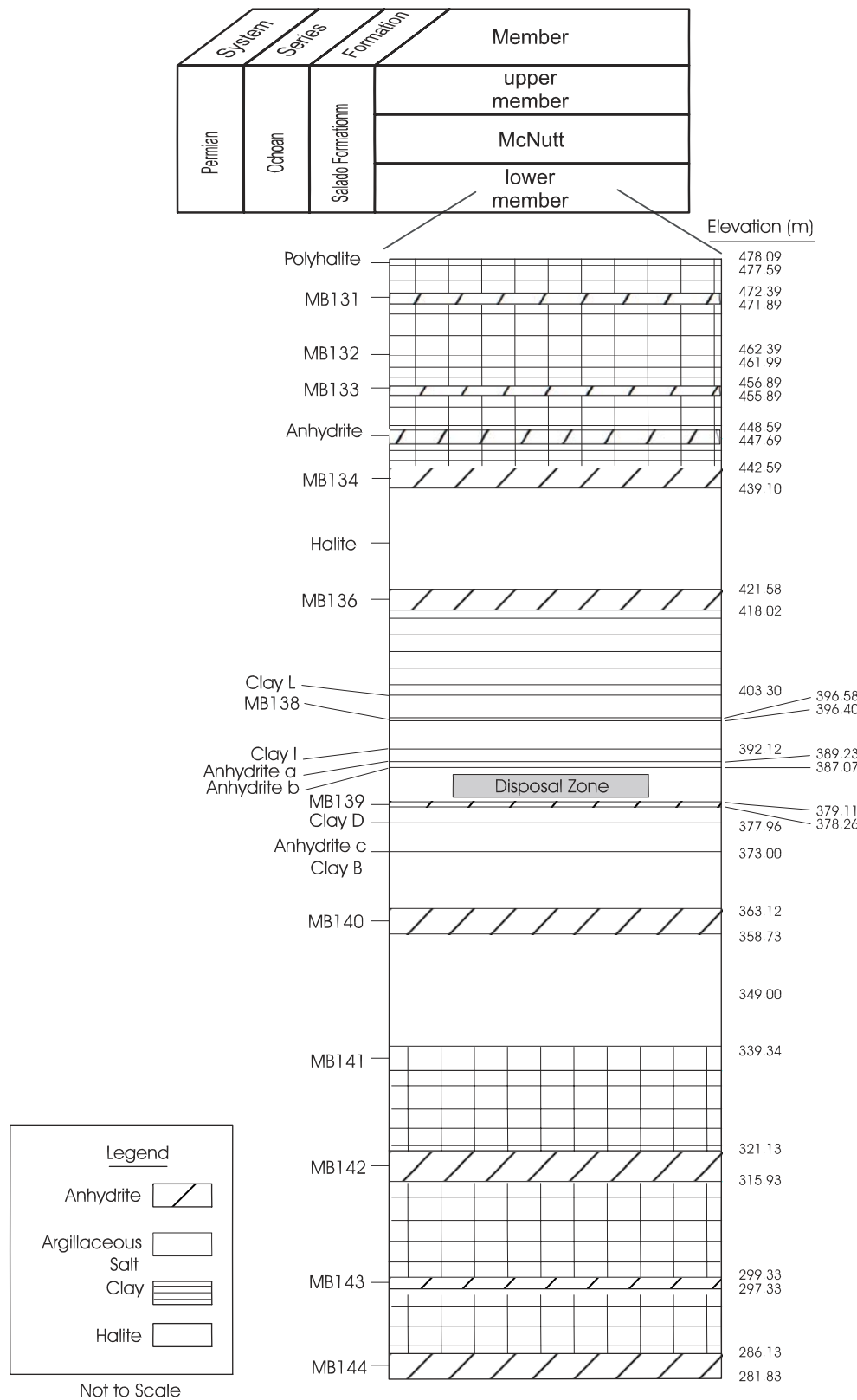
11 The Castile continues to be an object of research interest unrelated to the WIPP program as an  
12 example of evaporites supposedly deposited in deep water. Anderson (1993, pp. 12-13)  
13 discusses alternatives and contradictory evidence. Becker et al. (2002) presented a data set  
14 yielding a total Pb/U isochron age of  $251.5 \pm 2.8$  million years (Ma) for calcite from the Castile  
15 and inferred that the Permo-Triassic boundary could be younger than this date. This discussion  
16 contrasts with other data regarding age of the Salado, Rustler, and Dewey Lake Formations (see  
17 later sections), including evidence that later formations yield slightly older radiometric ages.  
18 Although these discussions and a resolution might eventually affect some concepts of Castile  
19 deposition and dissolution, this issue is largely of academic interest and bears no impact on the  
20 suitability of the Los Medaños region for the WIPP site. Additional discussion of Castile  
21 deformation and the associated WIPP studies appears in Section 2.1.6.1 and CCA Appendix  
22 DEF. The Castile is included in the conceptual model as described in Section 6.4.8. As shown  
23 in Appendix PA, Attachment PAR, Table PAR-43, no stratigraphic or lithologic parameters are  
24 of importance for this unit. Important hydrological parameters are discussed subsequently.

25 The EPA questioned DOE's geologic and geophysical basis for the probability (i.e., eight percent  
26 probability) of intercepting pressurized brine in the Castile Formation beneath the WIPP disposal  
27 panels, and therefore required this distribution to be revised (to a uniform distribution with a  
28 range of 0.01 to 0.6) in Performance Assessment Verification Testing (PAVT) (Docket A-93-02,  
29 Item II-I-25). The formation of Castile brine pockets as a result of Castile deformation was  
30 described in the CCA, and although DOE's discussion of the distribution and nature of fractures  
31 in the Castile was limited, parameters were modified to include larger Castile brine pockets in  
32 the PAVT. Further information on this topic is contained in EPA Technical Support Document  
33 for Section 194.14: Content of Compliance Certification Application, Section IV.C (Docket A-  
34 93-02, Item V-B-3), EPA Technical Support Document for Section 194.23: Parameter  
35 Justification Report (Docket A-93-02, Item V-B-14), and EPA Technical Support Document for  
36 Section 194.23: Review of TDEM Analysis of WIPP Brine Pockets (Docket A-93-02, Item V-  
37 B-30).

38     2.1.3.4 The Salado

39 The Salado is of interest because it contains the repository horizon and provides the primary  
40 natural barrier for the long-term containment of radionuclides. The following section provides  
41 basic information regarding the genesis and lithology of the Salado. Subsequent sections discuss

- 1 Salado deformation, Salado dissolution, and Salado hydrology. CCA Appendix GCR provides  
2 detailed information about the Salado from early site characterization studies.
- 3 The Salado is dominated by halite, in contrast to the underlying Castile. The Salado extends well  
4 beyond the Delaware Basin, and Lowenstein (1988, p. 592) has termed the Salado a saline  
5 "giant."
- 6 While the Fletcher Anhydrite Member, which is deposited on the Capitan Reef rocks, is defined  
7 by Lang (1939; 1942) as the base of the Salado, some investigators consider that the Fletcher  
8 Anhydrite Member may interfinger with anhydrites normally considered part of the Castile. The  
9 Castile-Salado contact is not uniform across the basin, and whether it is conformable is  
10 unresolved. Around the WIPP site, the Castile-Salado contact is commonly placed at the top of a  
11 thick anhydrite informally designated A3; the overlying halite is called the infra-Cowden salt and  
12 is included within the Salado. Bodine (1978, pp. 28 - 29) suggests that the clay mineralogy of  
13 the infra-Cowden in ERDA-9 cores changes at about 4.6 m (15 ft) above the lowermost Salado  
14 and that the lowermost clays are more like Castile clays. At the WIPP site, the DOE recognizes  
15 the top of the thick A3 anhydrite as the local contact for differentiating the Salado from the  
16 Castile and notes that the distinction is related only to nomenclature and has no relevance to the  
17 performance of the WIPP disposal system.
- 18 The Salado in the northern Delaware Basin is broadly divided into three informal members. The  
19 middle member is known locally as the McNutt Potash Zone (hereafter referred to as McNutt) or  
20 Member, and it includes 11 defined potash zones, 10 of which are of economic significance in  
21 the Carlsbad Potash District. The lower member and the upper member remain unnamed. The  
22 WIPP repository level is located below the McNutt in the lower member. Figure 2-12 shows  
23 details of the Salado stratigraphy near the excavated regions. Elements of this stratigraphy are  
24 important to the conceptual model. The conceptual model for the Salado is discussed in Section  
25 6.4.5. The thicknesses used in the model are given in Appendix PA, Attachment PAR, Table  
26 PAR-49.
- 27 Within the Delaware Basin, a system is used for numbering the more significant sulfate beds  
28 within the Salado, designating these beds as marker beds (MBs) from MB 100 (near the top of  
29 the formation) to MB 144 (near the base). The system is generally used within the Carlsbad  
30 Potash District as well as at and around the WIPP site. The repository is located between MB  
31 139 and MB 138.
- 32 In the central and eastern part of the Delaware Basin, the Salado is at its thickest, ranging up to  
33 about 600 m (2,000 ft) thick and consisting mainly of interbeds of sulfate minerals and halite,  
34 with halite dominating. The thinnest portions of the Salado consist of a brecciated residue of  
35 insoluble material a few tens-of-feet thick, which is exposed in parts of the western Delaware  
36 Basin. The common sulfate minerals are anhydrite ( $\text{CaSO}_4$ ), gypsum ( $\text{CaSO}_4 \cdot 2\text{H}_2\text{O}$ ) near the  
37 surface, and polyhalite ( $\text{K}_2\text{SO}_4 \cdot \text{MgSO}_4 \cdot 2\text{CaSO}_4 \cdot 2\text{H}_2\text{O}$ ). They form interbeds and are also  
38 found along halite grain boundaries. Isopach maps of various intervals of the Salado above the  
39 repository horizon have been provided to assist in understanding regional structure. These are  
40 Figures 4.3-4 to 4.3-7 in CCA Appendix GCR. A structure contour map of the Salado can be  
41 found in CCA Appendix GCR (Figure 4.4-10).



1

2 **Figure 2-12. Salado Stratigraphy in the Vicinity of the WIPP Disposal Zone**

1      **Table 2-2. Chemical Formulas, Distributions, and Relative Abundances of Minerals in the**  
 2      **Castile, Salado, and Rustler Formations**

Mineral	Formula	Occurrence and Abundance
Amesite	(Mg <sub>4</sub> Al <sub>2</sub> )(Si <sub>2</sub> Al <sub>2</sub> )O <sub>10</sub> (OH) <sub>8</sub>	S, R
Anhydrite	CaSO <sub>4</sub>	CCC, SSS, RRR (rarely near surface)
Calcite	CaCO <sub>3</sub>	S, RR
Carnallite	KMgCl <sub>3</sub> •6H <sub>2</sub> O	SS
Chlorite	(Mg,Al,Fe) <sub>12</sub> (Si,Al) <sub>8</sub> O <sub>20</sub> (OH) <sub>16</sub>	S, R
Corrensite	mixed-layer chlorite and smectite	S, R
Dolomite	CaMg(CO <sub>3</sub> ) <sub>2</sub>	RR
Feldspar	(K,Na,Ca)(Si,Al)O <sub>8</sub>	C, S, R
Glauberite	Na <sub>2</sub> Ca(SO <sub>4</sub> ) <sub>2</sub>	C, S (never near surface)
Gypsum	CaSO <sub>4</sub> •2H <sub>2</sub> O	CCC (only near surface), S, RRR
Halite	NaCl	CCC, SSS, RRR (rarely near surface)
Illite	K <sub>1-1.5</sub> Al <sub>4</sub> [Si <sub>7-6.5</sub> Al <sub>1-1.5</sub> O <sub>20</sub> ](OH) <sub>4</sub>	S, R
Kainite	KMgClSO <sub>4</sub> •3H <sub>2</sub> O	SS
Kieserite	MgSO <sub>4</sub> •H <sub>2</sub> O	SS
Langbeinite	K <sub>2</sub> Mg <sub>2</sub> (SO <sub>4</sub> ) <sub>3</sub>	S
Magnesite	MgCO <sub>3</sub>	C, S, R
Polyhalite	K <sub>2</sub> Ca <sub>2</sub> Mg(SO <sub>4</sub> ) <sub>4</sub> •2H <sub>2</sub> O	SS, R (never near surface)
Pyrite	FeS <sub>2</sub>	C, S, R
Quartz	SiO <sub>2</sub>	C, S, R
Serpentine	Mg <sub>3</sub> Si <sub>2</sub> O <sub>5</sub> (OH) <sub>4</sub>	S, R
Smectite	(Ca <sub>1/2</sub> ,Na) <sub>0.7</sub> (Al,Mg,Fe) <sub>4</sub> (Si,Al) <sub>8</sub> O <sub>20</sub> (OH) <sub>4</sub> •nH <sub>2</sub> O	S, R
Sylvite	KCl	SS

**Legend:**

C = Castile

S = Salado

R = Rustler

3 letters = abundant

2 letters = common

1 letter = rare or accessory

3      In the vicinity of the repository, authigenic quartz (SiO<sub>2</sub>) and magnesite (MgCO<sub>3</sub>) are also  
 4      present as accessory minerals. Interbeds in the salt are predominantly anhydrite with seams of  
 5      clay. The clays within the Salado are enriched in magnesium and depleted in aluminum (Bodine  
 6      1978, p. 1). The magnesium enrichment probably reflects the intimate contact of the clays with  
 7      brines derived from evaporating sea water, which are relatively high in magnesium.

8      Powers et al. (Chapter 7 of CCA Appendix GCR) studied the geochemistry of the rocks in the  
 9      vicinity of the disposal system. A partial list of minerals found in the Delaware Basin evaporites,  
 10     together with their chemical formulas, is given in Table 2-2. The table also indicates the relative  
 11     abundances of the minerals in the evaporite rocks of the Castile, Salado, and Rustler. Minerals  
 12     found either only at depth, removed from influence of weathering, or only near the surface, as  
 13     weathering products, are also identified.

1 Although the most common Delaware Basin evaporite mineral is halite, the presence of less  
2 soluble interbeds (dominantly anhydrite, polyhalite, and claystone) and more soluble admixtures  
3 (for example, sylvite, glauberite, kainite) has resulted in chemical and physical properties of the  
4 bulk Salado that are significantly different from those of pure halite layers contained within it.  
5 In particular, the McNutt, between MB 116 and MB 126, is locally explored and mined for  
6 potassium-bearing minerals of economic interest. Under differential stress, interbeds (anhydrite,  
7 polyhalite, magnesite, dolomite) may fracture while, under the same stress regime, pure halite  
8 would undergo plastic deformation. Fracturing of relatively brittle beds, for example, has locally  
9 enhanced the permeability, allowing otherwise nonporous rock to carry groundwater. Some  
10 soluble minerals incorporated in the rock salt can be radiometrically dated, and their dates  
11 indicate the time of their formation. The survival of such minerals is significant, in that such  
12 dating is impossible in pure halite or anhydrite.

13 Liquids were collected from fluid inclusions in the Salado halite and from seeps and boreholes  
14 within the WIPP drifts. Analysis of these samples indicated that there is compositional  
15 variability in the fluids that shows the effects of various phase transformations on brine  
16 composition. The fluid inclusions belong to a different chemical population than do the fluids  
17 emanating from the walls. It was concluded that much of the brine is completely immobilized  
18 within the salt and that the free liquid emanating from the walls is present as a fluid film along  
19 intergranular boundaries, mainly in clays and in fractures in anhydrites. Additional information  
20 can be found in CCA Appendix GCR, Sections 7.5 and 7.6.

21 Early investigators of the Salado recognized a repetitious vertical succession or cycle of beds in  
22 the Salado: clay - anhydrite - polyhalite - halite and minor polyhalite - halite. Later investigators  
23 described the cyclical units as clay - magnesite - anhydrite or polyhalite or glauberite - halite -  
24 argillaceous halite capped by mudstone. Lowenstein (1988, pp. 592 - 608) defined a  
25 depositional cycle (Type I) consisting of (1) basal mixed siliciclastic and carbonate (magnesite)  
26 mudstone, (2) laminated to massive anhydrite or polyhalite, (3) halite, and (4) halite with mud.  
27 Lowenstein also recognized repetitious sequences of halite and halite with mud as incomplete  
28 Type I cycles and termed them Type II cycles. Lowenstein (1988, pp. 592 - 608) interpreted the  
29 Type I cycles as having formed in a shallowing upward, desiccating basin beginning with a  
30 perennial lake or lagoon of marine origin and evaporating to saline lagoon and salt pan  
31 environments. Type II cycles are differentiated because they do not exhibit features of  
32 prolonged subaqueous deposition and also have more siliciclastic influx than do Type I cycles.

33 From detailed mapping of the Salado in the air intake shaft (AIS) at WIPP, Holt and Powers  
34 (1990a, pp. 2-26) interpreted depositional cycles of the Salado in terms of modern features such  
35 as those at Devil's Golf Course at Death Valley National Monument, California. The  
36 evaporative basin was desiccated, and varying amounts of insoluble residues had collected on the  
37 surface through surficial dissolution, eolian sedimentation, and some clastic sedimentation from  
38 temporary flooding caused from surrounding areas. The surface developed local relief that could  
39 be mapped in some cycles, while the action of continuing desiccation and exposure increasingly  
40 concentrated insoluble residues. Flooding, most commonly from marine sources, reset the  
41 sedimentary cycle by depositing a sulfate bed.

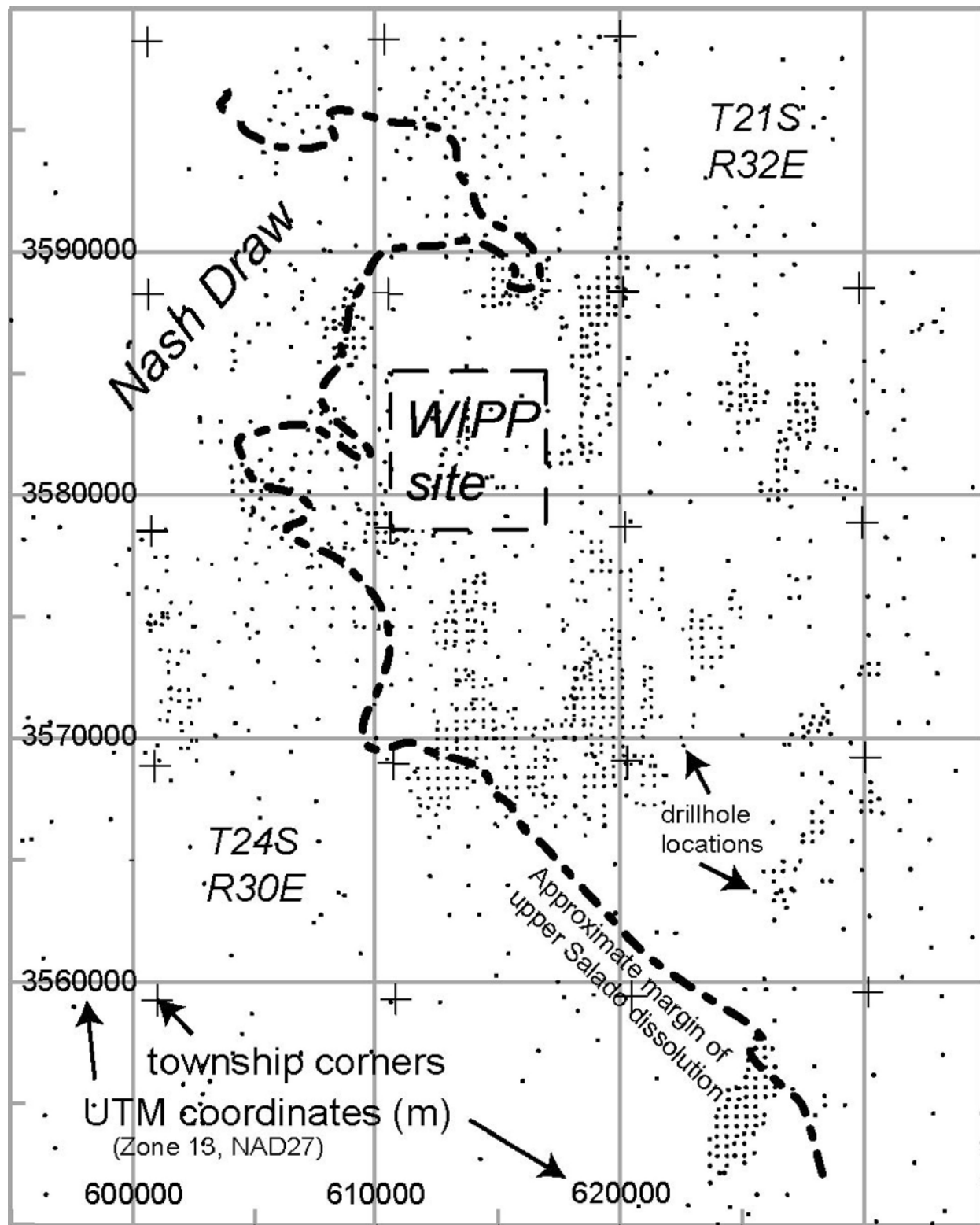
42 The details available from the shaft demonstrated the important role of syndepositional water  
43 level to water table changes that created solution pits and pipes within the halitic beds while they

1 were at the surface. Holt and Powers (1990a, Appendix F) concluded that passive halite cements  
2 filled the pits and pipes, as well as less dramatic voids, as the water table rose. Early diagenetic  
3 to synsedimentary cements filled the porosity early and rather completely with commonly clear  
4 and coarsely crystalline halite, reducing the porosity to a very small volume according to Casas  
5 and Lowenstein (1989).

6 Although Holt and Powers (1990a) found no evidence for postdepositional halite dissolution in  
7 the AIS, dissolution of the upper Salado halite has occurred west of the WIPP. Effects of  
8 dissolution are visible in Nash Draw and at other localities where gypsum karst has formed,  
9 where units above the Salado such as the Rustler Formation, Dewey Lake Redbeds, and post-  
10 Permian rocks have subsided. Dissolution studies are summarized in CCA Appendix DEF,  
11 Section DEF.3. The dissolution margin of upper Salado halite (see Figure 2-13), based on  
12 changes in thickness of the interval from the Culebra dolomite to the Vaca Triste Sandstone  
13 Member of the Salado, has been interpreted in detail by Powers (2002a, 2002b, 2003a), Holt and  
14 Powers (2002), and Powers et al. (2003). Powers (2002a, 2002b, 2003a) examined data from  
15 additional drillholes and noted that the upper Salado dissolution margin appears relatively  
16 narrow in many areas, and it directly underlies much of Livingston Ridge. The hydraulic  
17 properties of the Culebra correlate in part with dissolution of halite from the upper Salado (Holt  
18 and Yarbrough 2002; Powers et al. 2003), and the relationships are further described in Section  
19 2.2.1.4.1.2.

20 Within Nash Draw, Robinson and Lang (1938, pp. 87-88) recognized a zone equivalent to the  
21 upper Salado but lacking halite. Test wells in southern Nash Draw produced brine from this  
22 interval, and it has become known as the brine aquifer. Robinson and Lang (1938) considered  
23 this zone a residuum from dissolution of Salado halite (see Section 2.1.6.2). Jones et al. (1960)  
24 remarked that the residuum should be considered part of the Salado, though in geophysical logs  
25 it may resemble the lower Rustler. The approximate eastern limit of the residuum and brine  
26 aquifer lies near Livingston Ridge (the eastward margin of Nash Draw) and is marked by a  
27 thickening of the Salado (see Section 2.1.6.2.2).

28 At the center of the site, Holt and Powers (1984, pp. 4-9) recognized clasts of fossil fragments  
29 and mapped channeling in siltstones and mudstones above the halite; they considered these beds  
30 to be a normal part of the transition from the shallow evaporative lagoons and desiccated salt  
31 pans of the Salado to the saline lagoon of the lower Rustler. Although some Salado halite  
32 dissolution at the WIPP may have occurred before deposition of the Rustler clastics, this process  
33 was quite different from the subsurface removal of salt from the Salado in more recent time that  
34 caused the residuum and associated brine aquifer in Nash Draw.



2

Figure 2-13. Dissolution Margin for the Upper Salado

1 Geochronological investigations provide a means to confirm the physical evidence indicating  
2 that little or no rock-water interactions have occurred in the Salado at the WIPP since the Late  
3 Permian Period. Radiometric techniques provide a means of determining the approximate time  
4 of the latest episode of regional recrystallization of evaporite minerals, which can be inferred as  
5 the approximate time of the latest episode of freely circulating groundwater. Radiometric dates  
6 for minerals of the Salado are available from mines and boreholes in the vicinity of the WIPP  
7 (Register and Brookins, 1980, pp. 30-42; Brookins, 1980, pp. 29-31; Brookins, et al. 1980, pp.  
8 635-637; Brookins, 1981; and Brookins and Lambert, 1987, pp. 771-780). The distribution of  
9 dates shows that many of the rubidium-strontium (Rb-Sr) isochron determinations on evaporite  
10 minerals, largely sylvite ( $214 \pm 14$  million years ago), are in good agreement with potassium-  
11 argon (K-Ar) determinations on pure polyhalites (198 to 216 million years ago). (Potassium-  
12 argon ages for sylvite are significantly younger than Rb-Sr ages for the same rocks because of  
13 the loss of radiogenic argon. Radiogenic strontium, as a solid, is less mobile than argon and  
14 therefore the Rb-Sr isochron method is preferred for sylvite.) Renne et al. (1998) sampled  
15 langbeinite crystals from the Salado and obtained Ar-39/Ar-40 plateau ages of  $251 \pm 0.2$  Ma and  
16  $251 \pm 0.4$  Ma. Clay minerals have both Rb-Sr and K-Ar ages significantly older ( $390 \pm 77$   
17 million years [Register, 1981]) than the evaporite minerals, presumably reflecting the detrital  
18 origin of the clays.

19 One significantly younger recrystallization event has been identified in evaporites in the WIPP  
20 region and is a contact phenomenon associated with the emplacement of an Oligocene igneous  
21 dike (see Section 2.1.5.4). Polyhalite near the dike yields a radiometric age of 21 million years,  
22 compared to the 32- to 34-million-year age determined for the dike (Brookins, 1980, pp. 29-31;  
23 and Calzia and Hiss, 1978, p. 44) (this number was recalculated to  $34.8 \pm 0.8$  million years; CCA  
24 Appendix GCR, pp. 3 - 80). This exception notwithstanding, the results of radiometric  
25 determinations argue for the absence of pervasive recrystallization of the evaporites in the Salado  
26 in the last 200 million years. This conclusion is supported by the number of replicate  
27 determinations, the wide distribution of similarly dated minerals throughout the Delaware Basin,  
28 and the concordance of dates obtained by various radiometric methods.

29 The notion of extensive recrystallization of Salado evaporites has been raised again since the  
30 CCA was submitted. Hazen and Roedder (2001), reiterating some arguments presented by  
31 Roedder (1984) and O'Neill et al. (1986), suggested that halite has been extensively  
32 recrystallized by water moving through the Salado at unknown times. Stable isotope data from  
33 fluid inclusions within coarse, clear halite crystals were interpreted as signifying that modern  
34 meteoric water constituted part of the fluid inclusion. O'Neill et al. (1986) noted as well that the  
35 stable isotope data are consistent with meteoric water falling on a desiccated Salado salt pan  
36 surface. Powers and Hassinger (1985) and Holt and Powers (1990a, 1990b) interpret  
37 syndepositional dissolution pipes as a common feature of the Salado, with coarse, clear halite  
38 with large fluid inclusions formed on a desiccated salt pan. Powers et al. (2001) summarized the  
39 arguments against extensive recrystallization of Salado halite. Stein and Krumhansl (1988)  
40 found variable compositions of large fluid inclusions, and show that inclusion chemistry differs  
41 significantly from intercrystalline brines, indicating that fluid movement is very limited.  
42 Satterfield et al. (2002) also concluded that the coarse halite cements found in certain beds of the  
43 Salado are synsedimentary, based on ionic concentrations in fluid inclusions. Moreover,  
44 Beauheim and Roberts (2002) find extremely low permeability in Salado halite, showing that  
45 fluid movement, especially vertically, through the Salado is too limited and slow to create the

1 purported recrystallization. These findings are also consistent with indications that salt pan  
2 deposits are cemented quickly and thoroughly at shallow depths of burial (Casas and Lowenstein  
3 1989). The conclusion that Salado halite has not been pervasively recrystallized remains sound.

4 The Salado is of primary importance to the containment of waste. Because it is the principal  
5 natural barrier, many of the properties of the Salado have been characterized by the DOE, and  
6 numerical codes are used by the DOE to simulate the natural processes within the Salado that  
7 affect the disposal system performance.

8 Two conceptual models of the Salado are used in the performance assessment. One models the  
9 creep closure properties of the Salado and the other, the hydrological properties. The creep  
10 closure of the Salado is discussed in Appendix PA, Attachment PORSURF. This model uses key  
11 parameters derived from both in-situ measurements and laboratory testing on Salado core  
12 samples. Summaries of these parameters are in Butcher (1997). Appendix PORSURF  
13 Attachment 1, Table 2.

14 The second conceptual model is titled the Salado conceptual model and is discussed in Section  
15 6.4.5. This model divides the Salado into two lithologic units: impure halite and Salado  
16 interbeds. The impure halite in this conceptual model is characterized entirely by its  
17 hydrological parameters as shown in Table 6-16. The interbeds are characterized by both  
18 hydrological parameters in Table 6-17 and fracture properties in Table 6-19. This latter  
19 information is needed since the model in Section 6.4.5.2 incorporates the possibility of interbed  
20 fracturing should pressures in the repository become high enough. The modeling assumptions  
21 surrounding the fracturing model are discussed in Appendix PA, Attachment MASS, Section  
22 MASS-13.

23 **2.1.3.5 The Rustler**

24 The Rustler is the youngest evaporite-bearing formation in the Delaware Basin. It was originally  
25 named by Richardson in 1904 for outcrops in the Rustler Hills of Culberson County, Texas.  
26 Adams (1944, p. 1614) first used the names Culebra Member and Magenta Member to describe  
27 the two carbonates in the formation, indicating that Lang favored the names, although Lang did  
28 not use these names to subdivide the Rustler in his 1942 publication. Vine (1963, p. B1)  
29 extensively described the Rustler in Nash Draw and proposed the four formal names and one  
30 informal term that were used for the stratigraphic subdivisions of the Rustler. These are as  
31 follows (from the base): unnamed lower member, Culebra Dolomite Member, Tamarisk  
32 Member, Magenta Dolomite Member, and Forty-niner Member (Figure 2-14). Powers and Holt  
33 (1999) formalized the nomenclature for the lower Rustler, naming the Los Medaños Member for  
34 the exposures of the former “unnamed lower member” in the WIPP shafts and in boreholes in the  
35 vicinity of Los Medaños near the WIPP site. Four studies of the Rustler since Vine’s 1963 work  
36 contribute important information about the stratigraphy, sedimentology, and regional  
37 relationships while examining more local details as well. Eager (1983) published a report on  
38 relationships of the Rustler observed in the southern Delaware Basin as part of sulfur exploration  
39 in the area. Holt and Powers (1988, Section 5.0), reproduced

**Formal Stratigraphy  
After  
Lang (1935) and  
Powers and Holt (1999)**

Forty-niner  
Member

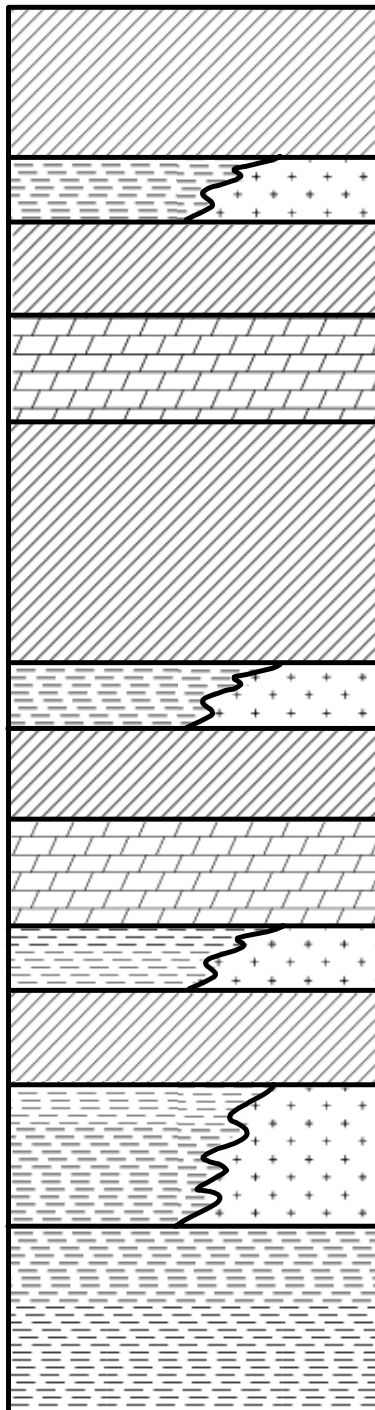
Magenta Dolomite  
Member

Tamarisk  
Member

Culebra Dolomite  
Member

Los Medaños  
Member

1  
2



**Informal Stratigraphy  
of  
Holt and Powers (1988)**

Anhydrite 5 (A5)

Mudstone-Halite 4 (M4/H4)

Anhydrite 4 (A4)

Magenta Dolomite

Anhydrite 3 (A3)

Mudstone-Halite 3 (M3/H3)

Anhydrite 2 (A2)

Culebra Dolomite

Mudstone-Halite 2 (M2/H2)

Anhydrite 1 (A1)

Mudstone-Halite 1 (M1/H1)

Bioturbated Clastic  
Interval

Figure 2-14. Rustler Stratigraphy

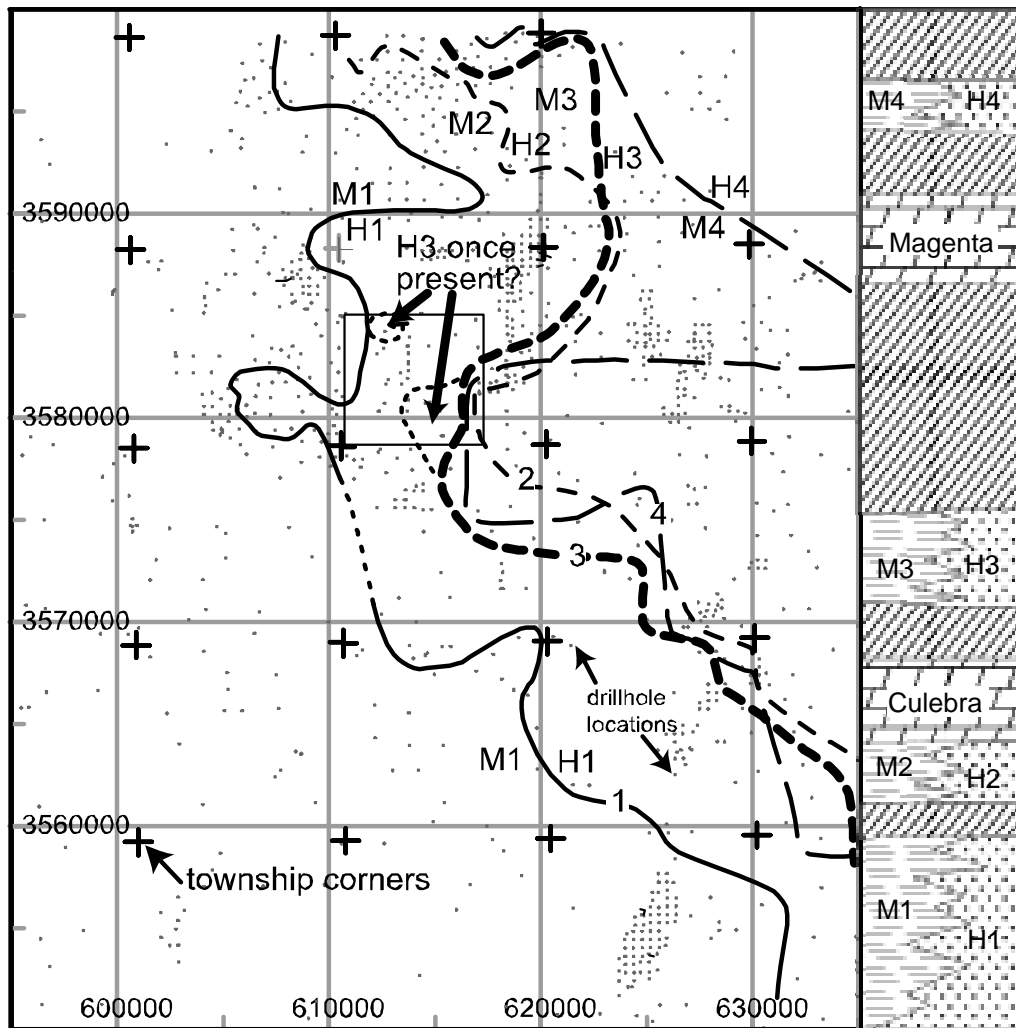
1 as CCA Appendix FAC, reported the details of sedimentologic and stratigraphic studies of  
2 WIPP shafts and cores as well as of geophysical logs from about 600 boreholes in southeastern  
3 New Mexico. Their work resulted in the more detailed subdivisions of the Rustler indicated in  
4 the right-hand column of Figure 2-14.

5 The Rustler is regionally extensive; a similar unit in the Texas panhandle is also called the  
6 Rustler. Within the area around WIPP, evaporite units of the Rustler are interbedded with  
7 significant siliciclastic beds and the carbonates. Both the Magenta and the Culebra extend  
8 regionally beyond areas of direct interest to the WIPP. In the general area of the WIPP, both the  
9 Tamarisk and the Forty-niner have similar lithologies: lower and upper sulfate beds and a  
10 middle unit that varies principally from mudstone to halite from west to east (Figure 2-14). In a  
11 general sense, halite in the Los Medaños broadly persists to the west of the WIPP site, and halite  
12 is found east of the center of the WIPP in the Tamarisk and the Forty-niner (Figure 2-15).

13 Two different explanations have been proposed over the history of the project to account for the  
14 observed distribution of halite in the non-dolomite members of the Rustler. The earliest  
15 researchers (e.g., Bachman [1985] and Snyder [1985]) assumed that halite had originally been  
16 present in all the non-sulfate intervals of the Forty-niner, Tamarisk, and Los Medaños Members,  
17 and that its present-day absence reflected post-depositional dissolution.

18 An alternative interpretation was presented by Holt and Powers (1988) following detailed  
19 mapping of the Rustler exposed in the WIPP ventilation (now waste) and exhaust shafts in 1984.  
20 Fossils, sedimentological features, and bedding relationships were identified in units that had  
21 previously been interpreted from boreholes as dissolution residues. Cores from existing  
22 boreholes, outcrops, geophysical logs, and petrographic data were also reexamined to establish  
23 facies variability across the area.

24 As a result of these studies, the Rustler was interpreted to have formed in variable depositional  
25 environments, including lagoon and saline playas, with two major episodes of marine flooding  
26 which produced the carbonate units. Sedimentary structures were interpreted to indicate  
27 synsedimentary dissolution of halite from halitic mudstones around a saline playa and fluvial  
28 transport of more distal clastic sediments. The halite in the Rustler, by this interpretation, has a  
29 present-day distribution similar to that at the time the unit was deposited. Some localized  
30 dissolution of halite may have occurred along the depositional margins, but not over large areas.  
31 Hence, the absence of halite in Rustler members at the WIPP site more generally reflects non-  
32 deposition than dissolution.



### Explanation

M#, H# indicate mudstone and halitic facies on each side of estimated halite margin (numbered line on map) for stratigraphic intervals as indicated in the column to the right (key on Figure 2-14). UTM coordinates (m) for Zone 13 (NAD27) are provided for easting and northing.

Two zones within the WIPP site boundary ("H3 once present?") indicate where halite may have been present west of the current boundary of H3 (marked by -----).

1  
2

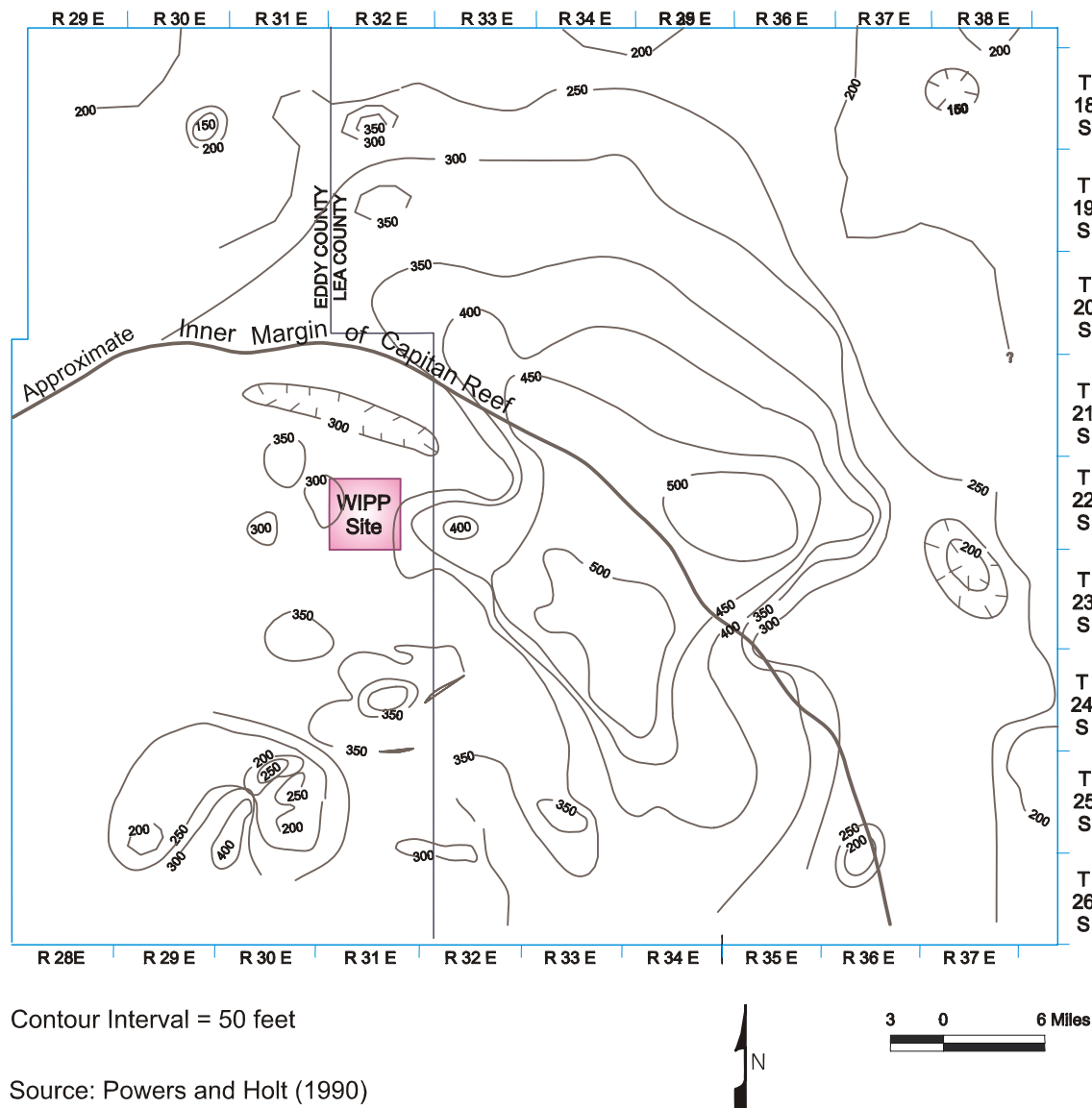
**Figure 2-15. Halite Margins for the Rustler Formation Members**

1 This hypothesis was tested and refined by subsequent investigations (e.g., Powers and Holt 1990,  
2 1999, 2000; Holt and Powers 1990a) and is now considered the accepted explanation for the  
3 present-day distribution of halite in the Rustler. Powers and Holt (1999) thoroughly described  
4 the sedimentary structures and stratigraphy of the Los Medaños as part of the procedure for  
5 naming the unit. This shows the basis for interpreting the depositional history of the member  
6 and for rejecting significant post-burial dissolution of halite in that unit. Powers and Holt (2000)  
7 further describe the lateral facies relationships in other Rustler units, especially the Tamarisk,  
8 developed on sedimentologic grounds, and rejected the concept of broad, lateral dissolution of  
9 halite from the Rustler across the WIPP site area.

10 As discussed in Section 2.2.1.4, regional Culebra transmissivity shows about six orders of  
11 magnitude variation across the area around the site and about three orders of magnitude across  
12 the site itself. Although some investigators have called attention to the broad relationship  
13 between the distribution of halite in the Rustler and variations in Culebra transmissivity and have  
14 attributed the variation to fracturing resulting from postdepositional dissolution of Rustler halite  
15 (see, for example, Snyder 1985, p. 10; and CCA Appendix DEF, Section DEF-3.2), CCA  
16 Appendix FAC and Powers and Holt 1990, 1999, 2000) largely rule out this explanation.  
17 Variations in transmissivity of the Culebra were correlated qualitatively to the thickness of  
18 overburden above the Culebra (see discussion in Section 2.1.5.2), the amount of dissolution of  
19 the upper Salado, and the distribution of gypsum fillings in fractures in the Culebra (Beauheim  
20 and Holt 1990). Subsequently, Holt and Yarbrough (2002) and Powers et al. (2003) related the  
21 variation in Culebra transmissivity more quantitatively to overburden thickness and dissolution  
22 of upper Salado halite. The DOE believes that variations in Culebra transmissivity are primarily  
23 caused by the relative abundance of open fractures in the unit, which may be related to each of  
24 these factors. As discussed in Section 6.4.6.2 and Appendix PA, Attachment TFIELD,  
25 uncertainty in spatial variability in the transmissivity of the Culebra has been incorporated in the  
26 PA.

27 In the region around the WIPP, the Rustler reaches a maximum thickness of more than 152 m  
28 (500 ft) (Figure 2-16), while it is about 91 to 107 m (300 to 350 ft) thick within most of the  
29 WIPP site. Much of the difference in Rustler thickness can be attributed to variations in the  
30 amount of halite contained in the formation. Variation in Tamarisk thickness accounts for a  
31 larger part of thickness changes than do variations in either the Los Medaños or the Forty-niner.  
32 Details of the Rustler thickness can be found in CCA Appendix GCR, 4-39 to 4-42 and Figure  
33 4.3-8. See also CCA Appendix FAC.

34 Much project-specific information about the Rustler is contained in CCA Appendix FAC. The  
35 WIPP shafts were a crucial element in Holt and Powers' 1988 study, exposing features not  
36 previously reported. Cores were available from several WIPP boreholes, and their lithologies  
37 were matched to geophysical log signatures to extend the interpretation throughout a larger area  
38 in southeastern New Mexico. These data are included in CCA Appendix FAC, Appendix II.



1

2

**Figure 2-16. Isopach Map of the Entire Rustler**

1    2.1.3.5.1 Los Medaños Member

2    The unit formerly referred to as the unnamed lower member has been named the Los Medaños  
3    Member. The Los Medaños rests on the Salado with apparent conformity at the WIPP site. It  
4    consists of significant proportions of bedded and burrowed siliciclastic sedimentary rocks with  
5    cross-bedding and fossil remains. These beds record the transition from strongly evaporative  
6    environments of the Salado to saline lagoonal environments. The upper part of the Los  
7    Medaños includes halitic and sulfatic beds within clastics. CCA Appendix FAC, pp. 6-8 and  
8    Powers and Holt (1999) interpret these as facies changes within a saline playa or lagoon  
9    environment, not dissolution residues from postdepositional dissolution.

10   According to CCA Appendix FAC, Figure 4-4, the Los Medaños ranges in thickness from about  
11   29 to 38 m (96 to 126 ft) within the site boundaries. The maximum thickness recorded during  
12   that study was 63 m (208 ft) southeast of the WIPP site. An isopach of the Los Medaños is  
13   shown as Figure 4-7 in CCA Appendix FAC.

14   Halite is present in the M1/H1 unit of the Los Medaños west of most of the site area (see Figure  
15   2-15 for an illustration of the halite margins). The drilling initiated during CRA-2004  
16   preparation to investigate Culebra transmissivity variations based on overburden and Salado  
17   dissolution will develop additional detailed information about distribution of halite in the Los  
18   Medaños. Cross-sections based on geophysical log interpretations by Holt and Powers (CCA  
19   Appendix FAC) and Powers and Holt (2000) show that the unit is thicker to the east where the  
20   halite is more abundant. The Los Medaños is incorporated into the conceptual model as  
21   described in Section 6.4.6.1. Model parameters are in Appendix PA, Attachment PAR, Table  
22   PAR- 27.

23   2.1.3.5.2 The Culebra Dolomite Member

24   The Culebra rests with apparent conformity on the Los Medaños, though the underlying unit  
25   ranges from claystone to its lateral halitic equivalent in the site area. West of the WIPP site, in  
26   Nash Draw, the Culebra is disrupted from dissolution of underlying halite. Holt and Powers  
27   (CCA Appendix FAC, Section 8.9.3) principally attribute this to dissolution of Salado halite,  
28   noting the presence of sedimentologic features in the lower Rustler (see also Powers and Holt  
29   1999). Culebra hydrology and its significance to disposal system performance are discussed in  
30   detail in Section 2.2.1.4.1.2.

31   The Culebra was described by Robinson and Lang (1938, p. 83) as a dolomite 11 m (35 ft) in  
32   thickness. The Culebra is generally brown, finely crystalline, locally argillaceous and  
33   arenaceous dolomite with rare to abundant vugs with variable gypsum and anhydrite filling;  
34   Adams (1944, p. 1614) noted that oölites are present in some outcrops as well. Holt and Powers  
35   (CCA Appendix FAC, pp. 5 - 11) describe the Culebra features in detail, noting that most of the  
36   Culebra is microlaminated to thinly laminated, while some zones display no depositional fabric.  
37   Holt and Powers (1984) described an upper interval of the Culebra consisting of medium brown,  
38   microlaminated carbonate that thickens up to 0.6 m (2 ft) in the vicinity of dome structures and is  
39   of probable algal origin. This is underlain by a 0.64-to 2.54-cm (0.25-to-1-in) thick bed of  
40   cohesive black claystone. Because of the unique organic composition of this thin layer, Holt and  
41   Powers (1988) did not include it in the Culebra for thickness computations, and this will be

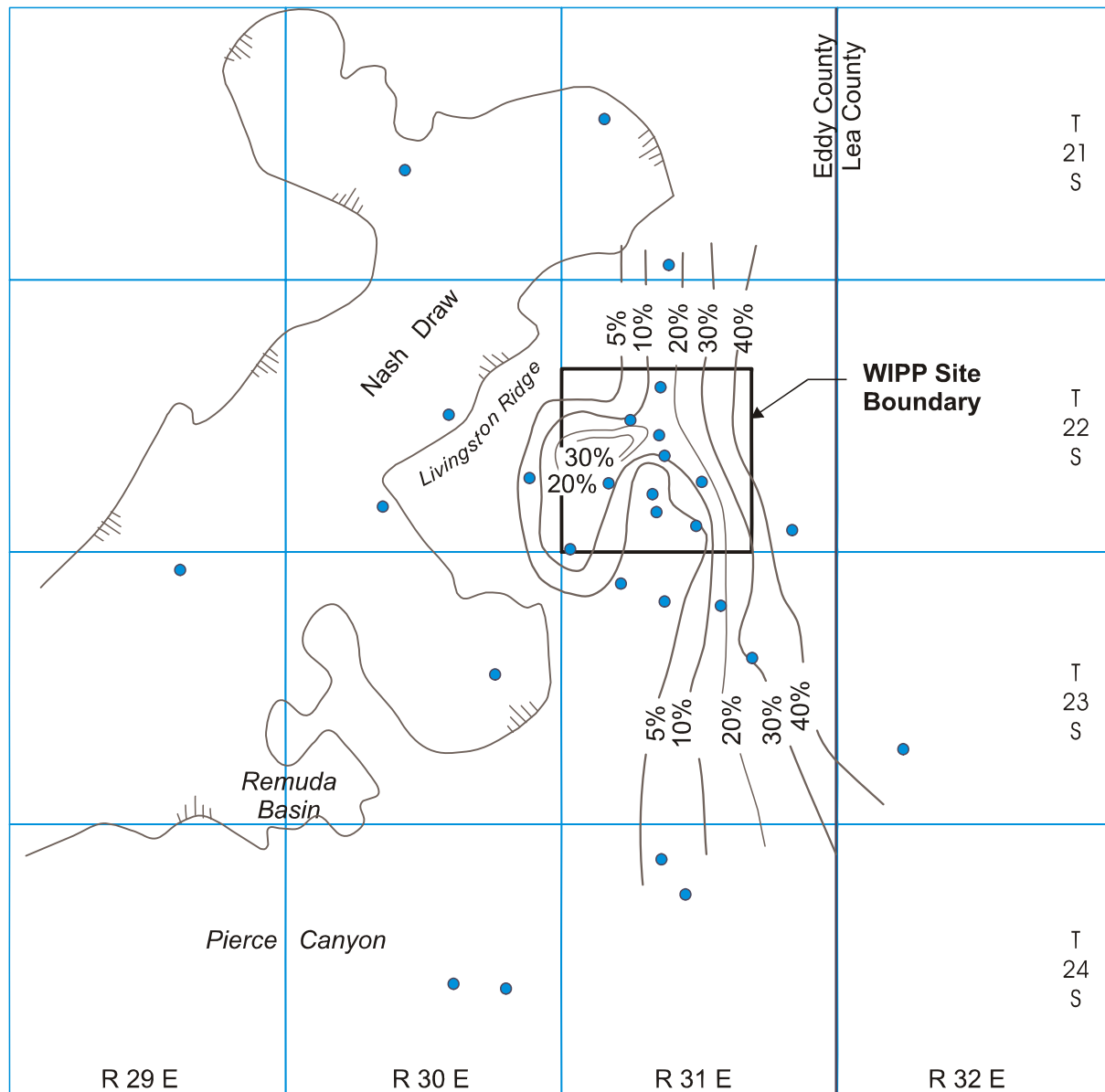
1 factored into discussions of Culebra thickness. Based on core descriptions from the WIPP  
2 project, Holt and Powers (CCA Appendix FAC) concluded that there is very little variation of  
3 depositional sedimentary features throughout the Culebra.

4 Vugs are an important part of Culebra porosity. They are commonly zoned parallel to bedding.  
5 In outcrop, vugs are commonly empty. In the subsurface, vugs range from open to partially  
6 filled or filled with anhydrite, gypsum, or clay (Holt and Powers 1990a, pp. 3-18 to 3-20).  
7 Lowenstein (1987, pp. 19 - 20) noted similar features. Holt and Powers (CCA Appendix FAC)  
8 attributed vugs partly to syndepositional growth as nodules and partly as later replacive textures.  
9 Lowenstein (1987, pp. 29 - 31) also described textures related to later replacement and alteration  
10 of sulfates. Vug or pore fillings vary across the WIPP site and contribute to the porosity  
11 structure of the Culebra. As pointed out by Holt and Powers (see CCA Appendix FAC, Section  
12 8.8), natural fractures filled with gypsum are common east of the WIPP site center and in a  
13 smaller area west of the site center (Figure 2-17). Section 2.1.5.2 discusses Culebra fracture  
14 mechanisms. Additional discussion of Culebra fractures and their role in groundwater flow and  
15 transport is in Section 2.2.1.4.1.1, Appendix PA, Attachment MASS, Sections MASS.14.4 and  
16 MASS.15.

17 Holt (1997) reexamined geological and hydrological data for the Culebra and developed a  
18 conceptual model for transport processes. In this document, Holt (1997) recognized several  
19 porosity types for the Culebra, and separated four Culebra units (CU) informally designated CU-  
20 1 through CU-4 from top to bottom. CU-1 differs from underlying units because it has been  
21 disrupted very little by syndepositional processes. Microvugs and interbeds provide most of the  
22 porosity, and the permeability of CU-1 is relatively limited. CU-2 and CU-3 likely contribute  
23 most of the flow in the Culebra, and the significant difference is that CU-2 includes more  
24 persistent silty dolomite interbeds. CU-2 and CU-3 include “small-scale bedding-plane  
25 fractures, networks of randomly oriented small-scale fractures and microfractures, discontinuous  
26 silty dolomite interbeds, large vugs hydraulically connected with microfractures and small-scale  
27 fractures, microvugs hydraulically connected with microfractures and intercrystalline porosity,  
28 blebs of silty dolomite interconnected with microfractures and intercrystalline porosity, and  
29 intercrystalline porosity” (Holt 1997, p. 2-19). Bedding-plane fractures dominate CU-4 at the  
30 base of the Culebra, and the unit shows some brittle deformation. CU-4 has not been isolated for  
31 hydraulic testing.

32 Holt (1997, p. I) also related porosity and solute transport, conceptualizing the medium “as  
33 consisting of advective porosity, where solutes are carried by the groundwater flow, and fracture-  
34 bounded zones of diffusive porosity, where solutes move through slow advection or diffusion.”  
35 Holt (1997) noted that length or time scales will govern how each porosity type will contribute to  
36 solute transport.

37 Swards et al. (1991, pp. IX-1) report that the Culebra is primarily dolomite with some quartz  
38 and clay. Clay minerals include corrensite, illite, serpentine, and chlorite. Clay occurs in bulk



● Boreholes Examined

Contour Interval = 10%

5% Line Shown for Clarity

1 Source: Beauheim and Holt (1990)

CCA-030-2

2 **Figure 2-17. Percentage of Natural Fractures in the Culebra Filled with Gypsum**

1 rock and on fracture surfaces. Even though these clays occur, the conceptual model discussed in  
 2 Section 6.4.6.2.1 takes no credit for their presence.

3 In the WIPP area, the Culebra varies in thickness. Depending on the area considered and the  
 4 horizons chosen for the upper and lower boundaries of the Culebra, different data sources  
 5 provide varying estimates (Table 2-3). Holt and Powers (CCA Appendix FAC, p. 4-4)  
 6 considered the organic-rich layer at the Culebra-Tamarisk contact separately from the Culebra in  
 7 interpreting geophysical logs.

8 Comparing data sets, Holt and Powers (CCA Appendix FAC) typically interpret the Culebra as  
 9 being about 1 m (about 3 ft) thinner than do other interpretations. In general, this reflects the  
 10 difference between including or excluding the unit at the Culebra-Tamarisk contact. The isopach  
 11 of the Culebra is shown as Figure 4.8 in CCA Appendix FAC.

12 LaVenue et al. (1988, Table B.1) calculated a mean thickness of 7.7 m (25 ft) for the Culebra  
 13 within their model domain based on thicknesses measured in 78 boreholes. Mercer (1983,  
 14 reproduced as CCA Appendix HYDRO) reported a data set similar to that of LaVenue et al. The  
 15 borehole database for the region of interest is provided in CCA Appendix BH.

16 The treatment of the Culebra in the conceptual model is discussed in Section 6.4.6.2 and  
 17 associated parameter values in Table 6-20. A more thorough discussion of Culebra features,  
 18 such as fractures, is provided in Appendix PA, Attachment MASS, Section MASS.15.

19 **Table 2-3. Culebra Thickness Data Sets**

Source	Data Set Location								
	T22S, R31E			T21-23S, R30-32E			Entire Set		
	n	ave	std dev	n	ave	std dev	n	ave	std dev
Richey (1989)	7	7.5 m	1.04 m	115	7.9 m	1.45 m	633	7.7 m	1.65 m
CCA Appendix FAC	35	6.4 m	0.59 m	122	7.0 m	1.26 m	508	6.5 m	1.89 m
LaVenue et al. (1988)							78	7.7 m	
Source	WIPP Potash Drillholes								
Jones (1978)				21	7.5 m	0.70 m			
CCA Appendix FAC				21	6.3 m	0.50 m			

Legend:

n number of boreholes or data points

ave average or mean

std dev standard deviation

m meters

20 2.1.3.5.3 The Tamarisk Member

21 Vine (1963, B14) named the Tamarisk for outcrops near Tamarisk Flat in Nash Draw. Outcrops  
 22 of the Tamarisk are distorted, and subsurface information was used to establish member

1 characteristics. Vine reported two sulfate units separated by a siltstone, about 1.5 m (5 ft) thick,  
2 interpreted by Jones et al. in 1960 as a dissolution residue.

3 The Tamarisk is generally conformable with the underlying Culebra. The transition is marked  
4 by an organic-rich unit interpreted as being present over most of southeastern New Mexico. The  
5 Tamarisk around the WIPP site consists of lower and upper sulfate units separated by a unit that  
6 varies from mudstone (generally to the west) to mainly halite (to the east). Near the center of the  
7 WIPP site, the lower anhydrite was partially eroded during deposition of the middle mudstone  
8 unit, as observed in the WIPP waste-handling and exhaust shafts. The lower anhydrite was  
9 completely eroded at WIPP-19. Before shaft exposures were available, the lack of the Lower  
10 Tamarisk anhydrite at WIPP-19 was interpreted as the result of dissolution and the mudstone was  
11 considered a cave filling.

12 Jones (1978) interprets halite to be present east of the center of the WIPP site based on  
13 geophysical logs and drill cuttings. Based mainly on cores and cuttings records from the WIPP  
14 potash drilling program, Snyder prepared a map showing the halitic areas of each of the  
15 noncarbonate members of the Rustler (Snyder 1985, Figure 4). A very similar map based on  
16 geophysical log characteristics was prepared by Holt and Powers (1988).

17 CCA Appendix FAC describes the mudstones and halitic facies in the middle of the Tamarisk  
18 and postulate that the unit formed in a salt-pan-to-mudflat system. Powers and Holt (2000) cited  
19 sedimentary features and the lateral relationships as evidence of syndepositional dissolution of  
20 halite in the marginal mudflat areas.

21 The Tamarisk thickness varies greatly in southeastern New Mexico, principally as a function of  
22 the thickness of halite in the middle unit. Within T22S, R31E, the thickness ranges from 26 to  
23 56 m (84 to 184 ft) for the entire Tamarisk and from 2 to 34 m (6 to 110 ft) for the interval of  
24 mudstone-halite between lower and upper anhydrites (CCA Appendix FAC, Figures 4-9 and 4-  
25 11). Expanded geophysical logs with corresponding lithology illustrate some of the lateral  
26 relationships for this interval (Figure 2-18; see also Powers and Holt 2000).

27 The Tamarisk is modeled as discussed in Section 6.4.6.3. Tamarisk parameter values are given  
28 in Appendix PA, Attachment PAR, Table PAR-24.

29 2.1.3.5.4 The Magenta Dolomite Member

30 Adams (1944, p. 1614) attributes the name Magenta Member to Lang, based on a feature named  
31 Magenta Point north of Laguna Grande de la Sal. According to CCA Appendix FAC the  
32 Magenta is a gypsumiferous dolomite with abundant primary sedimentary structures and well-  
33 developed algal features. It does not vary greatly in sedimentary features

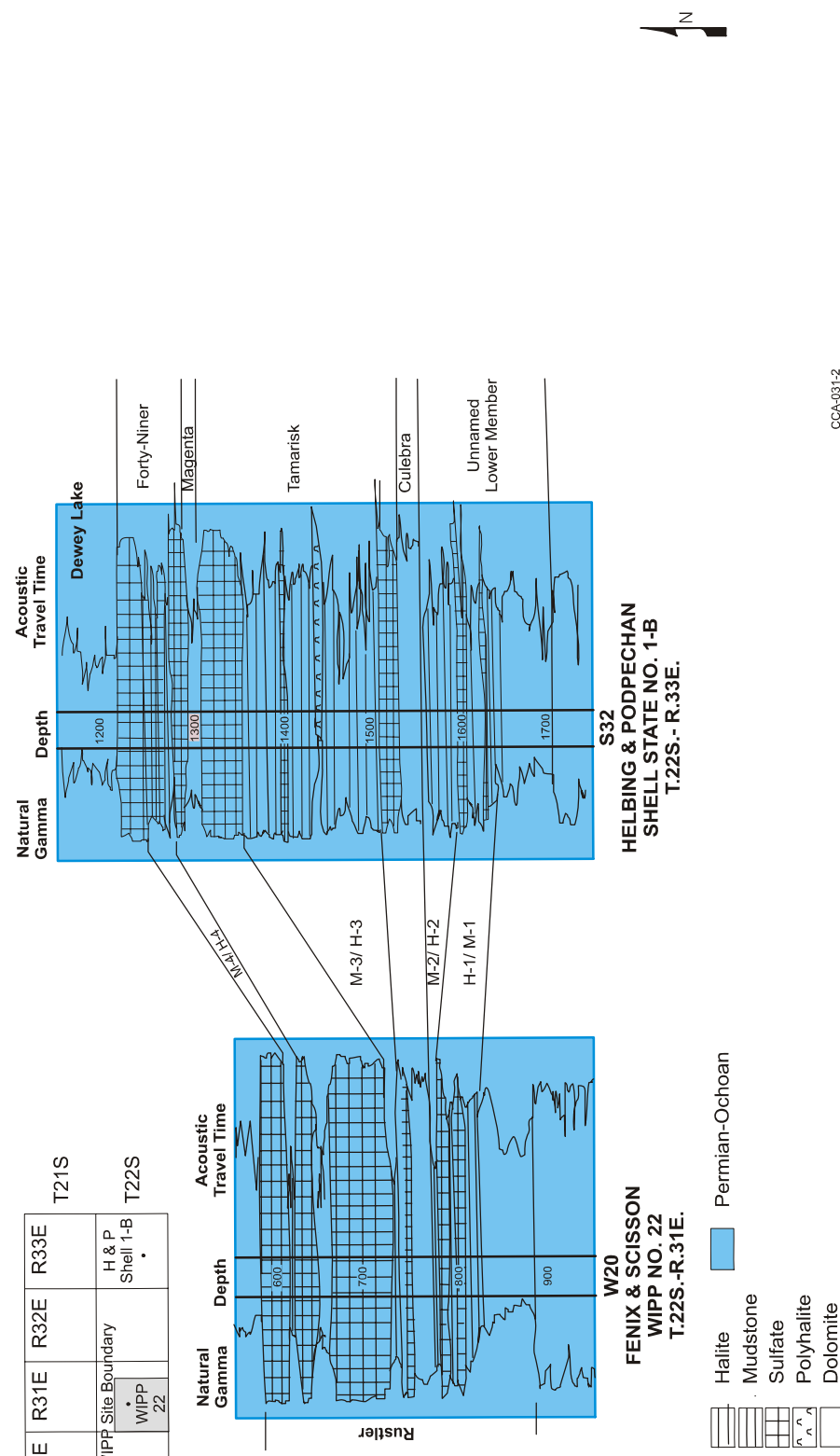


**Figure 2-18. Log Character of the Rustler Emphasizing Mudstone-Halite Lateral Relationships**

1 across the site area. CCA Appendix FAC, 5-22 reported that the Magenta varies from 7.0 to  
2 8.5 m (23 to 28 ft) around the WIPP site. CCA Appendix FAC did not include a regional  
3 Magenta isopach. Additional detail on the Magenta can be found in Section 4.3.2 of CCA  
4 Appendix GCR and in Sections 4.1.4, 4.2.4, and 5.4 of CCA Appendix FAC. The Magenta is  
5 included in the conceptual model as discussed in Section 6.4.6.4. Modeling values are in Table  
6 6-24.

7 **2.1.3.5.5 The Forty-niner Member**

8 Vine (1963) named the Forty-niner for outcrops at Forty-niner Ridge in eastern Nash Draw, but  
9 the unit is poorly exposed there. In the subsurface around the WIPP, the Forty-niner consists of  
10 basal and upper sulfates separated by a mudstone. It is conformable with the underlying  
11 Magenta. As with other members of the Rustler, geophysical log characteristics can be  
12 correlated with core and shaft descriptions to extend geological inferences across a large area  
13 (Holt and Powers 1988).

14 The Forty-niner varies from 13 to 23 m (43 to 77 ft) thick within T22S, R31E. East and  
15 southeast of the WIPP, the Forty-niner exceeds 24 m (80 ft), and some of the geophysical logs  
16 from this area indicate that halite is present in the beds between the sulfates. A regional isopach  
17 map of the Forty-niner is in CCA Appendix FAC (Figure 4-13). See also Powers and Holt  
18 (2000).

19 Within the waste-handling shaft, the Forty-niner mudstone displayed sedimentary features and  
20 bedding relationships indicating sedimentary transport. These beds are not known to have been  
21 described in detail prior to mapping in the waste-handling shaft at WIPP, and the features found  
22 there led Holt and Powers (CCA Appendix FAC) to reexamine the available evidence for, and  
23 interpretations of, dissolution of halite in Rustler units.

24 The inclusion of the Forty-niner in the conceptual model is discussed in Section 6.4.6.5.

25 **2.1.3.6 The Dewey Lake**

26 The nomenclature for rocks included in the Dewey Lake Formation was introduced during the  
27 1960s to clarify relationships between these rocks assigned to the Upper Permian and the  
28 Cenozoic Gatun Formation.

29 There are three main sources of data about the Dewey Lake in the area around WIPP. Miller  
30 reported the petrology of the unit in 1955 and 1966. Schiel (1988) described outcrops in the  
31 Nash Draw areas and interpreted geophysical logs of the unit in southeastern New Mexico and  
32 west Texas to infer the depositional environments and stratigraphic relationships in 1988 and  
33 1994. Holt and Powers (1990a) were able to describe the Dewey Lake in detail at the AIS for  
34 WIPP in 1990, confirming much of Schiel's (1988) information and adding data regarding the  
35 Lower Dewey Lake.

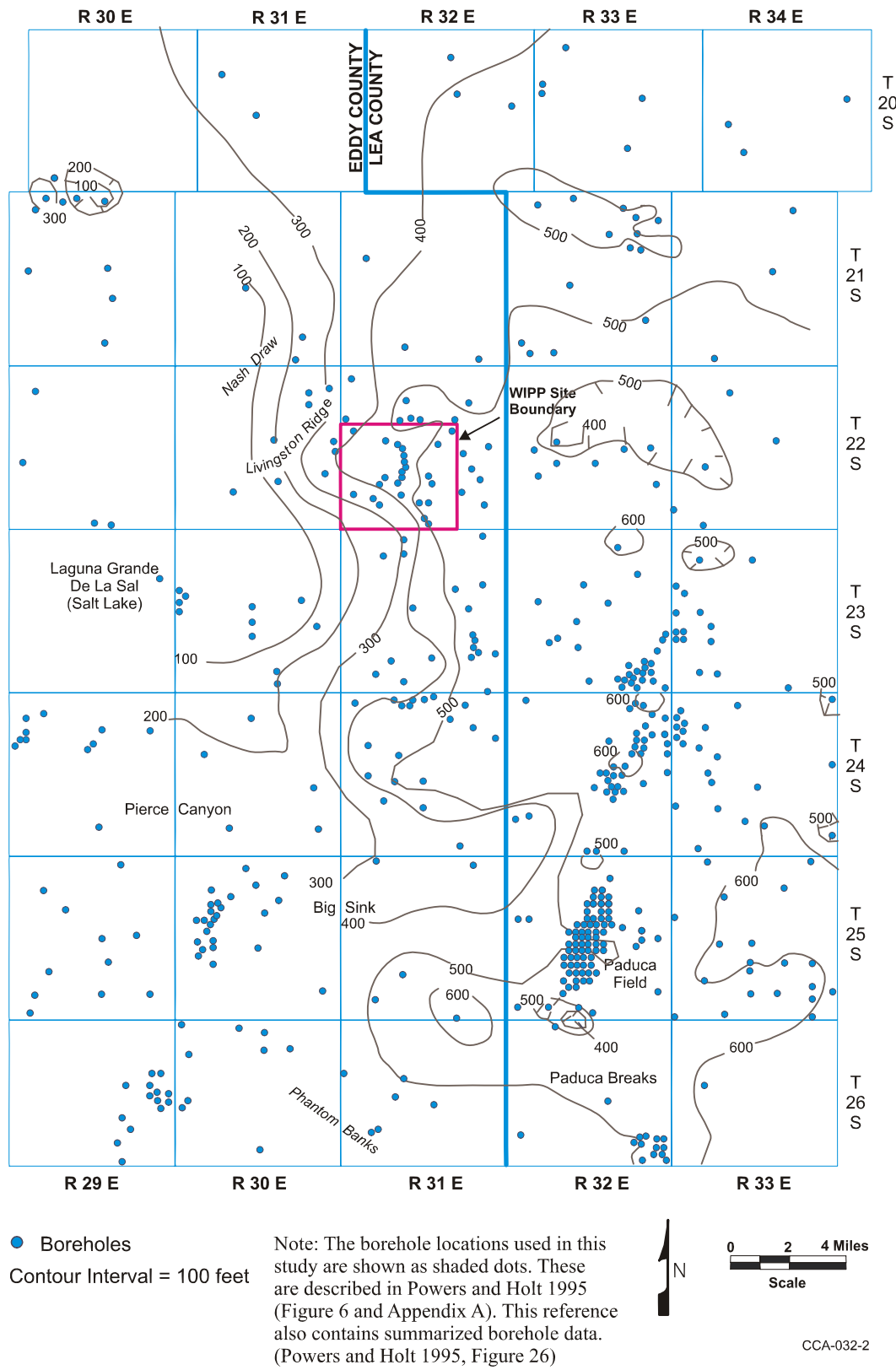
36 The Dewey Lake overlies the Rustler conformably, though local examples of the contact (for  
37 example, the AIS described by Holt and Powers (1990a) show minor disruption by dissolution of  
38 some of the upper Rustler sulfate. The formation is predominantly reddish-brown fine sandstone  
39 to siltstone or silty claystone with greenish-gray reduction spots. Thin bedding, ripple cross-

1 bedding, and larger channeling are common features in outcrops, and additional soft sediment  
2 deformation features and early fracturing from the lower part of the formation are described by  
3 Holt and Powers (1990a). Schiel (1988, p. 143; 1994, p. 9) attributed the Dewey Lake to  
4 deposition on “a large, arid fluvial plain subject to ephemeral flood events.”

5 There is no direct faunal or radiometric evidence of the age of the Dewey Lake in the vicinity of  
6 the WIPP site. It is assigned to the Ochoan Series, considered historically to be Late Permian in  
7 age, and it is regionally correlated with units of similar lithology and stratigraphic position.  
8 Schiel (1988, 1994) reviewed the limited radiometric data from lithologically similar rocks  
9 (Quartermaster Formation) and concluded that much of the unit could be Early Triassic in age.  
10 Renne et al. (1996) resampled tephra from the Quartermaster in the Texas panhandle area and  
11 found that radiometric data support the idea that the Quartermaster is mainly Triassic in age  
12 rather than Permian. Others have begun to infer as well that the Dewey Lake in the vicinity of  
13 the WIPP may be mostly Triassic (e.g., Powers and Holt 1999). These age relationships  
14 continue to be of academic interest because of the geologic significance of the Permo-Triassic  
15 boundary, but there is no significance for waste isolation at the WIPP.

16 Near the center of the WIPP site, Holt and Powers (1990a, Figure 5) mapped 152 m (498 ft) of  
17 the Dewey Lake (Figure 2-19). The formation is thicker to the east (Schiel 1994, Figure 2) of the  
18 WIPP site, in part because western areas were eroded before the overlying Triassic rocks were  
19 deposited.

20 The Dewey Lake contains fractures, which are filled with minerals to varying degrees. Both  
21 cements and fracture fillings have been examined and used to infer groundwater infiltration.  
22 Holt and Powers (1990a, pp. 3-10) described the Dewey Lake as cemented by carbonate above  
23 50 m (164.5 ft) in the AIS; some fractures in the lower part of this interval were also filled with  
24 carbonate, and the entire interval surface was commonly moist. Below this point, the cement is  
25 harder and more commonly anhydrite (Powers 2003b), the shaft is dry, and fractures are filled  
26 with gypsum. Powers (2002c; 2003b) reports core and geophysical log data supporting these  
27 vertical changes in natural mineral cements in the Dewey Lake over a larger region at a horizon  
28 that is believed to underlie known natural groundwater occurrences in the Dewey Lake. In areas  
29 where the Dewey Lake has been exposed to weathering after erosion of the overlying Santa  
30 Rosa, this cement boundary tends to generally parallel the eroded upper surface of the Dewey  
31 Lake, suggesting that weathering has affected the location of the boundary. Where the Dewey  
32 Lake has been protected by overlying rocks of the Santa Rosa, the cement change appears to be  
33 stratigraphically controlled but the data points are too few to be certain. Holt and Powers  
34 (1990a, pp. 3 - 11, Figure 16) suggested that the cement change might be related to infiltration of  
35 meteoric water. They also determined that some of the gypsum-filled fractures are  
36 syndepositional. Dewey Lake fractures include horizontal to subvertical trends, some of which  
37 were mapped in detail (Holt and Powers 1986, Figures 6, 7, and 8).



1

2

**Figure 2-19. Isopach of the Dewey Lake**

1   Lambert (1991, pp. 5 - 65) analyzed the deuterium/hydrogen (D/H) ratios of gypsum in the  
2   Rustler and gypsum veins in the Dewey Lake. He suggest that none of the gypsum formed from  
3   evaporitic fluid such as Permian seawater but that the D/H ratios all show influence of meteoric  
4   water. Furthermore, Lambert (1991, 5 – 66) infers that the gypsum D/H ratio is not consistent  
5   with modern meteoric water; it may, however, be consistent with older meteoric fluids. There is  
6   no obvious correlation with depth to indicate infiltration. Strontium isotope ratios ( $^{87}\text{Sr}/^{86}\text{Sr}$ )  
7   indicate no intermixing or homogenization of fluids between the Rustler and the Dewey Lake,  
8   but there may have been lateral movement of water within the Dewey Lake (Lambert 1991, pp.  
9   5 - 54). Dewey Lake carbonate-vein material shows a broader range of strontium ratios than  
10   does surface caliche, and the ratios barely overlap.

11   The treatment of the Dewey Lake in the conceptual model can be found in Section 6.4.6.6.  
12   Dewey Lake parameter values are in Table 6-25.

13   2.1.3.7 The Santa Rosa

14   There have been different approaches to the nomenclature of rocks of Triassic age in  
15   southeastern New Mexico. Bachman (1974) generally described the units as “Triassic,  
16   undivided” or as the Dockum Group, without dividing it. Vine (1963) used “Santa Rosa  
17   Sandstone,” and Santa Rosa has become common usage. Lucas and Anderson (1993a, 1993b)  
18   import other formation names that are unlikely to be useful for WIPP.

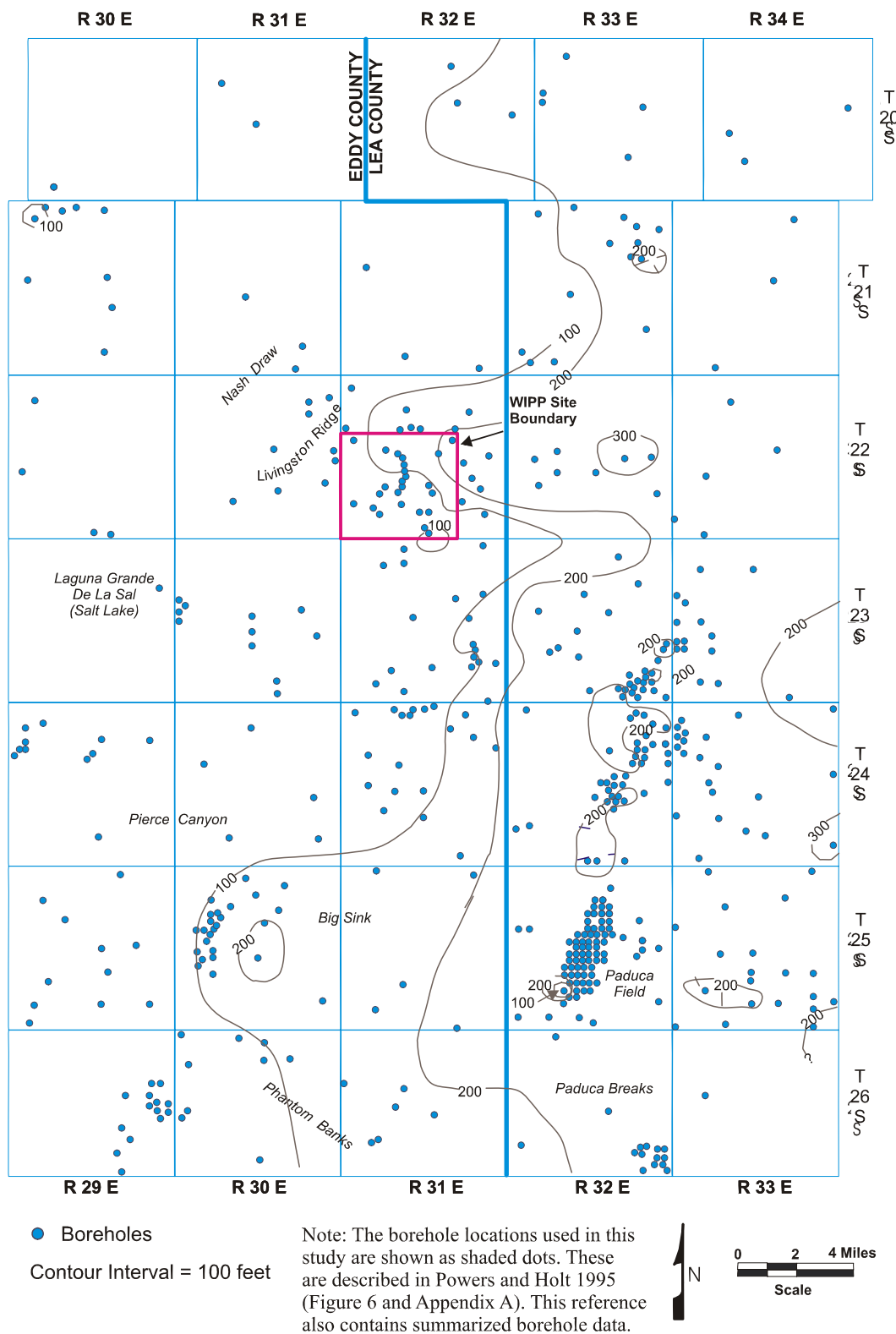
19   The Santa Rosa has been called disconformable over the Dewey Lake by Vine (1963, B25).  
20   These rocks have more variegated hues than the underlying uniformly colored Dewey Lake.  
21   Coarse-grained rocks, including conglomerates, are common, and the formation includes a  
22   variety of cross-bedding and sedimentary features (Lucas and Anderson 1993a, pp. 231 - 235).

23   Within the WIPP site boundary, the Santa Rosa is relatively thin to absent (Figure 2-20). At the  
24   AIS, Holt and Powers (1990a, Figure 5) attributed about 0.6 m (2 ft) of rock to the Santa Rosa.  
25   The Santa Rosa is a maximum of 78 m (255 ft) thick in potash holes drilled for WIPP east of the  
26   site boundary. The Santa Rosa is thicker to the east. The geologic data from design studies  
27   (Sargent et al. 1979) were incorporated with data from drilling to investigate shallow subsurface  
28   water in the Santa Rosa to provide structure and thickness maps of the Santa Rosa in the vicinity  
29   of the WIPP surface structures area (Powers 1997). These results are consistent with the broader  
30   regional distribution of the Santa Rosa.

31   The Santa Rosa and younger rocks are modeled in the WIPP PA as a single region as discussed  
32   in Section 6.4.6.7. The model parameters for this supra-Dewey Lake region are given in Table  
33   6-26.

34   2.1.3.8 The Gatuña

35   Lang (in Robinson and Lang 1938, p. 84) named the Gatuña for outcrops in the vicinity of  
36   Gatuña Canyon in the Clayton Basin. Rocks now attributed to the Gatuña in Pierce Canyon were  
37   once included in the Pierce Canyon Formation with rocks now assigned to the Dewey Lake. The  
38



1

2

**Figure 2-20. Isopach of the Santa Rosa**

1 formation has been mapped from the Santa Rosa, New Mexico, area south to the vicinity of  
2 Pecos, Texas. It is unconformable with underlying units.

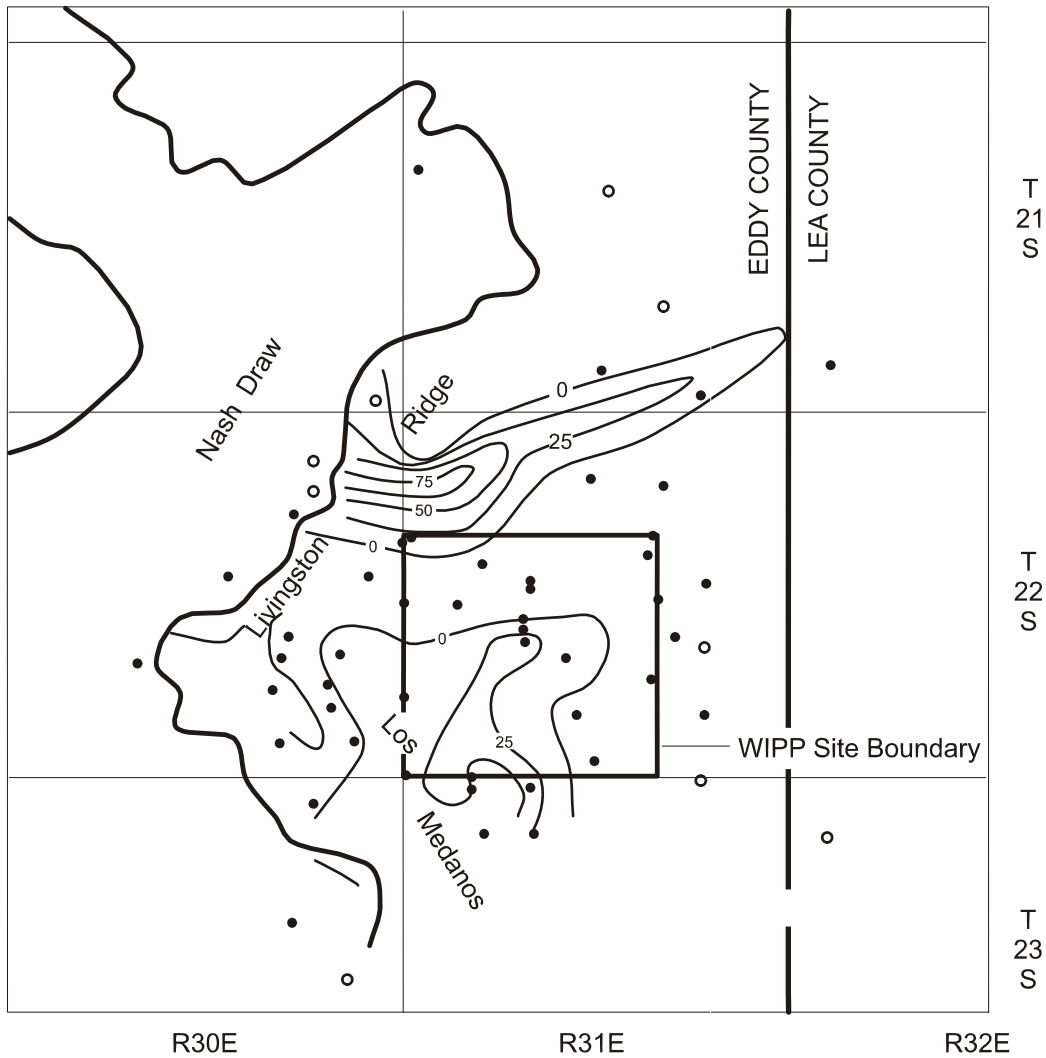
3 Vine (1963) and Bachman (1974) provided some limited description of the Gatuña. The most  
4 comprehensive study of the Gatuña is based on WIPP investigations and landfill studies for the  
5 City of Carlsbad and Eddy County (Powers and Holt 1993). Much of the formation is colored  
6 light reddish-brown. It is broadly similar to the Dewey Lake and the Santa Rosa, though the  
7 older units have more intense hues. The formation is highly variable, ranging from coarse  
8 conglomerates to claystones with some highly gypsiferous sections. Sedimentary structures are  
9 abundant. Analysis of lithofacies indicates that the formation is dominantly fluvial in origin with  
10 areas of low-energy deposits and evaporitic minerals.

11 The thickness of the Gatuña is not very consistent regionally, as shown in Figure 2-21. The  
12 thickness of the Gatuña ranges up to 91 m (300 ft) at Pierce Canyon, with thicker areas generally  
13 subparallel to the Pecos River. To the east, the Gatuña is thin or absent. Holt and Powers  
14 (1990a) reported about 2.7 m (9 ft) of undisturbed Gatuña in the AIS at WIPP. Powers (1997)  
15 integrated data from facility design geotechnical work (Sargent et al. 1979) and drilling to  
16 investigate shallow water to develop maps of the Gatuña in the vicinity of the WIPP surface  
17 facility. These maps are consistent with the broader regional view of the distribution of the  
18 Gatuña.

19 The Gatuña has been considered Pleistocene in age based on a volcanic glass in the Upper  
20 Gatuña along the eastern margin of Nash Draw that has been identified as the Lava Creek B ash,  
21 dated at 0.6 million years by Izett and Wilcox (1982). This upper-limit age is corroborated by  
22 the age determinations from the Mescalero caliche (hereafter referred to as the Mescalero) that  
23 overlies the Gatuña (see Section 2.1.3.9). An additional volcanic ash from the Gatuña in Texas  
24 yields consistent K-Ar and geochemical data, indicating that it is about 13 million years old at  
25 that location (Powers and Holt 1993, p. 271). Thus, the Gatuña ranges in age over a period of  
26 time that may be greater than that spanned by the Ogallala Formation (hereafter referred to as the  
27 Ogallala) on the High Plains east of WIPP.

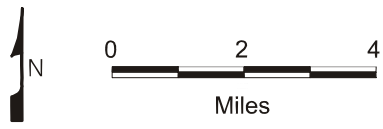
28   2.1.3.9 Mescalero Caliche

29 The Mescalero caliche is an informal stratigraphic unit apparently first differentiated by  
30 Bachman in 1974, though Bachman (1973, p. 17, p. 27) described the caliche on the Mescalero  
31 Plain. He differentiated the Mescalero from the older, widespread Ogallala caliche or caprock  
32 on the basis of textures, noting that breccia and pisolithic textures are much more common in the  
33 Ogallala caliche. The Mescalero has been noted over significant areas in the Pecos drainage,  
34 including the WIPP area, and it has been formed over a variety of substrates. Bachman (1973)  
35 described the Mescalero as a two-part unit: (1) an upper dense laminar caprock and (2) a basal,  
36 earthy-to-firm, nodular calcareous deposit. Machette (1985, p. 5) classified the Mescalero as  
37 having Stage V morphologies of a calcic soil (the more mature Ogallala caprock that occurs east  
38 of the WIPP site reaches Stage VI).



Modified from Mercer, J. W., 1983, Figure 1a

- Test Hole for Oil and Gas
  - Test Hole for Basic Data or Potash
- Contour Interval = 25 feet



CCA-071-2

1

## 2           **Figure 2-21. Isopach of the Gatuna**

3     Bachman (1976, Figure 8) provided structure contours on the Mescalero caliche for a large area  
4     of southeastern New Mexico, including the WIPP site. From the contours and Bachman's  
5     discussion of the Mescalero as a soil, it is clear that the Mescalero is expected to be continuous  
6     over large areas. Explicit WIPP data are limited mainly to boreholes, though some borehole  
7     reports do not mention the Mescalero. The unit may be as much as 3 m (10 ft) thick.

1 The Mescalero overlies the Gatuña and was interpreted by Bachman (1976) on basic  
2 stratigraphic grounds as having accumulated during the early-to-middle Pleistocene. Samples of  
3 the Mescalero from the vicinity of the WIPP were studied using uranium-trend methods.

4 Based on early written communication from Rosholt, Bachman (1985, p. 20) reports that the  
5 basal Mescalero began to form about 510,000 years ago and the upper part began to form about  
6 410,000 years ago; these ages are commonly cited in WIPP literature. The samples are  
7 interpreted by Rosholt and McKinney (1980, Table 5) in the formal report as indicating ages of  
8  $570,000 \pm 110,000$  years for the lower part of the Mescalero and  $420,000 \pm 60,000$  years for the  
9 upper part.

10 According to Bachman (1985, p. 19), where the Mescalero is flat-lying and not breached by  
11 erosion, it is an indicator of stability or integrity of the land surface over the last 500,000 years.  
12 An additional discussion of the Mescalero caliche can be found in CCA Appendix GCR, Section  
13 4.2.2.

14 2.1.3.10 Surficial Sediments

15 Soils of the region have developed mainly from Quaternary and Permian parent material. Parent  
16 material from the Quaternary System is represented by alluvial deposits of major streams, dune  
17 sand, and other surface deposits. These are mostly loamy and sandy sediments containing some  
18 coarse fragments. Parent material from the Permian System is represented by limestone,  
19 dolomite, and gypsum bedrock. Soils of the region have developed in a semiarid, continental  
20 climate with abundant sunshine, low relative humidity, erratic and low rainfall, and a wide  
21 variation in daily and seasonal temperatures. Subsoil colors are normally light brown to reddish  
22 brown but are often mixed with lime accumulations (caliche) that result from limited, erratic  
23 rainfall and insufficient leaching.

24 A soil association is a landscape with a distinctive pattern of soil types (series). It normally  
25 consists of one or more major soils and at least one minor soil. There are three soil associations  
26 within 8.3 km (5 mi) of the WIPP site: the Kermit-Berino, the Simona-Pajarito, and the Pyote-  
27 Maljamar-Kermit. Of these three associations, only the Kermit-Berino soil series has been  
28 mapped across the WIPP site by Chugg et al. (1952, Sheet No. 113). These are sandy soils  
29 developed on eolian material. The Kermit-Berino soils include active dune areas. The Berino  
30 soil has a sandy A horizon; the B horizons include more argillaceous material and weak-to-  
31 moderate soil structures. A and B horizons are described as noncalcareous, and the underlying C  
32 horizon is commonly caliche. Bachman (1980, p. 44) interpreted the Berino soil as a paleosol  
33 that is a remnant B horizon of the underlying Mescalero. Rosholt and McKinney (1980, Table 5)  
34 applied uranium-trend methods to samples of the Berino soil from the WIPP site area. Rosholt  
35 and McKinney (1980) interpreted the age of formation of the Berino soil as  $330,000 \pm 75,000$   
36 years.

37 Generally, the Berino Series, which covers about 50 percent of the site, consists of deep,  
38 noncalcareous, yellow-red to red sandy soils that developed from wind-worked material of  
39 mixed origin. These soils are described as undulating to hummocky and gently sloping (zero to  
40 three percent slopes). The soils are the most extensive of the deep, sandy soils in the Eddy  
41 County area. Berino soils are subject to continuing wind and water erosion. If the vegetative

1 cover is seriously depleted, the water-erosion potential is slight, but the wind-erosion potential is  
2 very high. These soils are particularly sensitive to wind erosion in the months of March, April,  
3 and May, when rainfall is minimal and winds are highest. These soil characteristics are a  
4 consideration for the design of long-term passive controls such as monuments and markers (see  
5 CCA Appendix PIC, Section III).

6 The Kermit Series consists of deep, light-colored, noncalcareous, excessively drained loose  
7 sands, typically yellowish-red fine sand. The surface is undulating to billowy (from 0 to  
8 3 percent slopes) and consists mostly of stabilized sand dunes. Kermit soils are slightly to  
9 moderately eroded. Permeability is very high, and, if vegetative cover is removed, the water-  
10 erosion potential is slight, but the wind-erosion potential is very high.

11 Surface soils appear to play a role in the infiltration of precipitation. Mercer (CCA Appendix  
12 HYDRO) points out that where surface deposits are thickest, they may contain localized perched  
13 zones of groundwater. A more thorough discussion of this topic can be found in CCA Appendix  
14 HYDRO.

15 **2.1.3.11 Summary**

16 The stratigraphy and lithology at the WIPP site has been summarized from the lowermost pre-  
17 Cambrian units to the surface soils. While these are important for an understanding of the site  
18 and its stability, not all of these units are important to the performance of the disposal system.  
19 As a result, the DOE has developed a conceptual model that describes the lithology as 13  
20 discrete model regions ranging from the Castile to a region that generally includes units above  
21 the Dewey Lake. In this model, emphasis is placed on the Castile, the Salado, the five members  
22 of the Rustler, the Dewey Lake, and the supra-Dewey Lake units. The Salado is divided into five  
23 stratigraphic units to capture the variations in properties near the horizon of the repository (see  
24 Figure 6-14). The identification and definition of the appropriate modeling units is based on the  
25 identification of FEPs that can impact the performance of the disposal system. Details of the  
26 conceptual model can be found in Section 6.4.2.

27 **2.1.4 *Physiography and Geomorphology***

28 In this section, the DOE presents a discussion of the physiography and geomorphology of the  
29 WIPP site and surrounding area. This information is taken from DOE 1980 (pp. 7-21 to 7-23).  
30 Geomorphology and physiography are determined by the DOE (1980) to be features that are  
31 potentially important to disposal system performance. They are included in the consequence  
32 analysis through consideration of the topography and its influence on the regional water table.  
33 (See discussion of regional water table characteristics in Section 2.2.1.) Consequently,  
34 topographic information is presented in this section. In addition, several geomorphological  
35 processes have been screened out on the basis of either low consequence or low probability, as  
36 discussed in Appendix PA, Attachment SCR. These include weathering, erosion, sedimentation,  
37 and soil development. Information is presented in this section to support this screening. In order  
38 to perform this screening, such factors as slopes, proximity to watercourses, dissection, and  
39 historic and existing processes are important. These are presented in this section in terms of the  
40 regional and local physiographic and geomorphological characteristics. Tectonic processes that  
41 may alter the physiography of the region or site area are discussed in Section 2.1.5. In addition,

1   Section 2.1.6 presents more specific details on nontectonic processes identified during site  
2   characterization as having the potential for affecting the repository over the longer term and as  
3   requiring detailed investigation. These include halite deformation and dissolution.

4   2.1.4.1 Regional Physiography and Geomorphology

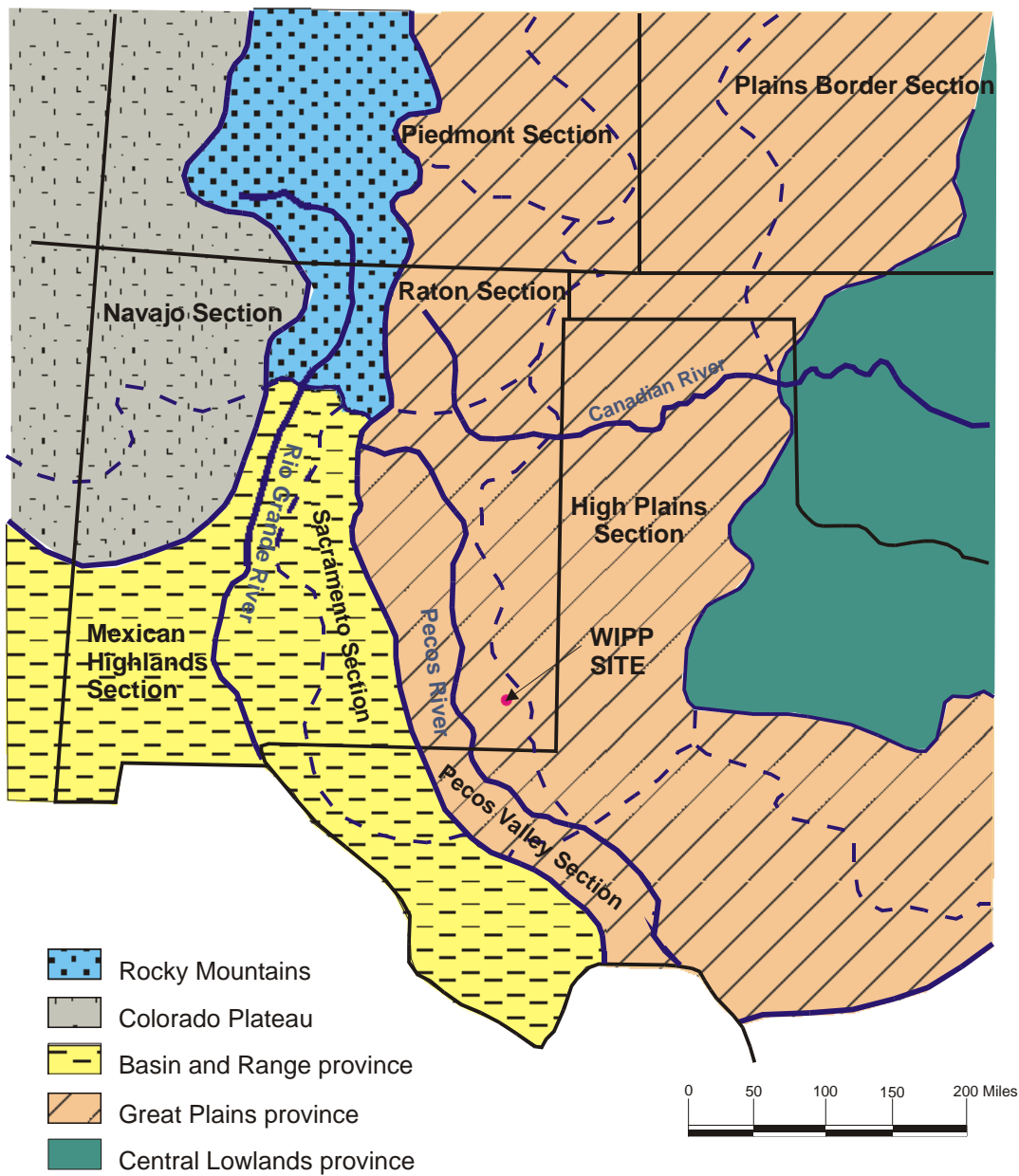
5   The WIPP site is in the Pecos Valley section of the southern Great Plains physiographic province  
6   (Figure 2-22), a broad, highland belt sloping gently eastward from the Rocky Mountains and the  
7   Basin and Range Province to the Central Lowlands Province. The Pecos Valley section itself is  
8   dominated by the Pecos River Valley, a long north-south trough that is from 8.3 to 50 km (5 to  
9   30 mi) wide and as much as 305 m (1,000 ft) deep in the north. The Pecos River System has  
10   evolved from the south, cutting headward through the Ogallala sediments and becoming  
11   entrenched some time after the Middle Pleistocene. It receives almost all the surface and  
12   subsurface drainage of the region; most of its tributaries are intermittent because of the semiarid  
13   climate. The surface locally has a karst terrain containing sinkholes, dolines, and solution-  
14   subsidence troughs from both surface erosion and subsurface dissolution. The valley has an  
15   uneven rock- and alluvium-covered floor with widespread solution-subsidence features, the  
16   result of dissolution in the underlying Upper Permian rocks. The terrain varies from plains and  
17   lowlands to rugged canyonlands, and contains such erosional features as scarps, cuestas, terraces,  
18   and mesas. The surface slopes gently eastward, reflecting the underlying rock strata. Elevations  
19   vary from more than 1,829 m (6,000 ft) in the northwest to about 610 m (2,000 ft) in the south.

20   The Pecos Valley section is bordered on the east by the virtually uneroded plain of the Llano  
21   Estacado. The Llano Estacado is part of the High Plains section of the Great Plains  
22   physiographic province and is a poorly drained eastward-sloping surface covered by gravels,  
23   wind-blown sand, and caliche that has developed since early-to-middle Pleistocene time. Few  
24   and minor topographic features are present in the High Plains section, formed when more than  
25   152 m (500 ft) of Tertiary silts, gravels, and sands were laid down in alluvial fans by streams  
26   draining the Rocky Mountains. In many areas, the nearly flat surface is cemented by a hard  
27   caliche layer.

28   To the west of the Pecos Valley section are the Sacramento Mountains and the Guadalupe  
29   Mountains, part of the Sacramento section of the Basin and Range Province. The Capitan  
30   escarpment along the southeastern side of the Guadalupe Mountains marks the boundary  
31   between the Basin and Range and the Great Plains provinces. The Sacramento section has large  
32   basinal areas and a series of intervening mountain ranges (DOE 1980).

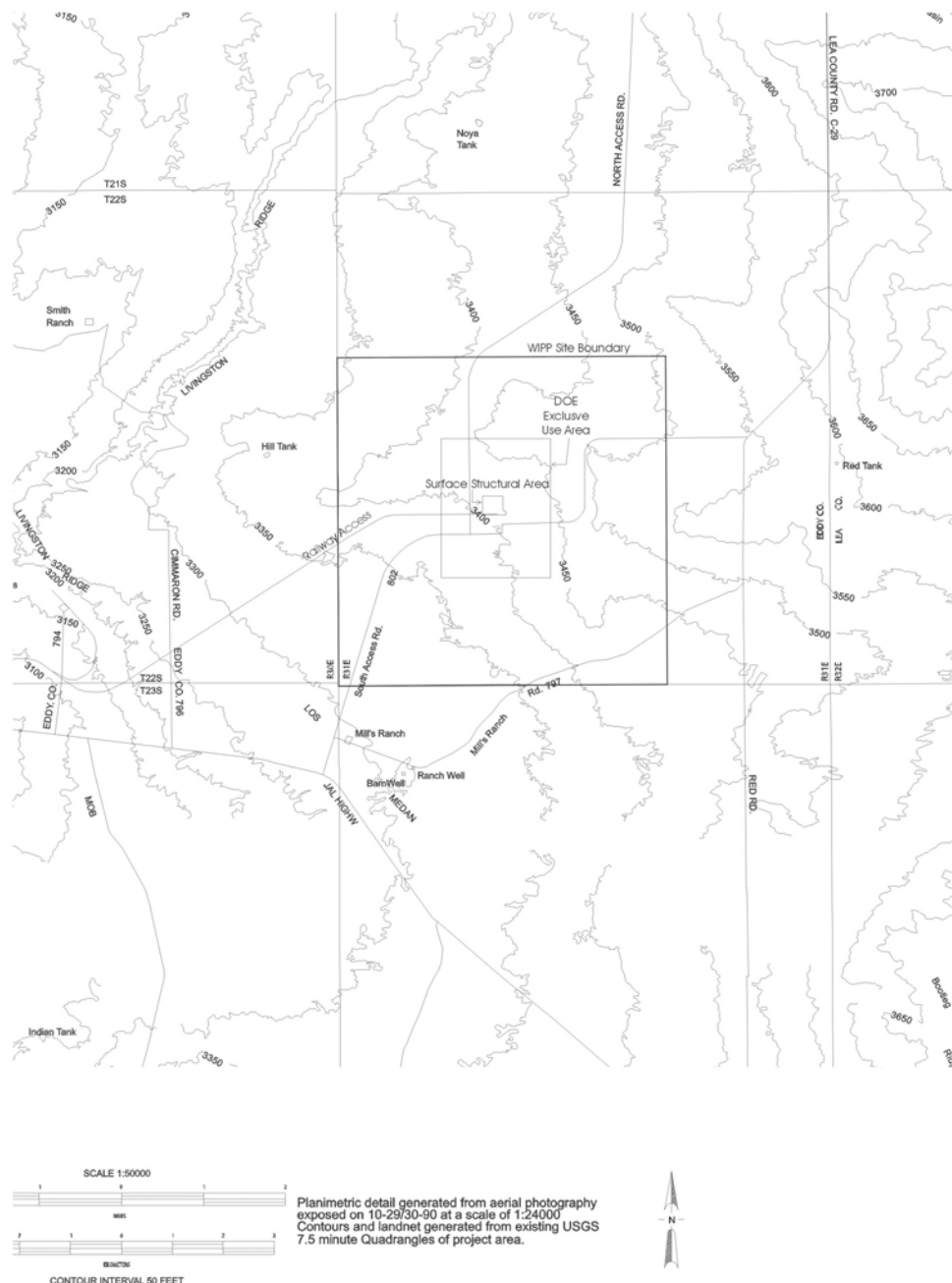
33   2.1.4.2 Site Physiography and Geomorphology

34   The land surface in the area of the WIPP site is a semiarid, wind-blown plain sloping gently to  
35   the west and southwest, and is hummocky with sand ridges and dunes. A hard caliche layer  
36   (Mescalero rocks) is typically present beneath the sand blanket and on the surface of the  
37   underlying Gatuña. Figure 2-23 is a topographic map of the area. Elevations at the site range  
38   from 1,088 m (3,570 ft) in the east to 990 m (3,250 ft) in the west. The average east-to-west  
39   slope is 9.4 m per kilometer (50 ft/mi).



1  
2

**Figure 2-22. Physiographic Provinces and Sections**



1

2 **Figure 2-23 Topographic Map of the Area Around the WIPP Site**

1 Livingston Ridge is the most prominent physiographic feature near the site. It is a west-facing  
2 escarpment that has about 23 m (75 ft) of topographic relief and marks the eastern edge of Nash  
3 Draw, the drainage course nearest to the site (see Figure 2-23). Nash Draw is a shallow 8-km-wide  
4 (5-mi-wide) basin, 61 to 91 m (200 to 300 ft) deep and open to the southwest. It was  
5 caused, at least in part, by subsurface dissolution and the accompanying subsidence of overlying  
6 sediments. Livingston Ridge is the approximate boundary between terrain that has undergone  
7 erosion and/or solution collapse to the west and terrain that has been little affected to the east.

8 About 24 km (15 mi) east of the site is the southeast-trending San Simon Swale, a depression  
9 caused, at least in part, by subsurface dissolution. Between San Simon Swale and the site is a  
10 broad, low mesa named the Divide. Lying about 9.7 km (6 mi) east of the site and about 30 m  
11 (100 ft) above the surrounding terrain, it is a boundary between southwest drainage toward Nash  
12 Draw and southeast drainage toward San Simon Swale. The Divide is capped by the Ogallala  
13 and the overlying caliche, upon which have formed small, elongated depressions similar to those  
14 in the adjacent High Plains section to the east.

15 Surface drainage is intermittent; the nearest perennial stream is the Pecos River, 19 km (12 mi)  
16 southwest of the WIPP site boundary. The site's location near a natural divide protects it from  
17 flooding and serious erosion caused by heavy runoff. Should the climate become more humid,  
18 any perennial streams should follow the present basins, and Nash Draw and San Simon Swale  
19 would be the most eroded, leaving the area of the Divide relatively intact.

## 20 **2.1.5 Tectonic Setting and Site Structural Features**

21 The DOE has screened out, on the basis of either probability or consequence or both, all tectonic,  
22 magmatic, and structural related processes. The screening discussions can be found in Appendix  
23 PA, Attachment SCR. The information needed for this screening is included here and covers  
24 regional tectonic processes such as subsidence and uplift and basin tilting, magmatic processes  
25 such as igneous intrusion and events such as volcanism, and structural processes such as faulting  
26 and loading and unloading of the rocks because of long-term sedimentation or erosion.  
27 Discussions of structural events, such as earthquakes, are considered to the extent that they may  
28 create new faults or activate old faults. The seismicity of the area is considered in Section 2.6 for  
29 the purposes of determining seismic design parameters for the facility.

### 30 **2.1.5.1 Tectonics**

31 The processes and features included in this section are those more traditionally considered part of  
32 tectonics, processes that develop the broad-scale features of the earth. Salt dissolution is a  
33 different process that can develop some features resembling those of tectonics.

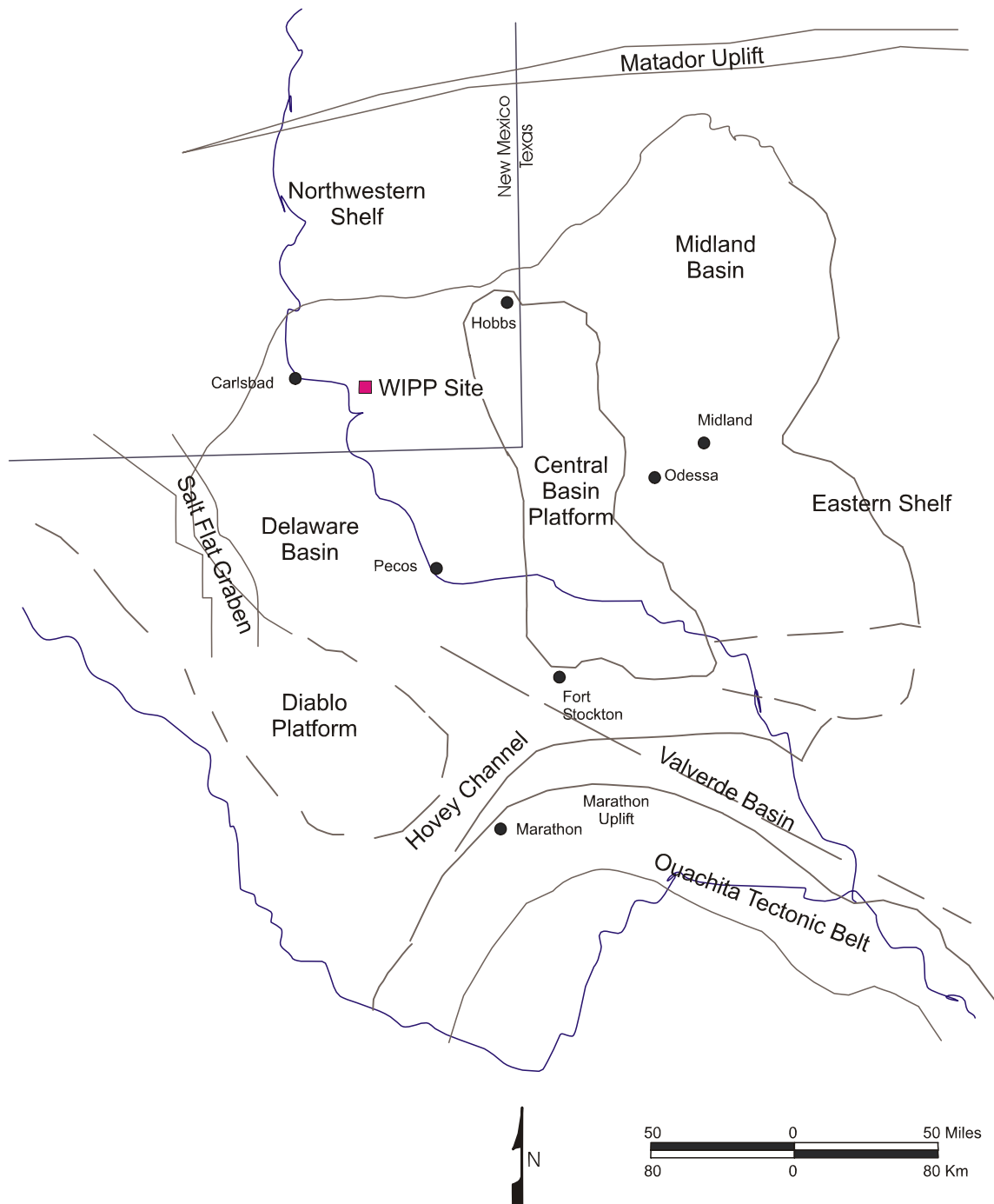
34 Most broad-scale structural elements of the area around the WIPP developed during the Late  
35 Paleozoic (CCA Appendix GCR, pp. 3-58 to 3-77). There is little historical or geological  
36 evidence of significant tectonic activity in the vicinity, and the level of stress in the region is low.  
37 The entire region tilted slightly during the Tertiary, and activity related to Basin and Range  
38 tectonics formed major structures southwest of the area. Seismic activity is specifically  
39 addressed in a separate section.

1 Broad subsidence began in the area as early as the Ordovician, developing a sag called the  
2 Tobosa Basin. By Late Pennsylvanian to Early Permian time, the Central Basin Platform  
3 developed (Figure 2-24), separating the Tobosa Basin into two parts: the Delaware Basin to the  
4 west and the Midland Basin to the east. The Permian Basin refers to the collective set of  
5 depositional basins in the area during the Permian Period. Southwest of the Delaware Basin, the  
6 Diablo Platform began developing either in the Late Pennsylvanian or Early Permian. The  
7 Marathon Uplift and Ouachita tectonic belt limited the southern extent of the Delaware Basin.

8 According to Brokaw et al. (1972, p. 30), pre-Ochoan sedimentary rocks in the Delaware Basin  
9 show evidence of gentle downwarping during deposition, while Ochoan and younger rocks do  
10 not. A relatively uniform eastward tilt, generally from about 14 to 19 m/per km (75 to  
11 100 ft/mi), has been superimposed on the sedimentary sequence.<sup>1</sup> King (1948, pp. 108 and 121)  
12 generally attributes the uplift of the Guadalupe and Delaware mountains along the west side of  
13 the Delaware Basin to the later Cenozoic, though he also notes that some faults along the west  
14 margin of the Guadalupe Mountains have displaced Quaternary gravels.

---

<sup>1</sup> Local dip of the Salado has been determined by mapping in the WIPP underground excavations. This dip is modeled as one degree to the south, as discussed in Section 6.4.2.1.



CCA-036-2

1

2

**Figure 2-24. Structural Provinces of the Permian Basin Region**

- 1 King (1948, p. 144) also infers the uplift from the Pliocene-age deposits of the Llano Estacado.  
2 Subsequent studies of the Ogallala of the Llano Estacado show that it varies in age from  
3 Miocene (about 12 million years before present) to Pliocene (Hawley 1993). This is the most  
4 likely range for uplift of the Guadalupe Mountains and broad tilting to the east of the Delaware  
5 Basin sequence.
- 6 Analysis of the present regional stress field indicates that the Delaware Basin lies within the  
7 Southern Great Plains stress province. This province is a transition zone between the extensional  
8 stress regime to the west and the region of compressive stress to the east. An interpretation by  
9 Zoback and Zoback (1991, p. 350) of the available data indicates that the level of stress in the  
10 Southern Great Plains stress province is low. Changes to the tectonic setting, such as the  
11 development of subduction zones and a consequent change in the driving forces, would take  
12 much longer than 10,000 years to occur.
- 13 To the west of the Southern Great Plains province is the Basin and Range province, or  
14 Cordilleran Extension province, where according to Zoback and Zoback (1991, pp. 348 - 351),  
15 normal faulting is the characteristic style of deformation. The eastern boundary of the Basin and  
16 Range province is marked by the Rio Grande Rift. Sanford et al. (1991, p. 230) note that, as a  
17 geological structure, the rift extends beyond the relatively narrow geomorphological feature seen  
18 at the surface, with a magnetic anomaly at least 500 km (300 mi) wide. On this basis, the Rio  
19 Grande Rift can be regarded as a system of axial grabens along a major north-south trending  
20 structural uplift (a continuation of the Southern Rocky Mountains). The magnetic anomaly  
21 extends beneath the Southern Great Plains stress province, and regional-scale uplift of about  
22 1,000 m (3,300 ft) over the past 10 million years also extends into eastern New Mexico.
- 23 To the east of the Southern Great Plains province is the large Mid-Plate province that  
24 encompasses central and eastern regions of the conterminous United States and the Atlantic  
25 basin west of the Mid-Atlantic Ridge. The Mid-Plate province is characterized by low levels of  
26 paleo- and historic seismicity. Where Quaternary faulting has occurred, it is generally strike-slip  
27 and appears to be associated with the reactivation of older structural elements.
- 28 Zoback et al. (1991) report no stress measurements from the Delaware Basin. The stress field in  
29 the Southern Great Plains stress province has been defined from borehole measurements in west  
30 Texas and from volcanic lineaments in northern New Mexico. These measurements were  
31 interpreted by Zoback and Zoback (1991, p. 353) to indicate that the least principal horizontal  
32 stress is oriented north-northeast and south-southwest and that most of the province is  
33 characterized by an extensional stress regime.
- 34 There is an abrupt change between the orientation of the least principal horizontal stress in the  
35 Southern Great Plains and the west-northwest orientation of the least principal horizontal stress  
36 characteristic of the Rio Grande Rift. In addition to the geological indications of a transition  
37 zone as described above, Zoback and Zoback (1980, p. 6134) point out that there is also evidence  
38 for a sharp boundary between these two provinces. This is reinforced by the change in crustal  
39 thickness from about 40 km (24 mi) beneath the Colorado Plateau to about 50 km (30 mi) or  
40 more beneath the Southern Great Plains east of the Rio Grande Rift. The base of the crust within  
41 the Rio Grande Rift is poorly defined but is shallower than that of the Colorado Plateau  
42 (Thompson and Zoback 1979, p. 152). There is also markedly lower heat flow in the Southern

1 Great Plains (typically  $< 60 \text{ mWm}^{-2}$ ) reported by Blackwell et al. (1991, p. 428) compared with  
2 that in the Rio Grande Rift (typically  $> 80 \text{ mWm}^{-2}$ ) reported by Reiter et al. (1991, p. 463).

3 On the eastern boundary of the Southern Great Plains province, there is only a small rotation in  
4 the direction of the least principal horizontal stress. There is, however, a change from an  
5 extensional, normal faulting regime to a compressive, strike-slip faulting regime in the Mid-Plate  
6 province. According to Zoback and Zoback (1980, p. 6134), the available data indicate that this  
7 change is not abrupt and that the Southern Great Plains province can be viewed as a marginal  
8 part of the Mid-Plate province.

9 **2.1.5.2 Loading and Unloading**

10 Loading and unloading during the geological history since deposition is considered an influence  
11 on the hydrology of the Permian units because of its possible effect on the development of  
12 fractures.

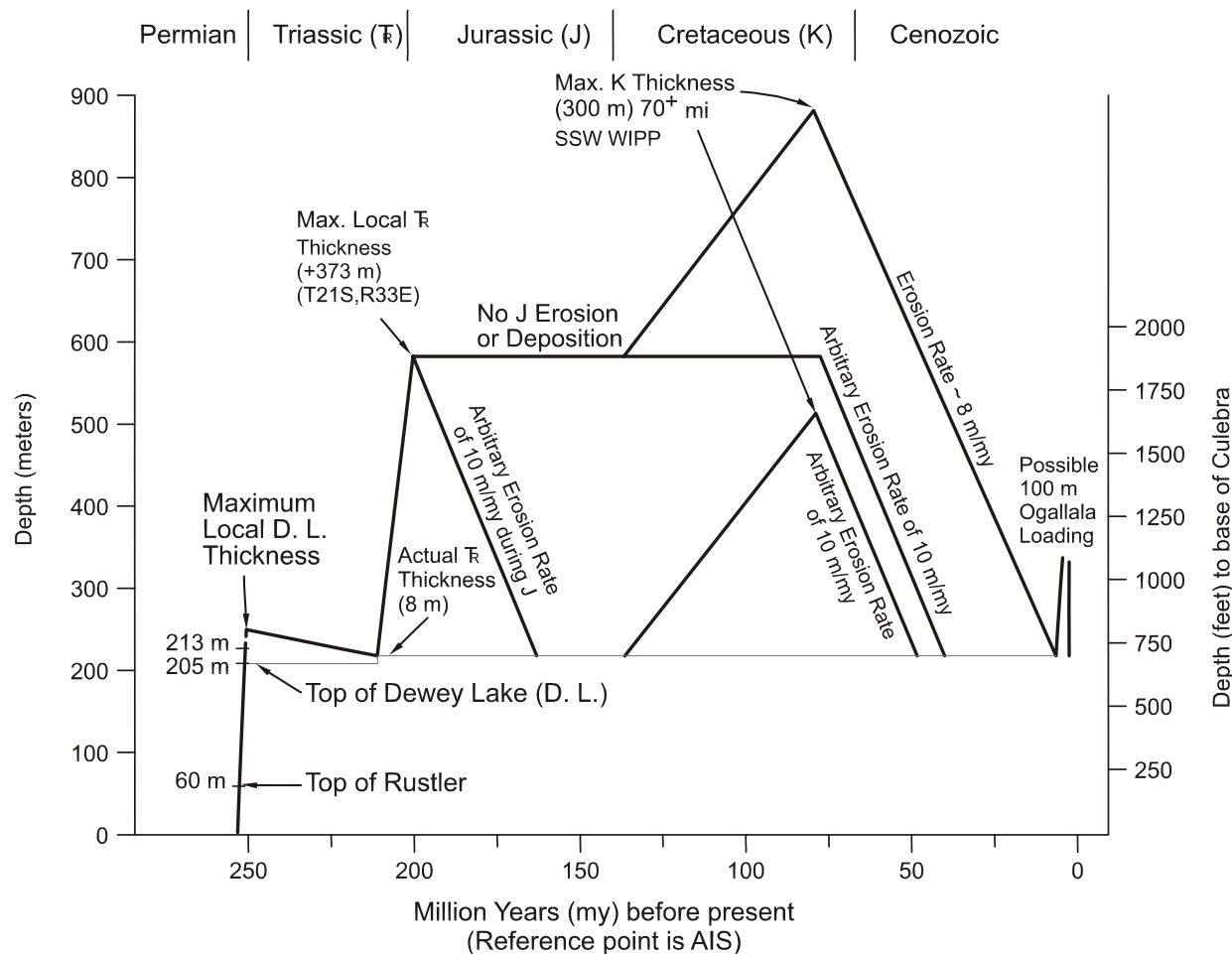
13 The sedimentary loading, depth of total burial, and erosion events combine in a complex history  
14 reconstructed here from regional geological trends and local data. The history is presented in  
15 Figure 2-25 with several alternatives, depending on the inferences that are drawn, ranging from  
16 minimal to upper-bound estimates (Powers and Holt 1995, Section 5.3). Borns (1987) also made  
17 a generalized estimate of loading that is similar. The estimates are made with a reference point  
18 and depth to the Culebra at the AIS.

19 Given the maximum local thickness of the Dewey Lake, the maximum load at the end of the  
20 Permian was no more than approximately 240 m (787 ft). Given the present depth to the Culebra  
21 from the top of the Dewey Lake in the AIS, approximately 35 m (115 ft) of Dewey Lake might  
22 have been eroded during the Early Triassic before additional sediments were deposited. The  
23 Triassic thickness at the AIS is approximately 8 m (26 ft). Northeast of the WIPP site (T21S,  
24 R33E), Triassic rocks (Dockum Group) have a maximum local thickness of approximately  
25 373 m (1,233 ft). This thickness is a reasonable estimate of the maximum thickness also attained  
26 at the WIPP site prior to the Jurassic Period. At the end of the Triassic, the total thickness at the  
27 WIPP site may have then attained approximately 586 m (1,863 ft) in two similar loading stages  
28 of a few million years each, over a period of approximately 50 million years.

29 The Jurassic outcrops nearest to the WIPP site are in the Malone Mountains of west Texas.  
30 There is no evidence that Jurassic rocks were deposited at or in the vicinity of the WIPP site.

31 As a consequence, the Jurassic is considered a time of erosion or nondeposition at the site,  
32 though erosion is most likely.

33 Widespread erosion during the Jurassic obviously cannot be broadly inferred for the area or there  
34 would not be thick Triassic rocks still preserved. Triassic rocks of this thickness are preserved  
35 nearby, indicating either pre-Jurassic tilting or that erosion did not occur until later (but still after  
36 tilting to preserve the Triassic rocks near the WIPP site). It is also possible that the immediate  
37 site area had little Triassic deposition or erosion, but very limited Triassic deposition (that is, 8 m  
38 [26 ft]) at the WIPP site seems unlikely.



Note: The estimates are made with a reference point and depth to the base of the Culebra at the AIS. Source: Powers and Holt 1995, Figure 34.

CCA-037-2

1

## 2      Figure 2-25. Loading and Unloading History Estimated to the Base of the Culebra

3 Lang (1947) reported fossils from Lower Cretaceous rocks in the Black River Valley southwest  
 4 of the WIPP site. Bachman (1980, p. 28) also reported similar patches of probable Cretaceous  
 5 rocks near Carlsbad and south of White's City. From these reports, it is likely that some  
 6 Cretaceous rocks were deposited at the WIPP site. Approximately 110 km (70 mi) south-  
 7 southwest of the WIPP site, significant Cretaceous outcrops of both Early and Late Cretaceous  
 8 age have a total maximum thickness of approximately 300 m (1,000 ft). Southeast of the WIPP,  
 9 the nearest Cretaceous outcrops are thinner and represent only the Lower Cretaceous. Based on  
 10 outcrops, a maximum thickness of 300 m (1,000 ft) of Cretaceous rocks could be estimated for  
 11 the WIPP site. Compared to the estimate of Triassic rock thickness, it is less likely that  
 12 Cretaceous rocks were this thick at the site. The uppermost lines of Figure 2-25 summarize the  
 13 assumptions of maximum thickness of these units.

1 A more likely alternative is that virtually no Cretaceous rocks were deposited, followed by  
2 erosion of remaining Triassic rocks during the Late Cretaceous to the Late Cenozoic. Such  
3 erosion may also have taken place over an even longer period, beginning with the Jurassic  
4 Period. Ewing (1993) favors Early Cretaceous uplift and erosion for the Trans-Pecos Texas area,  
5 but does not analyze later uplift and erosional patterns.

6 In the general vicinity of the WIPP site, there are outcrops of Cenozoic rock from the Late  
7 Miocene (Gatuña and Ogallala Formations). There is little reason to infer any significant Early  
8 Cenozoic sediment accumulation at the WIPP site. Erosion is the main process inferred to have  
9 occurred during this period and an average erosion rate of approximately 10 m (33 ft) per million  
10 years is sufficient during the Cenozoic to erode the maximum inferred Triassic and Cretaceous  
11 thickness prior to Gatuña and Ogallala deposition. Significant thicknesses of Cretaceous rocks  
12 may not have been deposited, however, and average erosion rates could have been lower.

13 Maximum-known Gatuña thickness in the area around the WIPP is approximately 100 m  
14 (330 ft); at the WIPP site, the Gatuña is very thin to absent. Ogallala deposits are known from  
15 the Divide east of the WIPP site, as well as from the High Plains further east and north. On the  
16 High Plains northeast of the WIPP, the upper Ogallala surface slopes to the southeast at a rate of  
17 approximately 4 m/km (20 feet per mile). A straight projection of the 1,250-m (4,100-ft) contour  
18 line from this High Plains surface intersects the site area, which is at an elevation slightly above  
19 1,036 m (3,400 ft). This difference in elevation of 213 m (700 ft) represents one estimate,  
20 probably near an upper bound, of possible unloading subsequent to deposition of the Ogallala  
21 Formation.

22 Alternatively, the loading and unloading of the Ogallala could have been closer to 100 m  
23 (330 ft). In any case, it would have occurred as a short-lived pulse over a few million years at  
24 most.

25 While the above inferences about greater unit thicknesses and probable occurrence are  
26 permissible, a realistic assessment suggests a more modest loading and unloading history  
27 (Powers and Holt 1995). It is likely that the Dewey Lake accumulated to near local maximum  
28 thickness of approximately 240 m (787 ft) before being slightly eroded prior to the deposition of  
29 Triassic rocks. It also is most probable that the Triassic rocks accumulated at the site to near  
30 local maximum thickness. In two similar cycles of rapid loading, the Culebra was buried to a  
31 depth of approximately 650 m (2,132 ft) by the end of the Triassic.

32 It also seems unlikely that a significant thickness of Cretaceous rock accumulated at the WIPP  
33 site. Erosion probably began during the Jurassic, slowed or stopped during the Early Cretaceous  
34 as the area was nearer or at base level, and then accelerated during the Cenozoic, especially in  
35 response to uplift as Basin and Range tectonics encroached on the area and the basin was tilted  
36 more. Erosional beveling of Dewey Lake and Santa Rosa suggest considerable erosion since  
37 tilting in the mid-Cenozoic. Erosion rates for this shorter period could have been relatively high,  
38 resulting in the greatest stress relief on the Culebra and surrounding units. Some filling occurred  
39 during the Late Cenozoic as the uplifted areas to the west formed an apron of Ogallala sediment  
40 across much of the area, but it is not clear how much Gatuña or Ogallala sediment was deposited  
41 in the site area. From general reconstruction of Gatuña history in the area (Powers and Holt  
42 1993, p. 281), the DOE infers that Gatuña or Ogallala deposits likely were not much thicker at

1 the WIPP site than they are now. The loading and unloading spike (Figure 2-25) representing  
2 Ogallala thickness probably did not occur. Cutting and headward erosion by the Pecos River has  
3 created local relief and unloading by erosion.

4 At the WIPP site, this history is a little complicated by dissolution, though locally (for example,  
5 Nash Draw) the effects of erosion and dissolution are more significant. The underlying  
6 evaporites have responded to foundering of anhydrite in less dense halite beds. These have  
7 caused local uplift of the Culebra (as at ERDA 6) but little change in the overburden at the  
8 WIPP. Areas east of the WIPP site are likely to have histories similar to that of the site. West of  
9 the site, the final unloading is more complicated by dissolution and additional erosion leading to  
10 exposure of the Culebra along stretches of the Pecos River Valley.

11 **2.1.5.3 Faulting**

12 Fault zones are well known along the Central Basin Platform, east of WIPP, from extensive  
13 drilling for oil and gas, as reported by Hills (1984). Holt and Powers performed an analysis in  
14 1988 (CCA Appendix FAC, p. 4-14) of geophysical logs from oil and gas wells to examine the  
15 regional geology for the Rustler. This analysis showed that faults along the margin of the  
16 Central Basin Platform displaced Rustler rocks of at least Late Permian age. The overlying  
17 Dewey Lake shows marked thinning along the same trend, according to Schiel (1988, Figure 21),  
18 but the structure contours of the top of the Dewey Lake are not clearly offset. Schiel (1988)  
19 concluded that the fault was probably reactivated during the Dewey Lake's deposition, but  
20 movement ceased at least by the time the Santa Rosa was deposited. No surface displacement or  
21 fault has been reported along this trend.

22 Muehlberger et al. (1978) mapped Quaternary fault scarps along the Salt Basin graben west of  
23 both the Guadalupe and Delaware mountains. These are the nearest known Quaternary faults of  
24 tectonic origin to the WIPP. Kelley (1971) inferred the Carlsbad and Barrera faults along the  
25 eastern escarpment of the Guadalupe Mountains based mainly on vegetative lineaments. Hayes  
26 and Bachman (1979) reexamined the field evidence for these faults in 1979 and concluded that  
27 they were nonexistent. Figure 2-26 illustrates major regional structures, including faults.

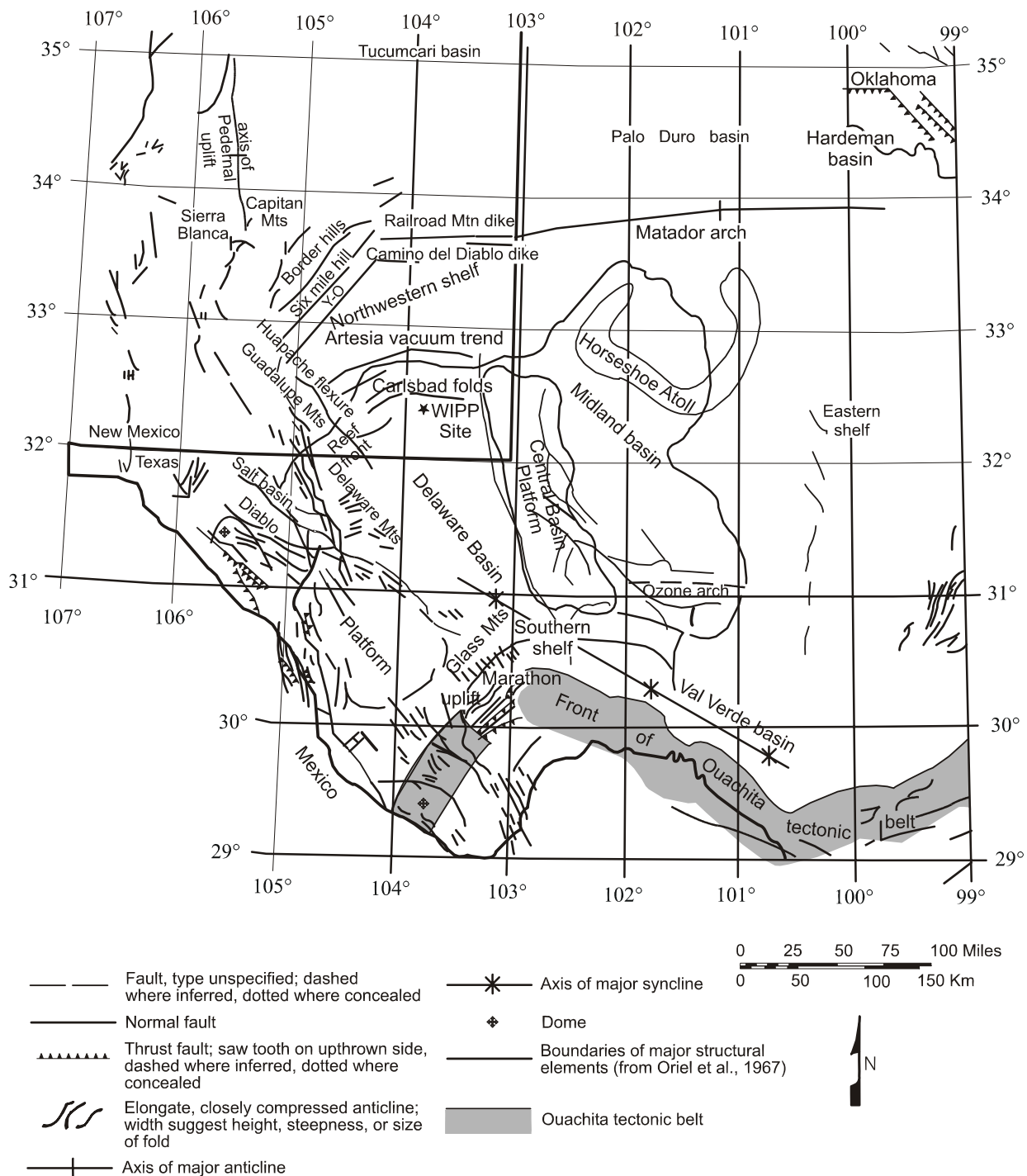
28 On a national basis, Howard et al. (1971, sheets 1 and 2) assessed the location and potential for  
29 activity of young faults. For the region around the WIPP site, Howard et al. (1971, sheet 1)  
30 located faults along the western escarpment of the Delaware and Guadalupe mountain trend.  
31 These faults were judged to be Late Quaternary (approximately the last 500,000 years) or older.

32 In summary, there are no known Quaternary or Holocene faults of tectonic origin that offset  
33 rocks at the surface nearer to the site than the western escarpment of the Guadalupe Mountains.  
34 A significant part of the tilt of basin rocks is attributed to a mid-Miocene to Pliocene uplift trend  
35 along the Guadalupe-Sacramento Mountains that is inferred on the basis of High Plains  
36 sediments of the Ogallala.

37 **2.1.5.4 Igneous Activity**

38 Within the Delaware Basin, only one feature of igneous origin is known to have formed since the  
39 Precambrian. An igneous lamprophyre dike or series of dikes occurs along a linear trace about

1 120 km (75 mi) long from the Yeso Hills south of White's City to the northeast of the WIPP site  
 2



CCA-070-2

3

4

**Figure 2-26. Regional Structures**

1 (Elliot Geophysical Company 1976). At its closest, the dike trend passes about 13 km (8 mi)  
2 northwest of the WIPP site center, as shown in Figure 2-27. Evidence for the extent of the dike  
3 includes outcroppings at Yeso Hills, subsurface intercepts in boreholes and mines, and airborne  
4 magnetic responses.

5 An early radiometric determination for the dike by Urry (1936) yielded an age of  $30 \pm$   
6 1.5 million years. Work on dike samples by Calzia and Hiss (1978) is consistent with earlier  
7 work, indicating an age of  $34.8 \pm 0.8$  million years.<sup>2</sup> Work by Brookins (1980) on polyhalite  
8 samples in contact with the dike indicated an age of about 21.4 million years. Volcanic ashes  
9 found in the Gatuña (Section 2.1.3.8) were airborne from distant sources and do not represent  
10 volcanic activity at the WIPP site.

## 11 **2.1.6 Nontectonic Processes and Features**

12 Nontectonic processes and features, which include evaporite deformation and dissolution of  
13 strata, are known to be active in the Delaware Basin. These processes are of interest because  
14 they represent mechanisms that are potentially disruptive to the repository in the long term. Both  
15 processes have been investigated extensively. The conclusions from these investigations are  
16 summarized in this section.

17 Halite in evaporite sequences is relatively plastic, which can lead to the process of deformation;  
18 it is also highly soluble, which can lead to the process of dissolution. Both processes  
19 (deformation and dissolution) can produce structural features similar to those produced by  
20 tectonic processes. The features developed by dissolution and deformation can be distinguished  
21 from similar-looking tectonic features where the underlying units do not reflect the same feature  
22 as do the evaporites. As an example, the evaporite deformation commonly does not affect the  
23 underlying Bell Canyon. Beds underlying areas of dissolved salt are not affected, but overlying  
24 units to the surface may be affected. The deformation in the Castile and Salado also tends to die  
25 out in overlying units, and the Rustler or the Dewey Lake may show little, if any, effects from  
26 deformed evaporites.

### 27 **2.1.6.1 Evaporite Deformation**

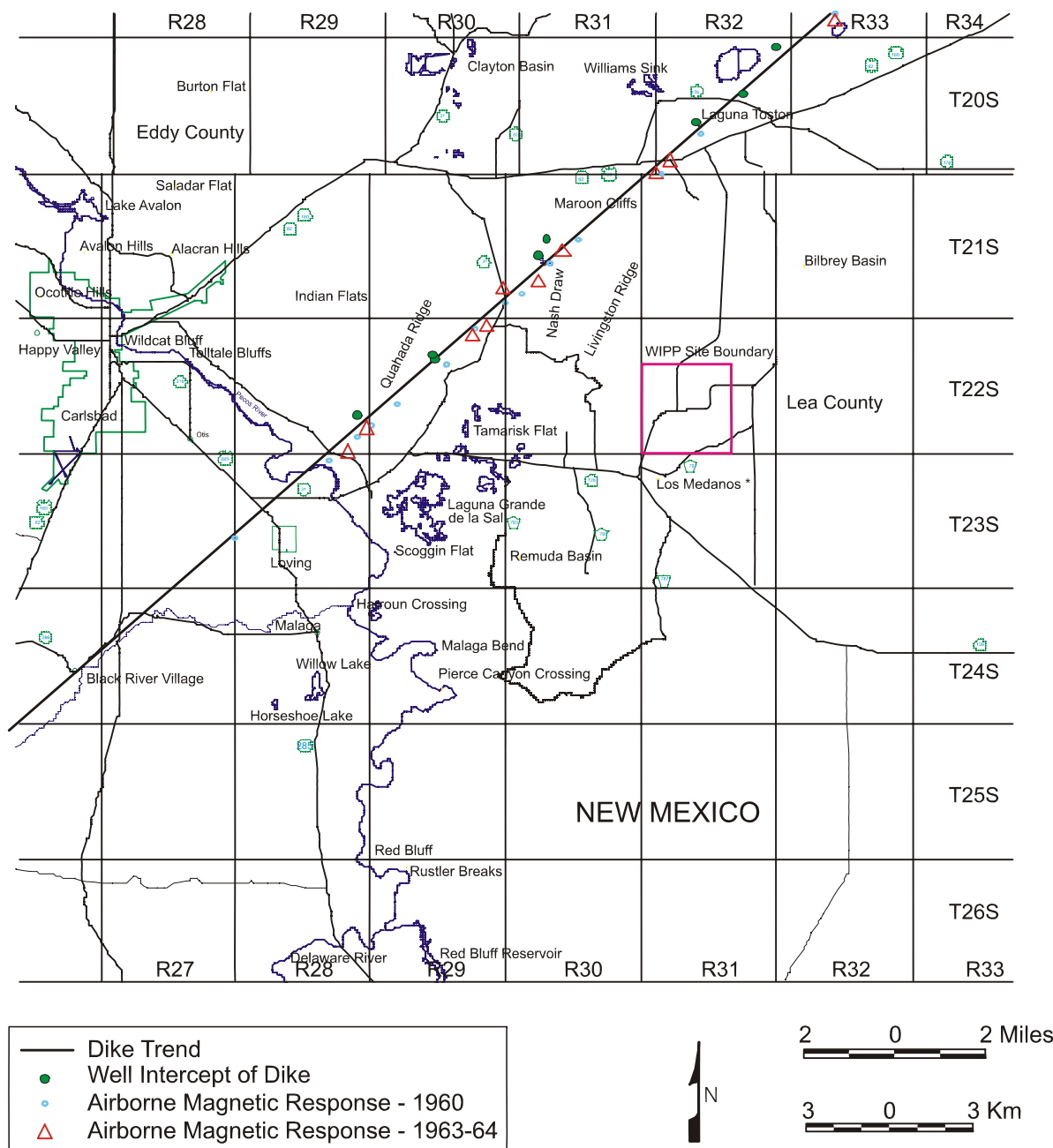
28 The most recent review of evaporite deformation in the northern Delaware Basin and original  
29 work to evaluate deformation is summarized here. More detail is provided in CCA Appendix  
30 DEF.

#### 31 **2.1.6.1.1 Basic WIPP History of Deformation Investigations**

32 The Castile has been known for many years to be deformed in parts of the Delaware Basin,  
33 especially along the northern margin. Jones et al. (1973) clearly showed the Castile to be thicker  
34 from the northwestern to northern part of the basin margin, just inside the Capitan Reef. A  
35 dissertation by Snider (1966, Figures 11 and 14) and a paper by Anderson et al. (1972, Figure  
36 10) also presented maps showing some evidence of thicker sections of Castile next to the

---

<sup>2</sup> Calzia and Hiss (1978, p. 44) reported 32.2 to 33.9 million years. However, Powers et al. 1978 (CCA Appendix GCR, p. 3-80) reported a recalculated value of  $34.8 \pm 0.8$  million years based on a change in measured decay constant.



Source: Elliot (1976)

CCA-076-2

1

2

**Figure 2-27. Igneous Dike in the Vicinity of the WIPP Site**

1 Capitan. ERDA-6 was drilled during 1975 as part of the program to characterize an initial site for  
2 WIPP. The borehole penetrated increasingly deformed beds through the Salado into the Castile,  
3 and, at 826 m (2,711 ft) depth, the borehole began to produce pressurized brine and gas.  
4 Anderson and Powers (1978, p. 79) and Jones (1981a) interpreted beds to have been displaced  
5 structurally by as much as 289.5 m (950 ft). Some of the lower beds may have pierced overlying  
6 beds. The beds were considered too structurally deformed to mine reasonably along single  
7 horizons for a repository. Therefore, the site was abandoned in 1975, and the current site was  
8 located in 1976 (CCA Appendix GCR). The deformed beds around ERDA-6 were considered  
9 part of a deformed zone within about 10 km (6 mi) of the inner margin of the Capitan Reef. As a  
10 consequence, the preliminary selection criteria were revised to prohibit locating a new site within  
11 10 km (6 mi) of the Capitan margin.

12 General criteria for the present site for the WIPP appeared to be met based on initial data from  
13 drilling (ERDA-9) and geophysical surveys. Beginning in 1977, the new site was more  
14 intensively characterized through geophysical surveys, including seismic reflection and drilling.  
15 Extensive seismic reflection work revealed good reflector quality in the southern part of the site  
16 and poor-quality or disturbed reflectors in a sector of the northern part of the site (see CCA  
17 Appendix DEF, Figure DEF-2.2). The area of disturbed reflectors became known as the  
18 disturbed zone, the area of anomalous seismic reflectors, or the zone of anomalous seismic  
19 reflection data. (The disturbed zone based on poor Castile seismic reflectors is completely  
20 different from the DRZ that describes the deformation around mined underground openings at  
21 the WIPP.)

22 Powers et al., in CCA Appendix GCR, Figures 4.4, 4.5, and 4.6, generally shows the disturbed  
23 zone beginning about 1.6 km (1 mi) north of the WIPP site center. Borns et al. (1983), included  
24 two areas south of the WIPP site as showing the same features of the disturbed zone. Neill et  
25 al.(1983) summarized the limits of the disturbed zone based on differing interpretations and  
26 included the area less than 1.6 km (1 mi) north of the site center, where the dip in the Castile  
27 begins to steepen. WIPP-11 was drilled in early 1978 about 5 km (3 mi) north of the site center  
28 over part of the disturbed zone where proprietary petroleum company data had also indicated  
29 significant seismic anomalies. The borehole encountered highly deformed beds within the  
30 Castile and altered thicknesses of halite units, but no pressurized brine and gas were found.

31 Less than 1.6 km (1 mi) north of the site center, seismic data indicated possible faulting of the  
32 upper Salado and the lower Rustler over the area of steepening Castile dips. Four boreholes  
33 (WIPP-18, -19, -21, -22) were drilled into the upper Salado and demonstrated neither faulting  
34 nor significant deformation of the Rustler-Salado contact. Lateral changes in the seismic  
35 velocity of the upper sections contributed to the interpretation of a possible fault and thus  
36 complicated interpretations of deeper structure.

37 WIPP-12 was located about 1.6 km (1 mi) north of the center of the site and drilled during 1978  
38 to a depth of 850 m (2,785 ft) in the upper Castile to determine the significance of structure on  
39 possible repository horizons. The top of the Castile was encountered at an elevation about 49 m  
40 (160 ft) above the same contact in ERDA-9 at the site center.

41 WIPP-12 was deepened during late 1981 to a depth of 1,200 m (3,925 ft) to test for possible  
42 brine and gas in the deformed Castile. The probability of encountering brine and gas was

1 considered low because ERDA-6 and other known brine reservoirs in the Castile occurred in  
2 areas with greater deformation. During drilling, fractured anhydrite in the upper Castile (lower  
3 A3) began to yield pressurized brine and gas. The borehole was deepened to the basal anhydrite  
4 (A1) of the Castile. Subsequent reservoir testing (Popielak et al. 1983) was conducted to  
5 estimate reservoir properties (see Section 2.2.1.2.2 and Section 6.4.8).

6 As a consequence of discovering pressurized brine and gas in WIPP-12, the EEG recommended  
7 that the design of the facility be changed and that proposed waste disposal areas in the north be  
8 moved or reoriented to the south. After additional drilling of DOE-1, the DOE concluded that  
9 the design change had advantages, and the disposal facilities were placed south of the site center.

10 A microgravity survey of the site was designed to delineate further the structure within the  
11 disturbed zone, based on the large density differences between halite and anhydrite. The gravity  
12 survey was unsuccessful in yielding any improved resolution of the Castile structure.

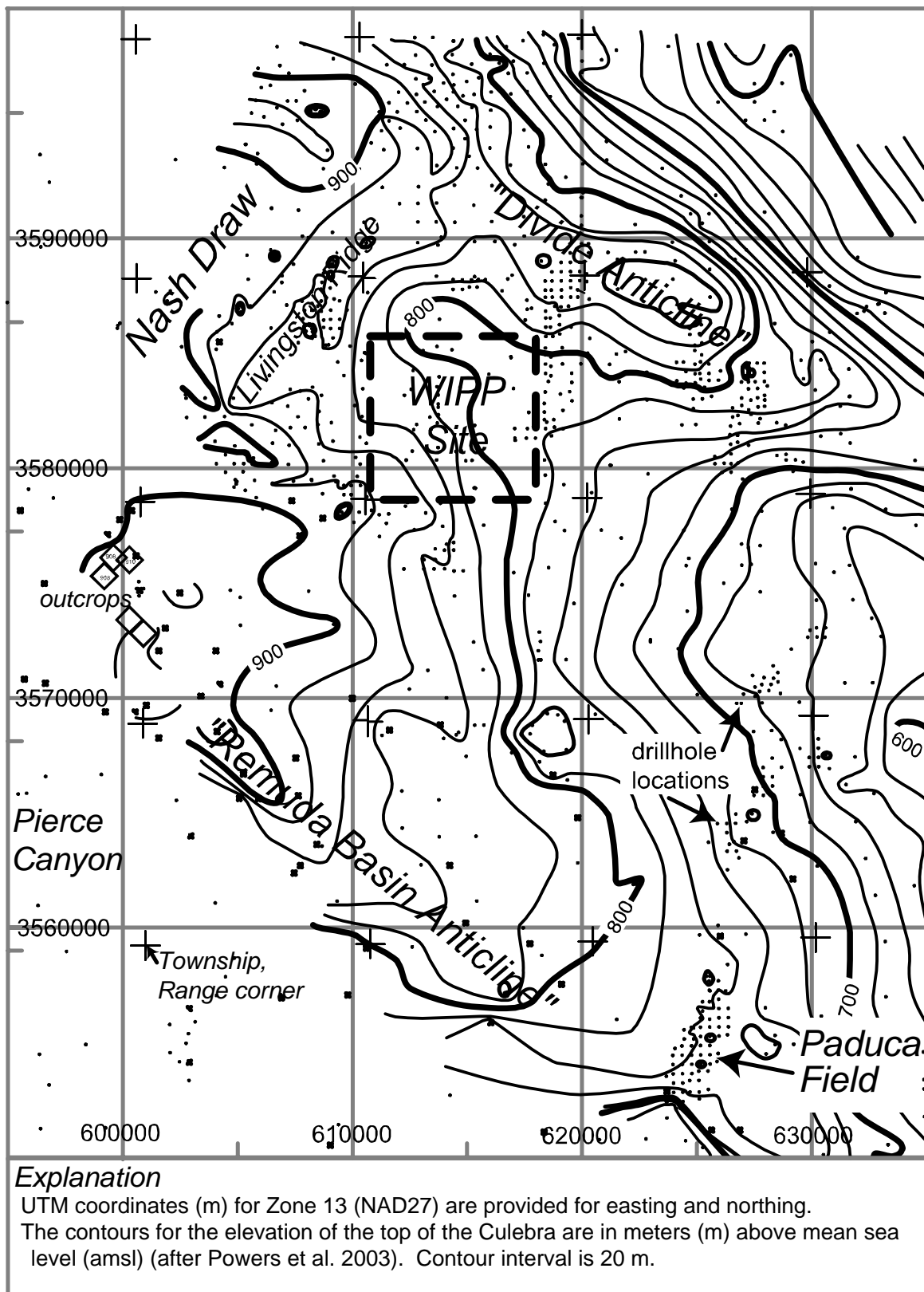
13 DOE-2 was the last WIPP borehole to examine structure within the Castile. Potash drillhole data  
14 suggested a low point in Salado units about 3.3 km (2 mi) north of the site center. It was  
15 proposed by Davies (1984, p. 175) that the Salado low might indicate deeper dissolution of  
16 Castile halite, somewhat similar to the dissolution causing breccia pipes (see Section 2.1.6.2 on  
17 evaporite dissolution). The borehole demonstrated considerable Castile deformation, but there  
18 was no indication that halite had been removed by dissolution (Mercer et al. 1987; Borns 1987).

#### 19 2.1.6.1.2 Extent of the Disturbed Zone at the Site

20 Nearby surface drilling, shafts, and underground drilling during early excavations at WIPP  
21 showed that the repository horizon varies modestly from the regional structure over the central  
22 part of the site; north of the site center, the beds dip gently to the south. Borns (1987) suggested  
23 that the south dip is probably related to the dip on the underlying Castile.

24 The upper surface of MB 139, under the repository horizon, exhibited local relief in the  
25 exploratory salt-handling shaft. Jarolimek et al. (1983, pp. 4 - 6) interpreted the relief as mainly  
26 caused by syndepositional growth of gypsum at the water-sediment interface to form mounds  
27 and by subsequent partial crushing. Jarolimek et al. (1983) concluded that the MB relief was not  
28 caused by deformation because the base of the MB showed no comparable relief. Based on  
29 concerns of the EEG, MB 139 was reevaluated. Borns (1985) found less relief on the upper  
30 surface of the MB in the areas they examined; he also concluded that depositional processes  
31 were responsible for the relief. In both cases, deformation is not thought to have caused the  
32 relief on MB 139.

33 For the investigation of geologic factors related to hydraulic properties of the Culebra, Powers  
34 (2002a; 2002b; 2003a) constructed elevation maps of the top of the Culebra for the region  
35 around the WIPP site. A simplified version (Figure 2-28) showing the elevations of the top of  
36 the Culebra in meters above mean sea level (m amsl) illustrates that deformation of the Castile  
37 propagated upward through the Culebra to the northeast of the WIPP site, forming a northwest-  
38 southeast trending anticline informally termed "the Divide anticline." Across the



1 WIPP site, the Culebra is slightly deformed by the deeper deformation, and the “disturbed zone”  
2 defined earlier geophysically is slightly evident at this horizon.

3   2.1.6.1.3 Deformation Mechanisms

4 In analyzing Castile structure in the northern Delaware Basin, Borns et al. (1983, p. 3) proposed  
5 five processes as the principal hypotheses to explain the structure: gravity foundering,  
6 dissolution, gravity sliding, gypsum dehydration, and depositional processes. Gravity foundering  
7 is the most comprehensive and best-accepted hypothesis of the five. It is based on the fact that  
8 anhydrite is much more dense (about 2.9 g/cm<sup>3</sup>) than halite (about 2.1 g/cm<sup>3</sup>), and anhydrite beds  
9 therefore have a potential for sinking into underlying halite. Regardless of which mechanism  
10 caused the disturbed zone, the important consideration is the long-term future effects. To  
11 evaluate this, Borns et al. (1983) postulated that both gravity-driven deformation mechanisms  
12 could be ongoing. The strain rates from such deformation are such that deformation would  
13 progress over the next 250,000 years and that such deformation would not directly jeopardize the  
14 disposal system.

15   2.1.6.1.4 Timing of Deformation of the Disturbed Zone at the Site

16 Jones (1981a, p. 18) estimated that deformation of the Castile and overlying rocks took place  
17 before the Ogallala Formation was deposited, as he believes the unit is undeformed. Anderson  
18 and Powers (1978, p. 79) inferred that data from ERDA-6 indicate that the Castile was deformed  
19 after the basin was tilted. Though these lines of evidence could be consistent with mid-Miocene  
20 deformation, there are other interpretations consistent with older deformation. There is no  
21 known evidence of surface deformation or other features to indicate recent deformation.

22   2.1.6.2 Evaporite Dissolution

23 Because evaporites are much more soluble than most other rocks, project investigators have  
24 considered it important to understand the dissolution processes and rates that occur within the  
25 site being considered for long-term isolation. These dissolution processes and rates constitute  
26 the limiting factor in any evaluation of the site. Over the course of the WIPP project, extensive  
27 resources have been committed to identify and study a variety of features in southeastern New  
28 Mexico interpreted to have been caused by dissolution. The subsurface distribution of halite for  
29 various units has been mapped. Several different kinds of surface features have been attributed  
30 to dissolution of salt or karst formation. The processes proposed or identified include point-  
31 source (brecciation), deep dissolution, shallow dissolution, and karst. These are each discussed  
32 in more detail in CCA Appendix DEF, Section DEF.3. Screening arguments relative to  
33 dissolution are presented in Appendix PA, Attachment SCR, FEPs N17 and N21 (including  
34 dissolution associated with abandoned boreholes in the discussion for FEP H34). These  
35 arguments are based principally on the observed rates and processes in the region. These are  
36 described below.

37   2.1.6.2.1 Brief History of Project Studies

38 Well before the WIPP project, several geologists recognized that dissolution is an important  
39 process in southeastern New Mexico, and that it contributed to the subsurface distribution of  
40 halite and to the surficial features. Early studies include those by Lee (1925), Maley and

1 Huffington (1953), and Olive (1957) Robinson and Lang (1938, p. 100) identified an area under  
2 Nash Draw where brine occurred at about the stratigraphic position of the upper Salado-basal  
3 Rustler and considered that salt had been dissolved to produce a dissolution residue. Vine (1963,  
4 p. B38 and B40) mapped Nash Draw and surrounding areas. Vine (1963) reported surficial  
5 domal structures, later called breccia pipes and identified as deep-seated dissolution and collapse  
6 features.

7 As the USGS and Oak Ridge National Laboratory (ORNL) began to survey southeastern New  
8 Mexico as an area in which to locate a repository site in salt, Brokaw et al. (1972) prepared a  
9 summary of the geology that included solution and subsidence as significant processes in  
10 creating the features of southeastern New Mexico. Brokaw et al. (1972) also recognized a  
11 solution residue at the top of the salt in the Salado in the Nash Draw area, and the unit commonly  
12 became known as the brine aquifer because it yielded brine. Brokaw et al. (1972) also  
13 interpreted the east-west decrease in thickness of the Rustler to be a consequence of removal by  
14 dissolution of halite and other soluble minerals.

15 During the early 1970s, the basic ideas about shallow dissolution of salt (generally from higher  
16 stratigraphic units and within a few hundred feet of the surface) were set out in a series of  
17 reports, as discussed in the following sections. Piper (1973; 1974) independently evaluated the  
18 geological survey data for ORNL. Claiborne and Gera (1974) concluded that salt was being  
19 dissolved too slowly from the near-surface units to affect a repository for several million years,  
20 at least.

21 By 1978, shallower drilling around the WIPP site to evaluate potash resources was interpreted by  
22 Jones (1978, p. 9), who felt that the Rustler included “dissolution debris, convergence of beds,  
23 and structural evidence for subsidence.” Halite in the Rustler has been reevaluated by the DOE,  
24 but there are only minor differences in inferred distributions among the various investigators.  
25 These investigators do have different explanations about how this distribution occurred (see  
26 Section 2.1.3.5 on Rustler stratigraphy): (1) through extensive dissolution of the Rustler’s halite  
27 after the Rustler was deposited, or (2) through syndepositional dissolution of halite from saline  
28 mud flat environments during Rustler deposition.

29 Anderson (1978) and Anderson et al. (1978) reevaluated halite distribution in deeper units,  
30 especially the Castile and Salado formations. They identified local anomalies proposed as  
31 features developed after deep dissolution of halite by water flowing upward from the underlying  
32 Bell Canyon. Anderson (1978) mapped geophysical log signatures of the Castile and interpreted  
33 lateral thinning and change from halite to non-halite lithology as evidence of lateral dissolution  
34 of deeper units (part of deep dissolution), and proposed that deep dissolution might threaten the  
35 WIPP site. In response to Anderson’s (1978) developing concepts, ERDA-10 was drilled south  
36 of the WIPP area during the latter part of 1977. ERDA-10 intercepted a stratigraphic sequence  
37 without evidence of solution residues in the upper Castile.

38 A set of annular or ring fractures is evident in the surface around San Simon Sink, about 30 km  
39 (18 mi) east of the WIPP site. Nicholson and Clebsch (1961, p. 14) suggested that San Simon  
40 Sink developed as a result of deep-seated collapse. WIPP-15 was drilled at about the center of  
41 the sink to a depth of 245 m (811 ft) to obtain samples for paleoclimatic data and stratigraphic  
42 data to interpret collapse. Anderson (1978) and Bachman (1980) both interpret San Simon Sink

1 as dissolution and collapse features, and the annular fractures are not considered evidence of  
2 tectonic activity.

3 Following the work by Anderson, Bachman (1980, 1981) mapped surficial features in the Pecos  
4 Valley, especially at Nash Draw, and differentiated between those surface features in the basin  
5 that were formed by karst and those that were formed by deep collapse features over the Capitan.  
6 WIPP-32, WIPP-33, and two boreholes over the Capitan Reef were eventually drilled. Their  
7 data, which demonstrated the concepts proposed by Bachman (1980, 1981), are documented in  
8 Snyder et al. (1982, p. 65).

9 A final program concerning dissolution and karst was initiated following a microgravity survey  
10 of a portion of the site during 1980. Based on localized low-gravity anomalies, Barrows et al.  
11 (1983) interpreted several areas within the site as locations of karst. WIPP-14 was drilled during  
12 1981 at a low-gravity anomaly. It revealed normal stratigraphy through the zones proposed to be  
13 affected by karst. As a follow-up, Bachman (1985) also reexamined surface features around the  
14 WIPP and concluded that there was no evidence for active karst within the WIPP site. The  
15 nearest karst feature is northwest of the site boundaries at WIPP-33.

16 **2.1.6.2.2 Extent of Dissolution**

17 Within the Rustler, dissolution of halite is believed to have occurred only near the depositional  
18 margins, as discussed in Section 2.1.3.5. Figure 2-15 shows the only two areas where evidence  
19 has been found for halite dissolution from the M3/H3 horizon in the Tamarisk.

20 Upper intervals of the Salado thin dramatically west and south of the WIPP site (Figure 2-29)  
21 compared to deeper Salado intervals. There are no cores for further consideration of possible  
22 depositional variations. As a consequence, this zone of thinning is interpreted by the DOE as the  
23 edge of dissolution of the upper Salado.

24 **2.1.6.2.3 Timing of Dissolution**

25 The dissolution of Ochoan evaporites through the near-surface processes of weathering and  
26 groundwater recharge has been studied extensively (Anderson 1981; Lambert 1983a; Lambert  
27 1983b; Bachman 1984; and CCA Appendix FAC). The work of Lambert (1983a) was  
28 specifically mandated by the agreement between the DOE and the state of New Mexico to  
29 evaluate in detail the conceptual models of evaporite dissolution proposed by Anderson (1981).  
30 There was no clear consensus among investigators on the volume of rock salt removed. Hence,  
31

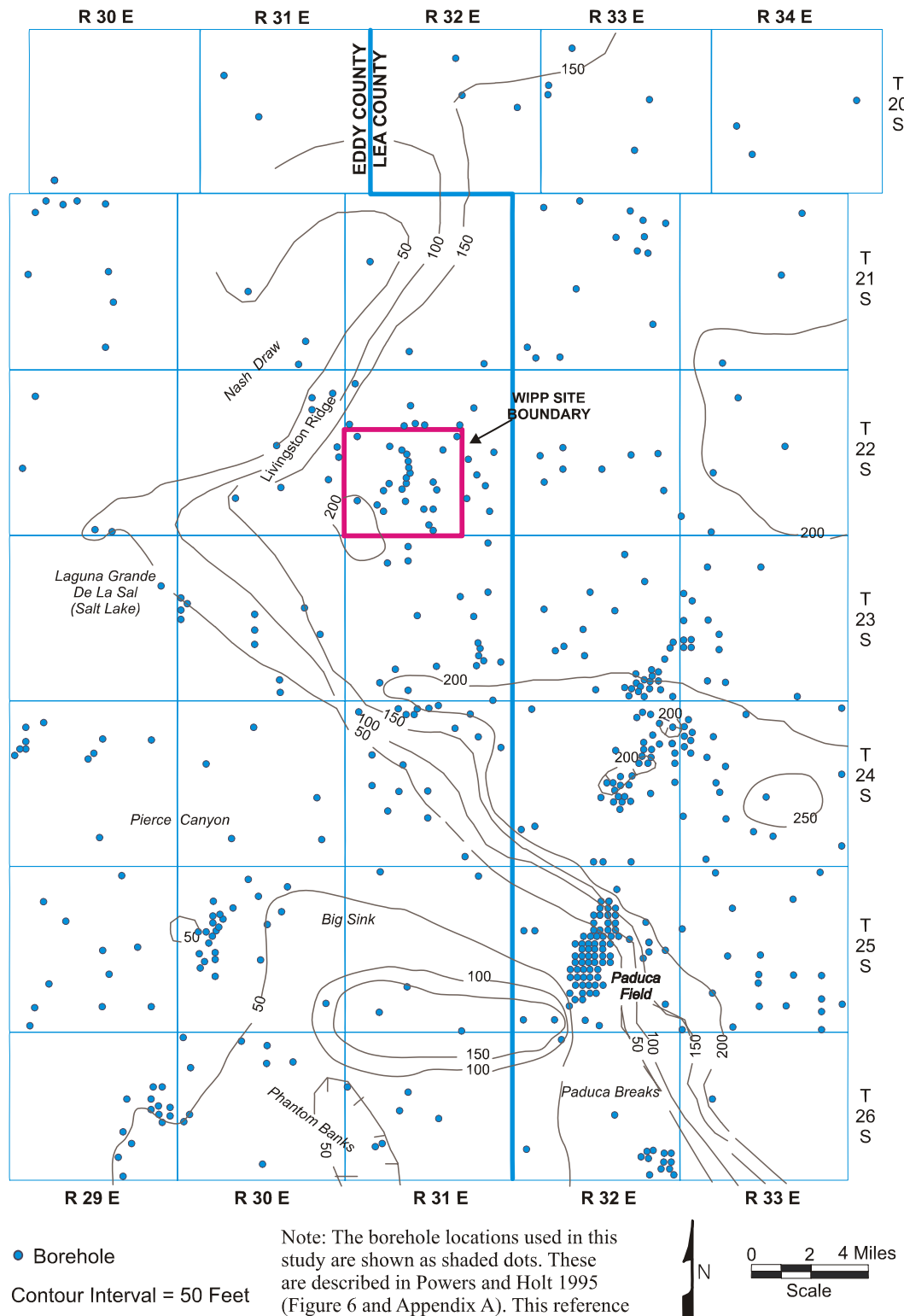


**Figure 2-29. Isopach from the Base of MB 103 to the Top of the Salado**

1 estimates of the instantaneous rate of dissolution vary significantly. Dissolution may have taken  
2 place as early as the Ochoan, during or shortly after deposition. For the Delaware Basin as a  
3 whole, Anderson (1981) proposed that up to 40 percent of the rock salt in the Castile and Salado  
4 formations was dissolved during the past 600,000 years. Lambert (1983b, p. 292) suggested that  
5 in many places the variations in salt-bed thicknesses inferred from borehole geophysical logs that  
6 were the basis for Anderson's (1981) calculation were depositional in origin, compensated by  
7 thickening of adjacent nonhalite beds, and were not associated with the characteristic dissolution  
8 residues. Borns and Shaffer (1985, p. 44 – 45) also suggested in 1985 a depositional origin for  
9 many apparent structural features attributed to dissolution.

10 Snyder (1985, p. 8), as well as earlier workers (for example, Vine 1963; Lambert 1983b; and  
11 Bachman 1984), attribute the variations in thickness in the Rustler, which crops out in Nash  
12 Draw, to postdepositional evaporite dissolution. Holt and Powers (CCA Appendix FAC, p. 9-2)  
13 have challenged this view and attribute the east-to-west thinning of salt beds in the Rustler to  
14 depositional facies variability rather than postdepositional dissolution. Bachman (1974, 1976,  
15 1980) envisioned several episodes of dissolution since the Triassic, each dominated by greater  
16 degrees of evaporite exhumation and a wetter climate, interspersed with episodes of evaporite  
17 burial and/or a drier climate. Evidence for dissolution after deposition of the Salado and before  
18 deposition of the Rustler along the western part of the Basin was cited by Adams (1944, p.  
19 1612). Others have argued that the evaporites in the Delaware Basin were above sea level and  
20 therefore potentially subject to dissolution, during the Triassic, Jurassic, Tertiary, and Quaternary  
21 periods. Because of discontinuous deposition, not all of these times are separable in the  
22 geological record of southeastern New Mexico. Bachman (1980) contends that dissolution was  
23 episodic during the past 225 million years as a function of regional base level, climate, and  
24 overburden.

25 There have been several attempts to estimate the rates of shallow dissolution in the basin.  
26 Bachman (1974) provided initial estimates of dissolution rates based on a reconstruction of Nash  
27 Draw relationships, including the observation that portions of the Gatuña were deposited over  
28 areas of active dissolution and subsidence of the underlying evaporites. Though these rates  
29 indicate no hazard to the WIPP related to Nash Draw dissolution, Bachman (1980, p. 85) later  
30 reconsidered the Nash Draw relationships and concluded that pre-Cenozoic dissolution had also  
31 contributed to salt removal. Thus, the initial estimated rates were too high.

32 With regard to deep dissolution, Anderson concluded in 1978 that the integrity of the WIPP to  
33 isolate radioactive waste would not be jeopardized by dissolution within about one million years.  
34 Anderson and Kirkland (1980, pp. 66 - 69) expanded on the concept of brine density flow  
35 proposed by Anderson (1978) as a means of dissolving evaporites at a point by circulating water  
36 from the underlying Bell Canyon. Wood et al. (1982, p. 100) examined the mechanism and  
37 concluded that, while it was physically feasible, it would not be effective enough in removing  
38 salt to threaten the ability of the WIPP to isolate transuranic (TRU) waste.

39 2.1.6.2.4 Features Related to Dissolution

40 Bachman (1980, p. 97) separated breccia pipes, formed over the Capitan Reef by dissolution and  
41 collapse of a cylindrical mass of rock, from evaporite karst features that appear similar to breccia  
42 pipes. There are surficial karst features, including sinks and caves, in large areas of the basin.

1 Nash Draw is the result of combined dissolution and erosion. Within the site boundaries, there  
2 are no known surficial features caused by dissolution or karst.

3 The subsurface structure of the Culebra is shown in Figure 2-28. South of the WIPP site, an  
4 antiformal structure informally called the “Remuda Basin anticline” has been created by  
5 dissolution of salt from the underlying Salado to the southwest of the anticline. Beds generally  
6 dip to the east, and salt removed to the west created the other limb of the structure. Units below  
7 the evaporites apparently do not show the same structure.

8 **2.2 Surface Water and Groundwater Hydrology**

9 The DOE has determined that the hydrological characteristics of the disposal system are  
10 important because contaminant transport via fluid flow has a potential to impact the performance  
11 of the disposal system. In addition, the EPA has provided numerous criteria related to  
12 groundwater in 40 CFR § 194.14(a). At the WIPP site, one of the DOE’s selection criteria was  
13 to choose a location that would minimize this impact. This was accomplished when the DOE  
14 selected (1) a host formation that contains little groundwater and transmits it poorly, (2) a  
15 location where the effects of groundwater flow are minimal and predictable, (3) an area where  
16 groundwater use is low, (4) an area where there are no permanent surface waters, (5) an area  
17 where future groundwater use is unlikely, and (6) a repository host rock that will not likely be  
18 affected by anticipated possible long-term climate changes within 10,000 years.

19 The following discussion summarizes the characteristics of the groundwater and surface water at  
20 and around the WIPP site. This summary is based on data collection programs that were  
21 initiated with the WIPP program and that continue to some extent today. The purpose of these  
22 programs was to provide information sufficient for the development and use of predictive models  
23 of the groundwater movement at the WIPP site.

24 For a comprehensive understanding of the impact of groundwater and surface water on the  
25 disposal system, the following factors have been evaluated:

26 *Groundwater*

- 27     • Horizontal and vertical flow fluxes and velocities,  
28     • Hydraulic interconnectivity between rock units,  
29     • Hydraulic parameters (porosity, etc.),  
30     • General groundwater use, and  
31     • Chemistry (including, but not limited to, salinity, mineralization, age, Eh, and pH).

32 *Surface Water*

- 33     • Regional precipitation and evapotranspiration rates,  
34     • Location and size of surface-water bodies,

- 1     • Water volume, flow rate, and direction,
- 2     • Drainage network,
- 3     • Hydraulic connection with groundwater,
- 4     • Soil hydraulic properties (infiltration), and
- 5     • General water chemistry and use.

6     Changes to the hydrological system due to human activity are evaluated in Chapter 6.0.

7     The specifics of groundwater modeling are found in Section 6.4.6, Appendix PA, Attachment  
8     MASS, Section MASS.14.2. The hydrological system is divided into four segments for the  
9     discussion in this chapter. These are: (1) the rock units below the Salado, which may impact the  
10    disturbed (human intrusion) performance of the disposal system, (2) the Salado, which mostly  
11    addresses the undisturbed performance of the disposal system, (3) the rock units above the  
12    Salado, which essentially impact only the disturbed (human intrusion) performance of the  
13    disposal system, and (4) the surface waters. The groundwater regime is discussed in  
14    Section 2.2.1, and the surface-water regime in Section 2.2.2.

15    The WIPP site lies within the Pecos River drainage area (Figure 2-23, see also Section 2.2.2,  
16    Figure 2-43). As discussed in the Final Environmental Impact Statement (FEIS) (DOE 1980,  
17    Section 7.1.1), the climate is semiarid, with a mean annual precipitation of about 0.33 m (13 in.),  
18    a mean annual runoff of 2.5 to 5 mm (0.1 to 0.2 in.), and a mean annual pan evaporation of more  
19    than 2.5 m (100 in.). Runoff is practically nonexistent and the WIPP does not have a well  
20    defined drainage pattern. The general movement of runoff can be inferred from the topography  
21    in Figure 2-23. Only one stream flow gaging station has been operated in the vicinity. This is at  
22    the location shown as Hill Tank in Figure 2-23. Observations at Hill Tank are discussed in  
23    Section 2.2.2.

24    Additional information about climatic conditions at the WIPP is given in Section 2.5.2. Brackish  
25    water with total dissolved solids (TDS) concentrations of more than 3,000 parts per million is  
26    common in the shallow wells near the WIPP site. Surface waters typically have high TDS  
27    concentrations, particularly of chloride, sulfate, sodium, magnesium, and calcium. Additional  
28    information about water quality is given in Section 2.4.2.

## 29    *2.2.1 Groundwater Hydrology*

30    At the WIPP site, the DOE has obtained groundwater hydrologic data from conventional and  
31    special-purpose test configurations in multiple surface boreholes. Geophysical logging of the  
32    boreholes has provided hydrologic information on the rock strata intercepted. Pressure  
33    measurements, fluid samples, and ranges of rock permeability have been obtained for selected  
34    formations through the use of standard and modified drill-stem tests. Slug injection or  
35    withdrawal tests and other flow-rate tests have provided data to aid in the estimation of  
36    transmissivity and storage. The hydraulic heads of groundwaters within many water-bearing  
37    zones in the region have been mapped from measured depths to water in the boreholes. Since the

1 CCA was submitted to the EPA in 1996, the DOE has implemented a number of monitoring  
2 programs (see Appendix MON-2004), including the Groundwater Monitoring Program, to meet  
3 the assurance requirements of 40 CFR § 191.14(b). In addition to the groundwater monitoring  
4 program, other hydrologic data gathered since the CCA come from logging of new or  
5 replacement wells, piezometers, special-purpose field investigations, and surveys of drilling  
6 practices in the Delaware Basin. A data summary of all these activities is provided in Appendix  
7 DATA.

8 Historically, the DOE has obtained hydrological data principally from a conventional well-  
9 monitoring network (Figures 2-3 through 2-6 are maps of the well locations) comprising 71 wells  
10 located on 45 separate wellpads (DOE 2003). Most of the 71 wells are completed only to a  
11 single hydrologic unit; however, six are multiple-completions to allow monitoring of two or  
12 more units in the same well. Hydrologic information (such as hydraulic head) is obtained at 80  
13 completion intervals within the 71 wells. The focus of the hydrological monitoring is the Rustler  
14 (comprising 72 of the 80 monitored intervals) because this formation contains two of the most  
15 transmissive saturated units, the Culebra and Magenta Dolomites, which are important to the  
16 modeling of releases during various human intrusion scenarios. Limited hydrological monitoring  
17 of the Bell Canyon, Dewey Lake, and Santa Rosa also occurs.

18 Rock units that are shown in the conceptual models in Section 6.4 to be important to disposal  
19 system performance from a hydrological standpoint are the Castile, the Salado, the Rustler, and  
20 the Dewey Lake (Figures 2-30 and 2-31). However, other units which are discussed due to their  
21 significance in screening hydrological processes or because they are less important to the  
22 conceptual model include the Bell Canyon, the Capitan, the Rustler-Salado contact zone, and the  
23 supra-Dewey Lake units. These will also be discussed because they are features of the  
24 groundwater flow system of the WIPP region.

25 The Bell Canyon is of interest to the DOE because it is the first regionally continuous water-  
26 bearing unit beneath the WIPP and is the target stratigraphic horizon for salt-water injection by  
27 industry outside of the WIPP site boundary. The halite and anhydrite layers of the Castile  
28 provide a hydrologic barrier between the Salado and the underlying Bell Canyon. The Castile is  
29 of interest to PA because it contains isolated high-permeability zones containing pressurized  
30 brine. As discussed in Section 2.1.6.1, several such zones of pressurized brine have been  
31 intercepted by boreholes near the WIPP site, and one or more of these zones may exist at the  
32 WIPP site.

33 The Salado comprises low-permeability beds of variable composition. The low permeability of  
34 the Salado provides a hydrologic barrier in all directions between the repository and the  
35 accessible environment or more transmissive beds. At the repository horizon, a much higher

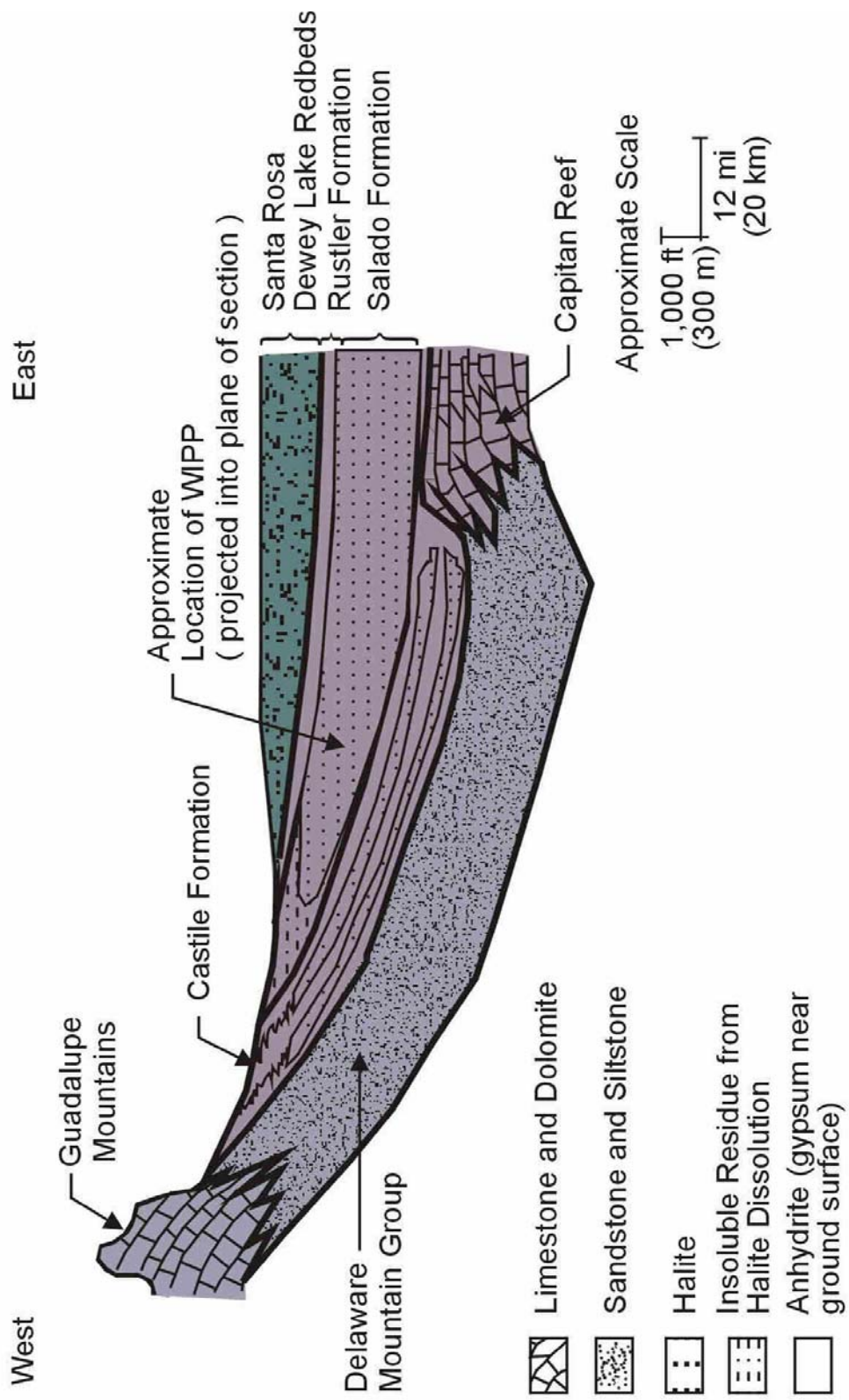
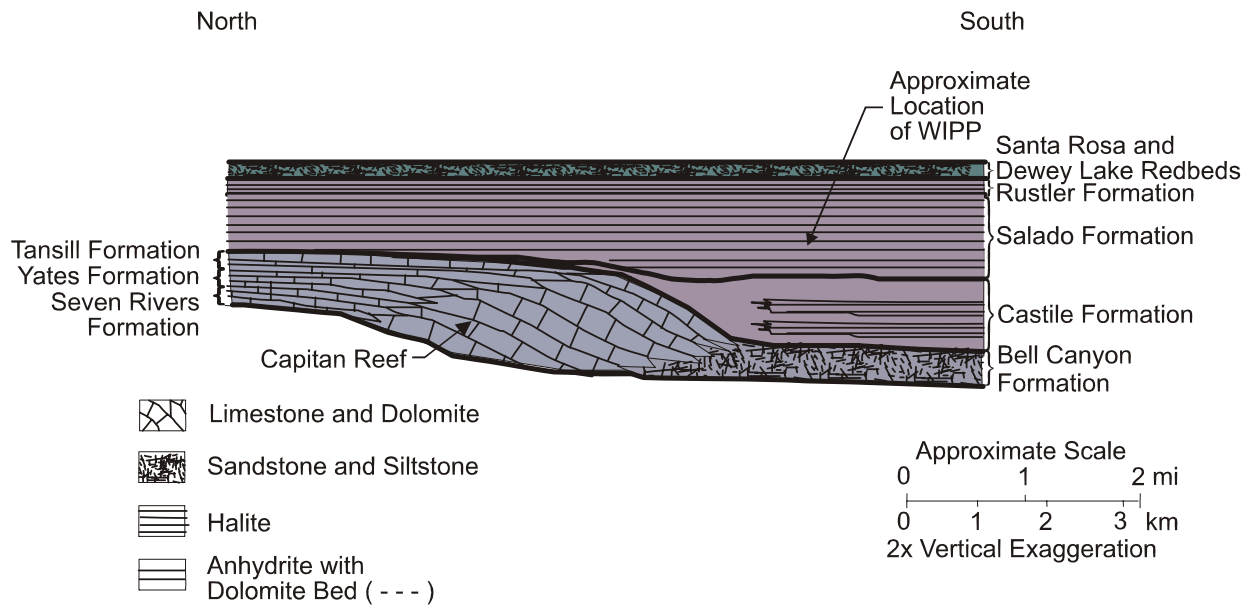


Figure 2-30. Schematic West-East Cross Section through the North Delaware Basin

CCA-043-2



CCA-044-2

1

## 2      **Figure 2-31. Schematic North-South Cross Section through the North Delaware Basin**

3      permeability DRZ forms locally in the salt around the waste emplacement rooms and operational  
 4      drifts. As described in Appendix DATA, the DRZ is of limited extent compared to the  
 5      significant thickness of the Salado low-permeability beds surrounding the repository horizon.

6      The Rustler contains two laterally transmissive members. The Culebra is the first laterally  
 7      continuous unit located above the WIPP underground facility to display hydraulic conductivity  
 8      sufficient to warrant investigation for lateral contaminant transport. It is also the most  
 9      transmissive continuously saturated unit above the WIPP repository. Therefore, except for a  
 10     release directly to the surface, the Culebra provides the most direct pathway between the WIPP  
 11     underground and the accessible environment. The hydrology and fluid geochemistry of the  
 12     Culebra are complex and, as a result, have received a great deal of study (see, for example,  
 13     LaVenue et al. 1988, 1990; Haug et al. 1987; and Siegel et al. 1991. The Magenta, although  
 14     more transmissive than the anhydrite and claystone members of the Rustler, has lower  
 15     transmissivity than the Culebra, and is unfractured at the WIPP.

16     There was no inflow of water from the Dewey Lake into the WIPP shafts after they were  
 17     completed and prior to their lining, indicating unsaturated conditions or low transmissivity.  
 18     However, since 1995, routine inspections of the WIPP exhaust shaft have revealed water  
 19     entering the shaft at a depth of approximately 24 m (80 ft) at a location where no water had been  
 20     observed during construction (the DOE is investigating the source and extent of this water; see  
 21     Sections 2.2.1.4.2.1 and Appendix DATA). The quantity and quality of water in the Dewey  
 22     Lake is also monitored in a deeper fractured zone in the Dewey Lake at well WQSP-6a (WIPP  
 23     MOC 1995).

1 The Santa Rosa is shallow and unsaturated at the site (with the exception of a perched water  
 2 table directly below the WIPP surface structures; see Section 2.2.1.4.2.2 and Appendix DATA),  
 3 and apparently receives recharge only through infiltration.

4 In conclusion, at the WIPP site, the DOE recognizes the Salado as the most significant  
 5 nontransmissive unit and the Culebra and the Magenta as the most significant transmissive units.  
 6 Other units are considered to have less important roles. The DOE's sampling and analysis of  
 7 non-Salado groundwater has focused on the Culebra and Magenta, and their hydrologic  
 8 background, presented here, is more detailed than for other non-Salado rock units. Table 2-4  
 9 provides an overview of the hydrologic characteristics of the Rustler rock units at the WIPP site  
 10 and the Rustler-Salado contact zone in Nash Draw. In developing this position on modeling the  
 11 hydrology of the WIPP, the DOE considered several modeling approaches. These are  
 12 summarized in CCA Appendix MASS, Section MASS.14.1 in general and Section MASS.15.1  
 13 for the Culebra. The DOE's conceptual models for hydrology are in Sections 6.4.5 and 6.4.6.

14 **Table 2-4. Hydrologic Characteristics of the Rustler at the WIPP and in Nash Draw**

<b>Member</b>	<b>Thickness (meters)</b>		<b>Transmissivity (square meters per second)</b>		<b>Porosity</b>	
	<b>max</b>	<b>min</b>	<b>max</b>	<b>min</b>	<b>max</b>	<b>min</b>
Forty-niner	23	13	$8 \times 10^{-8}$	$3 \times 10^{-9}$	—	—
Magenta	8.5	7	$4 \times 10^{-4}$	$1 \times 10^{-9}$	0.25	0
Tamarisk	56	26	$2.7 \times 10^{-11}$	—	—	—
Culebra	11.6	4	$1 \times 10^{-3}$	$1 \times 10^{-9}$	0.30	0.03
Los Medaños	38	29	$2.9 \times 10^{-10}$	$2.2 \times 10^{-13}$	—	—
Rustler-Salado Contact Zone in Nash Draw	18	3	$8.6 \times 10^{-6}$	$3.2 \times 10^{-11}$	0.33	0.15

15 The EPA sought information supporting the conceptualization of the disposal system and the  
 16 major site-related characteristics included in the PA modeling during the compliance review  
 17 process for Section 194.14(a)(3). In general, the EPA concluded that the groundwater hydrology  
 18 information for the various geologic and hydrostratigraphic units at the WIPP site identified the  
 19 important characteristics of the PA and was therefore technically sufficient. The EPA also noted  
 20 that the primary hydrogeologic units of concern relative to containment capability of the WIPP  
 21 are the Castile, Salado, Rustler, and the Dewey Lake.

22 The EPA noted that the potential for fluid migration through Salado marker beds and the Culebra  
 23 were acknowledged by DOE and included in the PA calculations. While the Dewey Lake is a  
 24 potential underground source of drinking water (Section 8.2.2), DOE's modeling indicated that  
 25 radionuclides will not reach the Dewey Lake, thus removing the formation as a unit needing  
 26 consideration as a pathway (Docket A-93-02, Item II-G-26 and Docket A-93-02, Item II-G-28).  
 27 The EPA concluded that Salado marker beds, and the Culebra were adequately identified and  
 28 characterized to the level necessary for PA calculations.

1    2.2.1.1 Conceptual Models of Groundwater Flow

2    The DOE addresses issues related to groundwater flow and radionuclide transport within the  
3    context of a conceptual model of how the natural hydrologic system works on a large scale. The  
4    conceptual model of regional flow around the WIPP that is presented here is based on widely  
5    accepted concepts of regional groundwater flow in groundwater basins (see, for example,  
6    Hubbert 1940; Tóth 1963; and Freeze and Witherspoon 1967).

7    See CCA Appendix MASS, Sections MASS.14.1 and MASS.14.2 for a summary of the DOE's  
8    activities leading to the acceptance of the groundwater basin model as a reasonable  
9    representation of groundwater flow in the region.

10   An idealized groundwater basin is a three-dimensional closed hydrologic unit bounded on the  
11   bottom by an impermeable rock unit (units with much smaller permeability than the units above),  
12   on the top by the ground surface, and on the sides by groundwater divides. The water table is the  
13   upper boundary of the region of saturated liquid flow. All rocks in the basin are expected to  
14   have finite permeability; in other words, hydraulic continuity exists throughout the basin. This  
15   means that the potential for liquid flow from any unit to any other units exists, although the  
16   existence of any particular flow path is dependent on a number of conditions related to gradients  
17   and permeabilities. All recharge to the basin is by infiltration of precipitation to the water table  
18   and all discharge from the basin is by flow across the water table to the land surface.

19   Differences in elevation of the water table across an idealized basin provide the driving force for  
20   groundwater flow. The pattern of groundwater flow depends on the lateral extent of the basin,  
21   the shape of the water table, and the heterogeneity of the permeability of the rocks in the basin.  
22   Water flows along gradients of hydraulic head from regions of high head to regions of low head.  
23   The highest and lowest heads in the basin occur at the water table at its highest and lowest  
24   points, respectively. Therefore, groundwater flows from the elevated regions of the water table,  
25   downward across confining layers (layers with relatively small permeability), then laterally along  
26   more conductive layers, and finally upward to exit the basin in regions where the water table  
27   (and by association, the land surface) is at low elevations. Recharge is necessary to maintain  
28   relief on the water table, without which flow does not occur.

29   Groundwater divides are boundaries across which it is assumed that no groundwater flow occurs.  
30   In general, these are located in areas where groundwater flow is dominantly downward (recharge  
31   areas) or where groundwater flow is upward (discharge areas). Topography and surface-water  
32   drainage patterns provide clues to the location of groundwater divides. Ridges between creeks  
33   and valleys may serve as recharge-type divides, and rivers, lakes, or topographic depressions  
34   may serve as discharge-type divides.

35   In the groundwater basin model, rocks can be classified into hydrostratigraphic units. A  
36   hydrostratigraphic unit is a continuous region of rock across which hydraulic properties are  
37   similar or vary within described or stated limits. The definition of hydrostratigraphic units is a  
38   practical exercise to separate rock regions with similar hydrologic characteristics from rock  
39   regions with dissimilar hydrologic characteristics. Although hydrostratigraphic units often are  
40   defined to be similar to stratigraphic units, this need not be the case. Hydrostratigraphic unit  
41   boundaries can reflect changes in hydraulic properties related to differences in composition,

1 fracturing, dissolution, or a variety of other factors that may not be reflected in the definition of  
2 stratigraphic formations.

3 Confining layers in a groundwater basin model can be characterized as allowing vertical flow  
4 only. The amount of vertical flow occurring in a confining layer generally decreases in relation  
5 to the depth of the layer. Flow in conductive units is more complicated. In general, flow will be  
6 lateral through conductive units. The magnitude (in other words, volume flux) of lateral flow is  
7 related to the thickness, conductivity, and gradient present in the unit. Gradients generally  
8 decrease in deeper units. The direction of flow is generally related to the distance the unit is  
9 from the land surface. Near the land surface, flow directions are influenced primarily by the  
10 local slope of the land surface. In deeper conductive units, flow directions are generally oriented  
11 parallel to the direction between the highest and lowest points in a groundwater basin. Thus,  
12 flow rates, volumes, and directions in conductive units in a groundwater basin are generally not  
13 expected to be the same.

14 In the WIPP region, the Salado provides an extremely low-permeability layer that forms the base  
15 for a regional groundwater-flow basin in the overlying rocks of the Rustler, Dewey Lake, and  
16 Santa Rosa. The Castile and Salado together form their own groundwater system, and they  
17 separate flow in units above them from that in units below. Because of the plastic nature of  
18 halite and the resulting low permeability, fluid pressures in the evaporites are more related to  
19 lithostatic stress than to the shape of the water table in the overlying units, and regionally neither  
20 vertical nor horizontal flow will occur as a result of natural pressure gradients in time scales  
21 relevant to the disposal system. (On a repository scale, however, the excavations themselves  
22 create pressure gradients that may induce flow near the excavated region.) Consistent with the  
23 recognition of the Salado as the base of the groundwater basin of primary interest, the following  
24 discussion is divided into three sections: hydrology of units below the Salado, hydrology of the  
25 Salado, and hydrology of the units above the Salado. The DOE has implemented the  
26 groundwater basin model in the conceptual model for groundwater flow within the rocks above  
27 the Salado. The details of the model are discussed in Section 6.4.6. Key modeling assumptions  
28 associated with the implementation are provided in Appendix PA, Attachment MASS, Section  
29 MASS.14.2.

30 Technical issues related to the Castile brine, Salado marker bed permeability, and Culebra  
31 hydraulic properties (e.g., transmissivity variation) were raised by the EPA in a letter dated  
32 December 19, 1996 (Docket A-93-02, Item II-I-01). The DOE provided additional information  
33 regarding these issues in letters dated January 24, 1997; February 7, 1997; April 15, 1997; June  
34 13, 1997; June 27, 1997; and July 3, 1997 (Docket A-93-02, Items II-I-03, II-I-07, II-I-24, II-H-  
35 44, II-H-45, and II-H-46, respectively).

36 A request was made in the December 19, 1996 EPA letter (Docket A-93-02, Item II-I-01) that  
37 DOE provide general hydraulic characteristic information for all geologic units within the  
38 disposal system by revising a partially complete table included in the letter. The DOE letter,  
39 dated February 14, 1997 (Docket A-93-02, Item II-I-08), transmitted the summary table  
40 providing the EPA with additional groundwater hydrology information related to hydraulic  
41 conductivity, storage coefficients, transmissivity, permeability, thickness, matrix and fracture  
42 characteristics, and hydraulic gradients for each of the geologic units in the WIPP disposal  
43 system. This information was reproduced as Figure IV-10 in EPA Technical Support Document

1 for Section 194.14: Content of Compliance Certification Application (Docket A-93-02, Item V-  
2 B-3).

3 In addition, the EPA in the December 19, 1996 EPA letter (Docket A-93-02, Item II-I-01)  
4 required the DOE to include the following in the discussion of conceptual models for  
5 groundwater flow: (1) the estimated infiltration at the surface and to the Dewey Lake, and (2) the  
6 estimated vertical flow of groundwater into other transmissive units within the area surrounding  
7 the WIPP. The DOE provided the estimates in a letter dated February 26, 1997 (Docket A-93-  
8 02, Item II-I-10) to EPA.

9    2.2.1.2 Units Below the Salado

10 Units of interest to the WIPP project below the Salado are the Bell Canyon and the Castile.  
11 These units have quite different hydrologic characteristics. Because of its potential to contain  
12 brine reservoirs below the repository, the hydrology of the Castile is regarded as having the most  
13 potential of all units below the Salado to impact the performance of the disposal system.

14    2.2.1.2.1 Hydrology of the Bell Canyon Formation

15 The Bell Canyon is considered for the purposes of regional groundwater flow to form a single  
16 hydrostratigraphic unit about 300 m (1,000 ft) thick. Tests at five boreholes (Atomic Energy  
17 Commission [AEC]-7, AEC-8, ERDA-10, DOE-2, and Cabin Baby [CB]-1) (CCA Appendix  
18 HYDRO, pp. 29-31; Beauheim et al. 1983, pp. 4-9 to 4-12; Beauheim 1986, p. 61-1]) indicate a  
19 range of hydraulic conductivities for the Bell Canyon from  $1.7 \times 10^{-7}$  to  $3.5 \times 10^{-12}$  m/s ( $5 \times$   
20  $10^{-2}$  ft/day to  $1 \times 10^{-6}$  ft/day). The pressure measured in the Bell Canyon at the DOE-2 and  
21 CB-1 boreholes at the time of the CCA ranged from 12.6 to 13.3 megapascals. Under the current  
22 groundwater-monitoring program, Bell Canyon water levels are measured in only two wells: CB-  
23 1 and AEC-8 (see locations in Figure 2-6).

24 After recovery from well work in 1999, the Bell Canyon water levels at CB-1 have remained  
25 steady for more than three years at 919 m (3,015 ft) above mean sea level (SNL 2003a). In  
26 contrast, since the beginning of 1994, the Bell Canyon water levels at AEC-8 have steadily risen  
27 by more than 32 m (106 ft) at a rate of approximately 0.5 m/month (1.6 ft/month) and stood at  
28 over 933.4 m (3,062 ft) above mean sea level (SNL 2003a) at the end of 2002. This water-level  
29 rise is hypothesized to be the result of deterioration of the well and not a response to actual Bell  
30 Canyon hydrologic conditions at this location. The well will be inspected and repaired or  
31 plugged and abandoned, as necessary, according to the requirements of DOE's groundwater  
32 monitoring program (see Appendix MON-2004).

33 Fluid flow in the Bell Canyon is markedly influenced by the presence of the extremely low-  
34 permeability Castile and Salado above it, which effectively isolate the Bell Canyon from  
35 interaction with overlying units except where the Castile is absent because of erosion or  
36 nondeposition, such as in the Guadalupe Mountains, or where the Capitan Reef is the overlying  
37 unit (Figures 2-30 and 2-31). Because of the isolating nature of the Castile and Salado, fluid  
38 flow directions in the Bell Canyon are sensitive only to gradients established over very long  
39 distances. At the WIPP, the brines in the Bell Canyon flow northeasterly under an estimated  
40 hydraulic gradient of 4.7 to 7.6 m/km (25 to 40 ft/mi) and discharge into the Capitan aquifer.

1 Velocities are on the order of tenths of feet per year, and groundwater yields from wells in the  
2 Bell Canyon are 2.3 to 5.8 liters (0.6 to 1.5 gallons) per minute. The fact that flow directions in  
3 the Bell Canyon under the WIPP are inferred to be almost opposite to the flow directions in units  
4 above the Salado (see Section 2.2.1.4) is not of concern because, as discussed above, the  
5 presence of the Castile and Salado makes the flow in the Bell Canyon sensitive to gradients  
6 established over long distances, whereas flow in the units above the Salado is sensitive to  
7 gradients established by more local variations in water table elevation.

8 As discussed in Appendix DATA, oil companies are currently involved in deep-well injection at  
9 several locations outside of the WIPP site boundary. Specifically, salt water (brine) produced  
10 during oil-field exploitation is injected into the Bell Canyon and Brushy Canyon Formations.  
11 For nearly four years, the DOE has monitored injection rates and pressures for a cluster of six of  
12 these salt water injection wells located approximately 1.6 to 2.4 km (1 to 1.5 mi) northeast of  
13 well H-9. Table 2-5 summarizes the depth intervals of the injection zones for each well. The  
14 cluster of six wells is currently injecting approximately 800 to 950 m<sup>3</sup> per day (5,000 to 6,000  
15 barrels per day) of salt water; however, in previous years, injection has ranged from  
16 approximately 480 to 1270 m<sup>3</sup> per day (3,000 to 8,000 barrels per day) (SNL 2003a). Wellhead  
17 injection pressures typically range between 5.5 to 6.9 MPa (800 to 1,000 psi). Because only two  
18 Bell Canyon wells are currently being monitored, the effect of salt-water injection on Bell  
19 Canyon water levels is speculative, but water levels in the Bell Canyon monitoring well nearest  
20 the cluster (i.e., CB-1, Figure 2-6) indicate no response to the injection. Additional discussion on  
21 potential effects of salt-water injection on the WIPP hydrologic setting is provided below in  
22 Section 2.2.1.4.

23 2.2.1.2.2 Castile Hydrology

24 As described in Section 2.1.3, the Castile is dominated by low-permeability anhydrite and halite  
25 zones. However, fracturing in the upper anhydrite has generated isolated regions with much  
26 greater permeability than the surrounding intact anhydrite. These regions are located in the area  
27 of structural deformation, as discussed in Section 2.1.6.1.1. The higher-permeability regions of  
28 the Castile contain brine at pressures greater than hydrostatic and have been referred to as brine  
29 reservoirs (see Figure 2-32). The fluid pressure measured by Popielak et al. (1983) in the WIPP-  
30 12 borehole (12.7 megapascals) is greater than the nominal hydrostatic pressure for a column of  
31 equivalent brine at that depth (11.1 megapascals).

32 Therefore, under open-hole conditions, brine could flow upward to the surface through a  
33 borehole.

34 Results of hydraulic tests performed in the ERDA-6 and WIPP-12 boreholes suggest that the  
35 extent of the highly permeable portions of the Castile is limited. As discussed in Section 2.1.3.3  
36 and modeled in Section 6.4.8, the vast majority of brine is thought to be stored in low-  
37 permeability microfractures; about five percent of the overall brine volume is stored in large

1           **Table 2-5. Depth Intervals of the Injection Zones of Six Salt-Water Injection Wells**  
 2           **Located Near Well H-9 (after SNL 2003a)**

Injection Well	Depth Interval of Injection Zone, feet <sup>(1)</sup>
Cal Mon #5	4,484 – 5,780 <sup>(2)</sup>
Sand Dunes 28F#1 <sup>(3)</sup>	4,295 – 5,570 <sup>(2)</sup>
Pure Gold B F#20 <sup>(3)</sup>	7,740 – 7,774 <sup>(4)</sup>
Todd 26F#2	4,460 – 5,134 <sup>(2)</sup>
Todd 26F#3	4,390 – 6,048 <sup>(2)</sup>
Todd 27F#16	4,694 – 5,284 <sup>(2)</sup>

<sup>(1)</sup> Below ground surface, bgs

<sup>(2)</sup> Bell Canyon Formation

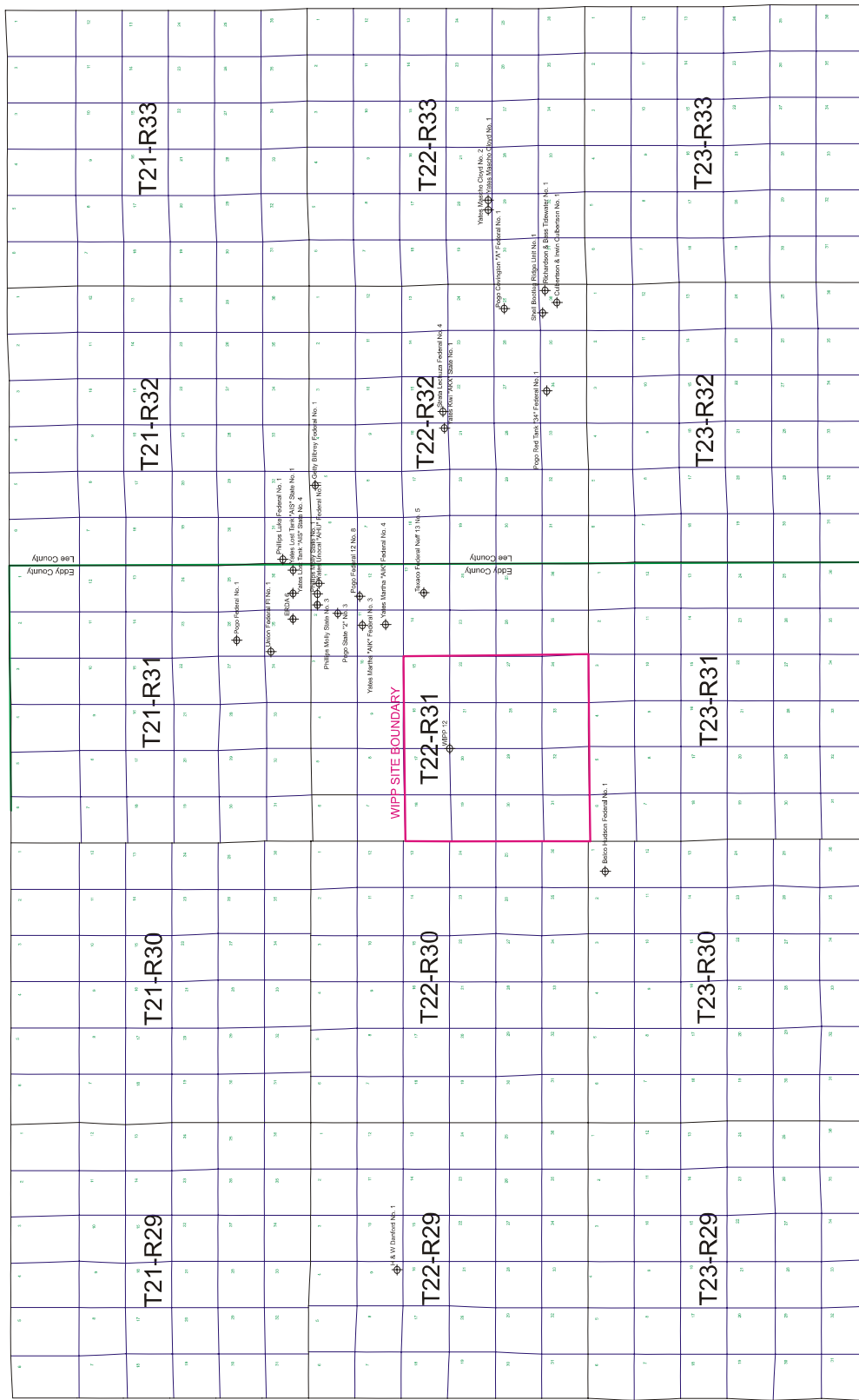
<sup>(3)</sup> Wells hydraulically connected to same manifold

<sup>(4)</sup> Brushy Canyon Formation

3       open fractures. The volumes of the ERDA-6 and WIPP-12 brine reservoirs were estimated by  
 4       Popielak et al. (1983) to be  $100,000 \text{ m}^3$  ( $3.5 \times 10^6 \text{ ft}^3$ ) and  $2,700,000 \text{ m}^3$  ( $9.5 \times 10^7 \text{ ft}^3$ ),  
 5       respectively. The conceptual model of the Castile brine region is discussed in Section 6.4.8. The  
 6       model uses parameter values derived from the ERDA-6 and WIPP-12 tests for quantifying some  
 7       reservoir characteristics. The derivation of some model parameters in Appendix PA, Attachment  
 8       PAR, Table PAR-44 from the data discussed here is also given in CCA Appendix MASS,  
 9       Section MASS.18.

10      A geophysical survey using time-domain electromagnetic (TDEM) methods was completed over  
 11     the WIPP-12 brine reservoir and the waste disposal panels (The Earth Technology Corporation  
 12     1988). The TDEM measurements detected a conductor interpreted to be the WIPP-12 brine  
 13     reservoir and also indicated that similar brine occurrences may be present within the Castile  
 14     under a portion of the waste disposal panels. Powers et al. (1996) used 354 drill holes and 27  
 15     Castile brine occurrences to establish that there is an eight percent probability of a hole drilled  
 16     into the waste panel region encountering brine in the Castile. This analysis was included as CCA  
 17     Appendix MASS, Attachment 18-6.

18      Initially, the EPA found that DOE's discussion of the size, orientation, and repressurization  
 19     potential of the Castile brine reservoirs was not well supported (Docket A-93-02, Item II-I-27).  
 20     The EPA required the probability of encountering a brine reservoir to be sampled between a  
 21     range of 1 and 60 percent in the PAVT (Docket A-93-02, Item II-G-26 and Docket A-93-02,  
 22     Item II-G-28). In addition, the EPA modified the values for parameters such as bulk  
 23     compressibility of Castile rock so that the brine reservoir sampling used in the PA would better  
 24     represent the larger, higher-end possible brine volumes. Further information on the EPA review  
 25     of these parameters may be found in CARD 23—Models and Computer Codes (EPA 1998f),  
 26     EPA Technical Support Document for Section 23: Models and Computer Codes (Docket A-93-  
 27     02, Item V-B-6), and EPA Technical Support Document for Section 23: Ground



Note: Full-sized map of this figure is in a pocket at the end of this volume.

♦ Castile Brine Well Locations

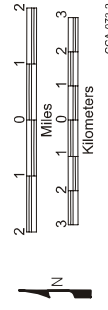


**Figure 2-32. Recent Occurrences of Pressurized Brine in the Castle**

1 Water Flow and Contaminant Transport Modeling at WIPP (Docket A-93-02, Item V-B-7). The  
2 PAVT used modified Castile brine reservoir characteristics and showed that the WIPP still meets  
3 the containment requirements (Docket A-93-02, Item II-G-26, Figure 7-2).

4 Based on these analyses, there was no significant impact on releases over the range of  
5 probabilities sampled. However, the DOE identified this parameter as a compliance monitoring  
6 parameter (see Appendix DATA) and conducts annual surveys as part of the Delaware Basin  
7 Monitoring Program (see Appendix MON-2004) to identify Castile brine encounters by drillers  
8 in the basin. Since the CCA, these surveys have identified five additional brine encounters.  
9 Appendix DATA provides extensive information pertinent to the brine reservoirs. The Delaware  
10 Basin Monitoring Annual Report (DOE 2002a), for example, documents three of the five Castile  
11 brine encounters. Two were located near well ERDA-6 northeast of the WIPP site and one was  
12 located to the southwest of the site. In the two encounters northeast of the site, reports indicated  
13 several hundred barrels of brine per hour were produced, but all brine was contained within the  
14 pits; thus, it was not necessary to file a report with the New Mexico Oil Conservation Division.  
15 In the other encounter, initial flows of from 64 to 79 m<sup>3</sup> (400 to 500 barrels) per hour were  
16 observed, but flow dissipated within hours of the encounter. Because of the relatively large  
17 number of boreholes (345 wells in the nine-township area drilled between 1996 and 2002), the  
18 five brine encounters that occurred do not substantially change the probability defined by Powers  
19 et al. (1996) and are unlikely to have any significant impact on PA given the large range of  
20 probabilities sampled in the PAVT analyses.

21 The origin of brine in the Castile has been investigated geochemically. Popielak et al. (1983, p.  
22 2) concluded that the ratios of major and minor element concentrations in the brines indicate that  
23 these fluids originated from ancient seawater and that no evidence exists for fluid contribution  
24 from present meteoric waters. The Castile brine chemistries from the ERDA-6 and WIPP-12  
25 reservoirs are distinctly different from each other and from local groundwaters. These  
26 geochemical data indicate that brine in reservoirs has not mixed to any significant extent with  
27 other waters and has not circulated. The brines are saturated, or nearly so, with respect to halite  
28 and, consequently, have little potential to dissolve halite. The chemical composition of Castile  
29 brine is given in Table 2-6. It's the use of the chemical composition of Castile brine as a  
30 parameter in the conceptual model of repository performance is discussed in Appendix PA.

31    2.2.1.3 Hydrology of the Salado

32 As described in Section 2.1.3, the Salado consists mainly of halite and anhydrite. A considerable  
33 amount of information about the hydraulic properties of these rocks has been collected through  
34 field and laboratory experiments. Appendix PA summarizes this information.

35 Hydraulic testing in the Salado in boreholes in the WIPP underground repository provided  
36 quantitative estimates of the hydraulic properties controlling brine flow through the Salado  
37 (Beauheim et al. 1991a; Beauheim et al. 1993; Domski et al. 1996; Roberts et al. 1999). This  
38 work was summarized by Beauheim and Roberts (2002). The stratigraphic intervals tested

1

**Table 2-6. WIPP Salado and Castile Brine Compositions**

	<b>Salado Brine Average (n between 82 and 96)</b>		<b>Castile ERDA-6</b>	<b>Castile WIPP-12</b>
Specific Gravity	1.22	± 0.01	1.216	1.215
pH	6.1		6.17	7.06
Sodium	79100	± 2,100	112000	138000
Potassium	15900	± 800	3800	2900
Calcium	282	± 38	490	350
Magnesium	22700	± 1,400	450	1600
Boron	1450	± 120	680	990
Lithium	nd		240	280
Silicon	1.6	± 0.7	21	27
Strontium	1.6	± 0.6	18	19
Ammonium	148	± 16	1119	476
Nitrate	0.8	(median)	2746	2436
Chloride	193000	± 4,000	170000	178000
Sulfate	17000	± 900	16000	18000
Bromide	1500	± 60	880	510
Iodide	14.8	± 3.1	28	24
Alkalinity (as HCO <sub>3</sub> <sup>-</sup> equivalent) <sup>1</sup>	883	± 123	2600	2700
Total Organic Carbon	54	± 50	nd	nd
Total Dissolved Solids	374000	± 13,000	330000	328000

<sup>1</sup> Alkalinity measured to an endpoint pH of 2.5 and expressed as equivalent bicarbonate.

Legend:

nd not determined

Note: All determinants reported in units of milligrams per liter (mg/L), except for pH and Specific Gravity. Only determinants with a concentration in excess of 10 mg/L in at least one of the brines are shown. Data taken from DOE (1994, Table 3-3) and Popeliak et al. (1983, Table C.2).

- 2 include both pure and impure halite, as well as anhydrite. Tests influence rock as far as 10 m (33  
 3 ft) distant from the test zone and therefore provide results representative of rock beyond the zone  
 4 of mechanical disturbance associated with drilling of the test boreholes. Because tests close to  
 5 the repository are within the DRZ that surrounds the excavated regions (see Section 3.2), results  
 6 of the tests farthest from the repository are most representative of undisturbed conditions.  
 7 Fifty-nine intervals were isolated and monitored and/or tested in 27 boreholes. Thirty-five of the  
 8 intervals isolated halite beds, and 24 isolated anhydrite beds. Permeability estimates were  
 9 obtained from 14 of the halite intervals and 16 of the anhydrite intervals. Interpreted

1 permeabilities using a Darcy-flow model vary from  $2 \times 10^{-23}$  to  $3 \times 10^{-16} \text{ m}^2$  for impure halite  
2 intervals, with the lower values representing halite with few impurities and the higher values  
3 representing intervals within the DRZ of the excavations. Interpreted formation pore pressures  
4 vary from atmospheric to 9.8 MPa for impure halite, with the lower pressures showing the  
5 effects of the DRZ. Tests in pure halite show no observable response, indicating either  
6 extremely low permeability ( $< 10^{-23} \text{ m}^2$ ), or no flow whatsoever, even though appreciable  
7 pressures are applied to the test intervals.

8 Interpreted permeabilities using a Darcy-flow model vary from  $2 \times 10^{-20}$  to  $9 \times 10^{-18} \text{ m}^2$  for  
9 anhydrite intervals. Interpreted formation pore pressures vary from atmospheric to 14.8 MPa for  
10 anhydrite intervals (Beauheim and Roberts 2002 p. 82). Lower values are caused by  
11 depressurization near the excavation.

12 As discussed in Beauheim and Roberts (2002), permeabilities of some tested intervals have been  
13 found to be dependent on the pressures at which the tests were conducted, which is interpreted as  
14 the result of fracture apertures changing in response to changes in effective stress. Flow  
15 dimensions inferred from most test responses are subradial, meaning that flow to/from the test  
16 boreholes is not radially symmetric but is derived from a subset of the rock volume. The  
17 subradial flow dimensions are believed to reflect channeling of flow through fracture networks,  
18 or portions of fractures, that occupy a diminishing proportion of the radially available space, or  
19 through percolation networks that are not “saturated” (that is, fully interconnected). This is  
20 probably related to the directional nature of the permeability created or enhanced by excavation  
21 effects. Other test responses indicate flow dimensions between radial and spherical, which may  
22 reflect propagation of pressure transients above or below the plane of the test interval or into  
23 regions of increased permeability (e.g., closer to an excavation). The variable stress and pore-  
24 pressure fields around the WIPP excavations probably contribute to the observed non-radial flow  
25 dimensions.

26 The properties of anhydrite interbeds have also been investigated in the laboratory. Tests were  
27 performed on three groups of core samples from MB 139 as part of the Salado Two-Phase Flow  
28 Laboratory Program. The laboratory experiments provided porosity, intrinsic permeability, and  
29 capillary pressure data. Analysis of capillary pressure test results indicates a threshold pressure  
30 of less than 1 MPa. Both laboratory and field data were used to establish hydraulic parameters  
31 for the Salado for PA as summarized in CCA Appendix PAR (Tables PAR-6 and PAR-7).

32 The EPA believed the DOE’s initial information on anhydrite characteristics and response to  
33 high pressure was unclear. In response, the DOE provided the EPA with data on modeling  
34 implementation and anhydrite characterization clarifying DOE’s approach to anhydrite fracture  
35 properties under pressurized conditions. The EPA concluded that while fracture distribution and  
36 subsequent fluid flow in the Salado marker beds cannot be detailed, the general application of  
37 fracturing and subsequent fluid flow appears to be an adequate representation of overall site  
38 conditions. The EPA also concluded that DOE’s modeling of fractures within Salado anhydrite  
39 marker beds is acceptable. For further discussion on this topic, see CARD 23—Models and  
40 Computer Codes, Section 1.3.2.

41 Fluid pressure above hydrostatic is a hydrologic characteristic of the Salado (and the Castile) that  
42 plays a potentially important role in the repository behavior. It is difficult to measure natural

1 pressures in these formations accurately because the boreholes or repository excavations required  
2 to access the rocks decrease the stress in the region measured. Stress released instantaneously  
3 decreases fluid pressure in the pores of the rock, so measured pressures must be considered as a  
4 lower bound of the natural pressures. Stress effects related to test location and the difficulty of  
5 making long-duration tests in lower-permeability rocks result in higher pore pressures observed  
6 to date in anhydrites. The highest observed pore pressures in halite-rich units, near Room Q, are  
7 on the order of 9 MPa, whereas the highest pore pressures observed in anhydrite are  
8 approximately 12 MPa (Beauheim and Roberts 2002, p. 82). Far-field pore pressures in halite-  
9 rich and anhydrite beds in the Salado at the repository level are expected to be similar because  
10 the anhydrites are too thin and of too low permeabilities to have liquid pressures much different  
11 than those of the surrounding salt. For comparison, the hydrostatic pressure for a column of  
12 brine at the depth of the repository is about 7 MPa, and the lithostatic pressure calculated from  
13 density measurements in ERDA-9 is about 15 MPa.

14 Fluid pressures in sedimentary basins that are much higher or much lower than hydrostatic are  
15 referred to as abnormal pressures by the petroleum industry, where they have received  
16 considerable attention. In the case of the Delaware Basin evaporites, the high pressures are  
17 almost certainly maintained because of the large compressibility and plastic nature of the halite  
18 and, to a lesser extent, the anhydrite. The lithostatic pressure at a particular horizon must be  
19 supported by a combination of the stress felt by both the rock matrix and the pore fluid. In  
20 highly deformable rocks, the portion of the stress that must be borne by the fluid exceeds  
21 hydrostatic pressure but cannot exceed lithostatic pressure.

22 Brine content within the Salado is estimated at 1 to 2 percent by weight, although the thin clay  
23 seams have been inferred by Deal et al. (1993, pp. 4-3) to contain up to 25 percent brine by  
24 volume. Where sufficient permeability exists, this brine will move towards areas of lower  
25 hydraulic potential, such as a borehole or mined section of the Salado.

26 Observation of the response of pore fluids in the Salado to changes in pressure boundary  
27 conditions at walls in the repository, in boreholes without packers, in packer-sealed boreholes, or  
28 in laboratory experiments is complicated by low permeability and low porosity. Qualitative data  
29 on brine flow to underground workings and exploratory boreholes were collected routinely  
30 between 1985 and 1993 under the Brine Sampling and Evaluation Program (BSEP) and have  
31 been documented in a series of reports (Deal and Case 1987; Deal et al. 1987, 1989, 1991a,  
32 1991b, 1993, and 1995). A discussion of alternative conceptual models for Salado fluid flow is  
33 given in Appendix PA, Attachment MASS, Section MASS.7. Additional data on brine inflow  
34 are available from the Large-Scale Brine Inflow Test (Room Q). Flow has been observed to  
35 move to walls in the repository, to boreholes without packers, and to packer-sealed boreholes.  
36 These qualitative and relatively short-term observations suggest that brine flow in the fractured  
37 DRZ is a complex process. In some locations, evidence for flow is no longer observed where it  
38 once was; in others, flow has begun where it once was not observed. In many cases,  
39 observations and experiments must last for months or years to obtain useful results.

40 For PA modeling, brine flow is a calculated term dependent on local hydraulic gradients and  
41 properties of the Salado units. Data on pore pressure and permeability of halite and anhydrite  
42 layers are available from the Room Q tests and other borehole tests as summarized in Beauheim

1 and Roberts (2002), and these data form the basis for the quantification of the material properties  
2 used in the PA. See Section 6.4.3.2 for a description of the repository fluid flow model.

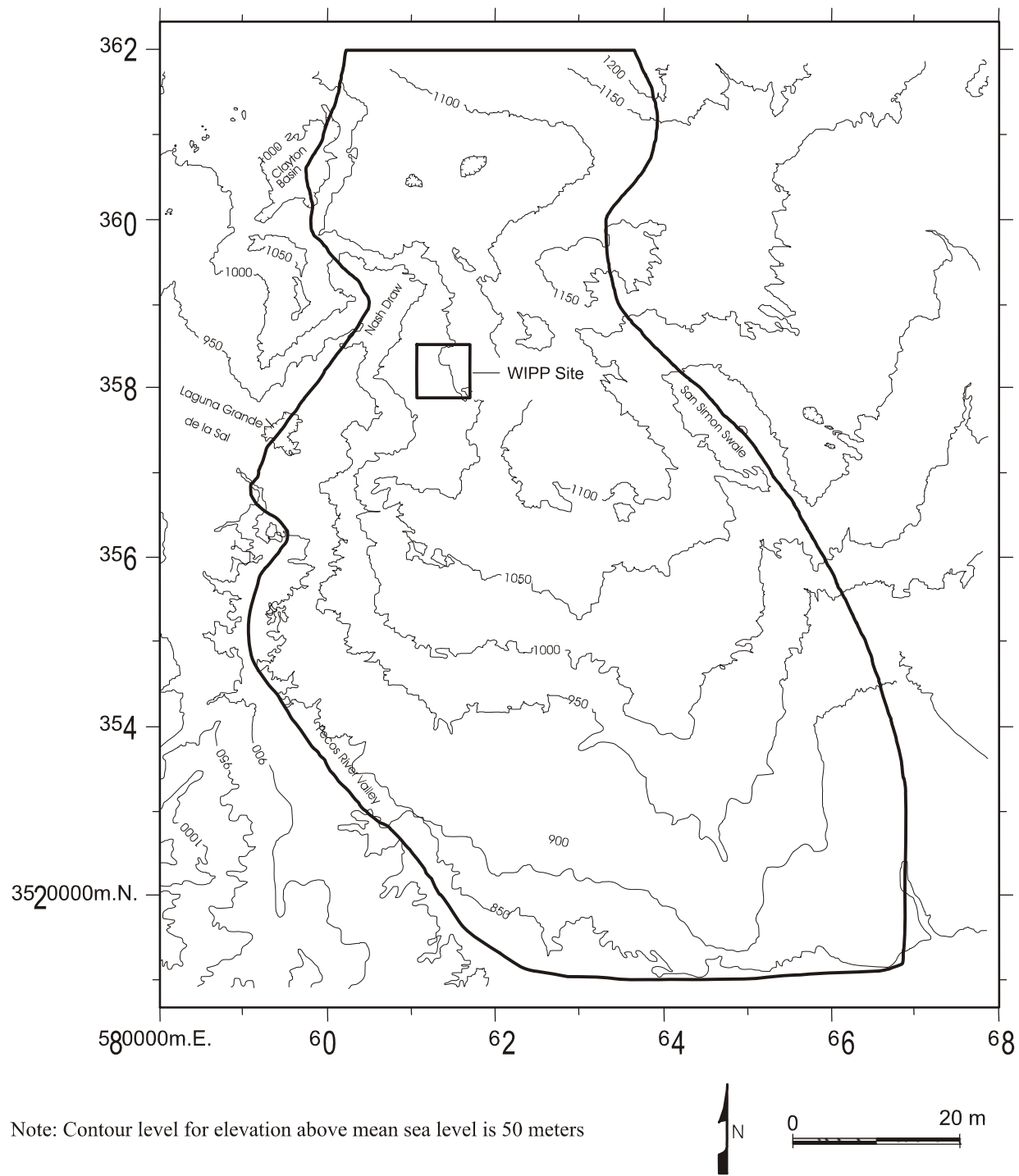
3 Because brine is an important factor in repository performance, several studies of its chemistry  
4 have been conducted. Initial investigations were reported in Powers et al. (CCA Appendix GCR,  
5 Section 7.5) and were continued once access to the underground was established. The most  
6 comprehensive data were developed by the BSEP (Deal and Case 1987; Deal et al. 1987, 1989,  
7 1991a, 1991b, 1993, 1995). Results are summarized in Table 2-6. CCA Appendix SOTERM  
8 discusses the role of brine chemistry in the conceptual model for actinide dissolution. The  
9 conceptual model is described in Section 6.4.3.5.

10 **2.2.1.4 Units Above the Salado**

11 In evaluating groundwater flow above the Salado, the DOE considers the Rustler, Dewey Lake,  
12 Santa Rosa, and overlying units to form a groundwater basin with boundaries coinciding with  
13 selected groundwater divides as discussed in Section 2.2.1.1. The model boundary follows Nash  
14 Draw and the Pecos River valley to the west and south and the San Simon Swale to the east  
15 (Figure 2-33). The boundary continues up drainages and dissects topographic highs along its  
16 northern part. These boundaries represent groundwater divides whose positions remain fixed  
17 over the past several thousand years and 10,000 years into the future. For reasons described in  
18 Section 2.2.1.2.1, the lower boundary of the groundwater basin is the upper surface of the  
19 Salado. Nash Draw and the Pecos River are areas where discharge to the surface occurs. Hunter  
20 (1985) described discharge at Surprise Spring and into saline lakes in Nash Draw. She reported  
21 groundwater discharge into the Pecos River between Avalon Dam north of Carlsbad and a point  
22 south of Malaga Bend as approximately  $0.92 \text{ m}^3/\text{s}$  ( $32.5 \text{ ft}^3/\text{s}$ ), mostly in the region near Malaga  
23 Bend.

24 Within this groundwater basin, hydrostratigraphic units with relatively high permeability are  
25 called conductive units, and those with relatively low permeability are called confining layers.  
26 The confining layers consist of halite and anhydrite and are perhaps five orders of magnitude less  
27 permeable than conductive units.

28 In a groundwater basin, the position of the water table moves up and down in response to  
29 changes in recharge. The amount of recharge is generally a very small fraction of the amount of  
30 rainfall; this condition is expected for the WIPP. Modeling of recharge changes within the  
31 groundwater basin as a function of climate variation is discussed in Section 6.4.9. The water  
32 table would stabilize at a particular position if the pattern of recharge remained constant for a  
33 long time. The equilibrated position depends, in part, on the distribution of hydraulic  
34 conductivity in all hydrostratigraphic units in the groundwater basin. However, the position of  
35 the water table depends mainly on the topography and geometry of the groundwater basin and  
36 the hydraulic conductivity of the uppermost strata. The position of the water table can adjust  
37 slowly to changes in recharge. Consequently, the water table can be at a position that is very  
38 much different from its equilibrium position at any given time. Generally, the water table drops



2 **Figure 2-33. Outline of the Groundwater Basin Model Domain on a Topographic Map**

1 very slowly in response to decreasing recharge but might rise rapidly in times of increasing  
2 recharge.

3 The asymmetry of response occurs because the rate at which the water table drops is limited by  
4 the rate at which water flows through the entire basin. In contrast, the rate at which the water  
5 table rises depends mainly on the recharge rate and the porosity of the uppermost strata. From  
6 groundwater basin modeling, the head distribution in the groundwater basin appears to  
7 equilibrate rapidly with the position of the water table.

8 The groundwater basin conceptual model (Corbet and Knupp 1996) described above has been  
9 implemented in a numerical model, as described in CCA Appendix MASS, Section MASS.14.2.  
10 This model has been used to simulate the interactive nature of flow through conductive layers  
11 and confining units for a variety of possible rock properties and climate futures. Thus, this  
12 model has allowed insight into the magnitude of flow through various units. The DOE has used  
13 this insight as a basis for model simplifications used in PA that are described here and in Chapter  
14 6.

15 One conclusion from the regional groundwater basin modeling is pertinent here. In general,  
16 vertical leakage through confining layers is directed downward over all of the controlled area.  
17 This downward leakage uniformly over the WIPP site is the result of a well-developed discharge  
18 area, Nash Draw and the Pecos River, along the western and southern boundaries of the  
19 groundwater basin. This area acts as a drain for the laterally conductive units in the groundwater  
20 basin, causing most vertical leakage in the groundwater basin to occur in a downward direction.  
21 This conclusion is important in PA simplifications related to the relative importance of lateral  
22 flow in the Magenta versus the Culebra, which will be discussed later in this chapter and in  
23 Section 6.4.6.

24 Public concern was expressed that groundwater flow to the spring supplying brine to Laguna  
25 Grande de la Sal could be related to the presence of karst features. The EPA examined  
26 information regarding the hydrology of the units above the Salado and DOE's conceptualization  
27 of the groundwater flow model, including supplementary information submitted in letters dated  
28 May 2, 1997 (Docket A-93-02, Item V-B-6 (6)), and May 14, 1997 (Docket A-93-02, Item II-I-  
29 31), and the EPA concluded that the information was adequate.

30 The EPA concluded, based on WIPP field observations and site-specific hydrologic information,  
31 there is no indication that any cavernous or other karst-related flow is present within the WIPP  
32 site boundary. The EPA concurred with DOE's conceptualization of groundwater flow in the  
33 Culebra, which includes the presence of fractures within the Culebra and recharge and discharge  
34 areas for groundwater that are more consistent with potential discharge to areas south and west  
35 of the WIPP.

### 36 2.2.1.4.1 Hydrology of the Rustler Formation

37 The Rustler is of particular importance for WIPP because it contains the most transmissive units  
38 above the repository. Fluid flow in the Rustler is characterized by very slow rates of vertical  
39 leakage through confining layers and faster lateral flow in conductive units. To illustrate this  
40 point, regional modeling with the groundwater basin model indicates that lateral specific

1 discharges in the Culebra, for example, are perhaps two to three orders of magnitude greater than  
2 the vertical specific discharges across the top of the Culebra.

3 Because of its importance, the Rustler continues to be the focus of studies to understand better  
4 the complex relationship between hydrologic properties and geology, particularly in view of  
5 water-level rises observed in the Culebra and Magenta (e.g., SNL 2003a; also see Appendix  
6 DATA). An example of the complex nature of Rustler hydrology is the variation in Culebra  
7 transmissivity (T). Culebra T varies over three orders of magnitude on the WIPP site itself and  
8 over six orders of magnitude on the scale of the regional groundwater basin model with lower T  
9 east of the site and higher T west of the site in Nash Draw (e.g., Beauheim and Ruskauff 1998).  
10 As discussed below, site investigations and studies (e.g., Holt and Powers 1988; Beauheim and  
11 Holt 1990; Powers and Holt 1995; Holt 1997; Holt and Yarbrough 2002; Powers et al. 2003)  
12 suggest that the variability in Culebra T can be explained largely by the thickness of Culebra  
13 overburden, the location and extent of upper Salado dissolution, and the occurrence of halite in  
14 the mudstone units bounding the Culebra (see Section 2.1.3.5).

15 **2.2.1.4.1.1 *Los Medaños***

16 The unnamed lower member was named the Los Medaños by Powers and Holt (1999). The Los  
17 Medaños is treated as a single hydrostratigraphic unit in WIPP models of the Rustler, although  
18 its composition varies. Overall, it acts as a confining layer. The basal interval of the Los  
19 Medaños, approximately 19.5 m (64 ft) thick, is composed of siltstone, mudstone, and claystone  
20 and contains the water-producing zones of the lowermost Rustler. Transmissivities of  $2.9 \times 10^{-10}$   
21  $\text{m}^2/\text{s}$  ( $2.7 \times 10^{-4}$   $\text{ft}^2/\text{day}$ ) and  $2.4 \times 10^{-10}$   $\text{m}^2/\text{s}$  ( $2.2 \times 10^{-4}$   $\text{ft}^2/\text{day}$ ) were reported by Beauheim  
22 (1987a, p. 50) from tests at well H-16 that included this interval. The porosity of the Los  
23 Medaños was measured in 1995 as part of testing at the H-19 hydropad (TerraTek 1996). Two  
24 claystone samples had effective porosities of 26.8 and 27.3 percent. One anhydrite sample had an  
25 effective porosity of 0.2 percent. The transmissivity values correspond to hydraulic  
26 conductivities of  $1.5 \times 10^{-11}$   $\text{m}/\text{s}$  ( $4.2 \times 10^{-6}$   $\text{ft}/\text{day}$ ) and  $1.2 \times 10^{-11}$   $\text{m}/\text{s}$  ( $3.4 \times 10^{-6}$   $\text{ft}/\text{day}$ ).  
27 Hydraulic conductivity in the lower portion of the Los Medaños is believed by the DOE to  
28 increase to the west in and near Nash Draw, where dissolution at the underlying Rustler-Salado  
29 contact has caused subsidence and fracturing of the sandstone and siltstone.

30 The remainder of the Los Medaños contains mudstones, anhydrite, and variable amounts of  
31 halite. The hydraulic conductivity of these lithologies is extremely low. It is for this reason the  
32 Los Medaños is treated as a single hydrostratigraphic unit that overall acts as a confining unit.  
33 The conceptual model incorporating the Los Medaños is discussed in Section 6.4.6.1. Important  
34 hydrologic model properties of the Los Medaños are summarized in Appendix PA.

35 As described in Section 2.1.3.5, the Los Medaños contains two mudstone layers: one in the  
36 middle of the Los Medaños and one immediately below the Culebra. An anhydrite layer  
37 separates the two mudstones. The lower and upper Los Medaños mudstones have been given the  
38 designations M1/H1 and M2/H2, respectively, by Holt and Powers (1988). This naming  
39 convention is used to indicate the presence of halite in the mudstone at some locations at and  
40 near the WIPP site. Powers (2002a) has mapped (Figure 2-15) the margins delineating the  
41 occurrence of halite in both mudstone layers. Whereas early researchers (e.g., Snyder 1985)  
42 interpreted the absence of halite west of these margins as evidence of dissolution, Holt and

1 Powers (1988) interpreted it as reflecting changes in the depositional environment, not  
2 dissolution. However, Holt and Powers (1988) concluded that dissolution of Rustler halite may  
3 have occurred along the present-day margins. The presence of halite in the Los Medaños  
4 mudstones is likely to affect the conductivity of the mudstones, but its greater importance is the  
5 implications it has for the conductivity of the Culebra. As discussed in Section 2.2.1.4.1.2, the  
6 Culebra transmissivity in locations where halite is present in M2/H2 and M3/H3 (a mudstone in  
7 the lower Tamarisk Member of the Rustler) is assumed to be an order of magnitude lower than  
8 where halite does not occur (Holt and Yarbrough 2002).

9 Fluid pressures in the Los Medaños have been continuously measured at well H-16 since 1987.  
10 During this period, the fluid pressure has remained relatively constant at between 190 and 195  
11 psi or a head of approximately 137 m (450 ft). Given the location of the pressure transducer (an  
12 elevation of 811.96 m amsl), the current elevation of the Los Medaños water level at H-16 is  
13 approximately 949 m amsl. No other wells in the WIPP monitoring network are completed to  
14 the Los Medaños. Thus, H-16 provides the only current head information for this member.

15 *2.2.1.4.1.2 The Culebra Dolomite Member*

16 The Culebra is of interest because it is the most transmissive saturated unit above the WIPP  
17 repository and hydrologic research has been concentrated on the unit for nearly two decades.  
18 Although it is relatively thin, it is an entire hydrostratigraphic unit in the WIPP hydrological  
19 conceptual model, and it is the most important conductive unit in this model. Implementation of  
20 the Culebra in the conceptual model is discussed in detail in Section 6.4.6.2. Model discussions  
21 cover groundwater flow and transport characteristics of the Culebra. These are supported by  
22 parameter values in Table 6-20, 6-21, 6-22, and 6-23. Additional background for the Culebra  
23 model is in CCA Appendix MASS, Sections MASS.14 and MASS.15.

24 The two primary types of field tests used to characterize the flow and transport characteristics of  
25 the Culebra are hydraulic tests and tracer tests.

26 The hydraulic testing consists of pumping, injection, and slug testing of wells across the study  
27 area (for example, Beauheim 1987a, p. 3). The most detailed hydraulic test data exist for the  
28 WIPP hydropads (for example, H-19). The hydropads generally comprise a network of three or  
29 more wells located within a few tens of meters of each other. Long-term pumping tests have  
30 been conducted at hydropads H-3, H-11, and H-19 and at well WIPP-13 (Beauheim 1987b;  
31 1989; Beauheim et al. 1995; Meigs et al. 2000). These pumping tests provided transient pressure  
32 data at the hydropad and over a much larger area. Tests often included use of automated data-  
33 acquisition systems, providing high-resolution (in both space and time) data sets. In addition to  
34 long-term pumping tests, slug tests and short-term pumping tests have been conducted at  
35 individual wells to provide pressure data that can be used to interpret the transmissivity at that  
36 well (Beauheim 1987a). (Additional short-term pumping tests have been conducted in the  
37 WQSP wells [Beauheim and Ruskauff 1998]). Detailed cross-hole hydraulic testing has been  
38 conducted at the H-19 hydropad (Beauheim 2000).

39 The hydraulic tests are designed to yield pressure data for the interpretation of such  
40 characteristics as transmissivity, permeability, and storativity. The pressure data from long-term  
41 pumping tests and the interpreted transmissivity values for individual wells are used for the

1 generation of transmissivity fields in PA flow modeling (see Appendix PA, Attachment TFIELD,  
2 Sections TFIELD 5.0 and TFIELD-6.0). Some of the hydraulic test data and interpretations are  
3 also important for the interpretation of transport characteristics. For instance, information about  
4 the vertical distribution of permeability interpreted from the hydraulic tests at a given hydropad  
5 is needed for interpretations of tracer test data at that hydropad.

6 To evaluate transport properties of the Culebra, a series of tracer tests were conducted at six  
7 locations (the H-2, H-3, H-4, H-6, H-11, and H-19 hydropads) near the WIPP site. Tests at the  
8 first five of these locations consisted of two-well dipole tests and/or multiwell convergent flow  
9 tests and are described in detail in Jones et al. (1992). Tracer tests at the H-19 hydropad and  
10 additional tracer tests performed at the H-11 hydropad are described in Meigs et al. (2000). The  
11 1995-1996 tracer test program consisted of single-well injection-withdrawal tests and multi-well  
12 convergent flow tests (Meigs and Beauheim 2001). Unique features of this testing program  
13 include the single-well test at both H-19 and H-11, the injection of tracers into six wells during  
14 the H-19 convergent-flow test, the injection of tracer into upper and lower zones of the Culebra  
15 at the H-19 hydropad, repeated injections under different convergent-flow pumping rates, and the  
16 use of tracers with different free-water diffusion coefficients. The 1995-1996 tracer tests were  
17 specifically designed to evaluate the importance of heterogeneity (both horizontal and vertical)  
18 and diffusion on transport processes.

19 The Culebra is a fractured dolomite with nonuniform properties both horizontally and vertically.  
20 Examination of core and shaft exposures has revealed that there are multiple scales of porosity  
21 within the Culebra including fractures ranging from microscale to potentially large, vuggy zones,  
22 and interparticle and intercrystalline porosity (Holt 1997). Porosity measurements made on core  
23 samples give porosity measurements ranging from 0.03 to 0.30 (Kelley and Saulnier 1990;  
24 TerraTek 1996). This large range in porosity for small samples is expected given the variety of  
25 porosity types within the Culebra. However, the effective porosity for flow and transport at  
26 larger scales will have a smaller range due to the effects of spatial averaging. The core  
27 measurements indicate that the Culebra has significant quantities of connected porosity.

28 Flow in the Culebra occurs within fractures, within vugs where they are connected by fractures,  
29 and to some extent within interparticle porosity where the porosity (and permeability) is high,  
30 such as chalky lenses. At any given location, flow will occur in response to hydraulic gradients  
31 in all places that are permeable. When the permeability contrast between different scales of  
32 connected porosity is large, the total porosity can effectively be conceptualized by dividing the  
33 system into advective porosity (often referred to as fracture porosity) and diffusive porosity  
34 (often referred to as matrix porosity). The advective porosity can be defined as the portion of the  
35 porosity where flow is the dominant process (for example fractures and to some extent vugs  
36 connected by fractures and interparticle porosity). Diffusive porosity can be defined as the  
37 portion of the porosity where diffusion is the dominant process (for example, intercrystalline  
38 porosity and to some extent microfractures, vugs and portions of the interparticle porosity.)

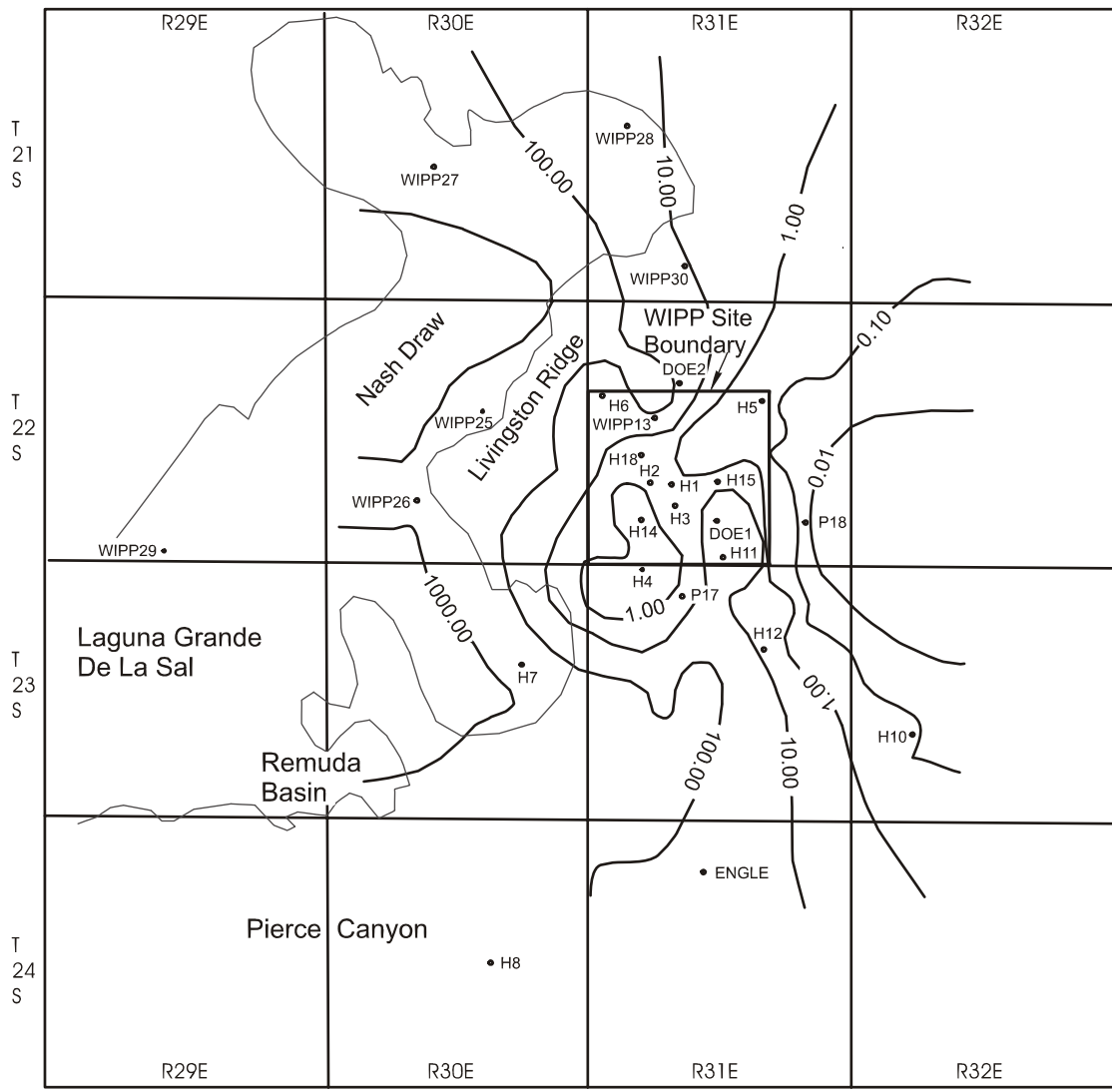
39 For the Culebra in the vicinity of the WIPP site, defining advective porosity is not a simple  
40 matter. In some regions the permeability of the fractures is inferred to be significantly larger  
41 than the permeability of the other porosity types, thus advective porosity can be conceptualized  
42 as predominantly fracture porosity (low porosity). In some regions, there appear to be no high  
43 permeability fractures. This may be due to a lack of large fractures or may be the result of

1 gypsum fillings in a portion of the porosity. Where permeability contrasts between porosity  
2 types are small, the advective porosity can be conceptualized as a combination of fractures, vugs  
3 connected by fractures, and permeable portions of the interparticle porosity. In each case, the  
4 diffusive porosity can be conceptualized as the porosity where advection is not dominant.

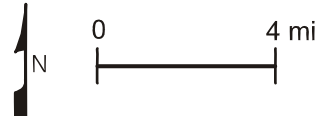
5 The major physical transport processes that affect actinide transport through the Culebra include  
6 advection (through fractures and other permeable porosity), diffusion from the advective porosity  
7 into the rest of the connected porosity (diffusive porosity) and dispersive spreading due to  
8 heterogeneity. Diffusion can be an important process for effectively retarding solutes by  
9 transferring mass from the porosity where advection (flow) is the dominant process into other  
10 portions of the rock. Diffusion into stagnant portions of the rock also provides access to  
11 additional surface area for sorption. Further discussion of transport of actinides in the Culebra as  
12 either dissolved species or as colloids is given in Section 6.4.6.2. Parameter values determined  
13 from tests of the Culebra are given in CCA Appendix PAR and are described in Section  
14 6.4.6.2.2. A summary of input values to the conceptual model is in Tables 6-22 and 6-23.

15 Fluid flow in the Culebra is dominantly lateral and southward except in discharge areas along the  
16 west or south boundaries of the basin. Where transmissive fractures exist, flow is dominated by  
17 fractures but may also occur in vugs connected by microfractures and interparticle porosity.  
18 Regions where flow is dominantly through vugs connected by microfractures and interparticle  
19 porosity have been inferred from pumping tests and tracer tests. Flow in the Culebra may be  
20 concentrated along zones that are thinner than the total thickness of the Culebra. In general, the  
21 upper portion of the Culebra is massive dolomite with a few fractures and vugs, and appears to  
22 have low permeability. The lower portion of the Culebra appears to have many more vuggy and  
23 fractured zones and to have significantly higher permeability (Meigs and Beauheim 2001).

24 There is strong evidence that the permeability of the Culebra varies spatially and varies  
25 sufficiently that it cannot be characterized with a uniform value or range over the region of  
26 interest to the WIPP. The transmissivity of the Culebra varies spatially over six orders of  
27 magnitude from east to west in the vicinity of the WIPP (Figure 2-34). Over the site, Culebra  
28 transmissivity varies over three to four orders of magnitude. CCA Appendix TFIELD, Section  
29 TFIELD.2 contains the data used to develop Figure 2-34, which shows variation in  
30 transmissivity in the Culebra in the WIPP region. Attachment TFIELD to Appendix P provides  
31 the modeling rationale and addresses how data collected over a number of years were correlated  
32 for the generation of transmissivity fields.



- Observation Well



Note: Transmissivities are given in square feet per day. Figure is modified from Cauffman et al. 1990 (Figure 5.22a). See Appendix TFIELD for details of the performance assessment implementation.

CCA-046-2

1

2

## Figure 2-34. Transmissivities of the Culebra

- 3 Transmissivities are from about  $1 \times 10^{-9} \text{ m}^2/\text{s}$  ( $1 \times 10^{-3} \text{ ft}^2/\text{day}$ ) at well P-18 east of the WIPP  
 4 site to about  $1 \times 10^{-3} \text{ m}^2/\text{s}$  ( $1 \times 10^3 \text{ ft}^2/\text{day}$ ) at well H-7 in Nash Draw (see Figure 2-2 for the  
 5 locations of these wells and see Figure 4-8 in CCA Appendix FAC for a Culebra isopach map).
- 6 Transmissivity variations in the Culebra are believed to be controlled by the relative abundance  
 7 of open fractures rather than by primary (that is, depositional) features of the unit. Lateral

1 variations in depositional environments were small within the mapped region, and primary  
2 features of the Culebra show little map-scale spatial variability, according to Holt and Powers  
3 (CCA Appendix FAC). Direct measurements of the density of open fractures are not available  
4 from core samples because of incomplete recovery and fracturing during drilling, but observation  
5 of the relatively unfractured exposures in the WIPP shafts suggests that the density of open  
6 fractures in the Culebra decreases to the east.

7 Recent investigations have made a significant contribution to the understanding of the large  
8 variability observed for Culebra transmissivity (e.g., Holt and Powers 1988; Beauheim and Holt  
9 1990; Powers and Holt 1995; Holt 1997; Holt and Yarbrough 2002; Powers et al. 2003). The  
10 spatial distribution of Culebra transmissivity is believed to be due strictly to deterministic post-  
11 depositional processes and geologic controls (Holt and Yarbrough 2002). The important  
12 geologic controls include Culebra overburden thickness, dissolution of the upper Salado, and the  
13 occurrence of halite in the mudstone Rustler units (M2/H2 and M3/H3) above and below the  
14 Culebra (Holt and Yarbrough 2002). Culebra transmissivity is inversely related to thickness of  
15 overburden because stress relief associated with erosion of overburden (see Section 2.1.5.2)  
16 leads to fracturing and opening of preexisting fractures. Culebra transmissivity is high where  
17 dissolution of the upper Salado has occurred and the Culebra has subsided and fractured.  
18 Culebra transmissivity is observed to be low where halite is present in overlying and/or  
19 underlying mudstones. Presumably, high Culebra transmissivity leads to dissolution of nearby  
20 halite (if any). Hence, the presence of halite in mudstones above and/or below the Culebra can  
21 be taken as an indicator for low Culebra transmissivity. Details of the geologic-based  
22 transmissivity model for the Culebra are given in Attachment TFIELD (Section TFIELD-3.0) to  
23 Appendix PA and summarized below.

24 The Culebra has been tested hydraulically at 42 locations, yielding reliable transmissivity values.  
25 These values ( $\log T$ ) are plotted as a function of depth to Culebra (overburden thickness) in  
26 Figure 2-35. As shown, the Culebra transmissivities fall into two populations separated by a  
27 cutoff (termed ‘high-T’ cutoff) equal to -5.4 ( $\log T$  [ $m^2/s$ ]). These data suggest a bimodal  
28 distribution for transmissivity with one population having high transmissivity and the other low  
29 transmissivity, with the difference attributed to open, interconnected fractures (“fracture  
30 interconnectivity”) for the high-transmissivity population (Holt and Yarbrough 2002). Using  
31 these data, Holt and Yarbrough (2002) constructed a linear Culebra transmissivity model relating  
32  $\log T$  to the deterministic geologic controls described above. The linear model is expressed as  
33 follows:

34 
$$Y(\mathbf{x}) = \beta_1 + \beta_2 d(\mathbf{x}) + \beta_3 I_f(\mathbf{x}) + \beta_4 I_D(\mathbf{x}), \quad (2.1)$$

35 where  $Y(x)$  is  $\log T(x)$ ,  $\beta_i$  ( $i = 1$  to 4) are regression coefficients,  $x$  is a two-dimensional location  
36 vector,  $d(x)$  is the overburden thickness at  $x$  (expressed in UTM coordinates and

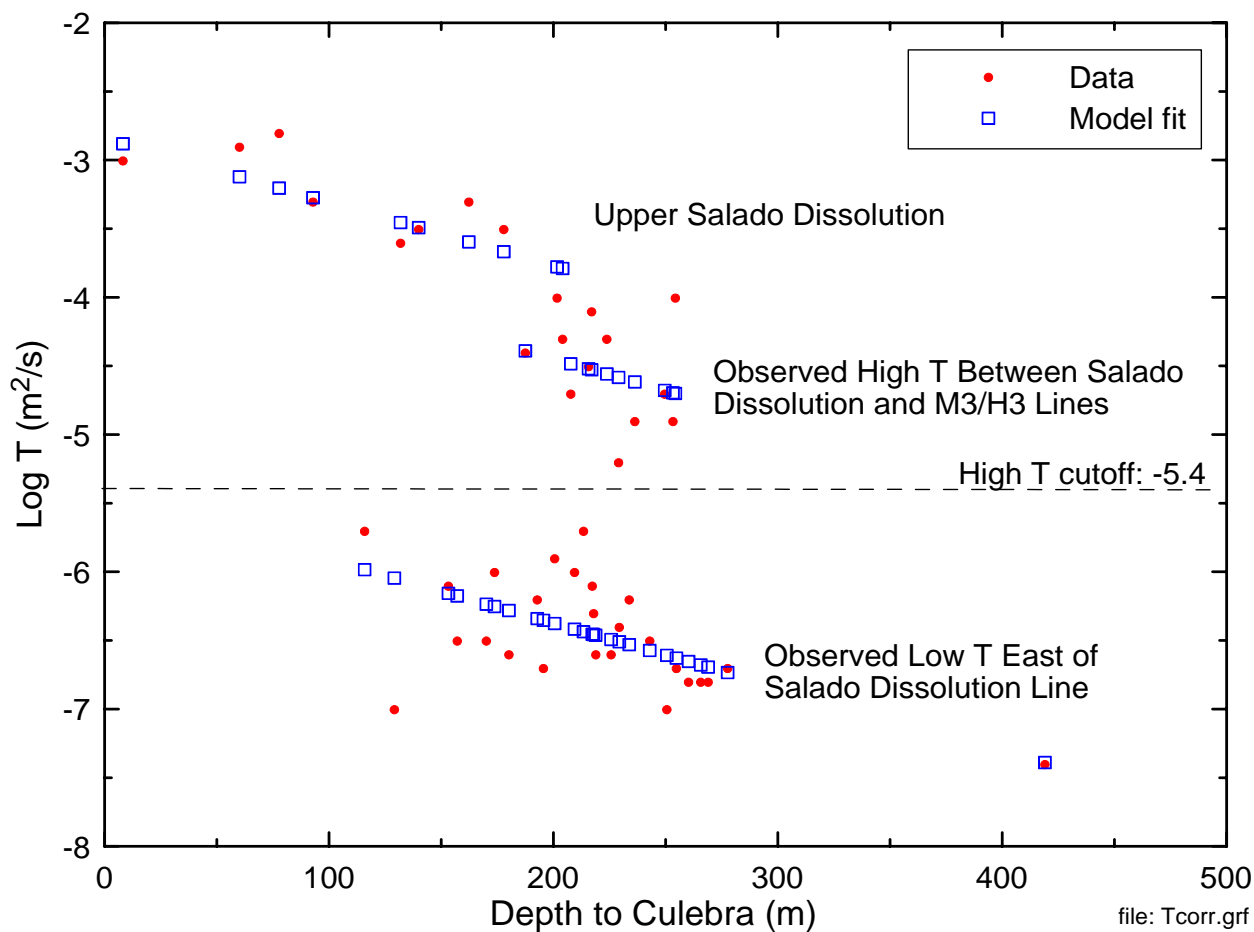


**Figure 2-35. Correlation Between Culebra Transmissivity ( $\log T$  ( $m^2/s$ )) and Overburden Thickness for Different Geologic Environments (after Holt and Yarbrough 2002)**

meters),  $I_f(x)$  is the fracture-interconnectivity indicator at  $x$  (equal to 1 when  $\log T$  ( $m^2/s$ )  $> -5.4$  or 0 when  $\log T$  ( $m^2/s$ )  $< -5.4$ ), and  $I_D(x)$  is the dissolution indicator (equal to 1 when Salado dissolution has occurred at  $(x)$  and 0 when it has not). In this model, coefficient  $\beta_1$  is the intercept value,  $\beta_2$  is the slope of  $Y(x)/d(x)$ , and  $\beta_3$  and  $\beta_4$  represent adjustments to the intercept for the occurrence of open, interconnected fractures and Salado dissolution, respectively. Based on linear-regression analysis, Holt and Yarbrough (2002) estimated the coefficients in Equation (2.1). These estimates are summarized in Table 2-7. Predictions of the Culebra transmissivity model represented by Equation (2.1) are shown in Figure 2-35.

The regression model expressed by Equation (2.1) cannot adequately predict transmissivity in the regions where halite is present both in M2/H2 and M3/H3. In these regions, Culebra

**Table 2-7. Estimates of Culebra Transmissivity Model Coefficients**

$\beta_1$	$\beta_2$	$\beta_3$	$\beta_4$
-5.441	$-4.636 \times 10^{-3}$	1.926	0.678

1 porosity is thought to be at least partially filled with halite, reducing transmissivity. For these  
2 regions, Equation (2.1) is modified as follows:

3

$$Y(\mathbf{x}) = \beta_1 + \beta_2 d(\mathbf{x}) + \beta_3 I_f(\mathbf{x}) + \beta_4 I_D(\mathbf{x}) + \beta_5 I_H(\mathbf{x}). \quad (2.2)$$

4  $I_H(\mathbf{x})$  is a halite indicator function equal to 1 in locations where halite occurs in both the M2/H2  
5 and M3/H3 intervals and 0 otherwise. The coefficient  $\beta_5$  is equal to -1 to assure that the model  
6 in Equation (2.2) reduces the predicted transmissivity values by one order of magnitude where  
7 halite occurs in both the M2/H2 and M3/H3 intervals.

8 In the region east of the upper Salado dissolution margin and west of the M2/H2 and M3/H3  
9 margins, high transmissivity depends, in part, on the absence of gypsum fracture fillings. No  
10 method has yet been determined for predicting whether fractures will or will not be filled with  
11 gypsum at a given location, so the distribution of high and low transmissivity is treated  
12 stochastically in this region. Predictions of transmissivity in this region make use of an isotropic  
13 spherical variogram model. Fitted parameters for the variogram model are described in  
14 Attachment TFIELD (Section TFIELD-4.3) of Appendix PA.

15 Geochemical and radioisotope characteristics of the Culebra have been studied. There is  
16 considerable variation in groundwater geochemistry in the Culebra. The variation has been  
17 described in terms of different hydrogeochemical facies that can be mapped in the Culebra (see  
18 Section 2.4.2). A halite-rich hydrogeochemical facies exists in the region of the WIPP site and  
19 to the east, approximately corresponding to the regions in which halite exists in units above and  
20 below the Culebra (Figure 2-15), and in which a large portion of the Culebra fractures are  
21 gypsum filled (Figure 2-17). An anhydrite-rich hydrogeochemical facies exists west and south  
22 of the WIPP site, where there is relatively less halite in adjacent strata and where there are fewer  
23 gypsum-filled fractures.

24 The Culebra groundwater geochemistry studies continue. Culebra water quality is evaluated  
25 semiannually at six wells, three north (WQSP-1, WQSP-2, and WQSP-3) and three south  
26 (WQSP-4, WQSP-5, and WQSP-6) (WIPP MOC 1995) of the surface structures area (see Figure  
27 2-3 for well locations). Five rounds of semiannual sampling of water quality completed before  
28 the first receipt of waste at the WIPP were used to establish the initial Culebra water-quality  
29 baseline for major ion species including  $\text{Na}^+$ ,  $\text{Ca}^{2+}$ ,  $\text{Mg}^{2+}$ ,  $\text{K}^+$ ,  $\text{Cl}^-$ ,  
30  $\text{SO}_4^{2-}$ , and  $\text{HCO}_3^{2-}$  (Crawley and Nagy 1998). In 2000, this baseline was expanded to include  
31 five additional rounds of sampling that were completed before first receipt of RCRA-regulated  
32 waste (IT Corporation 2000). Table 2-8 gives the 95 percent confidence intervals presented in  
33 SNL (2001) for the major ion species determined from the 10 rounds (semiannual sampling for 5  
34 years) of baseline sampling. Culebra water quality is extremely variable among the six sampling  
35 wells, as shown by the  $\text{Cl}^-$  concentrations that range from approximately 6,000 mg/L at WQSP-6  
36 to 130,000 mg/L at WQSP-3.

37 Radiogenic isotopic signatures suggest that the age of the groundwater in the Culebra is on the  
38 order of 10,000 years or more (see, for example, Lambert 1987, Lambert and Carter 1987, and  
39 Lambert and Harvey 1987). The radiogenic ages of the Culebra groundwater and the  
40 geochemical differences provide information potentially relevant to the groundwater flow  
41 directions and groundwater interaction with other units and are important constraints on

1   **Table 2-8. Ninety-Five Percent Confidence Intervals for Culebra Water-Quality Baseline**

Well I.D.	Cl <sup>-</sup> Conc. (mg/L)	SO <sub>4</sub> <sup>2-</sup> Conc. (mg/L)	HCO <sub>3</sub> <sup>-</sup> Conc. (mg/L)	Na <sup>+</sup> Conc. (mg/L)	Ca <sup>2+</sup> Conc. (mg/L)	Mg <sup>2+</sup> Conc. (mg/L)	K <sup>+</sup> Conc. (mg/L)
WQSP-1	31100-39600	4060-5600	45-54	15850-21130	1380-2030	940-1210	322-730
WQSP-2	31800-39000	4550-6380	43-53	14060-22350	1230-1730	852-1120	318-649
WQSP-3	113900-145200	6420-7870	23-51	62600-82700	1090-1620	1730-2500	2060-3150
WQSP-4	53400-63000	5620-7720	31-46	28100-37800	1420-1790	973-1410	784-1600
WQSP-5	13400-17600	4060-5940	42-54	7980-10420	902-1180	389-535	171-523
WQSP-6	5470-6380	4240-5120	41-54	3610-5380	586-777	189-233	113-245

2 conceptual models of groundwater flow. Previous conceptual models of the Culebra (see for  
 3 example, Chapman 1986, Chapman 1988, LaVenue et al. 1990, and Siegel et al. 1991) have not  
 4 been able to consistently relate the hydrogeochemical facies, radiogenic ages, and flow  
 5 constraints (that is, transmissivity, boundary conditions, etc.) in the Culebra.

6 The groundwater basin modeling that was conducted, although it did not model solute transport  
 7 processes, provides flow fields that can be used to develop the following concepts that help  
 8 explain the observed hydrogeochemical facies and radiogenic ages. The groundwater basin  
 9 model combines and tests three fundamental processes: (1) it calculates vertical leakage, which  
 10 may carry solutes into the Culebra; (2) it calculates lateral fluxes in the Culebra (directions as  
 11 well as rates); and (3) it calculates a range of possible effects of climate change. The presence of  
 12 the halite-rich groundwater facies is explained by vertical leakage of solutes into the Culebra  
 13 from the overlying halite-containing Tamarisk by advective or diffusive processes. Because  
 14 lateral flow rates here are low, even slow rates of solute transport into the Culebra can result in  
 15 high solute concentration. Vertical leakage occurs slowly over the entire model region, and thus  
 16 the age of groundwater in the Culebra is old, consistent with radiogenic information. Lateral  
 17 fluxes within the anhydrite zone are larger because of higher transmissivity, and where the halite  
 18 and anhydrite facies regions converge, the halite facies signature is lost by dilution with  
 19 relatively large quantities of anhydrite facies groundwater. Response of groundwater flow in the  
 20 Culebra as the result of increasing recharge is modeled through the variation in climate,  
 21 discussed in Section 6.4.9.

22 Groundwater levels in the Culebra in the WIPP region were measured prior to the CCA in  
 23 numerous wells (Figure 2-2). The Culebra monitoring wells as of the end of 2002 are shown in  
 24 Figures 2-3 and 2-4; plugged and abandoned wells are not shown in these figures. Beginning in  
 25 1989, a general

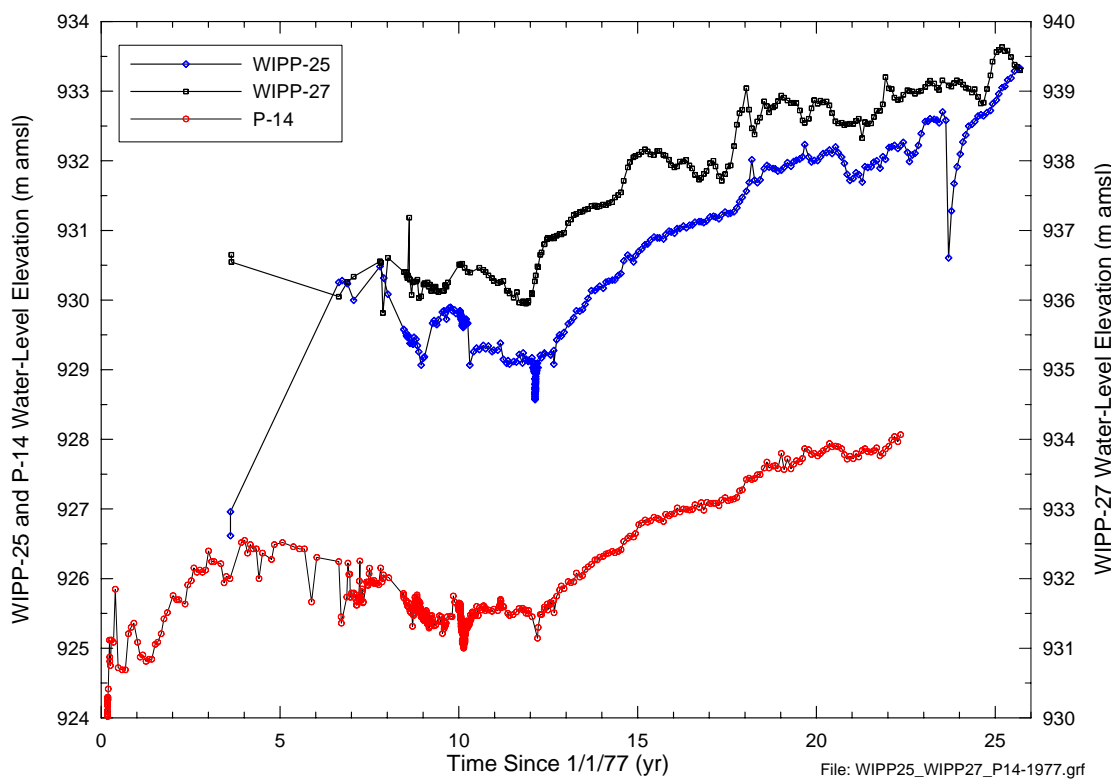


**Figure 2-36. Water-level Trends in Nash Draw Wells and at P-14 (see Figure 2-2 for well locations)**

long-term rise has been observed in both Culebra and Magenta water levels (Figure 2-36) over a broad area of the WIPP site including Nash Draw (SNL 2003a). At the time of the CCA this long-term rise was recognized, but was thought (outside of Nash Draw) to represent recovery from the accumulation of hydraulic tests that had occurred since the late 1970s and the effects of grouting around the WIPP shafts to limit leakage. Water levels in Nash Draw were thought to respond to changes in the volumes of potash mill effluent discharged into the draw (Silva 1996); however, correlation of these water levels with potash mine discharge cannot be proven because sufficient data on the timing and volumes of discharge are not available. As the rise in water levels has continued since 1996, observed heads have exceeded the ranges of uncertainty established for the steady-state heads in most of the 32 wells used in the calibration of the transmissivity fields described in CCA Appendix TFIELD. Although recovery from the hydraulic tests and shaft leakage has unquestionably occurred, the DOE has implemented a program to identify other potential causes for the water-level rises (SNL 2003b).

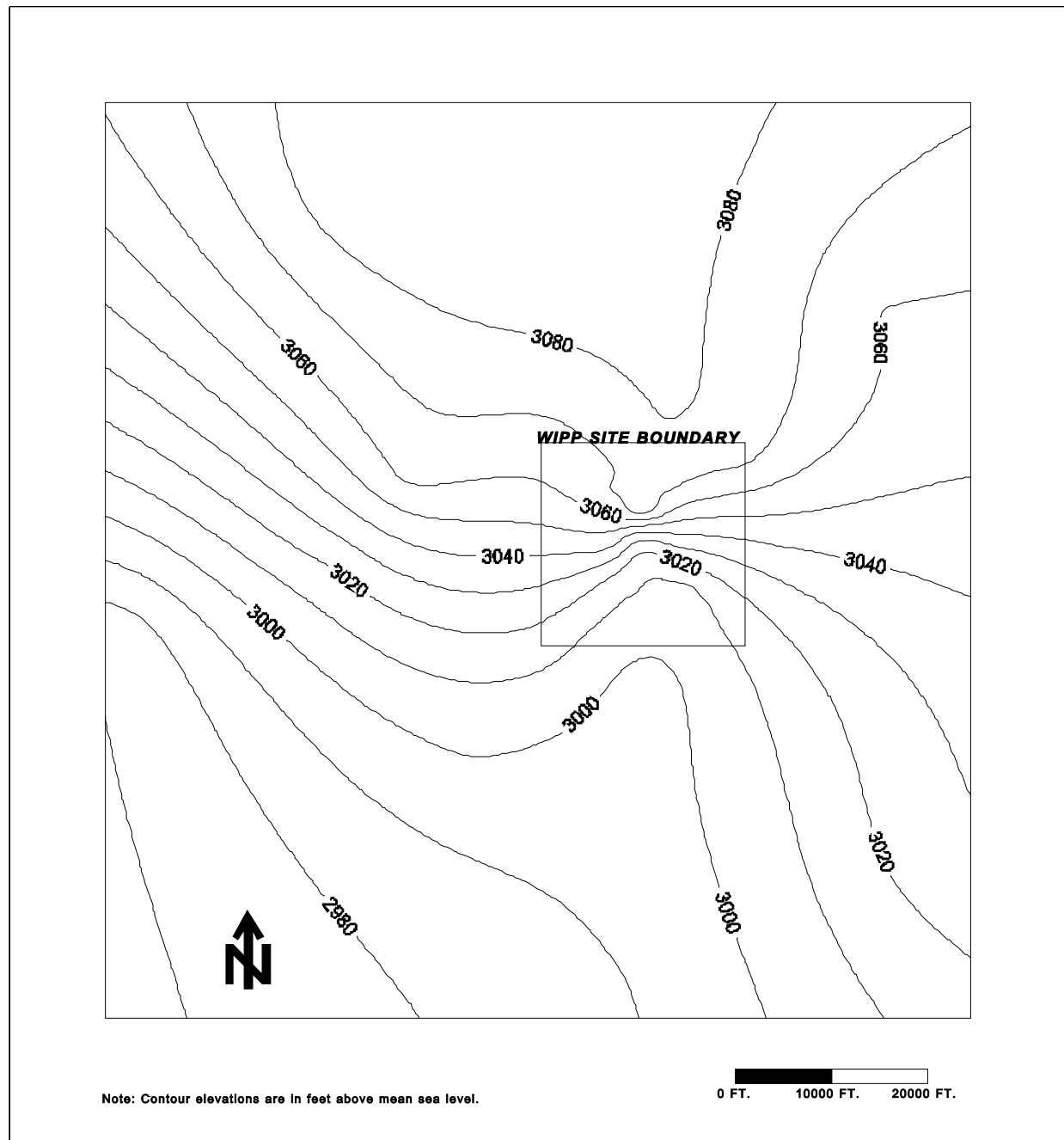
Potentiometric surface maps of the freshwater head in the Culebra in December 1998 and December 2002 are shown in Figures 2-37a, 2-37b and 2-37c, respectively. The maps are generally similar and indicate no changes in flow directions across the WIPP site over that period. Figure 2-37c shows the changes in heads at the wells monitored in both December 1998 and December 2002. Freshwater heads in most wells increased by 2-4 ft from 1998 to 2002. The largest rise was 4.84 ft at DOE-1. Only one well, AEC-7, showed a drop over this period (-0.85 ft) larger than potential measurement error.

1 Although Culebra heads have been rising, the head distribution in the Culebra (see Figures 2-  
2 37a, 2-37b and 2-37c) is consistent with groundwater basin modeling results (discussed in  
3 Appendix PA, Attachment MASS, Section MASS.14.2) indicating that the generalized direction  
4 of groundwater flow remains north to south. However, caution should be used when making  
5 assumptions based on groundwater-level data alone. Studies in the Culebra have shown that  
6 fluid density variations in the Culebra can affect flow direction (Davies 1989, p. 35). The  
7 fractured nature of the Culebra, coupled with variable fluid densities, can also cause localized  
8 flow patterns to differ from general flow patterns. Water-level rises in the vicinity of the H-9  
9 hydropad, about 10.46 km (6.5 mi) south of the site, are not thought to be caused by either WIPP  
10 activities or potash mining discharge and have been included in the DOE program to investigate  
11 Culebra water-level rises in general. The DOE continues to monitor groundwater levels  
12 throughout the region, but only water-level changes at or near the site have the potential to  
13 impact the prediction of disposal system performance. The DOE has implemented water-level  
14 changes in its conceptual model through variations in climate as discussed in Section 6.4.9.  
15 These variations bring the water table to the surface for some calculations. The DOE has also  
16 used recent (late 2000) Culebra heads in flow and transport calculations for this recertification  
17 application, as discussed in Appendix PA, Attachment TFIELD, Section TFIELD-6.2.

18 Inferences about vertical flow directions in the Culebra have been made from well data collected  
19 by the DOE. Beauheim (1987a) reported flow directions toward the Culebra from both the Los  
20 Medaños and the Magenta over the WIPP site, indicating that the Culebra acts as a drain for the  
21 units around it. This indication is consistent with results of groundwater basin modeling. A  
22 more detailed discussion of Culebra flow and transport can be found in Appendix PA,  
23 Attachment TFIELD

24 In response to an EPA letter dated March 19, 1997 (Docket A-93-02, Item II-I-17), supplemental  
25 information to the CCA pertinent to groundwater flow and geochemistry within the Culebra was  
26 provided by the DOE in a letter dated May 14, 1997 (Docket A-93-02, Item II-I-31). In that  
27 letter, the DOE explained the conceptual model of Culebra groundwater flow used in the CCA.  
28 The CCA conceptual model, referred to as the groundwater basin model, offers a three-  
29 dimensional approach to treatment of supra-Salado rock units, and assumes that vertical leakage  
30 (albeit very slow) occurs between rock units of the Rustler (where hydraulic gradients exist).  
31 Flow in the Culebra is considered transient, but is not expected to change significantly over the  
32 next 10,000 years. This differs from previous interpretations, wherein no flow was assumed  
33 between the Rustler units.

34 In an attachment to the May 14, 1997 letter, the DOE concluded that the presence of anhydrite  
35 within the Rustler units did not preclude slow downward infiltration, as previously argued by the  
36 DOE, and that the observed geochemistry and flow directions can be explained with different  
37 recharge areas and Culebra travel paths. The EPA reviewed the groundwater flow and recharge  
38 conceptualization and concluded that it provides a realistic representation of site conditions.

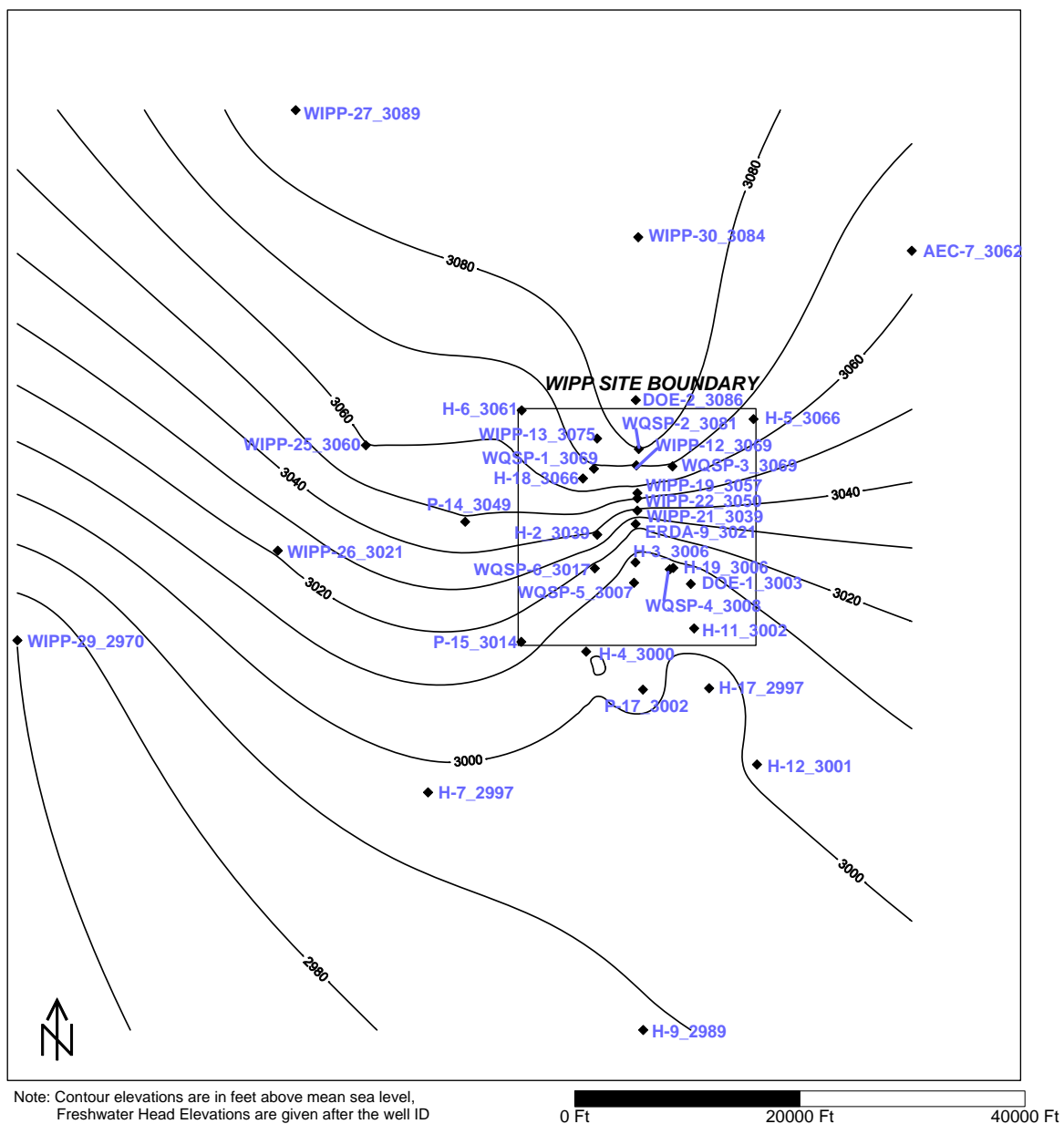


1

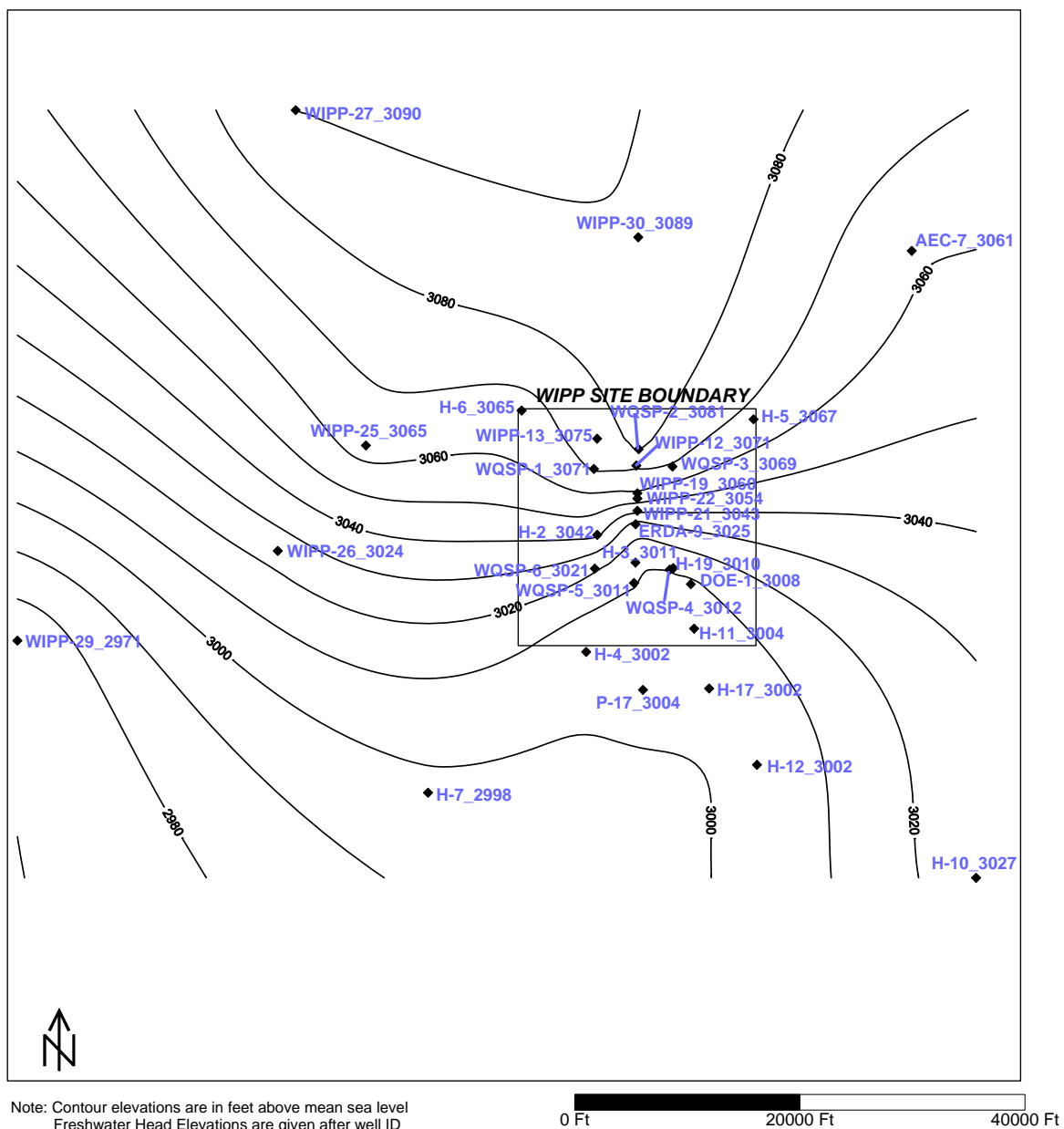
2

**Figure 2-37. Hydraulic Heads in the Culebra**

3



1  
2      Figure 2-37a. Potentiometric Surface. Expresses as Equivalent Freshwater Head, of the  
3      Culebra in December 1998.



1      Figure 2-37b. Potentiometric Surface, Expressed as Equivalent Freshwater Head, of the Culebra  
2      in December 2002.  
3  
4

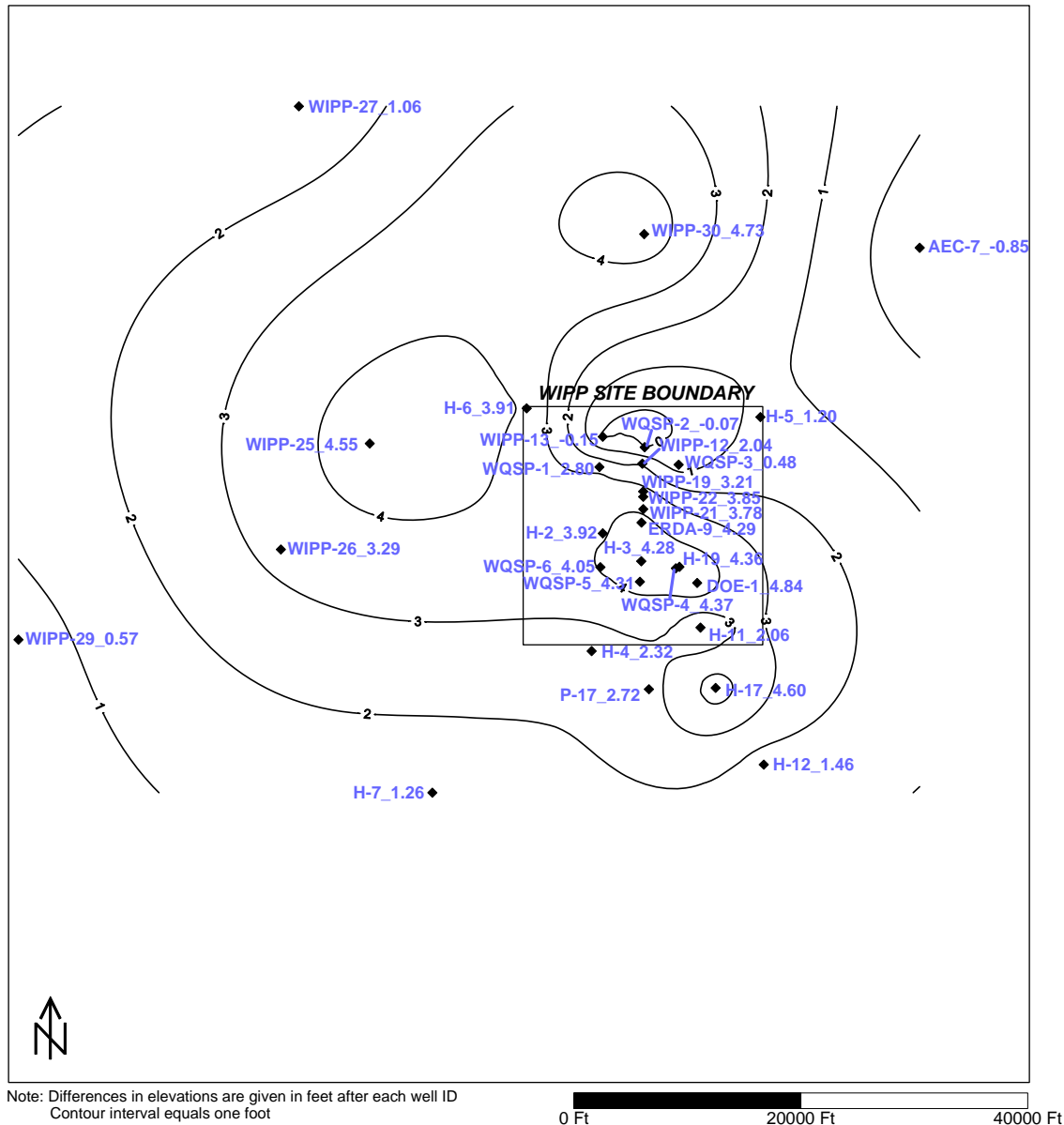


Figure 2-37c. Changes in Freshwater Heads in the Culebra Between December 1998 and December 2002.

During the CCA review, the EPA found that information on the Culebra in the CCA lacked a detailed discussion on the origin of the transmissivity variations relative to fracture infill/dissolution, integration of climatic change, and loading/unloading events. These are important aspects to understanding not only current transmissivity differences, but also potential future transmissivity variations that could affect PA calculations. The EPA's review stated, however, that the determination of the specific origin of fractures was not necessary because conditions were not expected to change during the regulatory period.

1 The DOE provided supplemental information in letters in 1997 (Docket A-93-02, Items II-I-03,  
2 II-I-24, II-I-31, II-H-44, and II-H-46) indicating that dissolution of fracture fill (which has the  
3 potential to alter fracture permeability) is unlikely to occur. The EPA accepted the DOE's  
4 position that infiltrating waters would most likely become saturated with calcium sulfate and  
5 consequently would not dissolve anhydrite or gypsum fracture fill. Further information on the  
6 EPA review of anhydrite and gypsum fracture fill dissolution is contained in EPA Technical  
7 Support Document for Section 194.14: Content of Compliance Certification Application,  
8 Section IV.C (Docket A-93-02, Item V-B-3).

9 The Sandia National Laboratories Annual Compliance Monitoring Parameter Assessment reports  
10 the annual assessment of the Compliance Monitoring Parameters (COMPs) pursuant to the SNL  
11 Analysis Plan, AP-069. The first assessment, for calendar year 1998 (SNL 2000a), showed that  
12 changes in Culebra water levels were considered minor. During the assessment of the COMP  
13 'changes in groundwater flow' for calendar year 2001 (SNL 2002), estimated freshwater Culebra  
14 heads in 15 wells were identified as above the ranges of uncertainty estimated for steady-state  
15 conditions at those wells. At 8 of the 15 wells, the measured water levels exceed the uncertainty  
16 range before being converted to freshwater head. In these cases, conversion to freshwater head  
17 using any feasible fluid density can only increase the deviation from the range. The freshwater  
18 head values from late 2000 were used to calibrate the Culebra transmissivity (T) fields used to  
19 simulate the transport of radionuclides through the Culebra (Appendix PA, Attachment  
20 TFIELD).

21 Because transport through the Culebra is a minor component of the total predicted releases from  
22 the repository, these changes in head values have little or no effect on the total releases to the  
23 accessible environment. The COMP assessment for the calendar year 2001 concluded that the  
24 current head values do not indicate a condition adverse to the predicted performance of the  
25 repository. However, because Culebra water levels are above expected values at most wells,  
26 work has been initiated to investigate the reason for the change and further evaluate the impact  
27 on performance.

28 Additional background for the Culebra model is in Appendix PA, Attachment TFIELD.  
29 Additional information on long-term pumping test data is documented in Meigs et al. (2000) and  
30 slug tests and short-term pumping tests are documented in Beauheim et al. (1991b) and  
31 Beauheim and Ruskauff (1998).

32 Several new publications on the Culebra updating the original CCA information have been  
33 released. Transport properties and tracer tests of the Culebra performed at the H-11 and H-19  
34 hydropads are described in Meigs et al. (2000). The 1995-96 tracer test program, which  
35 consisted of single-well injection-withdrawal tests and multiwell convergent flow tests, is  
36 documented in Meigs and Beauheim (2001). The higher permeability of the lower Culebra has  
37 been addressed in Meigs and Beauheim (2001, p. 1116).

38 *2.2.1.4.1.3 Tamarisk*

39 The Tamarisk acts as a confining layer in the groundwater basin model. Attempts were made in  
40 two wells, H-14 and H-16, to test a 2.4-m (7.9-ft) sequence of the Tamarisk that consists of  
41 claystone, mudstone, and siltstone overlain and underlain by anhydrite. Permeability was too

1 low to measure in either well within the time allowed for testing; consequently, Beauheim  
2 (1987a, pp. 108-110) estimated the transmissivity of the claystone sequence to be one or more  
3 orders of magnitude less than that of the tested interval in the Los Medaños (that is, less than  
4 approximately  $2.7 \times 10^{-11} \text{ m}^2/\text{s}$  [ $2.5 \times 10^{-5} \text{ ft}^2/\text{day}$ ]). The porosity of the Tamarisk was measured  
5 in 1995 as part of testing at the H-19 hydropad (TerraTek 1996). Two claystone samples had an  
6 effective porosity of 21.3 to 21.7 percent. Five anhydrite samples had effective porosities of 0.2  
7 to 1.0 percent.

8 Fluid pressures in the Tamarisk have been measured continuously at well H-16 since 1987.  
9 From 1998 through 2002, the pressures increased approximately 20 psi, from 80 to 100 psi (185  
10 to 230 ft of water), probably in a continuing recovery response to shaft grouting conducted in  
11 1993 to reduce leakage. Given the location of the pressure transducer, the elevation of Tamarisk  
12 water level has increased from 899 to 913 m amsl (2,950 to 2,995 ft amsl) during this period.  
13 Currently, no other wells in the WIPP monitoring network are completed to the Tamarisk. Thus,  
14 H-16 provides the only information on Tamarisk head levels.

15 Similar to the Los Medaños, the Tamarisk includes a mudstone layer (M3/H3) that contains  
16 halite in some locations at and around the WIPP site. This layer is considered to be important  
17 because of the effect it has on the spatial distribution of transmissivity of the Culebra as  
18 described in Section 2.2.1.4.1.2. The M3/H3 margin is described in Section 2.1.3.5 and mapped  
19 in Figure 2-15.

20 The Tamarisk is incorporated into the conceptual model as discussed in Section 6.4.6.3. The role  
21 of the Tamarisk in the groundwater basin model is in CCA Appendix MASS, Section  
22 MASS.14.1. Tamarisk hydrological model parameters are in Appendix PA, Attachment PAR,  
23 Table PAR-25.

24 **2.2.1.4.1.4 Magenta**

25 The Magenta is a conductive hydrostratigraphic unit about 7.9 m (26 ft) thick at the WIPP. The  
26 Magenta is saturated except near outcrops along Nash Draw, and hydraulic data are available  
27 from 22 wells including 7 wells recompleted to the Magenta between 1995 and 2002 (SNL  
28 2003a). According to Mercer (CCA Appendix HYDRO, p. 65), transmissivity ranges over five  
29 orders of magnitude from  $1 \times 10^{-9}$  to  $4 \times 10^{-4} \text{ m}^2/\text{s}$  ( $4 \times 10^{-3}$  to  $3.75 \times 10^2 \text{ ft}^2/\text{day}$ ). A slug test  
30 performed in H-9c, a recompleted Magenta well (see Figure 2-5 for well location), yielded a  
31 transmissivity of  $6 \times 10^{-7} \text{ m}^2/\text{s}$  (0.56  $\text{ft}^2/\text{day}$ ), which is consistent with Mercer's findings (SNL  
32 2003a). The porosity of the Magenta was measured in 1995 as part of testing at the H-19  
33 hydropad (TerraTek 1996). Four samples had effective porosities ranging from 2.7 to 25.2  
34 percent.

35 The hydraulic transmissivities of the Magenta, based on sparse data, show a decrease from west  
36 to east, with slight indentations of the contours north and south of the WIPP that correspond to  
37 the topographic expression of Nash Draw. In most locations, the hydraulic conductivity of the  
38 Magenta is one to two orders of magnitude less than that of the Culebra. The Magenta does not  
39 have hydraulically significant fractures in the vicinity of the WIPP. Treatment of the Magenta in  
40 the model is discussed in Section 6.4.6.4 with modeling parameters in Table 6-24.

1 Based on Magenta water levels measured in the 1980s (Lappin et al. 1989) when a wide network  
2 of Magenta monitoring wells existed, the hydraulic gradient in the Magenta across the site varies  
3 from 3 to 4 m/km (16 to 20 ft/mi) on the eastern side, steepening to about 6 m/km (32 ft/mi)  
4 along the western side near Nash Draw (Figure 2-38).

5 Regional modeling using the groundwater basin model indicates that leakage occurs into the  
6 Magenta from the overlying Forty-niner and out of the Magenta downward into the Tamarisk.  
7 Regional modeling also indicates that flow directions in the Magenta are dominantly westward,  
8 similar to the slope of the land surface in the immediate area of the WIPP. This flow direction is  
9 different than the dominant flow direction in the next underlying conductive unit, the Culebra.  
10 This difference is consistent with the groundwater basin conceptual model, in that flow in  
11 shallower units is expected to be more sensitive to local topography.

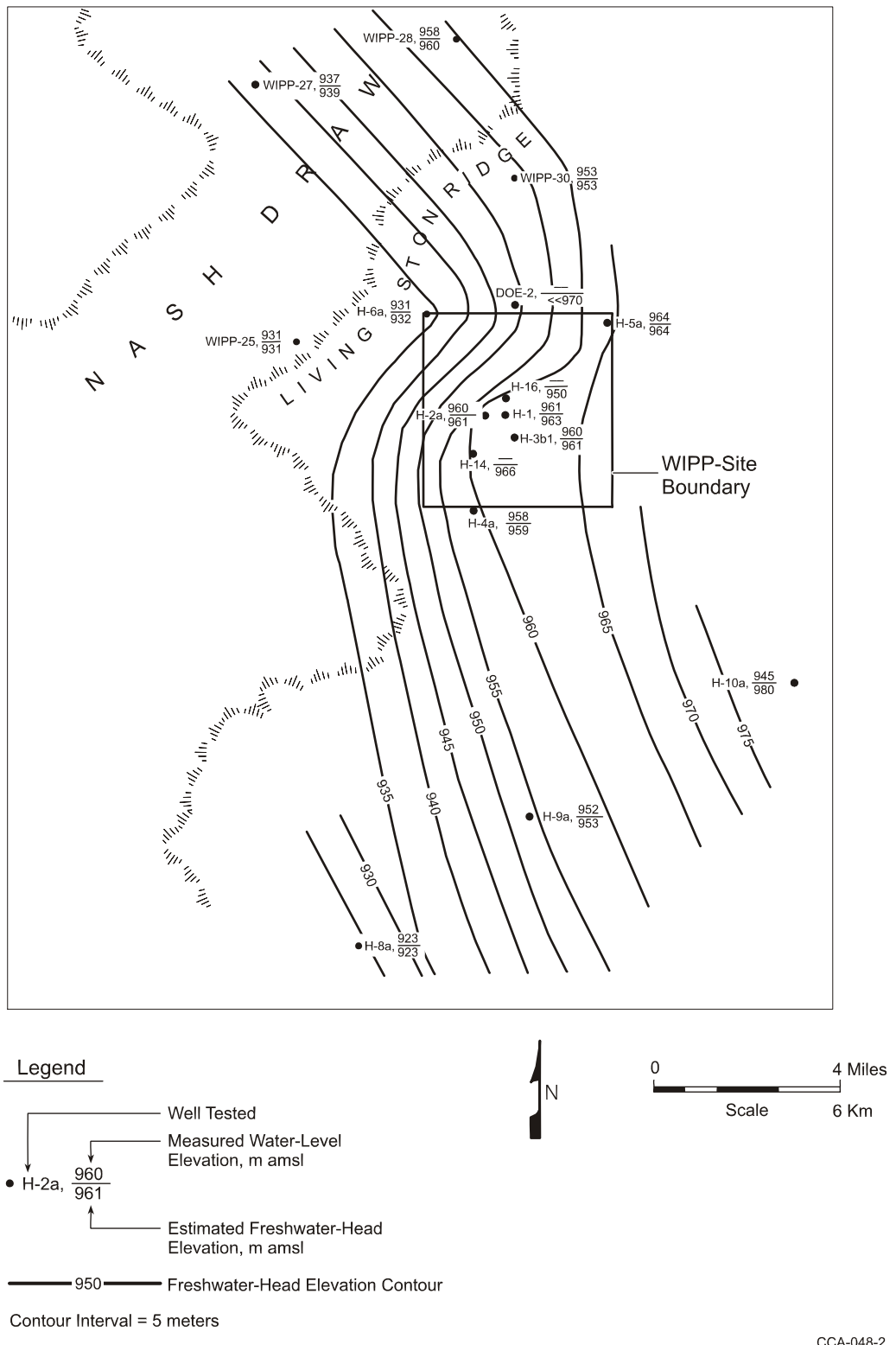
12 Inferences about vertical flow directions in the Magenta have been made from well data  
13 collected by the DOE. Beauheim (1987a, p. 137) reported flow directions downwards out of the  
14 Magenta over the WIPP site, consistent with results of groundwater basin modeling.

15 However, Beauheim (1987a, p. 139) concluded that flow directions between the Forty-niner and  
16 Magenta would be upward in the three boreholes from which reliable pressure data are available  
17 for the Forty-niner (H-3, H-14, and H-16), which is not consistent with the results of  
18 groundwater modeling. This inconsistency may be the result of local heterogeneity in rock  
19 properties that affect flow on a scale that cannot be duplicated in regional modeling.

20 As is the case for the Culebra, groundwater elevations in the Magenta have changed over the  
21 period of observation. The pattern of changes is similar to that observed for the Culebra (see  
22 Section 2.2.1.4.1.2), and is being investigated under the current DOE hydrology program (SNL  
23 2003b).

24 *2.2.1.4.1.5 Forty-niner*

25 The Forty-niner is a confining hydrostratigraphic layer about 20 m (66 ft) thick throughout the  
26 WIPP area and consists of low-permeability anhydrite and siltstone. Tests by Beauheim (1987a,  
27 119-123 and Table 5-2) in H-14 and H-16 yielded transmissivities of about  $3 \times 10^{-8}$  to  $8 \times 10^{-8}$   
28 m<sup>2</sup>/s ( $3 \times 10^{-2}$  to  $7 \times 10^{-2}$  ft<sup>2</sup>/day) and  $3 \times 10^{-9}$  to  $6 \times 10^{-9}$  m<sup>2</sup>/s ( $5 \times 10^{-3}$  to  $6 \times 10^{-3}$  ft<sup>2</sup>/day),  
29 respectively, for the medial siltstone unit of the Forty-niner. Tests of the siltstone in H-3d  
30 provided transmissivity estimates of  $3.8 \times 10^{-9}$  to  $4.8 \times 10^{-9}$  m<sup>2</sup>/s ( $3.5 \times 10^{-3}$  to  $4.5 \times 10^{-3}$  ft<sup>2</sup>/day)  
31 (Beauheim et al. 1991b, Table 5-1). The porosity of the Forty-niner was measured as part of  
32 testing at the H-19 hydropad (TerraTek 1996). Three claystone samples had effective porosities  
33 ranging from 9.1 to 24.0 percent. Four anhydrite samples had effective porosities ranging from  
34 0.0 to 0.4 percent. Model consideration of the Forty-niner is in Section 6.4.6.5. Modeling  
35 parameters are in CCA Appendix PAR, Table PAR-27.



1

2

**Figure 2-38. Hydraulic Heads in the Magenta (1980s)**

CCA-048-2

1 Fluid pressures in the Forty-niner have been measured continuously at well H-16, approximately  
2 13.9 m (45.6 ft) from the well of the AIS, since 1987. The pressures cycle in a sinusoidal  
3 fashion on an annual basis. These cycles correlate with cycles observed in rock bolt loads in the  
4 WIPP shafts (DOE 2002c), and presumably reflect seasonal temperature changes causing the  
5 rock around the shafts to expand and contract. From 1998 through 2002, the pressures have  
6 cycled between 40 and 70 psi (90 and 160 ft of fresh water). Given the location of the pressure  
7 transducer, the elevation of Forty-niner water level has varied between 899 to 920 m (2,950 to  
8 3,020 ft) amsl during this period. Through April 2002, Forty-niner water levels were also  
9 measured monthly at H-3d as part of the WIPP groundwater monitoring program. Measurements  
10 were discontinued after April 2002 because of an obstruction in the well. The April 2002 Forty-  
11 niner water level elevation determined at H-3d was 942 m (3,092 ft) amsl. Differences in Forty-  
12 niner water levels at H-16 and H-3d are probably due, in part, to differences in the densities of  
13 the fluids in the wells. No other wells in the WIPP monitoring network are completed to the  
14 Forty-niner.

15 2.2.1.4.2 Hydrology of the Dewey Lake and the Santa Rosa

16 The Dewey Lake and the Santa Rosa, and surficial soils, overlie the Rustler and are the  
17 uppermost hydrostratigraphic units considered by the DOE. The Dewey Lake and overlying  
18 rocks are more permeable than the anhydrites at the top of the Rustler. Consequently, basin  
19 modeling indicates that most (probably more than 70 percent) of the water that recharges the  
20 groundwater basin (that is, percolates into the Dewey Lake from surface water) flows only in the  
21 rocks above the Rustler. As modeled, the rest leaks vertically through the upper anhydrites of  
22 the Rustler and into the Magenta or continues downward to the Culebra. More flow occurs into  
23 the Rustler units at times of greater recharge. Even though it carries most of the modeled  
24 recharge, lateral flow in the Dewey Lake is slow because of its low permeability in most areas.

25 A saturated, perched-water zone has been identified in the lower Santa Rosa directly below the  
26 operational area of the WIPP (DOE 1999; INTERA 1997a; INTERA 1997b; DES 1997). The  
27 zone occurred at a location that previously had been dry or only partially saturated. Details are  
28 provided in Appendix DATA and a summary provided in Section 2.2.1.4.2.2.

29 2.2.1.4.2.1 *Dewey Lake*

30 The Dewey Lake contains a productive zone of saturation, probably under water-table  
31 conditions, in the southwestern to south-central portion of the WIPP site and south of the site.  
32 Several wells operated by the J.C. Mills Ranch south of the WIPP site produce sufficient  
33 quantities of water from the Dewey Lake to supply livestock. Short-term production rates of 5.7  
34 to 6.8 m<sup>3</sup>/hr (25 to 30 gpm) were observed in boreholes P-9 (Jones 1978, Vol. 1., pp. 167- 168),  
35 WQSP-6, and WQSP-6a (see CCA Appendix USDW). Based on a single hydraulic test  
36 conducted at WQSP-6a (Figure 2-6), Beauheim and Ruskauff (1998) estimated the transmissivity  
37 of a 7.3m (24ft) fractured section of the Dewey Lake at  $3.9 \times 10^{-4}$  m<sup>2</sup>/s (360 ft<sup>2</sup>/day). The  
38 productive zone is typically found in the middle of the Dewey Lake, 55 to 81 m (180 to 265 ft)  
39 below ground surface and appears to derive much of its transmissivity from open fractures.  
40 Where present, the saturated zone may be perched or simply underlain by less transmissive rock.  
41 Fractures below the productive zone tend to be completely filled with gypsum. Open fractures

1 and/or moist (but not fully saturated) conditions have been observed at similar depths north of  
 2 the zone of saturation, at the H-1, H-2, and H-3 boreholes (CCA Appendix HYDRO, p. 69).

3 Under the groundwater monitoring program (Appendix MON-2004), water levels are measured  
 4 in two Dewey Lake wells, WQSP-6a and H-3d, located south of the WIPP site center (Figure 2-  
 5 6). Water levels in these two wells are currently 975 and 937 m (3,198 and 3,075 ft) amsl,  
 6 respectively. Water levels at WQSP-6a remain relatively constant. Over the past several years,  
 7 water levels at H-3d have risen about 0.3 m/yr (1 ft/yr). Future changes in the Dewey Lake  
 8 water table due to wetter conditions are part of the conceptual model discussed in Sections 6.4.6  
 9 and 6.4.9.

10 Similar to the six Culebra WQSP wells (WQSP-1 through WQSP-6), Dewey Lake water quality  
 11 is determined semiannually at WQSP-6a. Baseline concentrations for major ion species have  
 12 also been determined from ten rounds of sampling. The 95 percent confidence intervals for the  
 13 major ion species presented in SNL (2001) are shown in Table 2-9 and indicate the Dewey Lake  
 14 water at this location is relatively fresh. Major ion concentrations have been stable within the  
 15 baseline 95 percent confidence intervals for all 14 rounds of sampling conducted through May  
 16 2002 (Kehrman 2002).

17 **Table 2-9. Ninety-Five Percent Confidence Intervals for Dewey Lake**  
 18 **Water-Quality Baseline**

Well I.D.	Cl <sup>-</sup> Conc. (mg/L)	SO <sub>4</sub> <sup>2-</sup> Conc. (mg/L)	HCO <sub>3</sub> <sup>-</sup> Conc. (mg/L)	Na <sup>+</sup> Conc. (mg/L)	Ca <sup>2+</sup> Conc. (mg/L)	Mg <sup>2+</sup> Conc. (mg/L)	K <sup>+</sup> Conc. (mg/L)
WQSP-6a	433-764	1610-2440	97-111	253-354	554-718	146-185	1.8-9.2

19 Powers (1997) suggests that what distinguishes the low-transmissivity lower Dewey Lake from  
 20 the high-transmissivity upper Dewey Lake is a change in natural cements from carbonate (above)  
 21 to sulfate (below). Resistivity logs correlate with this cement change and show a drop in  
 22 porosity across the cement-change boundary. Similarly, porosity measurements made on eight  
 23 core samples from the Dewey Lake from well H-19b4 showed a range from 14.9 to 24.8 percent  
 24 for the four samples from above the cement change, and a range from 3.5 to 11.6 percent for the  
 25 four samples from below the cement change (TerraTek 1996). In the vicinity of the surface  
 26 structures area of the WIPP, Powers (1997) proposed the surface of the cement change is at a  
 27 depth of approximately 50 to 55 m (165 to 180 ft), is irregular, and trends downward  
 28 stratigraphically to the south and west of the site center.

29 During site characterization and initial construction of the WIPP shafts, the Dewey Lake did not  
 30 produce water within the WIPP shafts or in boreholes in the immediate vicinity of the panels.  
 31 However, since 1995, water has been observed leaking into the exhaust shaft at a depth of  
 32 approximately 24.4 m (80 ft) at the location of the Dewey Lake/ Santa Rosa contact (Docket A-  
 33 93-02, Item number 11-1-07, 1999; INTERA 1997a; INTERA 1997b). As described below in  
 34 Section 2.2.1.4.2.2, the water is interpreted to be from an anthropogenic source, including  
 35 infiltration from WIPP rainfall-runoff retention ponds and the WIPP salt storage area and

1 evaporation pond located at the surface. At the site center, thin cemented zones in the upper  
2 Dewey Lake retard, at least temporarily, downward infiltration of modern waters.

3 Saturation of the uppermost Dewey Lake was observed for the first time in 2001 as well C-2737  
4 was being drilled (Powers 2002c). Well C-2811 was then installed nearby to monitor this zone  
5 (Powers and Stensrud 2003). Because of the proximity of these two wells to the WIPP surface  
6 structures area, and the absence of water at this horizon when earlier wells were drilled, the  
7 saturation is assumed to be an extension of the anthropogenic waters described in the following  
8 section.

9 For modeling purposes, the hydraulic conductivity of the Dewey Lake, assuming saturation, is  
10 estimated to be  $10^{-8}$  m/sec ( $3 \times 10^{-3}$  ft/day), corresponding to the hydraulic conductivity of fine-  
11 grained sandstone and siltstone (Davies 1989, p. 110).

12 The Dewey Lake is the uppermost important layer in the hydrological model. Its treatment is  
13 discussed in Section 6.4.6.6 and Appendix PA, Attachment MASS, Section MASS.14.2. Model  
14 parameters are in Table 6-25 and in Appendix PA, Attachment PAR, Table PAR-22.

15 *2.2.1.4.2.2 Santa Rosa*

16 The Santa Rosa ranges from 0 to 91 m (0 to about 300 ft) thick and is present over the eastern  
17 half of the WIPP site. It is absent over the western portion of the site. It crops out northeast of  
18 Nash Draw. The Santa Rosa near the WIPP site may have a naturalwater-saturated thickness of  
19 limited extent. It has a porosity of about 13 percent and a specific capacity of 0.029 to 0.041  
20 L/s/m (0.14 to 0.20 gallons per minute per foot (gpm/ft) of drawdown, where it yields water in  
21 the WIPP region.

22 In May 1995, a scheduled inspection of the WIPP exhaust shaft revealed water emanating from  
23 cracks in the concrete liner at a depth of approximately 24.4 m (80 ft) below the shaft collar.  
24 Because little or no groundwater had been encountered at this depth interval previously (Bechtel  
25 1979; DOE 1983; Holt and Powers 1984, 1986), the DOE implemented a program in early 1996  
26 to investigate the source and extent of the water. The program included installation of wells and  
27 piezometers, hydraulic testing (pumping tests), water-quality sampling and analysis, and water-  
28 level and precipitation monitoring (Docket A-93-02, Item number 11-1-07, DOE 1999; INTERA  
29 1997a; DES 1997; INTERA 1997b).

30 In the initial phases of the investigation, three wells (C-2505, C-2506, and C-2507) and 12  
31 piezometers (PZ-1 through PZ-12) were installed within the surface structures area of the WIPP  
32 site (Figure 2-39). The three wells were located near the exhaust shaft and completed to the  
33 Santa Rosa/Dewey Lake contact (approximately 15 m [50 ft] below ground surface). Similarly,  
34 the piezometers were also completed to the Santa Rosa/Dewey Lake contact (approximately 16  
35 to 23 m [55 to 75 ft] below ground surface). All wells and piezometers, with the exception of  
36 PZ-8, encountered a saturated zone just above the Santa Rosa/Dewey Lake contact, but water did  
37 not appear to have percolated significantly into the Dewey Lake. PZ-8, the piezometer located  
38 farthest to the east in the study area, was a dry hole.

39 Subsequent to the well and piezometer installations, water-level, water-quality, and rainfall data  
40 were collected. In addition, hydraulic tests were performed to estimate hydrologic properties and

1 water production rates. These data suggest that the water present in the Santa Rosa below the  
2 WIPP surface structures area represents an unconfined, water-bearing horizon perched on top of  
3 the Dewey Lake (DES 1997). Pressure data collected from instruments located in the exhaust  
4 shaft show no apparent hydrologic communication between the Santa Rosa and other formations  
5 located stratigraphically below the Santa Rosa.

6 A water-level-surface map of the Santa Rosa in the vicinity of the WIPPsurface structures area  
7 indicates that a potentiometric high is located near the salt water evaporation pond and PZ-7  
8 (Figure 2-40). The water level at PZ-7 is approximately 1 m (3.3 ft) higher than the water levels  
9 in any other wells or piezometers. Water is presumed to move radially from this potentiometric  
10 high. The areal extent of the water is larger than the 80-acre investigative area shown in Figure  
11 2-39 (DES 1997) as evidenced by drilling records of C-2737 (Powers 2002c) located outside of  
12 and south of the WIPP surface structures area that indicate a Santa Rosa/Dewey Lake perched-  
13 water horizon at a depth of approximately 18 m (60 ft). The study of this water is ongoing.

14 Water-quality data for the perched Santa Rosa waters are highly variable and appear to be  
15 dominated by two anthropogenic sources: (1) runoff of rainfall into and infiltration from the  
16 retention ponds located to the south of the WIPP surface facilities, and (2) infiltration of saline  
17 waters from the salt storage area, the salt storage evaporation pond, and perhaps remnants of the  
18 drilling and tailings pit used during the construction of the WIPP salt shaft. The total dissolved  
19 solids (TDS) in the perched water range from less than 3,000 mg/L at PZ-10 to more than  
20 160,000 mg/L at PZ-3 (DES 1997). Concentration contours are known to shift with time. For  
21 example, the high-TDS zone centered at PZ-3 moved observably to the northeast toward PZ-9  
22 between February 1997 and October 2000 (DOE 2002b).

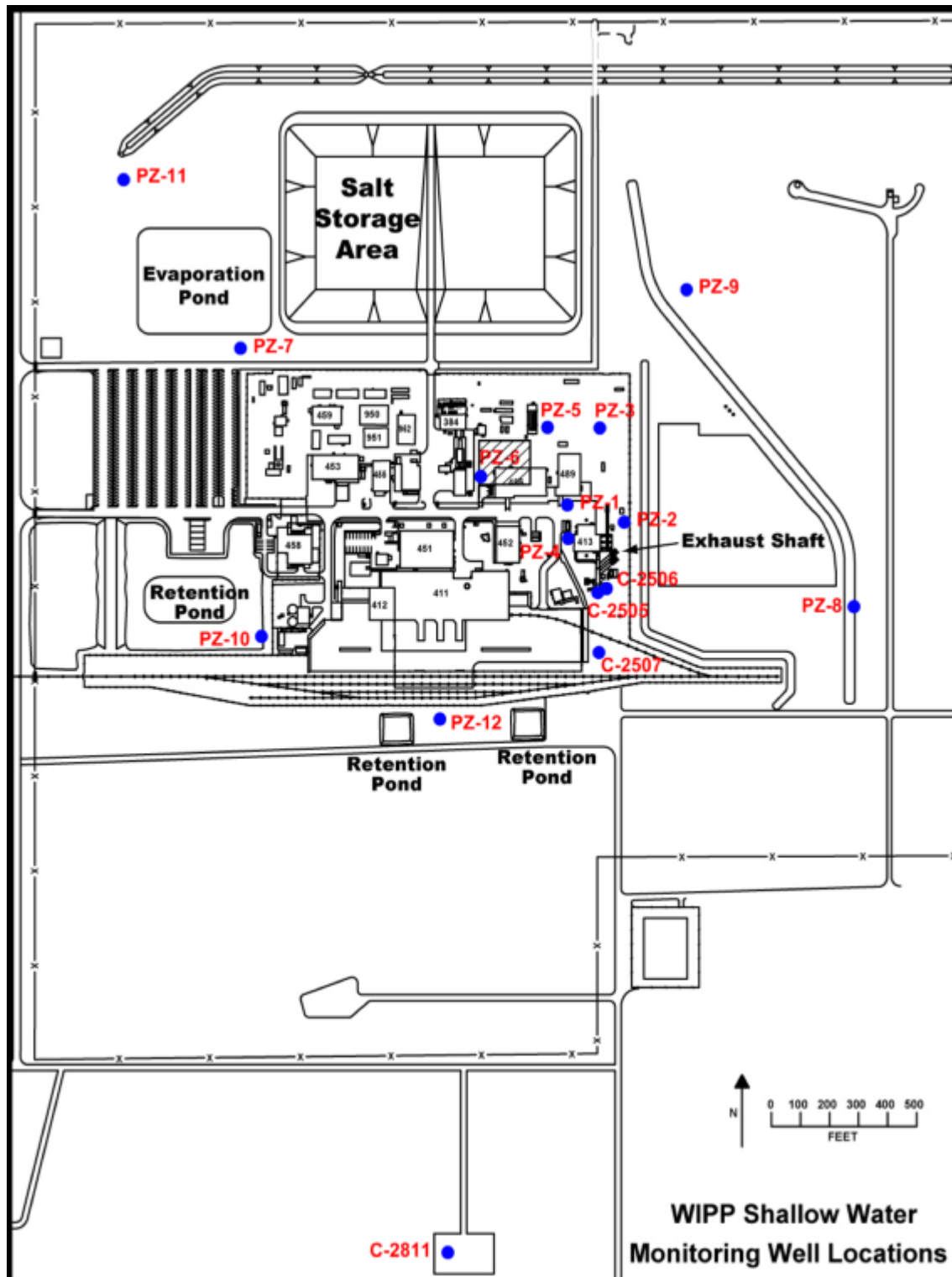
23 Hydraulic tests (Docket A-93-02, Item number 11-1-07, DOE; INTERA 1997a; DES 1997)  
24 conducted in the three wells and 12 piezometers indicate that the Santa Rosa behaves as a low-  
25 permeability, unconfined aquifer perched on the Dewey Lake. Hydraulic conductivity ranges  
26 from  $2.6 \times 10^{-8}$  to  $5.5 \times 10^{-5}$  m/s ( $7.4 \times 10^{-3}$  to 16 ft/day). The wells are capable of producing at  
27 rates of about 0.3 to 1.0 gpm. The estimated storativity value for the Santa Rosa is  $1 \times 10^{-2}$ .

28 **2.2.1.5 Hydrology of Other Groundwater Zones of Regional Importance**

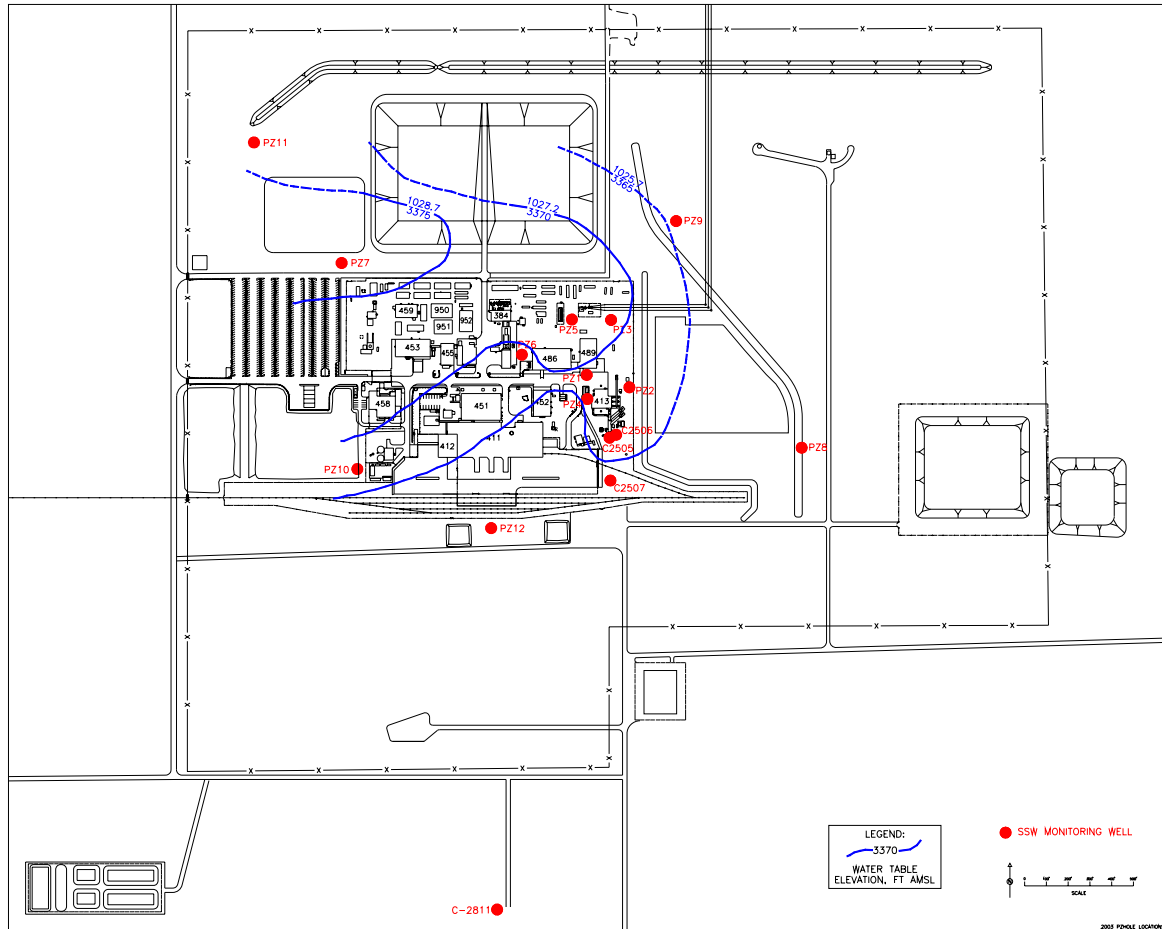
29 The groundwater regimes in the Capitan Limestone, which is generally regarded as the northern  
30 boundary of the Delaware Basin, and Nash Draw have been evaluated by the DOE as part of the  
31 WIPP project because of their importance in some processes, notably dissolution features, that  
32 the DOE has determined to be of low probability at the WIPP site.

33 **2.2.1.5.1 Capitan Limestone**

34 The Capitan Limestone (hereafter referred to as the Capitan), which outcrops in the southern end  
35 of the Guadalupe Mountains, is a massive limestone unit that grades basinward into recemented,  
36 partly dolomitized reef breccia and shelfward into bedded carbonates and evaporites. A deeply  
37 incised submarine canyon near the Eddy-Lea county line has been identified (Hiss 1976). This



1  
2 **Figure 2-39. Site Map of WIPP Surface Structures Area Showing Location of Wells (e.g.,**  
3 **C-2505) and Piezometers (e.g., PZ-1) (after INTERA 1997)**



1

2 **Figure 2-40. Santa Rosa Potentiometric Surface Map**

3 canyon is filled with sediments of lower permeability than the Capitan and, according to Hiss  
 4 (1975 p. 199), restricts fluid flow. The hydraulic conductivity of the Capitan ranges from  $3 \times$   
 5  $10^{-6}$  to  $9 \times 10^{-5}$  m/s (1 to 25 ft/day) in southern Lea County and is  $1.7 \times 10^{-5}$  m/s (5 ft/day) east  
 6 of the Pecos River at Carlsbad (CCA Appendix HYDRO, p. 34). Hiss (1975, p. 199) reported in  
 7 1975 that average transmissivities around the northern and eastern margins of the Delaware  
 8 Basin are  $0.01 \text{ m}^2/\text{s}$  (10,000 ft $^2$ /day) in thick sections and  $5.4 \times 10^{-4} \text{ m}^2/\text{s}$  (500 ft $^2$ /day) in incised  
 9 submarine canyons. Water table conditions are found in the Capitan aquifer southwest of the  
 10 Pecos River at Carlsbad; however, artesian conditions exist to the north and east. The hydraulic  
 11 gradient to the southeast of the submarine canyon near the Eddy-Lea county line has been  
 12 affected by large oil field withdrawals. The Capitan is recharged by percolation through the  
 13 northern shelf aquifers, by flow from the south and west from underlying basin aquifers (see  
 14 information on the Bell Canyon, Section 2.2.1.2.1), and by direct infiltration at its outcrop in the  
 15 Guadalupe Mountains. The Capitan is important in the regional hydrology because breccia pipes  
 16 in the Salado have formed over it, most likely in response to the effects of dissolution by  
 17 groundwater flowing in the Castile along the base of the Salado. See CCA Appendix DEF,  
 18 Section DEF.3.1 for a more thorough discussion of breccia pipe formation.

1    2.2.1.5.2 Hydrology of the Rustler-Salado Contact Zone in Nash Draw

2    As discussed in Sections 2.1.3.4 and 2.1.6.2.1, in Nash Draw the contact between the Rustler and  
3    the Salado is an unstructured residuum of gypsum, clay, and sandstone created by the dissolution  
4    of halite and has been known as the brine aquifer, Rustler-Salado residuum, and residuum. The  
5    residuum is absent under the WIPP site. It is clear that dissolution in Nash Draw occurred after  
6    deposition of the Rustler (see CCA Appendix DEF, Section DEF.3.2 for a discussion of lateral  
7    dissolution of the Rustler-Salado contact). As described previously, the topographic low formed  
8    by Nash Draw is a groundwater divide in the groundwater basin conceptual model of the units  
9    above the Salado. The brine aquifer is shown in Figure 2-41.

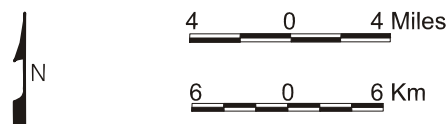
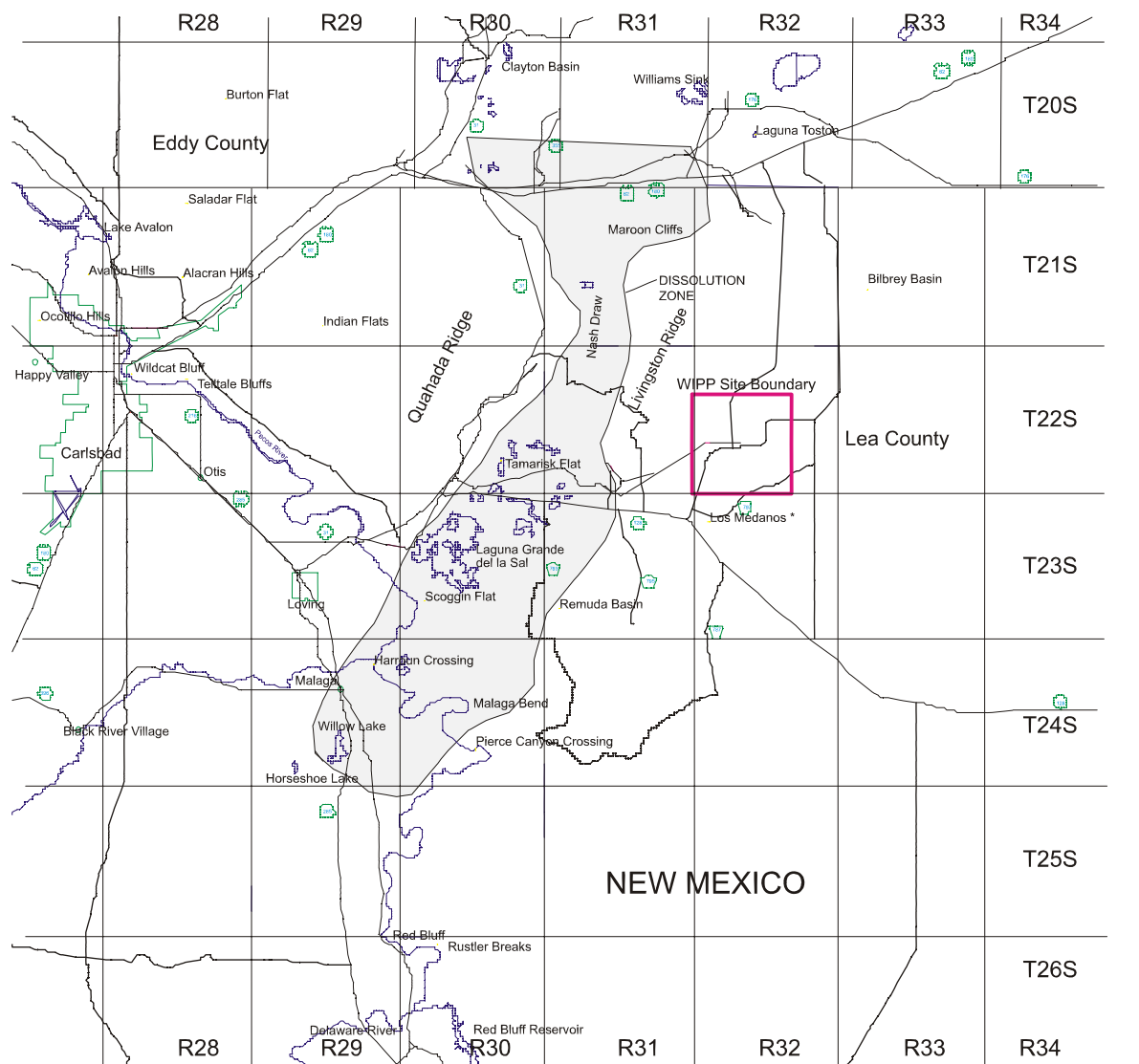
10    Robinson and Lang (1938) described the brine aquifer (Section 2.1.3.4) and suggested that the  
11    structural conditions that caused the development of Nash Draw might control the occurrence of  
12    the brine; thus, the brine aquifer boundary may coincide with the topographic surface expression  
13    of Nash Draw, as shown in Figure 2-33. Their studies show brine concentrated along a strip  
14    from 3.3 to 13 km (2 to 8 mi) wide and about 43 km (26 mi) long. Data from the test holes that  
15    Robinson and Lang (1938) drilled indicate that the residuum (containing the brine) ranges in  
16    thickness from 3 to 18 m (10.5 to 60 ft) and averages about 24 feet (7 meters).

17    Hydraulic properties were determined by Hale et al. (1954) primarily for the area between  
18    Malaga Bend on the Pecos River and Laguna Grande de la Sal. They calculated a transmissivity  
19    value of  $8.6 \times 10^{-3} \text{ m}^2/\text{s}$  (8,000 ft<sup>2</sup>/day) and estimated the potentiometric gradient to be  
20    0.27 m/km (1.4 ft/mi). In this area, the Rustler-Salado residuum apparently is part of a  
21    continuous hydrologic system, as evidenced by the coincident fluctuation of water levels in the  
22    test holes (as far away as Laguna Grande de la Sal) with pumping rates in irrigation wells along  
23    the Pecos River.

24    In the northern half of Nash Draw, the approximate outline of the brine aquifer as described by  
25    Robinson and Lang (1938) has been supported by drilling associated with the WIPP  
26    hydrogeologic studies. These studies also indicate that the main differences in areal extent occur  
27    along the eastern side where the boundary is very irregular and, in places (test holes P-14 and H-  
28    07), extends farther east than previously indicated by Robinson and Lang (1938).

29    Other differences from the earlier studies include the variability in thickness of residuum present  
30    in test holes WIPP-25 through WIPP-29. These holes indicate thicknesses ranging from 3.3 m  
31    (11 ft) in WIPP-25 to 33 m (108 ft) in WIPP-29 in Nash Draw, compared to 2.4 m (8 ft) in test  
32    hole P-14, east of Nash Draw. The specific geohydrologic mechanism that has caused  
33    dissolution to be greater in one area than in another is not apparent, although a general increase  
34    in chloride concentration in water from the north to the south may indicate the effects of  
35    movement down the natural hydraulic gradient in Nash Draw.

36    The average hydraulic gradient within the residuum in Nash Draw is about 1.9 m/km (10 ft/mi);  
37    in contrast, the average gradient at the WIPP site is 7.4 m/km (39 ft/mi) (CCA Appendix  
38    HYDRO, p. 50). This difference reflects the changes in transmissivity, which are as much as  
39    five orders of magnitude greater in Nash Draw. The transmissivity determined from aquifer tests  
40    in test holes completed in the Rustler-Salado contact residuum of Nash Draw ranges from



1 CCA-075-2

2 **Figure 2-41. Brine Aquifer in the Nash Draw (Redrawn from CCA Appendix HYDRO,**  
3 **Figure 14)**

1    $2.1 \times 10^{-10} \text{ m}^2/\text{s}$  ( $2 \times 10^{-4} \text{ ft}^2/\text{day}$ ) at WIPP-27 to  $8.6 \times 10^{-6} \text{ m}^2/\text{s}$  ( $9.8 \text{ ft}^2/\text{day}$ ) at WIPP-29. This  
2   is in contrast to the WIPP site proper, where transmissivities range from  $3.2 \times 10^{-11} \text{ m}^2/\text{s}$   
3   ( $3 \times 10^{-5} \text{ ft}^2/\text{day}$ ) at test holes P-18 and H-5c to  $5.4 \times 10^{-8} \text{ m}^2/\text{s}$  ( $5 \times 10^{-2} \text{ ft}^2/\text{day}$ ) at test hole P-  
4   14 (CCA Appendix HYDRO, p. 50). Locations and estimated hydraulic heads of these wells  
5   based on water-level measurements made in the 1980s (Lappin et al. 1989) are illustrated in  
6   Figure 2-42.

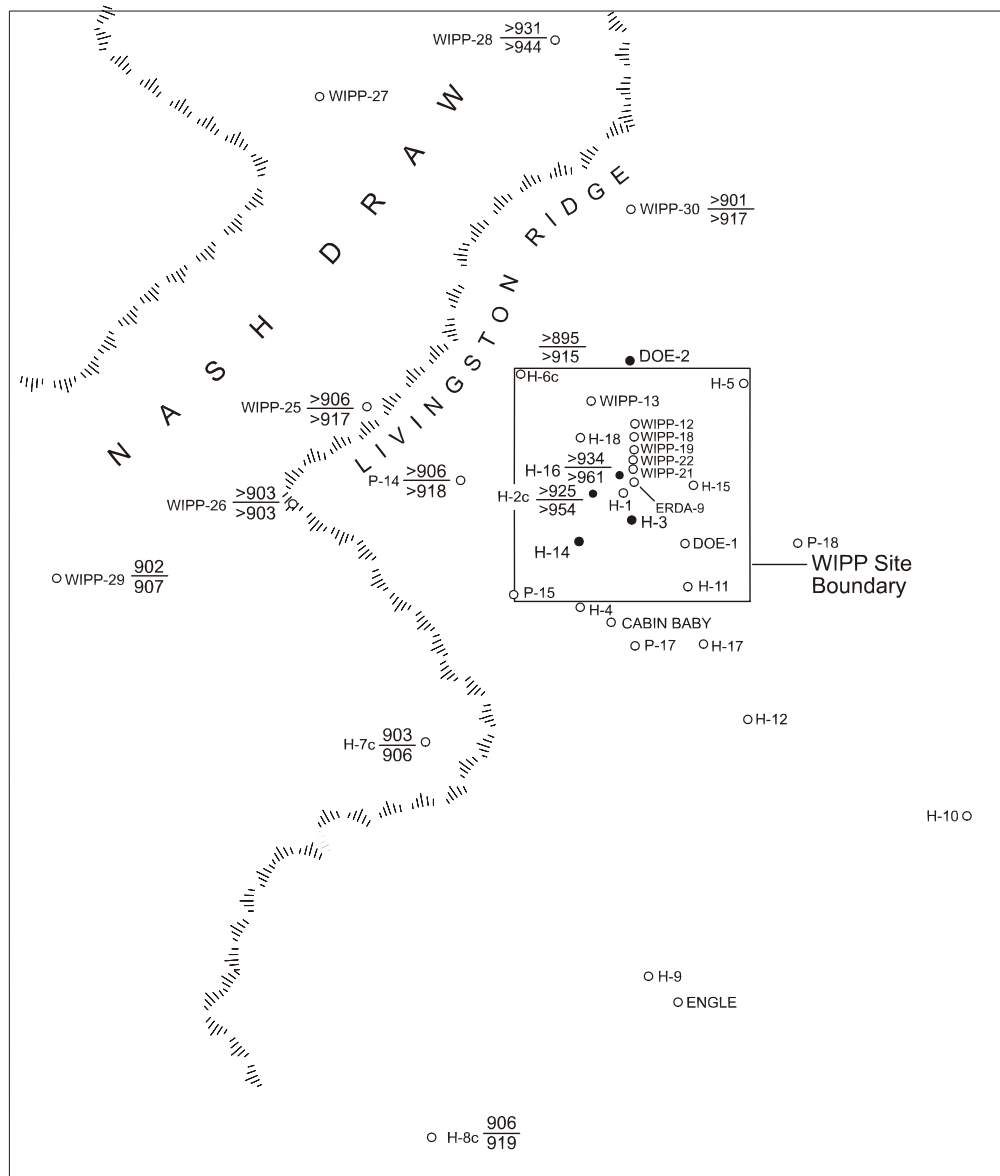
7   Hale et al. (1954) believed the Rustler-Salado contact residuum discharges to the alluvium near  
8   Malaga Bend on the Pecos River. Because the confining beds in this area are probably fractured  
9   because of dissolution and collapse of the evaporites, the brine (under artesian head) moves up  
10   through these fractures into the overlying alluvium and then discharges into the Pecos River.

11   According to CCA Appendix HYDRO, p. 55, water in the Rustler-Salado contact residuum in  
12   Nash Draw contains the largest concentrations of dissolved solids in the WIPP area, ranging  
13   from 41,500 mg/L in borehole H-1 to 412,000 mg/L in borehole H-5c. These waters are  
14   classified as brines. The dissolved mineral constituents in the brine consist mostly of sulfates  
15   and chlorides of calcium, magnesium, sodium, and potassium; the major constituents are sodium  
16   and chloride. Concentrations of the other major ions vary according to the spatial location of the  
17   sample, are probably directly related to the interaction of the brine and the host rocks, and reflect  
18   residence time within the rocks. Residence time of the brine depends upon the transmissivity of  
19   the rock. For example, the presence of large concentrations of potassium and magnesium in  
20   water is correlated with minimal permeability and a relatively undeveloped flow system.

21   The EPA's initial review of the CCA found the discussion of the Rustler/Salado contact to  
22   require clarification, particularly with respect to the possibility of the continued development and  
23   characteristics of a dissolution front along this contact, and the impact that continued dissolution  
24   within the brine aquifer residuum would have on the overlying units of the Rustler. The DOE  
25   discussed the rate and extent of dissolution processes further in supplemental information  
26   provided in a letter dated June 13, 1997 (Docket A-93-02, II-H-44). Based upon this  
27   information, the EPA concluded that, while dissolution may occur along the Rustler/Salado  
28   contact, it would not affect the WIPP's containment capabilities during the regulatory time  
29   period. Further discussion of this topic is contained in EPA Technical Support Document for  
30   Section 194.14: Content of Compliance Certification Application, Section IV.C.3 (Docket A-93-  
31   02, Item V-B-3).

32   **2.2.2 Surface-Water Hydrology**

33   The WIPP site is in the Pecos River basin, which contains about 50 percent of the drainage area  
34   of the Rio Grande Water Resources Region. The Pecos River headwaters are northeast of Santa  
35   Fe, and the river flows to the south through eastern New Mexico and western Texas to the Rio  
36   Grande. The Pecos River has an overall length of about 805 km (500 mi), a maximum basin  
37   width of about 209 km (130 mi), and a drainage area of about 115,301 km<sup>2</sup> (44,535 mi<sup>2</sup>). (About  
38   53,075 km<sup>2</sup> [20,500 mi<sup>2</sup>] contained within the basin have no external surface drainage and their  
39   surface waters do not contribute to Pecos River flows.) Figure 2-43 shows the Pecos River  
40   drainage area.



CCA-050-2

1

2 **Figure 2-42. Measured Water Levels of the Los Medaños and Rustler-Salado**  
3 **Contact Zone (1980s)**

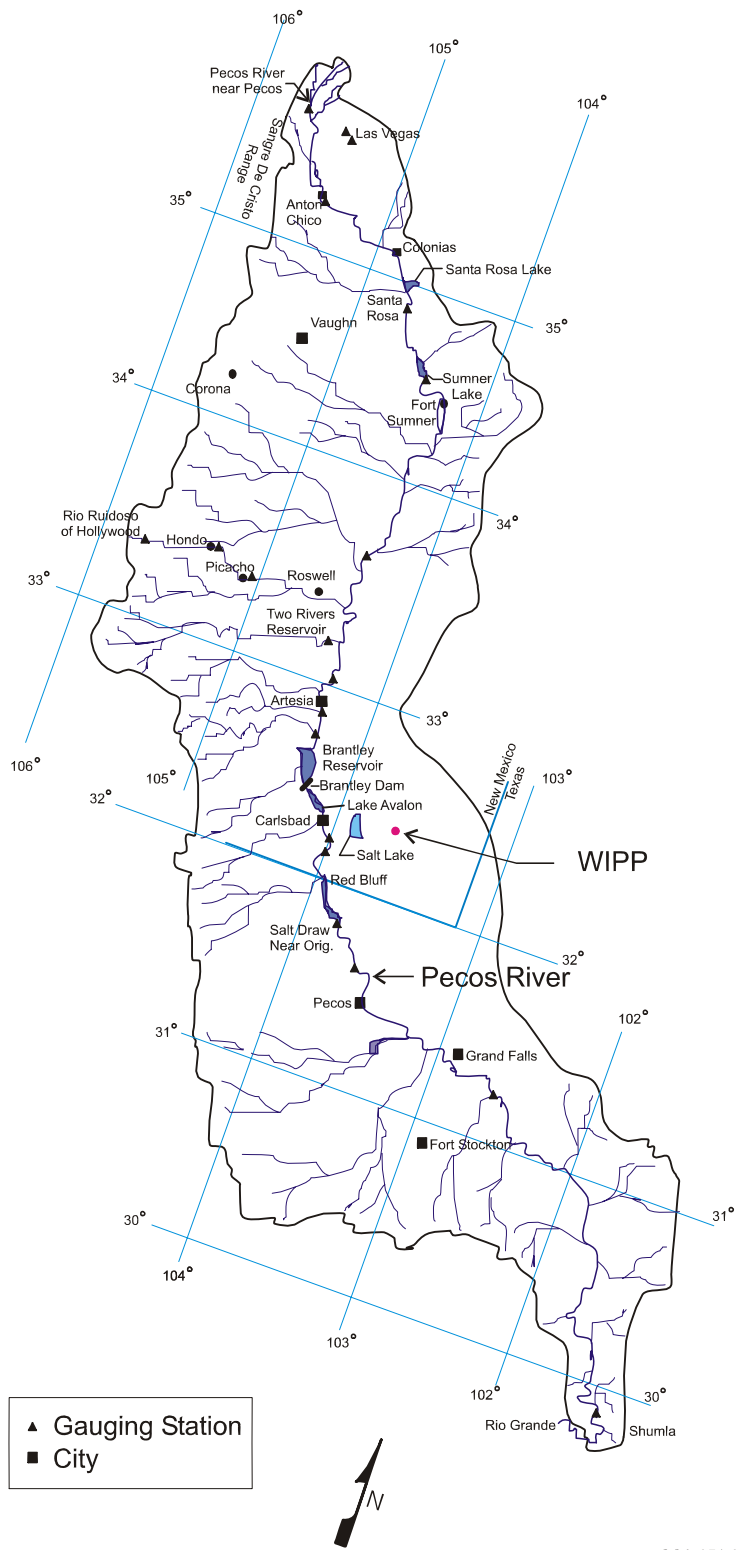
1 The Pecos River generally flows year-round, except in the reach below Anton Chico where the  
2 low flows percolate into the stream bed. The main stem of the Pecos River and its major  
3 tributaries have low flows, and the tributary streams are frequently dry. About 75 percent of the  
4 total annual precipitation and 60 percent of the annual flow result from intense local  
5 thunderstorms between April and September.

6 There are no perennial streams at the WIPP site. At its nearest point, the Pecos River is about 19  
7 km (12 mi) southwest of the WIPP site boundary. A few small creeks and draws are the only  
8 westward flowing tributaries of the Pecos River within 32 km (20 mi) north or south of the site.  
9 Nash Draw, the largest surface drainage feature east of the Pecos River in the WIPP region, is a  
10 closed depression and does not provide surface flow into the Pecos. Potash mining operations in  
11 and near Nash Draw likely contribute to the flow in Nash Draw. For example, the Mississippi  
12 Potash Inc. East operation located 11 to 13 km (7 to 8 mi) due north of the WIPP site disposes of  
13 mine tailings and refining-process effluent on its property and has done so since 1965. Records  
14 obtained from the New Mexico Office of the State Engineer show that since 1973, an average of  
15  $3 \times 10^6 \text{ m}^3$  (2,400 acre-feet [ac-ft]) of water per year has been pumped from local aquifers  
16 (Ogallala and Capitan) for use in the potash-refining process at that location (SNL 2003b).  
17 Based on knowledge of the potash refining process, approximately 90 percent of the pumped  
18 water is estimated to be discharged to the tailings pile. Geohydrology Associates (1978)  
19 estimated that approximately half of the brine discharged onto potash tailings piles in Nash Draw  
20 seeps into the ground annually, while the remainder evaporates. The Black River (drainage area:  
21 1,035 km<sup>2</sup> [400 mi<sup>2</sup>]) joins the Pecos from the west about 25 km (16 mi) southwest of the site.  
22 The Delaware River (drainage area: 1,812 km<sup>2</sup> [700 mi<sup>2</sup>]) and a number of small creeks and  
23 draws also join the Pecos River along this reach. The flow in the Pecos River below Fort  
24 Sumner is regulated by storage in Sumner Lake, Brantley Reservoir, Lake Avalon, and several  
25 other smaller irrigation dams.

26 Five major reservoirs are located on the Pecos River: Santa Rosa Lake, Sumner Lake, Brantley  
27 Reservoir, Lake Avalon, and the Red Bluff Reservoir, the last located just over the border in  
28 Texas (Figure 2-43). The storage capacities of these reservoirs and the Two Rivers Reservoir in  
29 the Pecos River Basin are shown in Table 2-10.

30 With regard to surface drainage onto and off of the WIPP site, there are no major natural lakes or  
31 ponds within 8 km (5 mi) of the site. Laguna Gatuña, Laguna Tonto, Laguna Plata, and Laguna  
32 Toston are playas more than 16 km (10 mi) north and are at elevations of 1,050 m (3,450 ft) or  
33 higher. Thus, surface runoff from the site (elevation 1,010 m [3,310 ft] above sea level) would  
34 not flow toward any of them. To the northwest, west, and southwest, Red Lake, Lindsey Lake,  
35 and Laguna Grande de la Sal are more than 8 km (5 mi) from the site, at elevations of 914 to  
36 1,006 m (3,000 to 3,300 ft). A low-flow investigation has been initiated by the USGS within the  
37 Hill Tank Draw drainage area, the most prominent drainage feature near the WIPP site. The  
38 drainage area is about 10.3 km<sup>2</sup> (4 mi<sup>2</sup>), with an average channel slope of 1 to 100, and the  
39 drainage is westward into Nash Draw. Two years of observations showed only four flow events.  
40 The USGS estimates that the flow rate for these events was under 0.057 m<sup>3</sup>/s (2 ft<sup>3</sup>/s) (DOE  
41 1980, pp. 7- 74).

42 As discussed in Section 2.5.2.3, the mean annual precipitation in the region is 0.33 m (13 in.),  
43 and the mean annual runoff is 2.5 to 5 mm (0.1 to 0.2 in.). The maximum recorded 24-hour



CCA-051-2

1  
2  
3

**Figure 2-43. Location of Reservoirs and Gauging Stations in the Pecos River Drainage Area**

1

**Table 2-10. Capacities of Reservoirs in the Pecos River Drainage**

Reservoir	River	Total Storage Capacity <sup>a</sup> (ac-ft)	Use <sup>b</sup>
Santa Rosa	Pecos	282000	FC
Sumner	Pecos	122100	IR, R
Brantley	Pecos	42000	IR, R, FC
Avalon	Pecos	5000	IR
Red Bluff	Pecos	310000	IR, P
Two Rivers	Rio Hondo	167900	FC

<sup>a</sup> Capacity below the lowest uncontrolled outlet or spillway.

<sup>b</sup> Legend:

FC flood control

IR irrigation

R recreation

P hydroelectric

2 precipitation at Carlsbad was 130 mm (5.12 in.) in August 1916. The predicted maximum 6-hour, 100-year precipitation event for the site is 91 mm (3.6 in.) and is most likely to occur 4 during the summer. The maximum recorded daily snowfall at Carlsbad was 254 mm (10 in.) in 5 December 1923.

6 The maximum recorded flood on the Pecos River occurred near the town of Malaga, New 7 Mexico, on August 23, 1966, with a discharge of 3,396 m<sup>3</sup> (120,000 ft<sup>3</sup>) per second and a stage 8 elevation of about 895 m (2,938 ft) amsl. The minimum surface elevation at the WIPP is over 91 m (300 ft) above the elevation of this maximum historic flood (DOE 1980, Section 7.4.1).

10 As discussed in the FEIS (DOE 1980, pp. 7- 71), more than 90 percent of the mean annual 11 precipitation at the site is lost by evapotranspiration. On a mean monthly basis, 12 evapotranspiration at the site greatly exceeds the available rainfall; however, intense local 13 thunderstorms may produce runoff and percolation.

14 Water quality in the Pecos River basin is affected by mineral pollution from natural sources and 15 from irrigation return flows (see Section 2.4.2.2 for discussion of surface-water quality). At 16 Santa Rosa, New Mexico, the average suspended-sediment discharge of the river is about 1,497 17 metric tons/day (1,650 tons/day). Large amounts of chlorides from Salt Creek and Bitter Creek 18 enter the river near Roswell. River inflow in the Hagerman area contributes increased amounts 19 of calcium, magnesium, and sulfate; and waters entering the river near Lake Arthur are high in 20 chloride. Below Brantley Reservoir, springs flowing into the river are usually submerged and 21 difficult to sample; springs that could be sampled had TDS concentrations of 3,350 to 22 4,000 mg/L. Concentrated brine entering at Malaga Bend adds an estimated 64 metric tons/day 23 (370 tons/day) of chloride to the Pecos River (CCA Appendix GCR, pp. 6-7).

1    **2.3 Resources**

2    At the outset of the repository program, the DOE understood the importance of resources in the  
3    vicinity of a disposal system. Several of the siting criteria emphasized avoidance of resources  
4    that would impact the performance of the disposal system. In this regard, the DOE selected a  
5    site that (1) maximized the use of federal lands, (2) avoided known oil and gas trends, (3)  
6    minimized the impacts on potash deposits, and (4) avoided existing drill holes. While the DOE  
7    could not meet all these criteria totally, it is shown that the favorable characteristics of the  
8    location compensate for any increased risks due to the presence of resources. Consequently, the  
9    DOE has prepared this section to discuss resources that may exist at or beneath the WIPP site.  
10   The topic of resources is used to broadly define both economic (mineral and nonmineral) and  
11   cultural resources associated with the WIPP site. These resources are important because they  
12   (1) provide evidence of past uses of the area and (2) indicate potential future use of the area with  
13   the possibility that such use could lead to disruption of the closed repository. Because of the  
14   depth of the disposal horizon, it is believed that only the mineral resources are of significance in  
15   predicting the long-term performance of the disposal system. However, the nonmineral and  
16   cultural resources are presented for completeness because they are included in the FEP screening  
17   discussions in Chapter 6 and Appendix PA, Attachment SCR. Information needed to make  
18   screening decisions includes natural resource distributions, including potable groundwaters, the  
19   distribution of drillholes, mines, excavations, and other man-made features that exploit these  
20   resources, the distribution of drillholes and excavation used for disposal or injection purposes,  
21   activities that significantly alter the land surface, agricultural activities that may affect the  
22   disposal system, archaeological resources requiring deep excavation to exploit, and technological  
23   changes that may alter local demographics. This information is presented here or is referenced.

24   With respect to minerals or hydrocarbons, reserves are the portion of resources that are economic  
25   at today's market prices and with existing technology. For hydrocarbons, proved (proven)  
26   reserves are an estimated quantity that engineering and geologic data analysis demonstrates, with  
27   reasonable certainty, is recoverable in the future from discovered oil and gas pools. Probable  
28   resources (extensions) consist of oil and gas in pools that have been discovered but not yet  
29   developed by drilling. Their presence and distribution can generally be surmised with a high  
30   degree of confidence. Probable resources (new pools) consist of oil and gas surmised to exist in  
31   undiscovered pools within existing fields. (Definitions are from NMBMMR 1995, V-2 and  
32   V-3.)

33   Mineral resource discussions are focused principally on hydrocarbons and potassium salts, both  
34   of which have long histories of development in the region. Development of either resource  
35   potentially could be disruptive to the disposal system. The information regarding the mineral  
36   resources concentrates on the following factors:

- 37     • number, location, depth, and present state of development, including penetrations through  
38       the disposal horizon,
- 39     • type of resource,
- 40     • accessibility, quality, and demand, and

- 1       • mineral ownership in the area.

2       The specific impacts of resource development are discussed in Section 6.4.6.2.3, where scenarios  
3       related to mineral development are included for evaluation of disposal system performance. This  
4       discussion uses information presented in CCA Appendices DEL and MASS as indicated in the  
5       following text. The discussion of cultural and economic resources is focused on describing past  
6       and present land uses unrelated to the development of minerals. The archaeological record  
7       supports the observation that changes in land use are principally associated with climate and the  
8       availability of forage for wild and domestic animals. In no case does it appear that past or  
9       present land use has had an impact on the subsurface beyond the development of shallow  
10      groundwater wells to water livestock.

11      **2.3.1 Extractable Resources**

12      The geologic studies of the WIPP site included the investigation of potential natural resources to  
13      evaluate the impact of denying access to these resources and other consequences of their  
14      occurrence. Studies were completed in support of the FEIS to ensure knowledge of natural  
15      resources, and the impacts of denying access were included in the decision-making process for  
16      WIPP. Of the natural resources expected to occur beneath the site, five are of practical concern:  
17      the two potassium salts sylvite and langbeinite, which occur in the McNutt; and the three  
18      hydrocarbons, crude oil, natural gas, and distillate liquids associated with natural gas, all three of  
19      which occur elsewhere in strata below the Castile. Other mineral resources beneath the site are  
20      caliche, salt, gypsum, and lithium; enormous deposits of these minerals near the site and  
21      elsewhere in the country are more than adequate (and more economically attractive) to meet  
22      future requirements for these materials. In 1995, the NMBMMR performed a reevaluation of the  
23      mineral resources at and within 1.6 km (1 mi) around the WIPP site. The following discussion is  
24      based in part on information from NMBMMR (1995).

25      **2.3.1.1 Potash Resources at the WIPP Site**

26      Throughout the Carlsbad Potash District, commercial quantities of potassium salts are restricted  
27      to the middle portion of the Salado, locally called the McNutt. A total of 11 zones (or distinct  
28      ore layers) have been recognized in the McNutt. Horizon Number 1 is at the base, and Number  
29      11 is at the top. The 11th ore zone is not mined.

30      The USGS uses three standard grades—low, lease, and high—to quantify the potash resources at  
31      the site. The USGS assumes that the lease and high grades comprise reserves because some  
32      lease-grade ore is mined in the Carlsbad Potash District. Most of the potash that is mined,  
33      however, is better typified as high-grade. Even the high-grade resources may not be reserves,  
34      however, if properties such as high clay content make processing uneconomical. The analysis in  
35      NMBMMR (1995) distinguishes between lease-grade ore and economically mineable ore.

36      The NMBMMR (1995) study contains a comprehensive summary of all previous potash resource  
37      evaluations. NMBMMR (1995, Chapter VII) used 40 existing boreholes drilled on and around  
38      the WIPP site to perform a reevaluation of potash resources. He selected holes that were drilled  
39      using brine so that the dissolution of potassium salts was inhibited. The conclusion reached is

1 that only the 4th and 10th ore zones contain economic potash reserves. The quantities are  
 2 summarized in Table 2-11.

3 **Table 2-11. Current Estimates of Potash Resources at the WIPP Site**

<b>Mining Unit</b>	<b>Product</b>	<b>Recoverable Ore (<math>10^6</math> tons)</b>	
		<b>Within the WIPP site</b>	<b>One-Mile Strip Adjacent to the WIPP site</b>
4th Ore Zone	Langbeinite	40.5 at 6.99%*	126.0 at 7.30%
10th Ore Zone	Sylvite	52.3 at 13.99%	105.0 at 14.96%

Source: NMBMMR 1995, Chapter VII.

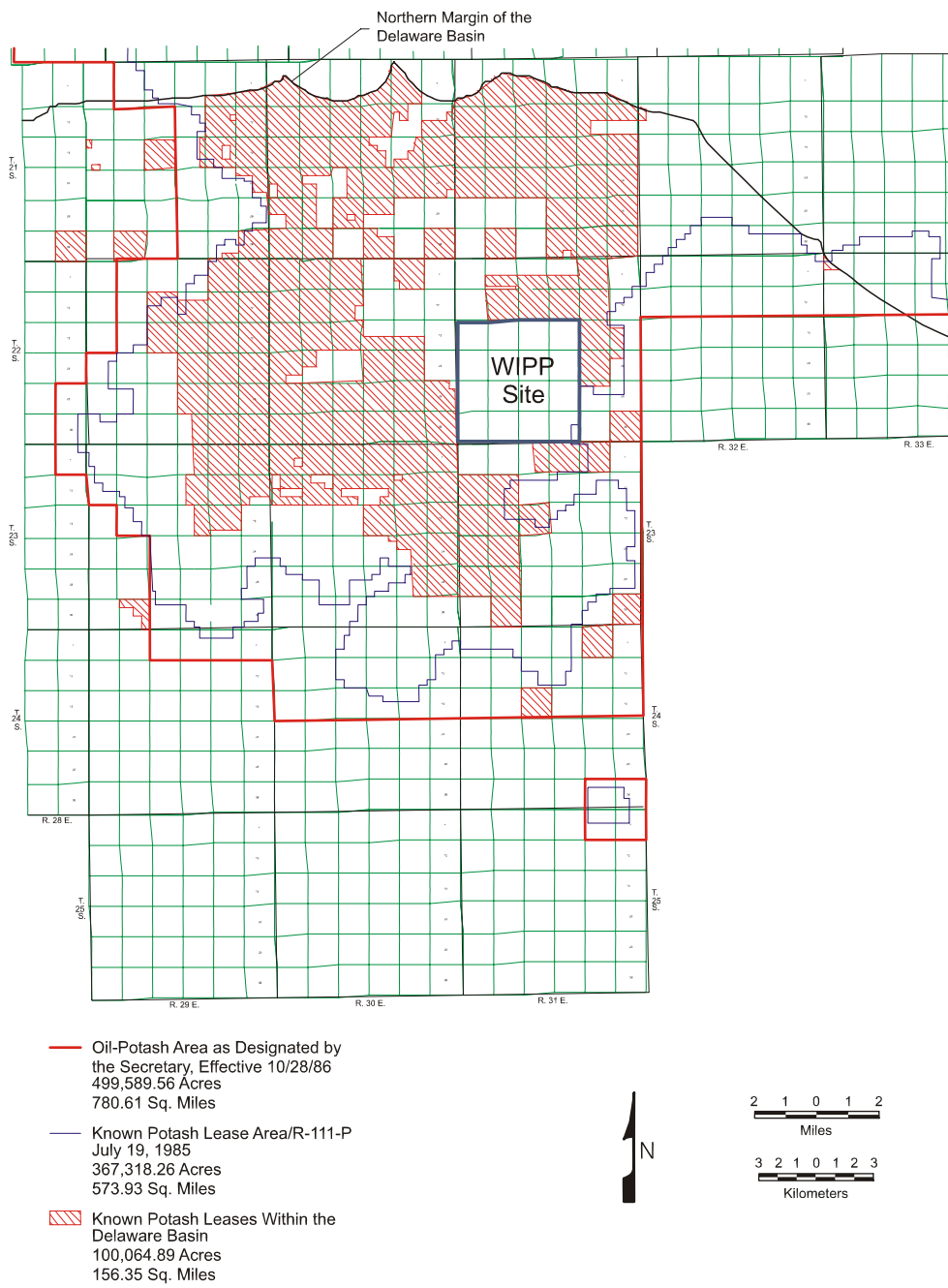
\* For example, read as  $40.5 \times 10^6$  tons of ore at a grade of 6.99 percent or higher.

4 Within the Carlsbad Known Potash Leasing Area, exploration holes have been drilled to evaluate  
 5 the grade of the various ore zones. These are included in the drillhole database in CCA  
 6 Appendix DEL. None of the economically minable reserves identified by the NMBMMR lies  
 7 directly above the waste panels. The known potash leases within the Delaware Basin are shown  
 8 in Figure 2-44 and are detailed in CCA Appendix DEL, Figure DEL-8. From information in this  
 9 figure and other data which is provided in CCA Appendix MASS, Attachment 15-5, DOE  
 10 evaluates the extent of future mining outside the land withdrawal area. The extent of possible  
 11 future mining within the controlled area is shown in Figure 2-45. The DOE also addresses this  
 12 subject with respect to PA in Section 6.4.6.2.3.

13 The EPA concluded that neither the DOE's nor the Department of Interior's (DOI) estimate  
 14 shows the area above the WIPP waste panels as containing mineable reserves. The DOE  
 15 provided supplemental information in a letter dated May 14, 1997, indicating that potash solution  
 16 mining and brine extraction do not need to be considered for the PA, based on low consequence  
 17 to the containment capability of the repository (Docket A-93-02, Item II-I-31). The EPA  
 18 reviewed the supplemental data and concurred with the DOE's conclusion. To obtain further  
 19 discussion on this topic, CARD 32-Section 32.B, CARD 33-Section 33A, and CARD 32-Section  
 20 32 F (Docket A-93-02, item III-B-2) may be referenced. Additional information is found in  
 21 FEPs screening discussions for solution mining for potash and solution mining for other  
 22 resources (FEPs H58 and H59) in Appendix PA, Attachment SCR.

### 23 2.3.1.2 Hydrocarbon Resources at the WIPP Site

24 In 1974, Foster of the NMBMMR conducted a hydrocarbon resource study in southeastern New  
 25 Mexico under contract to the ORNL. The study included an area of  $3,914 \text{ km}^2$  ( $1,512 \text{ mi}^2$ ). At  
 26 the time of that study, the proposed repository site was about 8 km (5 mi) northeast of the current  
 27 site. The 1974 NMBMMR evaluation included a more detailed study of a four-township area  
 28 centered on the old site; the present site is in the southwest quadrant of that area. The 1974  
 29 NMBMMR hydrocarbon resources study (Foster 1974) is presented in more detail in the FEIS  
 30 (DOE 1980, Section 9.2.3.5). The reader is referred to the FEIS or the original study for  
 31 additional information.



CCA-074-2

1  
2

**Figure 2-44. Known Potash Leases Within the Delaware Basin**

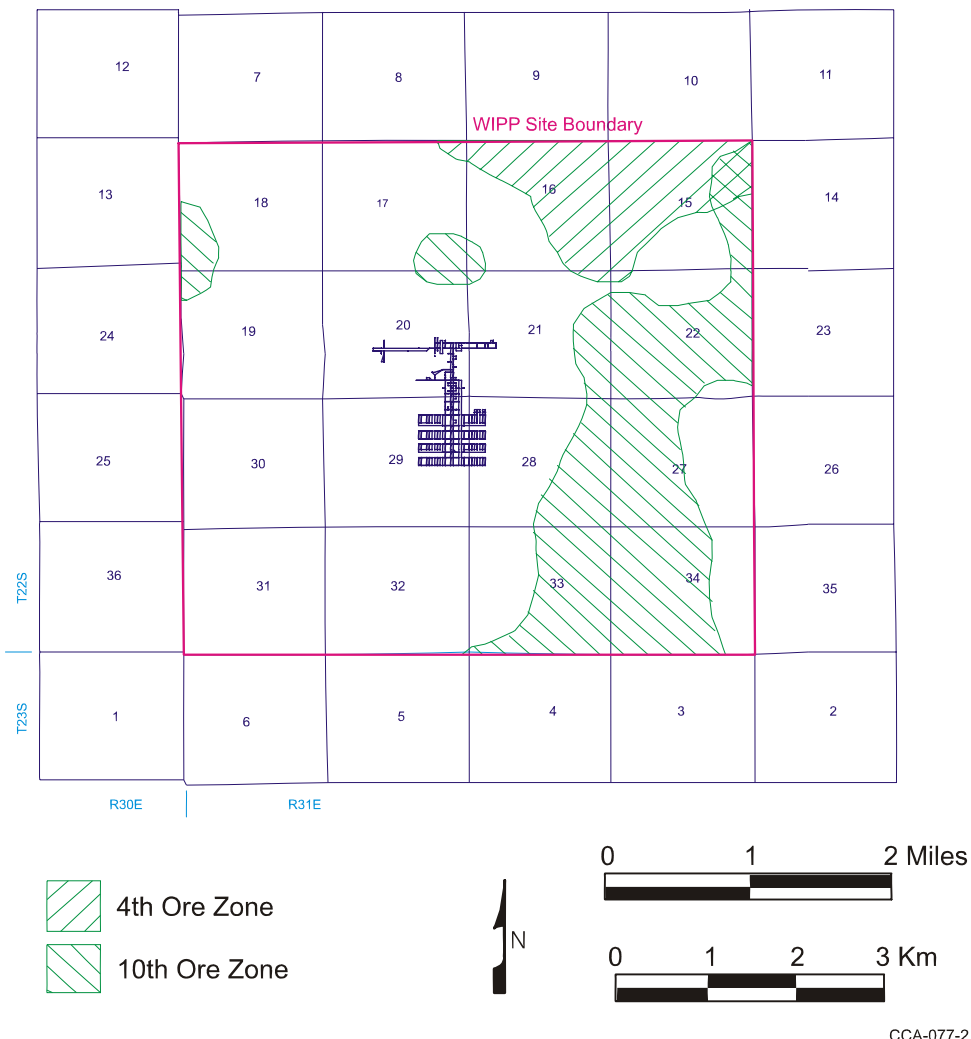


**Figure 2-45. Extent of Economically Mineable Reserves Inside the Site Boundary (Based on NMBMMR Report)**

- The resource evaluation was based both on the known reserves of crude oil and natural gas in the region and on the probability of discovering new reservoirs in areas where past unsuccessful drilling was either too widely spread or too shallow to have allowed discovery. Potentially productive zones were considered in the evaluation; therefore, the findings may be used for estimating the total hydrocarbon resources at the site. A fundamental assumption in the study was that the WIPP area has the same potential for containing hydrocarbons as the larger region studied for which exploration data are available. Whether such resources actually exist can be satisfactorily established only by drilling at spacings close enough to give a high probability of discovery.
- The NMBMMR 1995 mineral resource reevaluation contains a comprehensive summary of all previous evaluations. NMBMMR (1995, Chapter XI) provided a reassessment of hydrocarbon

resources within the WIPP site boundary and within the first mile adjacent to the boundary. Calculations were made for resources that are extensions of known, currently productive oil and gas resources that are thought to extend beneath the study area with reasonable certainty (called probable resources in the report). Qualitative estimates are also made concerning the likelihood that oil and gas may be present in undiscovered pools and fields in the area (referred to as possible resources). Possible resources were not quantified in the study. The results of the study are shown in Tables 2-12 and 2-13.

**Table 2-12. In-Place Oil within Study Area**

<b>Formation</b>	<b>Within WIPP Site (10<sup>6</sup> bbl<sup>a</sup>)</b>	<b>1-Mile Strip Adjacent to the WIPP Site (10<sup>6</sup> bbl)</b>	<b>Total (10<sup>6</sup> bbl)</b>
Delaware	10.33	20.8	31.13
Bone Spring	0.44	0.8	1.25
Strawn	0.4	0.4	0.8
Atoka	1.1	0.1	0.2
<b>Total</b>	<b>12.3</b>	<b>22.9</b>	<b>35.3</b>

Source: NMBMMR (1995, Chapter XI)

<sup>a</sup> bbl = barrel = 42 gallons**Table 2-13. In-Place Gas within Study Area**

<b>Formation</b>	<b>Gas Reserves (Mcf)<sup>a</sup></b>	
	<b>Within WIPP Site</b>	<b>1-Mile Strip Adjacent to the WIPP</b>
Delaware	18176	32873
Bone Springs	956	1749
Strawn	9600	9875
Atoka	123336	94410
Morrow	32000	28780

Source: NMBMMR (1995, Chapter XI)

<sup>a</sup> Mcf = thousand cubic feet

The DOE compiled statistics on the historical development of hydrocarbon resources in the Delaware Basin and included them in CCA Appendix DEL. For these purposes, the Delaware Basin is described as the surface and subsurface features that lie inside the boundary formed to the north, east, and west by the innermost edge of the Capitan Reef and formed to the south by a straight line drawn from the southeastern point of the Davis Mountains to the southwestern point of the Glass Mountains (see Figure 2-46).

Several important modeling parameters result from the study of hydrocarbon resources and the history of their exploitation. These include parameters related to the number of human intrusions, the size of boreholes, the operational histories of such holes, the plugging of these

1 holes, and the use of such holes for other purposes, such as liquid disposal. Each of these topics  
2 is discussed in detail in CCA Appendix DEL and Appendix PA, Attachment MASS, Section  
3 MASS.16 and is addressed in Sections 6.4.7 and 6.4.12. The distribution of existing boreholes is  
4 shown in Figure DEL-4 (CCA Appendix DEL) for the entire Delaware Basin and Figure 2-47 for  
5 the vicinity of the WIPP site. In addition, CCA Appendix DEL includes an assessment of  
6 current drilling and plugging practices in the Delaware Basin. CCA Appendix DEL also  
7 discusses the regulatory constraints placed on the use of wells for injection.

8    2.3.1.3 Other Resources

9 While the focus of studies at the WIPP has been on potash and hydrocarbon, other resources are  
10 known to occur within the Delaware Basin and are considered in the screening. For example,  
11 sulfur is produced in the vicinity of Orla, Texas. Sulfur wells are included in CCA Appendix  
12 DEL; however, no sulfur resources have been identified in the vicinity of the WIPP; therefore,  
13 there are no projected impacts. Another resource that is extensively produced is groundwater.  
14 Potable water occurs in numerous places within the Delaware Basin. Several communities rely  
15 solely on groundwater sources for drinking water. CCA Appendix DEL includes a distribution of  
16 groundwater wells in the Delaware Basin. All such wells in the vicinity of the WIPP are  
17 shallow, generally no deeper than the Culebra. An evaluation of underground sources of  
18 drinking water in the vicinity of the disposal system is presented in CCA Appendix USDW.  
19 Figure USDW-4 shows the distribution of groundwater wells in the vicinity of the disposal  
20 system. Sand, gravel, and caliche are produced in numerous areas within the Delaware Basin. In  
21 all cases, these are surface quarries that are generally shallow (10s of feet). No impact to the  
22 disposal system is expected from these activities.

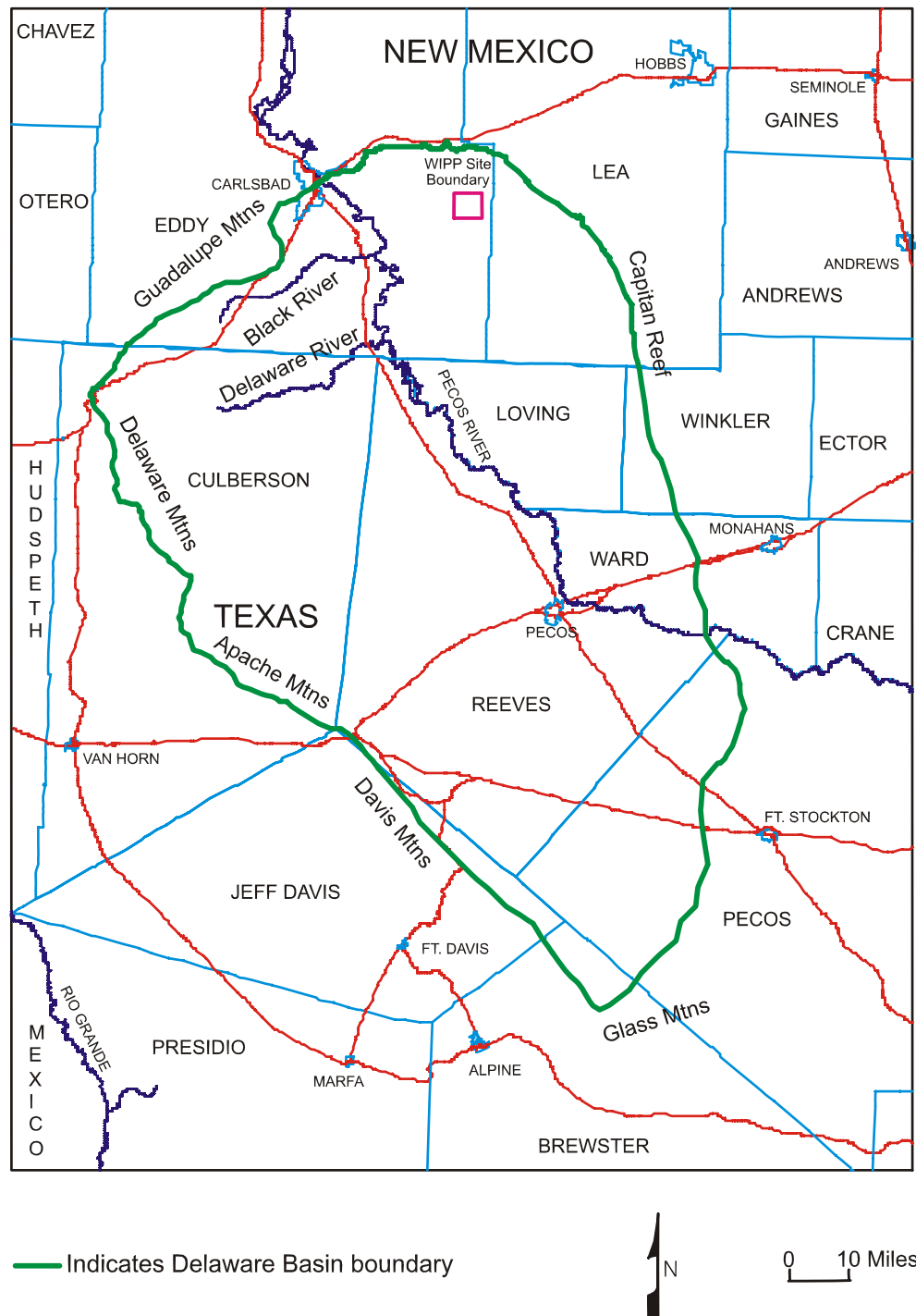
23    2.3.2 *Cultural and Economic Resources*

24 The demographics, land use, and history and archaeology of the WIPP site and its environs are  
25 characterized in the sections that follow.

26    2.3.2.1 Demographics

27 The WIPP facility is located 42 km (26 mi) east of Carlsbad in Eddy County in southeastern  
28 New Mexico and includes an area of 10,240 ac (approximately 41 km<sup>2</sup>) (16 mi<sup>2</sup>). The facility is  
29 located in a sparsely populated area with fewer than 30 permanent residents living within a 16-  
30 km (10-mi) radius of the facility. The area surrounding the facility is used primarily for grazing,  
31 potash mining, and hydrocarbon production. No resource development that would affect WIPP  
32 facility operations or the long-term integrity of the facility is allowed within the 10,240 ac that  
33 have been set aside for the WIPP project.

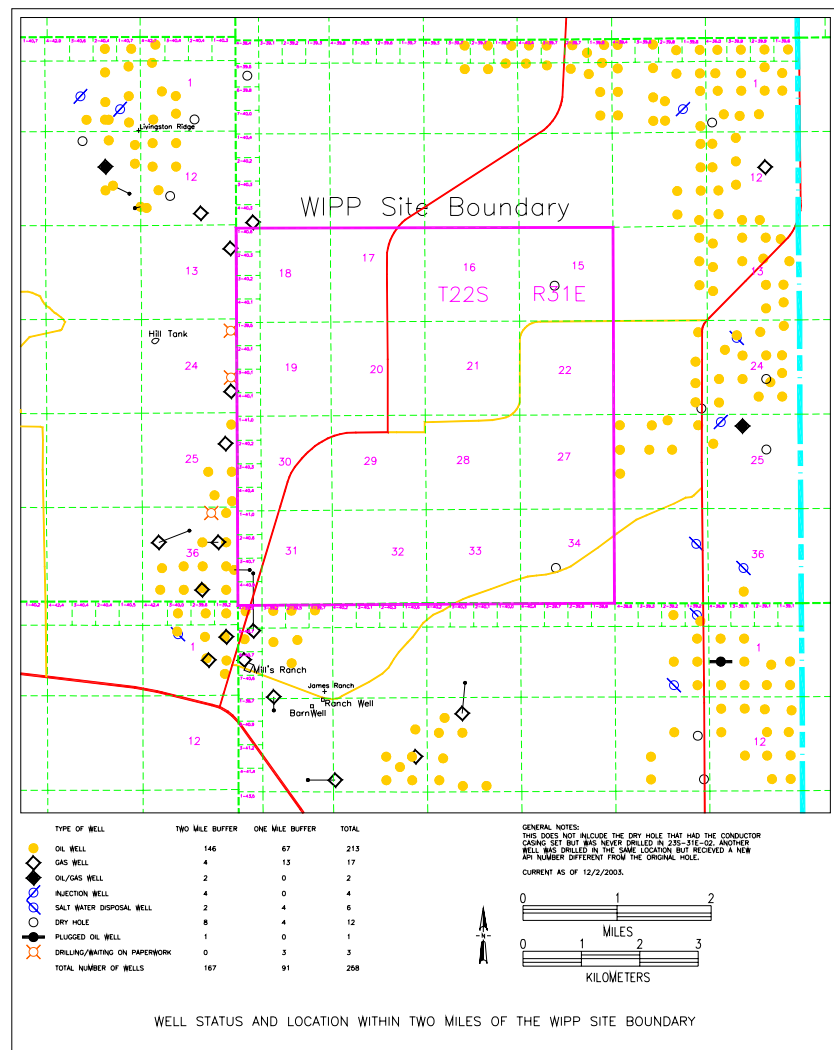
34 The permanent residence nearest to the WIPP site boundary is the J.C. Mills Ranch, which is  
35 2 km (1.2 mi) to the south. The community nearest to the WIPP site is the town of Loving, New  
36 Mexico, 29 km (18 mi) west-southwest of the site center. The population of Loving increased  
37 from 1,243 in 1990 to 1,326 in 2000. The nearest population center is the city of Carlsbad, New  
38 Mexico, 42 km (26 mi) west of the site. The population of



1  
2

CCA-072-2

**Figure 2-46. Delaware Basin Boundary**



1

2 **Figure 2-47. Distribution of Existing Petroleum Industry Boreholes Within Two Miles of  
3 the WIPP Site**

4 Carlsbad increased from 24,896 in 1990 to 26,870 in 2000. Hobbs, New Mexico, 58 km (36 mi)  
5 to the east of the site, had a population decrease from 29,115 in 1990 to 28,657 in 2000. Eunice,  
6 New Mexico, 64 km (40 mi) east of the site, had a 1990 population of 2,731 decrease to 2,562 in  
7 2000. Jal, New Mexico, 72 km (45 mi) southeast of the site, had a population of 2,153 in 1990  
8 decrease to 1,996 in 2000.

9 The WIPP site is located in Eddy County near the border of Lea County, New Mexico. The  
10 Eddy County population increased from 48,605 in 1990 to 51,658 in 2000. The Lea County  
11 population decreased from 55,765 in 1990 to 55,511 in 2000. Population figures are taken from  
12 the 1990 census (U.S. Department of Commerce, 1990) and the 2000 census (U.S. Census  
13 Bureau, 2000).

1    2.3.2.2 Land Use

2    At present, land within 16 km (10 mi) of the site is used for potash mining operations, active oil  
3    and gas wells, activities associated with hydrocarbon production, and grazing.

4    The WIPP Land Withdrawal Act (LWA) (U.S. Congress 1992) withdrew certain public lands  
5    from the jurisdiction of the Bureau of Land Management (BLM). The law provides for the  
6    transfer of the WIPP site lands from the DOI to the DOE and effectively withdraws the lands,  
7    subject to existing rights, from entry, sale, or disposition; appropriation under mining laws; or  
8    operation of the mineral and geothermal leasing laws. The LWA directed the Secretary of  
9    Energy to produce a management plan to provide for grazing, hunting and trapping, wildlife  
10   habitat, mining, and the disposal of salt and tailings.

11   Between 1978 and 1988, DOE acquired all active potash and hydrocarbon leases within the  
12   WIPP site boundary. These were acquired either through outright purchase or through  
13   condemnation. In one condemnation proceeding, the court awarded DOE the surface and top  
14   1.82 km (6,000 ft) of Section 31 and allowed the leaseholder to retain the subsurface below 1.82  
15   km (6,000 ft). This was allowed because analysis showed that wells developed within this lease  
16   below the 1.82-km (6,000ft) limit would be too far away from the waste panels to be of  
17   consequence to the WIPP (see, for example, Brausch et al. 1982). This is corroborated by the  
18   results of PA discussed in Section 6.2.5.1; and Appendix PA, Attachment SCR, FEP 56.  
19   Consequently, as the result of the DOE's acquisition activities, there are no producing  
20   hydrocarbon wells within the volumetric boundary defined by the land withdrawal (T22S, R31E,  
21   S15-22, 27-34). Two active wells were drilled to tap the oil and gas resources on the leases  
22   beneath Section 31. The James Ranch #13, drilled in 1982, is a gas well, and the James Ranch  
23   #27, drilled in 2000, is an oil well. Both wells are located on surface leases outside the WIPP  
24   site boundary. Both wells enter Section 31 below a depth of 1.82 km (6,000 ft) beneath ground  
25   level. Except for the leases in Section 31, the LWA prohibits all drilling into the controlled area  
26   unless such drilling is in support of the WIPP.

27   Grazing leases have been issued for all land sections immediately surrounding the WIPP facility.  
28   Grazing within the WIPP site lands occurs within the authorization of the Taylor Grazing Act of  
29   1934, the Federal Land Policy and Management Act (FLPMA), the Public Rangelands  
30   Improvement Act of 1978, and the Bankhead-Jones Farm Tenant Act of 1973.

31   The responsibilities of DOE include supervision of ancillary activities associated with grazing  
32   (for example, wildlife access to livestock water development), tracking of water developments  
33   inside WIPP lands to ensure that they are configured according to the regulatory requirements,  
34   and ongoing coordination with respective allottees. Administration of grazing rights is in  
35   cooperation with the BLM according to the memorandum of understanding (MOU) and the  
36   coinciding Statement of Work through guidance established in the East Roswell Grazing  
37   Environmental Impact Statement. The WIPP site is composed of two grazing allotments  
38   administered by the BLM: the Livingston Ridge (No. 77027), and the Antelope Ridge  
39   (No. 77032) (see Figure 7-2).

1    2.3.2.3 History and Archaeology

2    From about 10,000 B.C. to the late 1800s, the WIPP site and surrounding region were inhabited  
3    by nomadic aboriginal hunters and gatherers who subsisted on various wild plants and animals.  
4    From about A.D. 600 onward, as trade networks were established with Puebloan peoples to the  
5    west, domesticated plant foods and materials were acquired in exchange for dried meat, hides,  
6    and other products from the Pecos Valley and Plains. In the late 1500s, the Spanish  
7    Conquistadors encountered Jumano and Apachean peoples in the region who practiced hunting  
8    and gathering and engaged in trade with Puebloans. After the Jumanos abandoned the southern  
9    Plains region, the Comanches became the major population of the area. Neighboring populations  
10   with whom the Comanches maintained relationships ranging from mutual trade to open warfare  
11   included the Lipan, or Southern Plains Apache, several Puebloan Groups, Spaniards, and the  
12   Mescalero Apaches.

13   The best documented indigenous culture in the WIPP region is that of the Mescalero Apaches,  
14   who lived west of the Pecos. The lifestyle of the Mescalero Apaches represents a transition  
15   between the full sedentism of the Pueblos and the nomadic hunting and gathering of the  
16   Jumanos. In 1763, the San Saba expedition encountered and camped with a group of Mescaleros  
17   in Los Medaños. Expedition records indicate the presence of both Lipan and Mescalero Apaches  
18   in the region.

19   A peace accord reached between the Comanches and the Spaniards in 1786 resulted in two  
20   historically important economic developments: (1) organized buffalo hunting by Hispanic and  
21   Puebloan ciboleros, and (2) renewal and expansion of the earlier extensive trade networks by  
22   Comancheros. These events placed eastern New Mexico in a position to receive a wide array of  
23   both physical and ideological input from the Plains culture area to the east and north and from  
24   Spanish-dominated regions to the west and south. Comanchero trade began to mesh with the  
25   Southwest American trade influence in the early nineteenth century. However, by the late 1860s,  
26   the importance of Comanchero trade was cut short by Texan influence.

27   The first cattle trail in the area was established along the Pecos River in 1866 by Charles  
28   Goodnight and Oliver Loving. By 1868, Texan John Chisum dominated much of the area by  
29   controlling key springs along the river. Overgrazing, drought, and dropping beef prices led to  
30   the demise of open-range cattle ranching by the late 1880s.

31   Following the demise of open-range livestock production, ranching developed using fenced  
32   grazing areas and production of hay crops for winter use. Herd grazing patterns were influenced  
33   by the availability of water supplies as well as by the storage of summer grasses for winter  
34   feeding.

35   The town of Carlsbad was founded as Eddy in 1889 as a health spa. In addition to ranching, the  
36   twentieth century brought the development of the potash, oil, and gas industries that have  
37   increased the population eightfold in the last 50 years.

38   Although technological change has altered some of the aspects, ranching remains an important  
39   economic activity in the WIPP region. This relationship between people and the land is still an  
40   important issue in the area. Ranch-related sites dating to the 1940s and 1950s are common in

1 parts of the WIPP area. These will be considered historical properties within the next several  
2 years, and thus will be treated as such under current law.

3 The National Historic Preservation Act (NHPA) (16 USC Part 470 et seq.) was enacted to protect  
4 the nation's cultural resources in conjunction with the states, local governments, Indian tribes,  
5 and private organizations and individuals. The policy of the federal government includes:  
6 (1) providing leadership in preserving the prehistoric and historic resources of the nation,  
7 (2) administering federally owned, administered, or controlled prehistoric resources for the  
8 benefit of present and future generations, (3) contributing to the preservation of nonfederally  
9 owned prehistoric and historic resources, and (4) assisting state and local governments and the  
10 national trust for historic preservation in expanding and accelerating their historic preservation  
11 programs and activities. The act also established the National Register of Historic Places  
12 (National Register). At the state level, the State Historic Preservation Officer (SHPO)  
13 coordinates the state's participation in implementing the NHPA. The NHPA has been amended  
14 by two acts: the Archeological and Historic Preservation Act (16 USC Part 469 et seq.), and the  
15 Archeological Resource Protection Act (16 USC Part 470aa et seq.).

16 To protect and preserve cultural resources found within the WIPP site boundary, the WIPP  
17 submitted a mitigation plan to the New Mexico SHPO describing the steps to either avoid or  
18 excavate archaeological sites. A site was defined as a place used and occupied by prehistoric  
19 people. In May 1980, the SHPO made a determination of "no adverse effect from WIPP facility  
20 activities" on cultural resources. The Advisory Council on Historic Preservation concurred that  
21 the WIPP Mitigation Plan is appropriate to protect cultural resources.

22 Known historical sites (more than 50 years old) in southeastern New Mexico consist primarily of  
23 early twentieth century homesteads that failed, or isolated features from late nineteenth century  
24 and early twentieth century cattle or sheep ranching, or military activities. To date, no Spanish  
25 or Mexican sites have been identified. Historic components are rare but are occasionally noted  
26 in the WIPP area. These include features and debris related to ranching.

27 Since 1976, cultural resource investigations have recorded 98 archaeological sites and numerous  
28 isolated artifacts within the 41km<sup>2</sup> (16mi<sup>2</sup>) area enclosed by the WIPP site. In the central  
29 10.4km<sup>2</sup> (4mi<sup>2</sup>) area, 33 sites were determined to be eligible for inclusion on the National  
30 Register as archaeological districts. Investigations since 1980 have recorded an additional 14  
31 individual sites outside the central 10.4km<sup>2</sup> (4mi<sup>2</sup>) area that are considered eligible for inclusion  
32 on the National Register. The following major cultural resource investigations to date are broken  
33 out in the list that follows. Additional information can be found in the bibliography of CCA  
34 Chapter 2.

35 **1977.** The first survey of the area was conducted for SNL by Nielson of the Agency for  
36 Conservation Archaeology (ACA). This survey resulted in the location of 33 sites and 64  
37 isolated artifacts.

38 **1979.** MacLennan and Schermer of ACA conducted another survey to determine access roads  
39 and a railroad right-of-way for Bechtel, Inc. The survey encountered two sites and 12 isolated  
40 artifacts.

1   **1980.** Schermer conducted another survey to relocate the sites originally recorded by Nielson.  
2   This survey redescribed 28 of the original 33 sites.

3   **1981.** Hicks (1981a, 1981b) directed the excavation of nine sites in the WIPP core area.

4   **1982.** Bradley (Lord and Reynolds 1985) recorded one site and four isolated artifacts in an  
5   archaeological survey for a proposed water pipeline.

6   **1985.** Lord and Reynolds (1985) examined three sites within the WIPP core area that consisted  
7   of two plant-collecting and processing sites and one base camp used between 1000 B.C. and  
8   A.D. 1400. The artifacts recovered from the excavations are in the Laboratory of Anthropology  
9   at the Museum of New Mexico in Santa Fe.

10   **1987.** Mariah Associates, Inc. identified 40 sites and 75 isolates in an inventory of 2,460 ac in  
11   15 quarter-section units surrounding the WIPP site. In this investigation, 19 of the sites were  
12   located within the WIPP site's boundary. Sites encountered in this investigation tended to lack  
13   evident or intact features. Of the 40 new sites defined, 14 were considered eligible for inclusion  
14   in the National Register, 24 were identified as having insufficient data to determine eligibility,  
15   and 2 were determined to be ineligible for inclusion. The eligible and potentially eligible sites  
16   have been mapped and are avoided by DOE in its current activities at the WIPP site.

17   **1988–1992.** Several archaeological clearance reports have been prepared for seismic testing  
18   lines on public lands in Eddy County, New Mexico.

19   All archaeological sites are surface or near-surface sites, and no reasons exist (either geological  
20   or archeological) to suspect that deep drilling would uncover or investigate archaeological sites.

21   No artifacts were encountered during cultural resource surveys performed from 1992 until  
22   present. The following list provides examples of WIPP projects that required cultural resource  
23   surveys. All investigations were performed and reported in accordance with requirements  
24   established by the New Mexico Office of Cultural Affairs (OCA) and administered by the  
25   SHPO.

- 26   • SPDV site investigation into status of a previously recorded site (#LA 33175) to determine  
27   potential impacts from nearby reclamation activity. Assessment included minor surface  
28   excavation.
- 29   • WIPP well bore C-2737. Cultural resource investigation for well pad and access road.
- 30   • WIPP well bores WQSP 1-6 and 6a. Individual cultural resource investigations conducted  
31   for construction of each respective well pad and access road.
- 32   • WIPP well bores SNL 1, 2, 3, 9 and 12. Cultural resource investigations conducted for  
33   construction of each respective well pad and access road.
- 34   • WIPP well bore WTS 4. Cultural resource investigation conducted in support of siting and  
35   constructing reserve pits for well drilling and development.

1     • North Salt Pile Expansion. Cultural resource investigation conducted in support of the  
2       expansion of the North Salt Pile, a project designed to mitigate surface water infiltration.

3     All of the aforementioned archeological investigations received determinations of “No Adverse  
4       Affect” from the OCA and the SHPO. This determination serves as a clearance to proceed with  
5       work.

6     The Delaware Basin has been used in the past for an isolated nuclear test. This test, Project  
7       Gnome, took place in 1961 at a location approximately 13 km (8 mi) southwest of the WIPP.  
8       The primary objective of Project Gnome was to study the effects of an underground nuclear  
9       explosion in salt. The Gnome experiment involved the detonation of a 3.1-kiloton nuclear device  
10      at a depth of 361 m (1,200 ft) in the bedded salt of the Salado (Rawson et al. 1965). The  
11      explosion created a cavity of approximately 28,000 m<sup>3</sup> (1,000,000 ft<sup>3</sup>) and caused surface  
12      displacements over an area of about a 360m (1,200ft) radius. Fracturing and faulting caused  
13      measurable changes in rock permeability and porosity at distances up to approximately 100 m  
14      (330 ft) from the cavity. No earth tremors were reported at distances over 40 km (25 mi) from  
15      the explosion. Project Gnome was decommissioned in 1979.

## 16     **2.4 Background Environmental Conditions**

17     Background environmental conditions at and near the WIPP site were characterized prior to the  
18       initiation of the operation of the facility and are described in CCA Section 2.4. Because  
19       background characterization focuses on environmental conditions existing prior to operations, it  
20       is not meaningful to redefine background environmental conditions after operations began.  
21       Accordingly, information presented in CCA Section 2.4 is not repeated and updated in this  
22       recertification application.

## 23     **2.5 Climate and Meteorological Conditions**

24     The DOE did not consider climate directly in its site selection process, although criteria such as  
25       low population density and large tracts of federally owned land tend to favor arid and semi-arid  
26       areas in the western United States. The semi-arid climate around the WIPP is beneficial since it  
27       is a direct cause of the lack of a near surface water table and the minimization of radiation  
28       exposure pathways that involve surface or groundwater. Data used to interpret paleoclimates in  
29       the American southwest come from a variety of sources and indicate alternating arid and subarid  
30       to subhumid climates throughout the Pleistocene. The information in this section was taken from  
31       Swift (1992), and included in CCA Appendix CLI and references therein.

### 32     **2.5.1 Historic Climatic Conditions**

33     Prior to 18,000 years ago, radiometric dates are relatively scarce, and the record is incomplete.  
34     From 18,000 years ago to the present, however, the climatic record is relatively well constrained  
35       by floral, faunal, and lacustrine data. These data span the transition from the last full-glacial  
36       maximum to the present interglacial period; given the global consistency of glacial fluctuations  
37       described below, they can be taken to be broadly representative of extremes for the entire  
38       Pleistocene.

1 Early and middle Pleistocene paleoclimatic data for the southwestern United States are  
2 incomplete and permit neither continuous reconstructions of paleoclimates nor direct correlations  
3 between climate and glaciation prior to the last glacial maximum, which occurred 22,000 to  
4 18,000 years ago. Stratigraphic and soil data from several locations, however, indicate that  
5 cyclical alternation of wetter and drier climates in the Southwest had begun by the Early  
6 Pleistocene. Fluvial gravels in the Gatuña exposed in the Pecos River Valley of eastern New  
7 Mexico suggest wetter conditions 1.4 million years ago and again 600,000 years ago. The  
8 Mescalero caliche, exposed locally over much of southeastern New Mexico, suggests drier  
9 conditions 510,000 years ago, and loosely dated spring deposits in Nash Draw west of the WIPP  
10 imply wetter conditions occurring again later in the Pleistocene. The Blackwater Draw  
11 Formation of the southern High Plains of eastern New Mexico and western Texas, correlating in  
12 time to both the Gatuña Formation and the Mescalero caliche, contains alternating soil and eolian  
13 sand horizons that show at least six climatic cycles beginning more than 1.4 million years ago  
14 and continuing to the present.

15 Data used to construct the more detailed climatic record for the latest Pleistocene and Holocene  
16 come from six independent lines of evidence dated using carbon-14 techniques: plant  
17 communities preserved in packrat middens throughout the southwest, including sites in Eddy and  
18 Otero counties, New Mexico; pollen assemblages from lacustrine deposits in western New  
19 Mexico and other locations in the southwest; gastropod assemblages from western Texas;  
20 ostracod assemblages from western New Mexico; paleolake levels throughout the southwest; and  
21 faunal remains from caves in southern New Mexico.

22 Prior to the last glacial maximum 22,000 to 18,000 years ago, evidence from faunal assemblages  
23 in caves in southern New Mexico, including the presence of species such as the desert tortoise  
24 that are now restricted to warmer climates, suggests hot summers and mild, dry winters.  
25 Lacustrine evidence confirms the interpretation of a relatively dry climate prior to and during the  
26 glacial advance. Permanent water did not appear in what was later to become a major lake in the  
27 Estancia Valley in central New Mexico until some time before 24,000 years ago, and water  
28 depths in lakes at higher elevations in the San Agustin Plains in western New Mexico did not  
29 reach a maximum until sometime between 22,000 and 19,000 years ago. Ample floral and  
30 lacustrine evidence documents cooler, wetter conditions in the southwest during the glacial peak.  
31 These changes were not caused by the immediate proximity of glacial ice. None of the  
32 Pleistocene continental glaciations advanced farther southwest than northeastern Kansas, and the  
33 most recent, late-Wisconsinan ice sheet reached its limit in South Dakota, approximately 1,200  
34 km (750 mi) from WIPP. Discontinuous alpine glaciers formed at the highest elevations  
35 throughout the Rocky Mountains, but these isolated ice masses were symptoms, rather than  
36 causes, of cooler and wetter conditions and had little influence on regional climate at lower  
37 elevations. The closest such glacier to WIPP was on the northeast face of Sierra Blanca Peak in  
38 the Sacramento Mountains, approximately 220 km (135 mi) to the northwest.

39 Global climate models indicate that the dominant glacial effect in the southwest was the  
40 disruption and southward displacement of the westerly jet stream by the physical mass of the ice  
41 sheet to the north. At the glacial peak, major Pacific storm systems followed the jet stream  
42 across New Mexico and the southern Rocky Mountains, and winters were wetter and longer than  
43 either at the present or during the previous interglacial period.

1      Gastropod assemblages at Lubbock Lake in western Texas suggest mean annual temperatures 5°  
2      C (9° F) below present values. Both floral and faunal evidence indicate that annual precipitation  
3      throughout the region was 1.6 to 2.0 times greater than today's values. Floral evidence also  
4      suggests that winters may have continued to be relatively mild, perhaps because the glacial mass  
5      blocked the southward movement of arctic air. Summers at the glacial maximum were cooler  
6      and drier than at present, without a strongly developed monsoon.

7      The jet stream shifted northward following the gradual retreat of the ice sheet after 18,000 years  
8      ago, and the climate responded accordingly. By approximately 11,000 years ago, conditions  
9      were significantly warmer and drier than previously, although still dominated by winter storms  
10     and still wetter than today. Major decreases in total precipitation and the shift toward the  
11     modern monsoonal climate did not occur until the ice sheet had retreated into northeastern  
12     Canada in the early Holocene.

13     By middle Holocene time, the climate was similar to that of the present, with hot, monsoon-  
14     dominated summers and cold, dry winters. The pattern has persisted to the present, but not  
15     without significant local variations. Soil studies show that the southern High Plains were drier  
16     from 6,500 to 4,500 years ago than before or since. Gastropod data from Lubbock Lake indicate  
17     the driest conditions from 7,000 to 5,000 years ago (precipitation, 0.89 times present values;  
18     mean annual temperature, 2.5° C [4.5° F] higher than present values), with a cooler and wetter  
19     period 1,000 years ago (precipitation, 1.45 times present values; mean annual temperature, 2.5° C  
20     [4.5° F] lower than present). Plant assemblages from southwestern Arizona suggest steadily  
21     decreasing precipitation from the middle Holocene to the present, except for a brief wet period  
22     approximately 990 years ago. Stratigraphic work at Lake Cochise (the present Willcox playa in  
23     southeast Arizona) shows two mid-Holocene lake stands, one near or before 5,400 years ago and  
24     one between or before 3,000 to 4,000 years ago; however, both were relatively short-lived, and  
25     neither reached the maximum depths of the Late Pleistocene high stand that existed before  
26     14,000 years ago.

27     Inferred historical precipitation indicates that during the Holocene, wet periods were relatively  
28     drier and shorter in duration than those of the late Pleistocene. Historical records over the last  
29     several hundred years indicate numerous lower-intensity climatic fluctuations, some too short in  
30     duration to affect floral and faunal circulation. Sunspot cycles and the related change in the  
31     amount of energy emitted by the sun have been linked to historical climatic changes elsewhere in  
32     the world, but the validity of the correlation is uncertain. Correlations have also been proposed  
33     between volcanic activity and climatic change. In general, however, causes for past short-term  
34     changes are unknown.

35     The climatic record presented here should be interpreted with caution because its resolution and  
36     accuracy are limited by the nature of the data used to construct it. Floral and faunal assemblages  
37     change gradually and show only a limited response to climatic fluctuations that occur at  
38     frequencies that are higher than the typical life span of the organisms in question. For long-lived  
39     species such as trees, resolution may be limited to hundreds or even thousands of years.  
40     Sedimentation in lakes and playas has the potential to record higher-frequency fluctuations,  
41     including single-storm events, but only under a limited range of circumstances. Once water  
42     levels reach a spill point, for example, lakes show only a limited response to further increases in  
43     precipitation.

With these observations in mind, three significant conclusions can be drawn from the climatic record of the American southwest. First, maximum precipitation in the past coincided with the maximum advance of the North American ice sheet. Minimum precipitation occurred after the ice sheet had retreated to its present limits. Second, past maximum long-term average precipitation levels were roughly twice the present levels. Minimum levels may have been 90 percent of the present levels. Third, short-term fluctuations in precipitation have occurred during the present relatively dry, interglacial period, but they have not exceeded the upper limits of the glacial maximum.

Too little is known about the relatively short-term behavior of global circulation patterns to accurately predict precipitation levels over the next 10,000 years. The long-term stability of patterns of glaciation and deglaciation, however, do permit the conclusion that future climatic extremes are unlikely to exceed those of the late Pleistocene. Furthermore, the periodicity of glacial events suggests that a return to full-glacial conditions is highly unlikely within the next 10,000 years.

### **2.5.2 Recent Climatic Conditions**

Recent climatic conditions are provided to allow for the assessment of impacts of these factors on the disposal unit and the site. Data are taken from the WIPP environmental monitoring reports (see WEC 1991a, 1991b, 1992, 1993, 1994, 1995, 1996, 1997, 1998; WGESC 1999; ESRF 2000, 2001, 2002; and WRES 2003).

#### **2.5.2.1 General Climatic Conditions**

The climate of the region is semiarid, with generally mild temperatures, low precipitation and humidity, and a high evaporation rate. Winds are mostly from the southeast and moderate. In late winter and spring, there are strong west winds and dust storms. During the winter, the weather is often dominated by a high-pressure system situated in the central portion of the western United States and a low-pressure system located in north-central Mexico. During the summer, the region is affected by a low-pressure system normally situated over Arizona.

#### **2.5.2.2 Temperature Summary**

Temperatures are moderate throughout the year, although seasonal changes are distinct. The mean annual temperature in southeastern New Mexico is 63° F (17° C). In the winter (December through February), nighttime lows average near 23° F (-5° C), and maxima average in the 50s. The lowest recorded temperature at the nearest Class-A weather station in Roswell was -29° F (-34° C) in February 1905. In the summer (June through August), the daytime temperature exceeds 90° F (32° C) approximately 75 percent of the time. The National Weather Service documented 122° F (50° C) at the WIPP site as the record high temperature for New Mexico. This temperature was recorded on June 27, 1994. Table 2-14 shows the annual average, maximum, and minimum temperatures from 1990 through 2002.

1    **2.5.2.3 Precipitation Summary**

2    Precipitation is light and unevenly distributed throughout the year, averaging 28.2cm (11.1in.)  
 3    per year from 1995 through 2002. Winter is the season of least precipitation, averaging less than  
 4    1.5 cm (0.6 in.) of rainfall per month. Snow averages about 13 cm (5 in.) per year at the site and  
 5    seldom remains on the ground for more than a day. Approximately half the annual precipitation  
 6    comes from frequent thunderstorms in June through September. Rains are usually brief but  
 7    occasionally intense when moisture from the Gulf of Mexico spreads over the region. Monthly  
 8    average, maximum, and minimum precipitations recorded at the WIPP site from 1990 through  
 9    2002 are summarized in Figure 2-48.

10    **2.5.2.4 Wind Speed and Wind Direction Summary**

11    The frequencies of wind speeds and directions are depicted by wind roses in Figures 2-49  
 12    through 2-56 for the WIPP site.

13    **Table 2-14. Annual Average, Maximum, and Minimum Temperatures**

Year	Annual Average Temperature		Maximum Temperature		Minimum Temperature	
	(°C)	(°F)	(°C)	(°F)	(°C)	(°F)
1990	17.8	64	46.1	115	-13.9	7
1991	17.2	63	42.8	109	-7.8	18
1992	17.2	63	42.8	109	-10	14
1993	17.8	64	42.8	109	-18.9	-2
1994	17.8	64	50	122	-14.4	6
1995	17	63	42	107	-7	19
1996	17	63	41	106	-7	19
1997	16.3	61.4	38.6	101.5	-11.4	11.4
1998	18.3	64.9	41.6	106.9	-10.8	12.6
1999	18.1	64.6	40.9	105.6	-7.9	17.8
2000	17.4	63.3	40.2	104.4	-6.8	19.7
2001	17.5	63.5	39.5	103.2	-7.8	18.0
2002	17.5	63.5	39.8	103.7	-8.9	16.0
Average	17.5	63.5	42.2	107.9	-0.2	13.9

1    **2.6 Seismology**

2    The DOE used tectonic activity as a siting criterion. The intent was to avoid tectonic conditions  
3    such as faulting and igneous activity that would jeopardize waste isolation over the long term  
4    and to avoid areas where earthquake size and frequency could impact facility design and  
5    operations. The WIPP site met both aspects of this criterion fully. Long-term tectonic activity is  
6    discussed in Section 2.1.5. The favorable results of the seismic (earthquake) studies are  
7    discussed here. The purpose of the seismic studies is to build a basis from which to predict  
8    ground motions that the WIPP repository may be subjected to in the near and distant future. The  
9    concern about seismic effects in the near future, during the operational period, pertains mainly to  
10   the design requirements for surface and underground structures for providing containment during  
11   seismic events. The concern about effects occurring over the long term, after the repository has  
12   been decommissioned and sealed, pertains more to relative motions (faulting) within the  
13   repository and possible effects of faulting on the integrity of the salt beds and/or shaft seals.  
14   Updated seismic activity information is provided in Figures 2-57 and 2-58. In this discussion,  
15   the magnitudes are reported in terms of the Richter scale, and all intensities are based on the

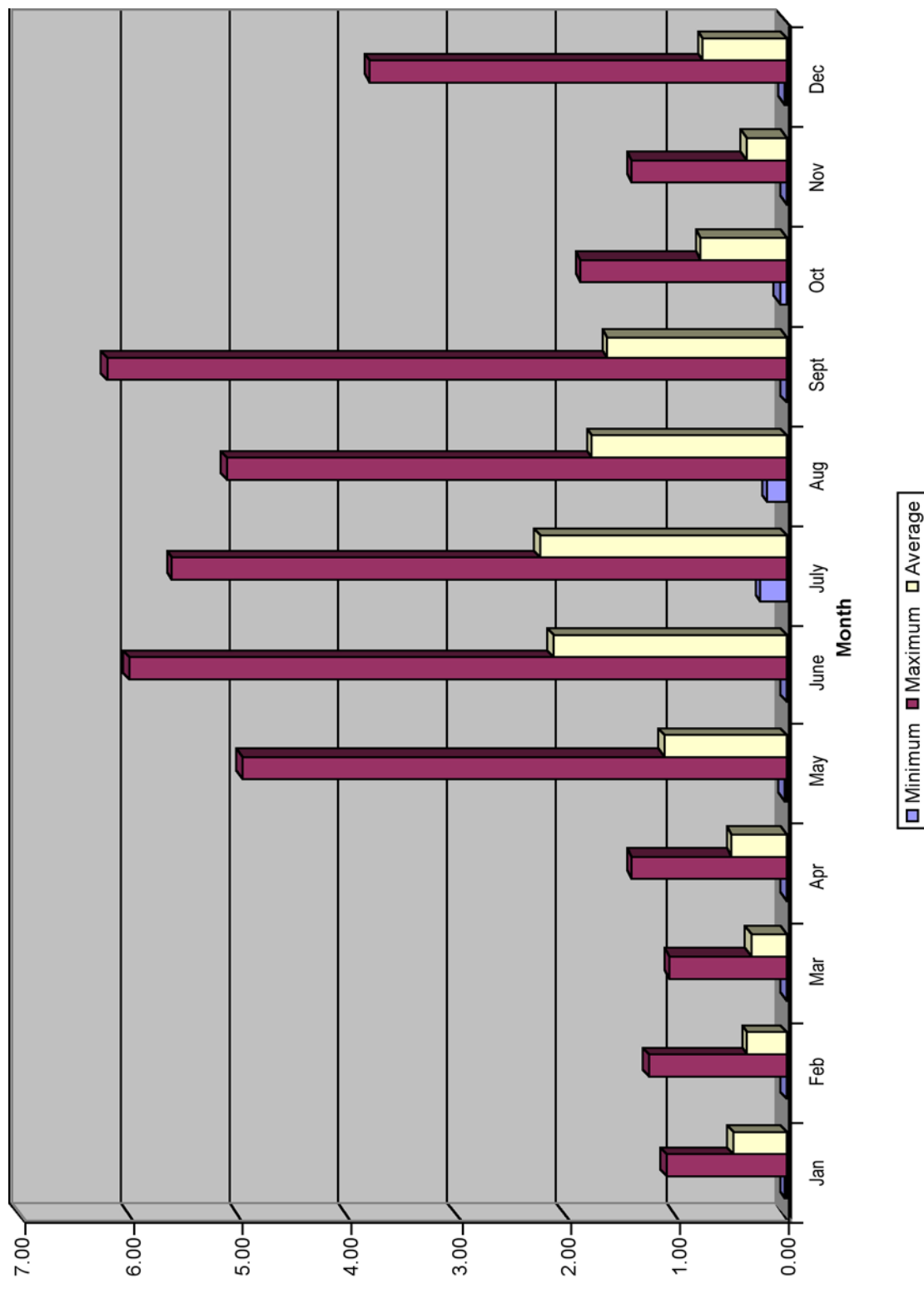
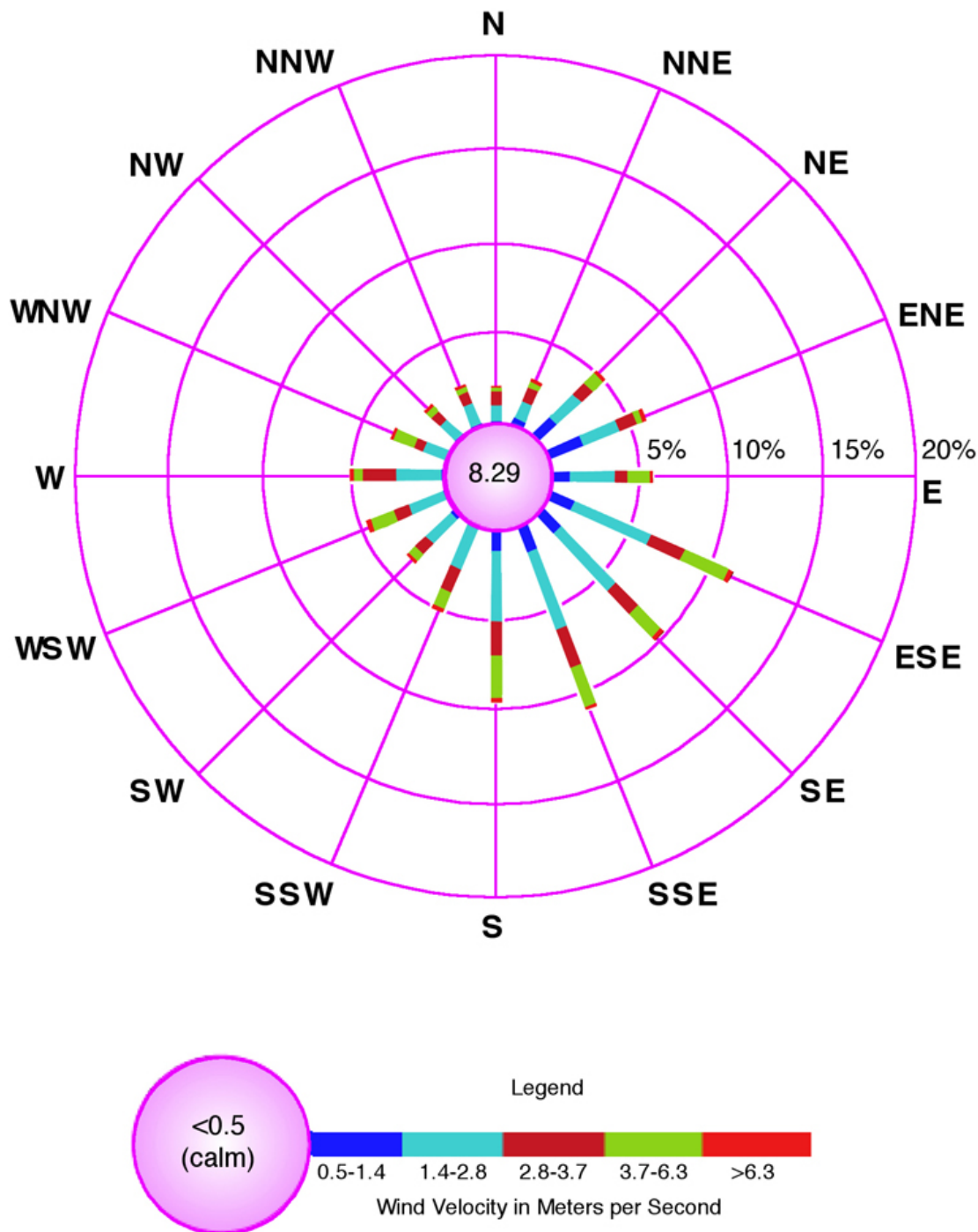
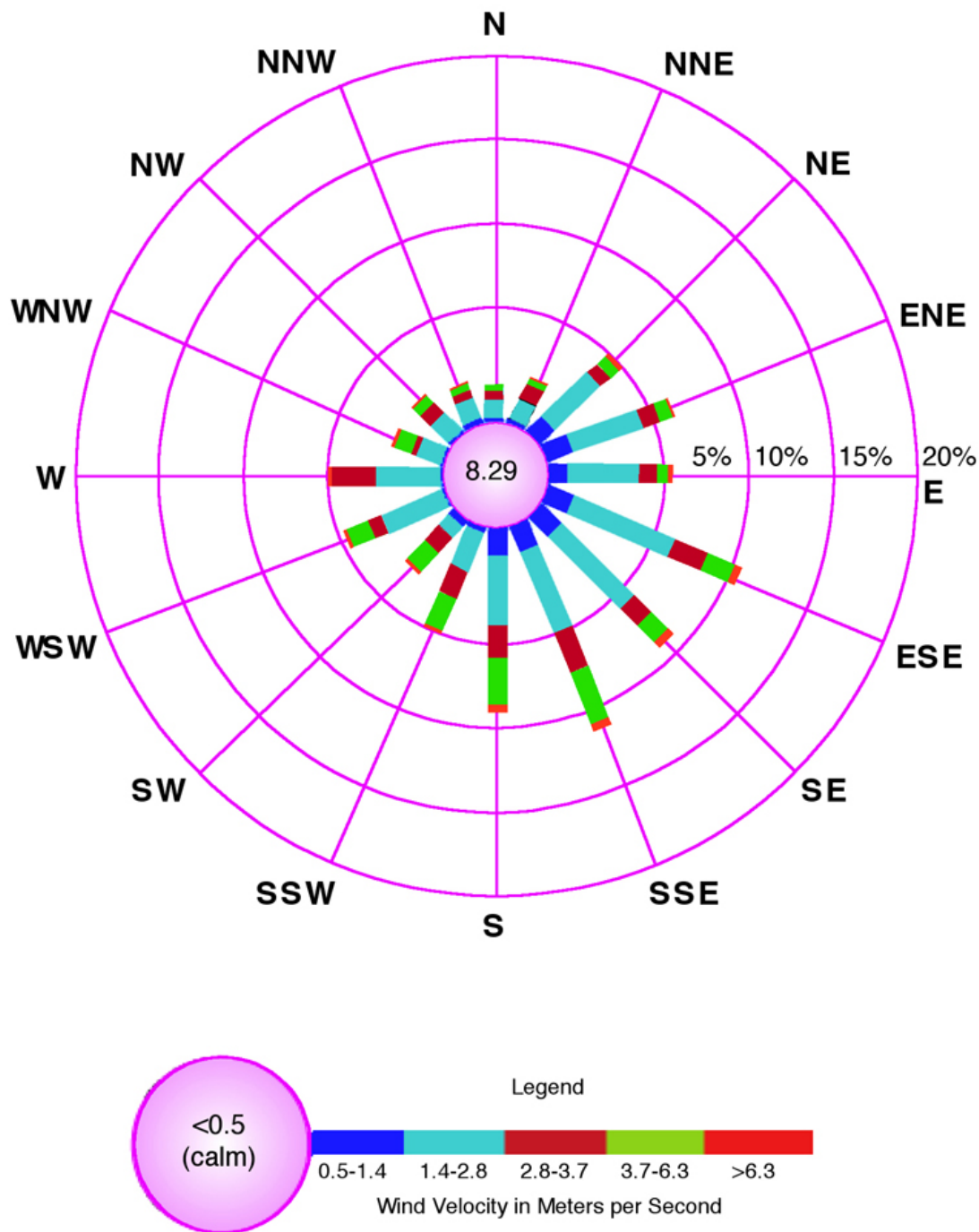


Figure 2-48. Monthly Precipitation for the WIPP Site from 1990-2002



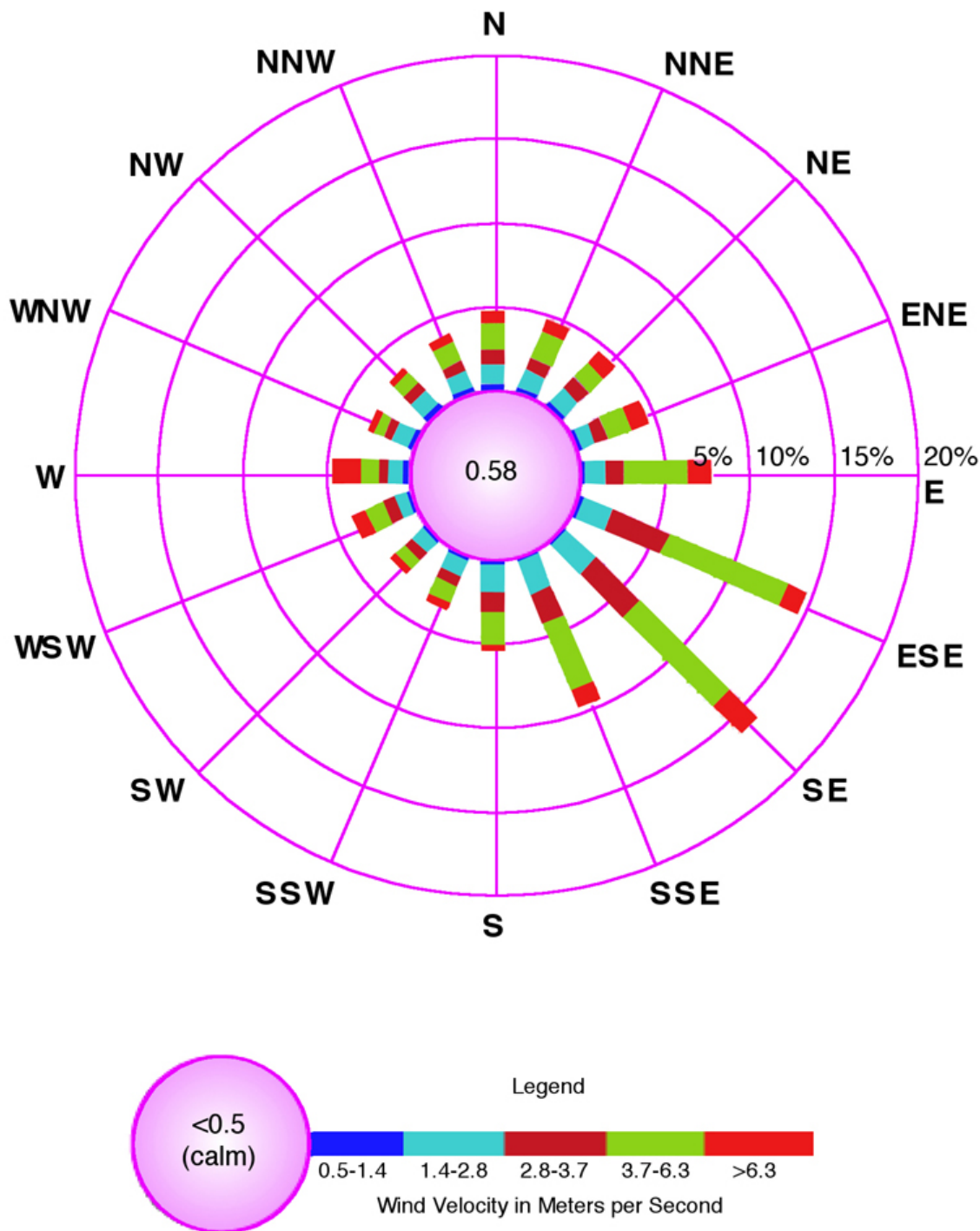
1

2 **Figure 2-49. 1995 Annual Wind Rose at 10-m (33-ft.) Height at WIPP Site**



1  
2

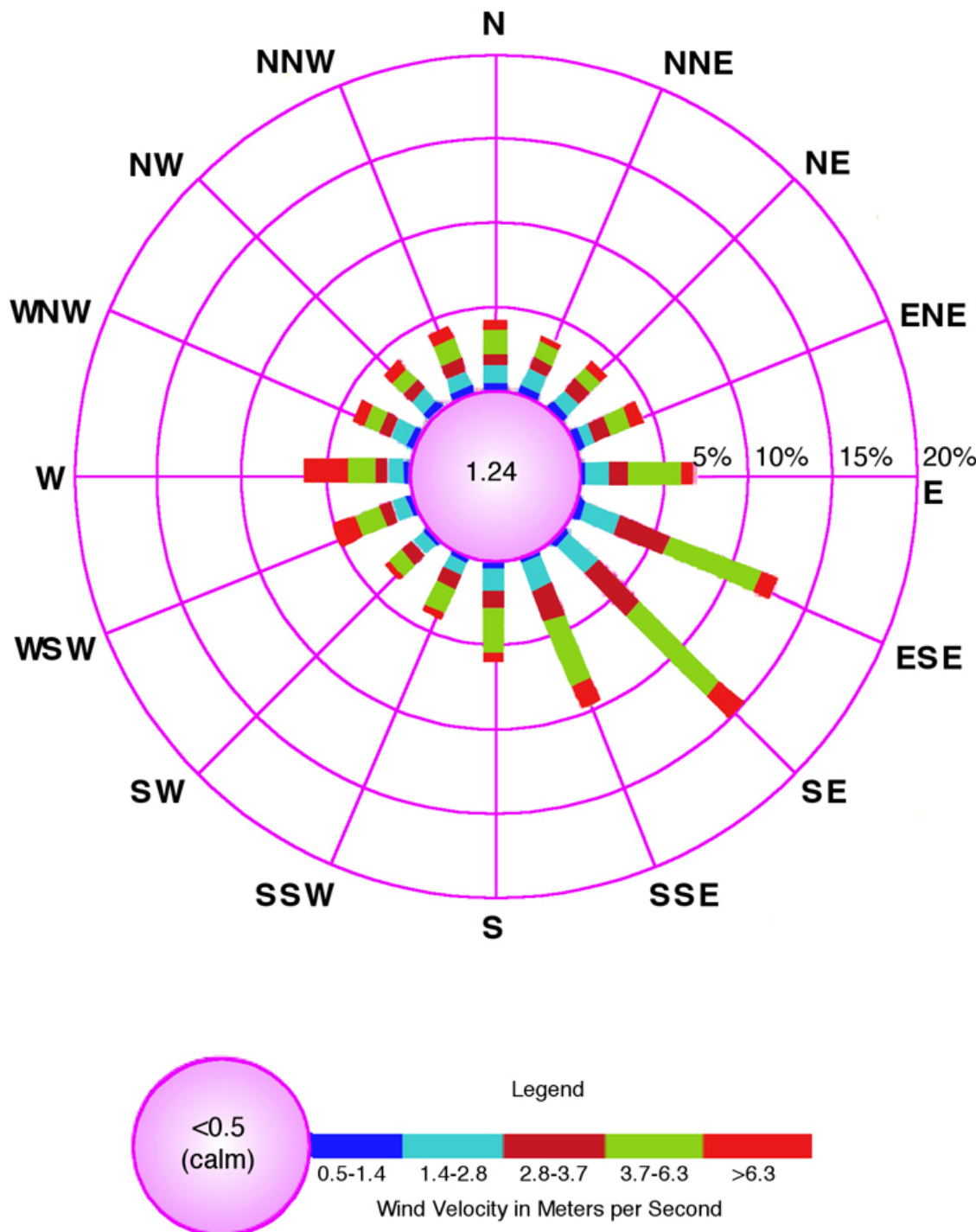
Figure 2-50. 1996 Annual Wind Rose at 10-m (33-ft.) Height at WIPP Site



1

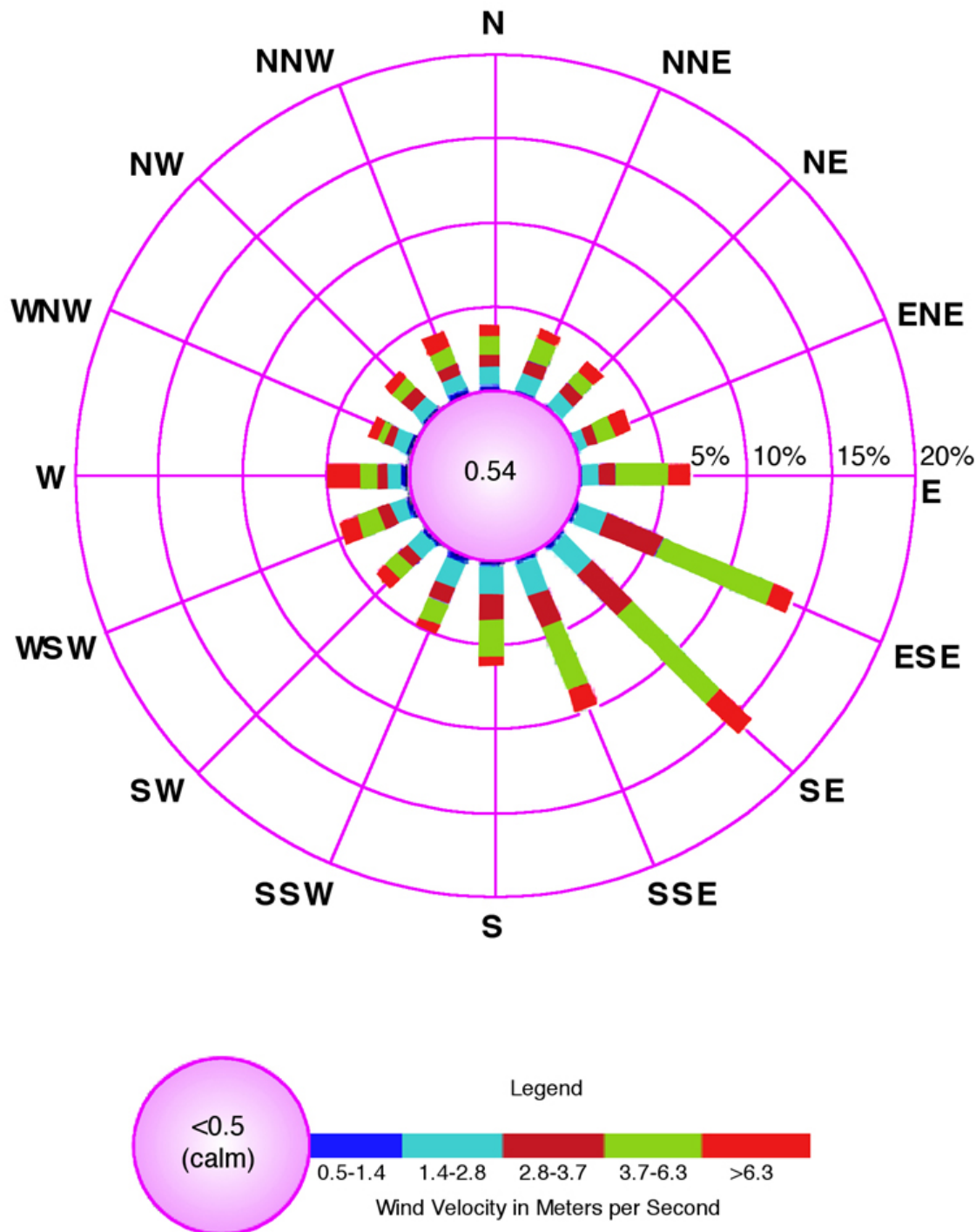
2

Figure 2-51. 1997 Annual Wind Rose at 10-m (33-ft.) Height at WIPP Site



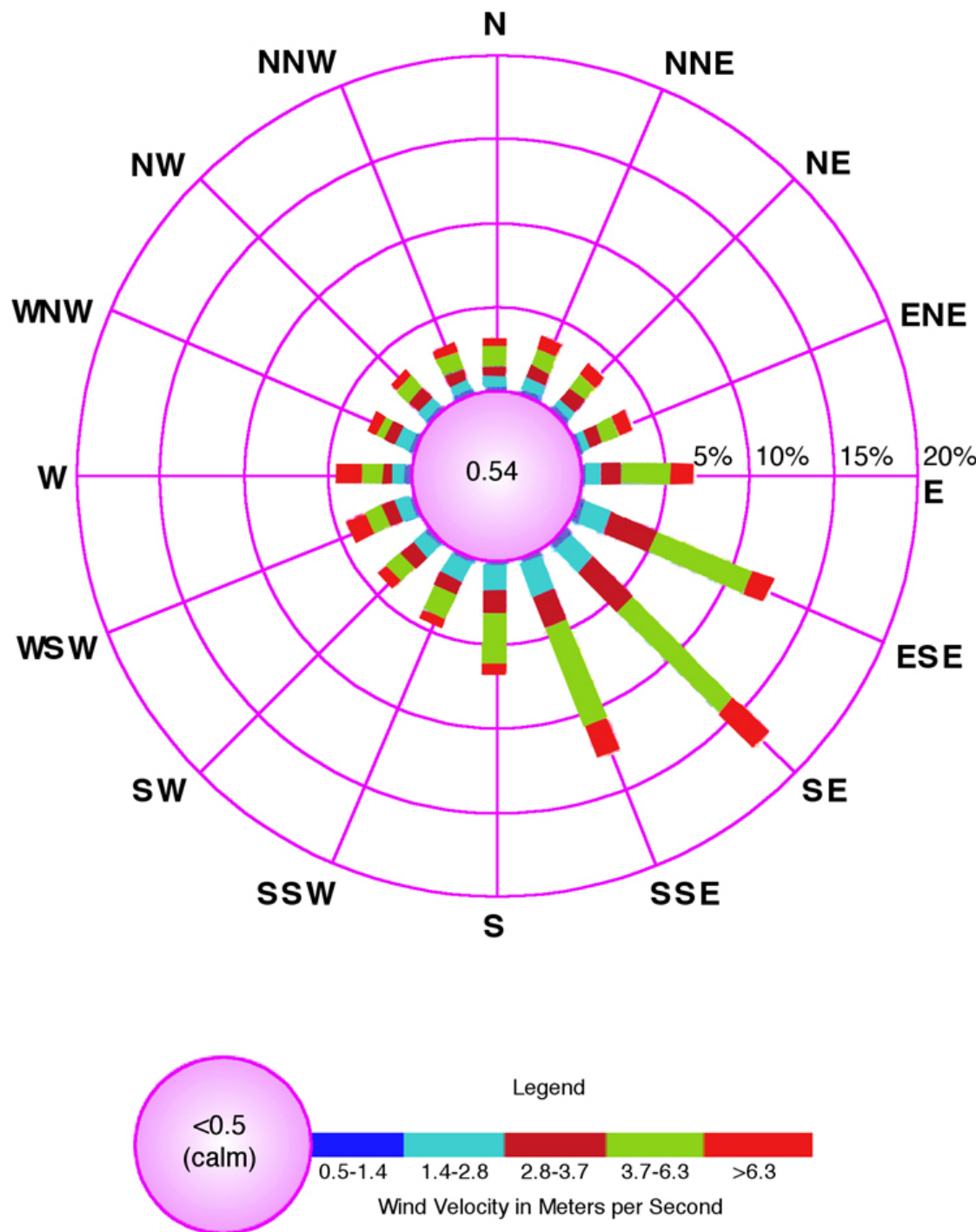
1  
2

**Figure 2-52. 1998 Annual Wind Rose at 10-m (33-ft.) Height at WIPP Site**



1  
2

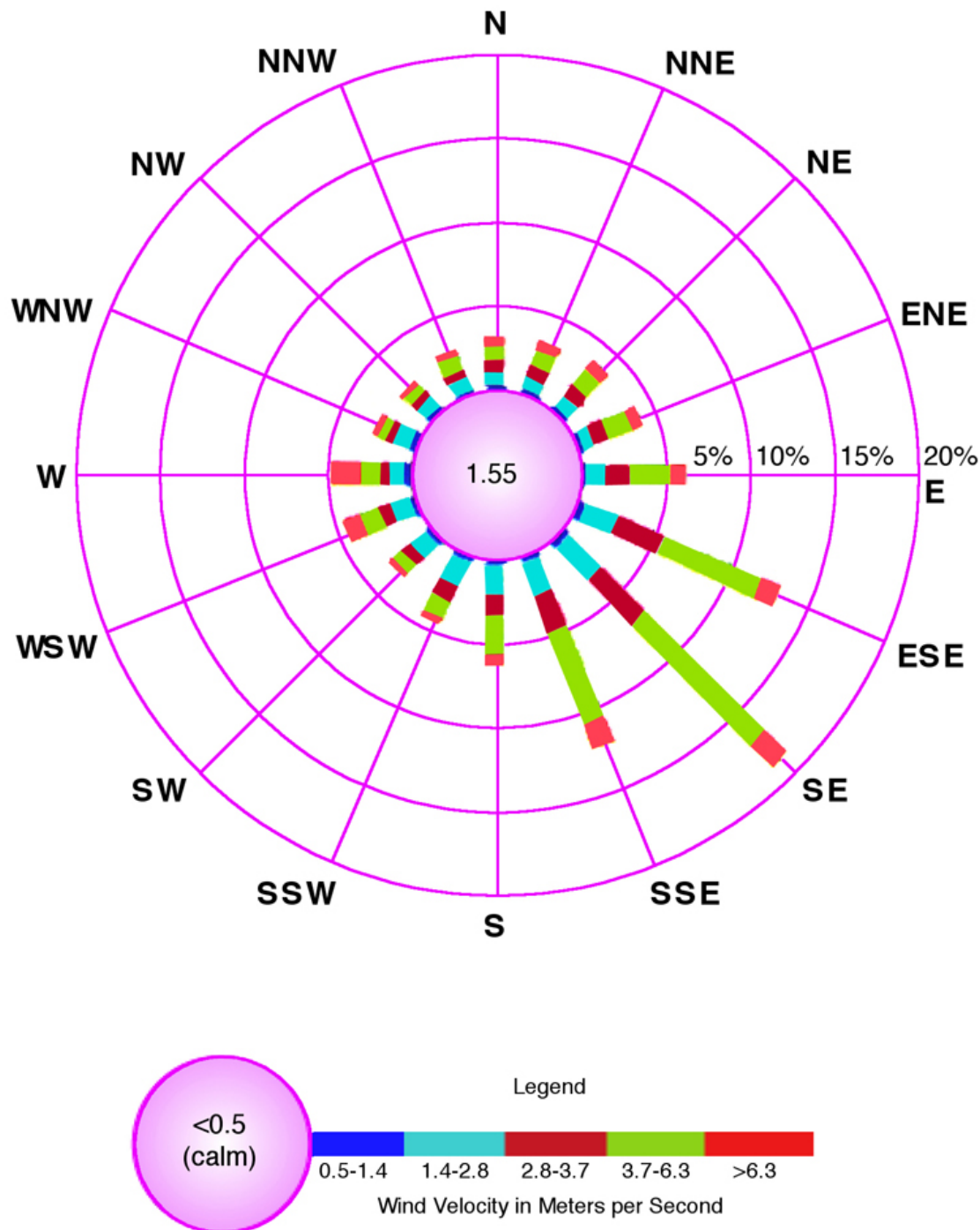
**Figure 2-53. 1999 Annual Wind Rose at 10-m (33-ft.) Height at WIPP Site**



1

2

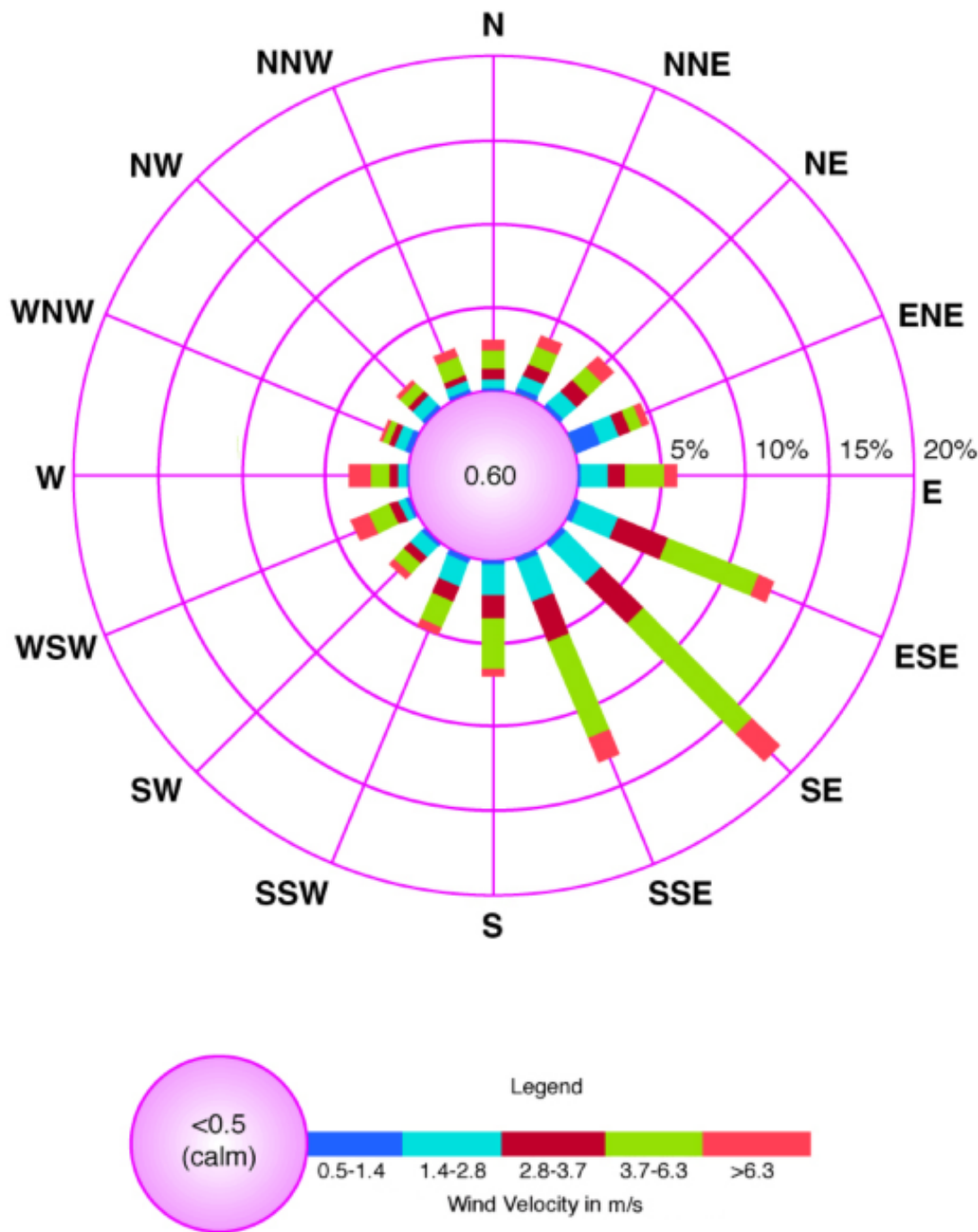
**Figure 2-54. 2000 Annual Wind Rose at 10-m (33-ft.) Height at WIPP Site**



1

2

**Figure 2-55. 2001 Annual Wind Rose at 10-m (33-ft.) Height at WIPP Site**



1  
2

**Figure 2-56. 2002 Annual Wind Rose at 10-m (33-ft.) Height at WIPP Site**

1 modified Mercalli intensity scale. Most of the magnitudes were determined by the New Mexico  
2 Institute of Mining and Technology or are described in CCA Appendix GCR and references  
3 therein.

4 **2.6.1 Seismic History**

5 Seismic data are presented in two time frames, before and after the time when seismographic  
6 data for the region became available. The earthquake record in southern New Mexico dates back  
7 only to 1923, and seismic instruments have been in place in the state since 1961. Various  
8 records have been examined to determine the seismic history of the area within 180 mi (288 km)  
9 of the site. With the exception of a weak shock in 1926 at Hope, New Mexico (approximately 64  
10 km [40 mi] northwest of Carlsbad), and shocks in 1936 and 1949 felt at Carlsbad, all known  
11 shocks in the region before 1961 occurred to the west and southwest of the site more than  
12 160 km (100 mi) away.

13 The strongest earthquake on record occurring within 288 km (180 mi) of the site was the  
14 Valentine, Texas earthquake of August 16, 1931. It has been estimated to have been of  
15 magnitude 6.4 on the Richter scale (Modified Mercalli Intensity of VIII). The Valentine  
16 earthquake was 208 km (130 mi) south-southwest of the site. Its Modified Mercalli Intensity at  
17 the site is estimated to have been V; this is believed to be the highest intensity felt at the site in  
18 this century.

19 In 1887, a major earthquake occurred in northeast Sonora, Mexico. Although about 536 km  
20 (335 mi) west-southwest of the site, it is indicative of the size of earthquakes possible in the  
21 eastern portion of the Basin and Range Province, west of the province containing the site. Its  
22 magnitude was estimated to have been 7.8 (VIII to IX in Modified Mercalli Intensity). It was  
23 felt over an area of 1.3 million km<sup>2</sup> (0.5 million mi<sup>2</sup>) (as far as Santa Fe to the north and Mexico  
24 City to the south); fault displacements near the epicenter were as large as 18 m (26 ft).

25 Since 1961, instrumental coverage has become comprehensive enough to locate most of the  
26 moderately strong earthquakes (local magnitude >3.5) in the region. Instrumentally determined  
27 shocks that occurred within 288 km (180 mi) of the site between 1961 and 1994 are shown in  
28 Figure 2-57. The distribution of these earthquakes may be biased by the fact that seismic  
29 stations were more numerous and were in operation for longer periods north and west of the site.  
30 Pre-1961 earthquakes can be found in CCA Appendix GCR, Figure 5.2-1.

31 Except for the activity southeast of the site, the distribution of epicenters since 1961 differs little  
32 from that of shocks before that time. There are two clusters, one associated with the Rio Grande  
33 Rift on the Texas-Chihuahua border and another associated with the Central Basin Platform in  
34 Texas near the southeastern corner of New Mexico. The latter activity was not reported before  
35 1964. It is not clear from the record whether earthquakes were occurring in the Central Basin  
36 Platform before 1964, although local historical societies and newspapers tend to confirm their  
37 absence before that time.

38 The April 14, 1995, earthquake near Marathon, Texas, was located 240 km (150 mi) south of the  
39 WIPP site. The USGS estimated that moment magnitude for this event was 5.7. At a distance of

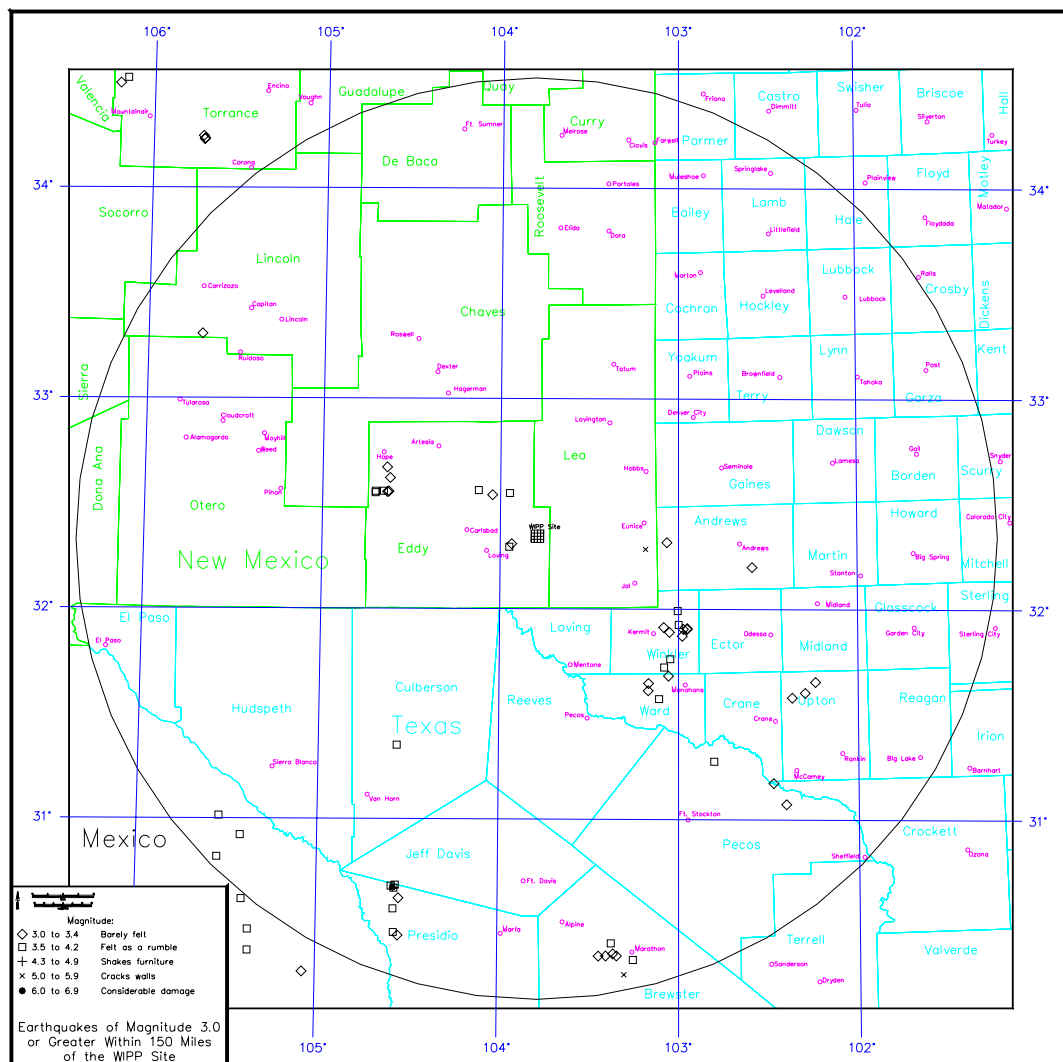


**Figure 2-57. Regional Earthquake Epicenters Occurring between 1961 and 2002**

- 240 km (149 mi), an event of magnitude 5.7 would produce a maximum acceleration at the WIPP site of less than 0.01 g (acceleration due to gravity).
- The Marathon earthquake should not be considered an unanticipated event. The shock occurred in the Basin and Range Province, a seismotectonic province with evidence for 24 Quaternary faults in West Texas and adjacent parts of Mexico. Two of these faults had recent surface-faulting events in the Holocene. Strong earthquakes have occurred within the West Texas part of the Basin and Range Province, most notably the  $M_w = 6.4$  (Richter) Valentine, Texas earthquake on August 15, 1931.
- The WIPP site is located within the Great Plains seismotectonic province, a region that has no evidence of Quaternary faulting, even above major buried structures such as the Central Basin Platform. Because the Great Plains seismotectonic province is geologically distinct from the Basin and Range Province and lacks evidence for recent faulting, the maximum possible or

1 credible earthquake for this region would be substantially smaller than that for the Basin and  
2 Range Province of West Texas.

3 **2.6.2 Seismic Risk**

4 Procedures exist that allow for formal determination of earthquake probabilistic design  
5 parameters. In typical seismic risk analyses of this kind, the region of study is divided into  
6 seismic source areas within which future events are considered equally likely to occur at any  
7 location. For each seismic source area, the rate of occurrence of events above a chosen threshold  
8 level is estimated using the observed frequency of historical events. The sizes of successive  
9 events in each source are assumed to be independent and exponentially distributed; the slope of  
10 the log number versus frequency relationship is estimated from the relative frequency of  
11 different sizes of events observed in the historical data. This slope, often termed the b value, is  
12 determined either for each seismic source individually or for all sources in the region jointly.  
13 Finally, the maximum possible size of events for each source is determined using judgement and  
14 the historical record. Thus, all assumptions underlying a measure of earthquake risk derived  
15 from this type of analysis are explicit, and a wide range of assumptions may be employed in the  
16 analysis procedure.

17 In this section, the particular earthquake risk parameter calculated is peak acceleration expressed  
18 as a function of annual probability of being exceeded at the WIPP site. The particular analysis  
19 procedure applied to the calculation of this probabilistic peak acceleration is taken from a  
20 computer program written by McGuire (1976). In that program, the seismic source zones are  
21 modeled geometrically as quadrilaterals of arbitrary shape. Contributions to site earthquake risk  
22 from individual source zones are integrated into the probability distribution of acceleration, and  
23 the average annual probability of exceedence then follows directly.

24 In the analysis, the principal input parameters are as follows: site region acceleration  
25 attenuation, source zone geometry, recurrence statistics, and maximum magnitudes. Based on  
26 these parameters, several curves showing probabilistic peak acceleration are developed, and the  
27 conclusions that may be drawn from these curves are considered. The data treated in this way  
28 are used to arrive at a general statement of risk from vibratory ground motion at the site during  
29 its active phase of development and use.

30 **2.6.2.1 Acceleration Attenuation**

31 The first input parameters considered have to do with acceleration attenuation in the site region  
32 as a function of earthquake magnitude and hypocentral distance. The risk analysis used in this  
33 study employs an attenuation law of the form

34 
$$a = b_1 \exp(b_2 M_L) R^{-b_3}, \quad (2.3)$$

35 where  $a$  is acceleration in  $\text{cm/s}^2$ ,  $M_L$  is Richter local magnitude, and  $R$  is the distance in km. The  
36 particular formula used in this study is based on a central United States model developed by  
37 Nuttli (1973). The formula coefficients  $b_1 = 17$ ,  $b_2 = 0.92$ , and  $b_3 = 1.0$  were selected. A  
38 justification for this assumption can be found in CCA Appendix GCR, Section 5.3.2.

### 1 2.6.2.2 Seismic Source Zones

Geologic, tectonic, and seismic evidence indicates that three seismic source zones may be used to adequately characterize the region. These are well approximated by the Basin and Range subregion, the Permian Basin subregion exclusive of the Central Basin Platform, and the Central Basin Platform itself. Specific boundaries are taken from a 1976 study by Algermissen and Perkins (1976) of earthquake risks throughout the United States. Additional details on this study are in CCA Appendix GCR, Section 5.3.2.

8 Site region seismic source zones are shown in Figure 2-58. Superposed on these zones are the  
9 earthquake epicenters of Figure 2-57. The zonation presented generally conforms with historical  
10 seismicity. The source zonation of Figure 2-58 has no explicit analog to the Permian Basin  
11 subregion exclusive of the Central Basin Platform. This is considered part of the broad  
12 background region.

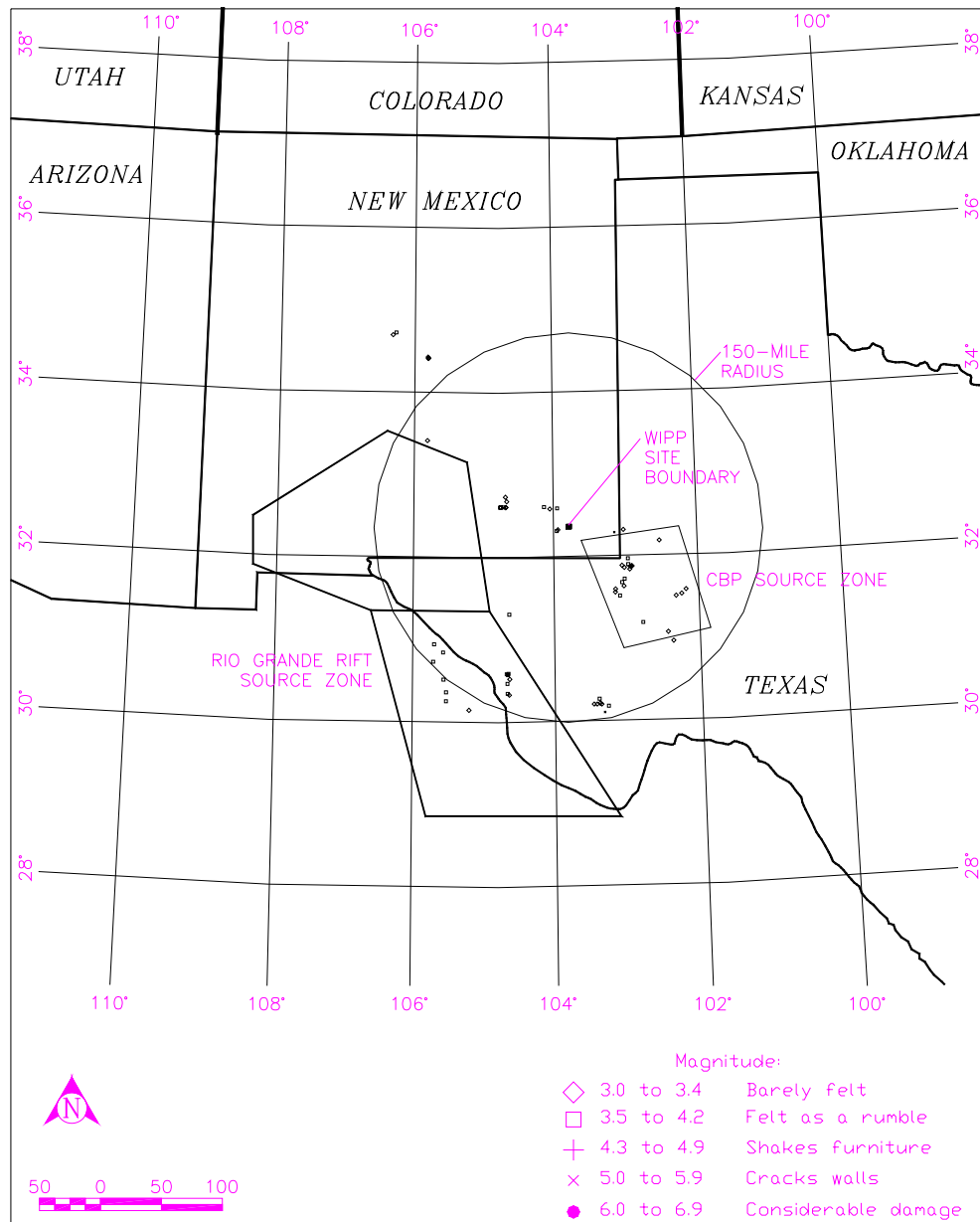
13 For the purposes of this study, some minor modifications of the Algermissen and Perkins (1976)  
14 source zones were made. Geologic and tectonic evidence suggests that the physiographic  
15 boundary between the Basin and Range and Great Plains provinces provides a good and  
16 conservative approximation of the source zones (CCA Appendix GCR). In addition, information  
17 from the Kermit seismic array (Appendix to Rogers and Malkiel 1979) indicates that the  
18 geometry used to model the limits of the Central Basin Platform source zone may be modified  
19 somewhat from the original analogous Algermissen and Perkins (1976) zone. These  
20 modifications are shown in Figure 2-59 and constitute the preferred model for the WIPP site  
21 region seismic source zones in this study. This model is preferred because it more completely  
22 considers geologic and tectonic information, as well as seismic data, and because it results in a  
23 more realistic development of risks at the WIPP facility.

With regard to earthquake focal depth, there is little doubt that the focal depths of earthquakes in the WIPP facility region should be considered shallow. Early instrumental locations were achieved using an arc intersection method employing travel-time-distance curves calculated from a given crustal model, and the assumption of focal depths of 5 km (3.1 mi), 10 km (6.2 mi), or, for later calculations, 8 km (5 mi). Good epicentral locations could generally be obtained under these assumptions. For conservatism, a focal depth of 5 km (3.1 mi) is used in all source zones of this study including that of the site. For smaller hypocentral distances, the form of the attenuation law adopted here severely exaggerates the importance of small, close shocks in the estimation of probabilistic acceleration at the WIPP site. Additional discussion is included CCA Appendix GCR, Chapter 5.

### 34 2.6.2.3 Source Zone Recurrence Formulas and Maximum Magnitudes

35 The risk calculation procedure used in this study requires that earthquake recurrence rates for  
36 each seismic source zone be specified. This is done formally by computing the constants  $a$  and  $b$   
37 in the equation

$$38 \qquad \log N = a - bM , \qquad (2.4)$$

**Figure 2-58. Seismic Source Zones**

where N is the number of earthquakes of magnitude greater than or equal to M within a specified area occurring during a specified period.

For the WIPP facility region, three formulas of this type are needed: one for the province west and southwest of the site (the Basin and Range subregion or Rio Grande Rift source zone), another for the province of the WIPP facility exclusive of the Central Basin Platform (the Permian Basin subregion or background source zone), and a final one for the Central Basin Platform. In practice, the difficulties in finding meaningful recurrence formulas for such small areas in a region of low historical earthquake activity are formidable.

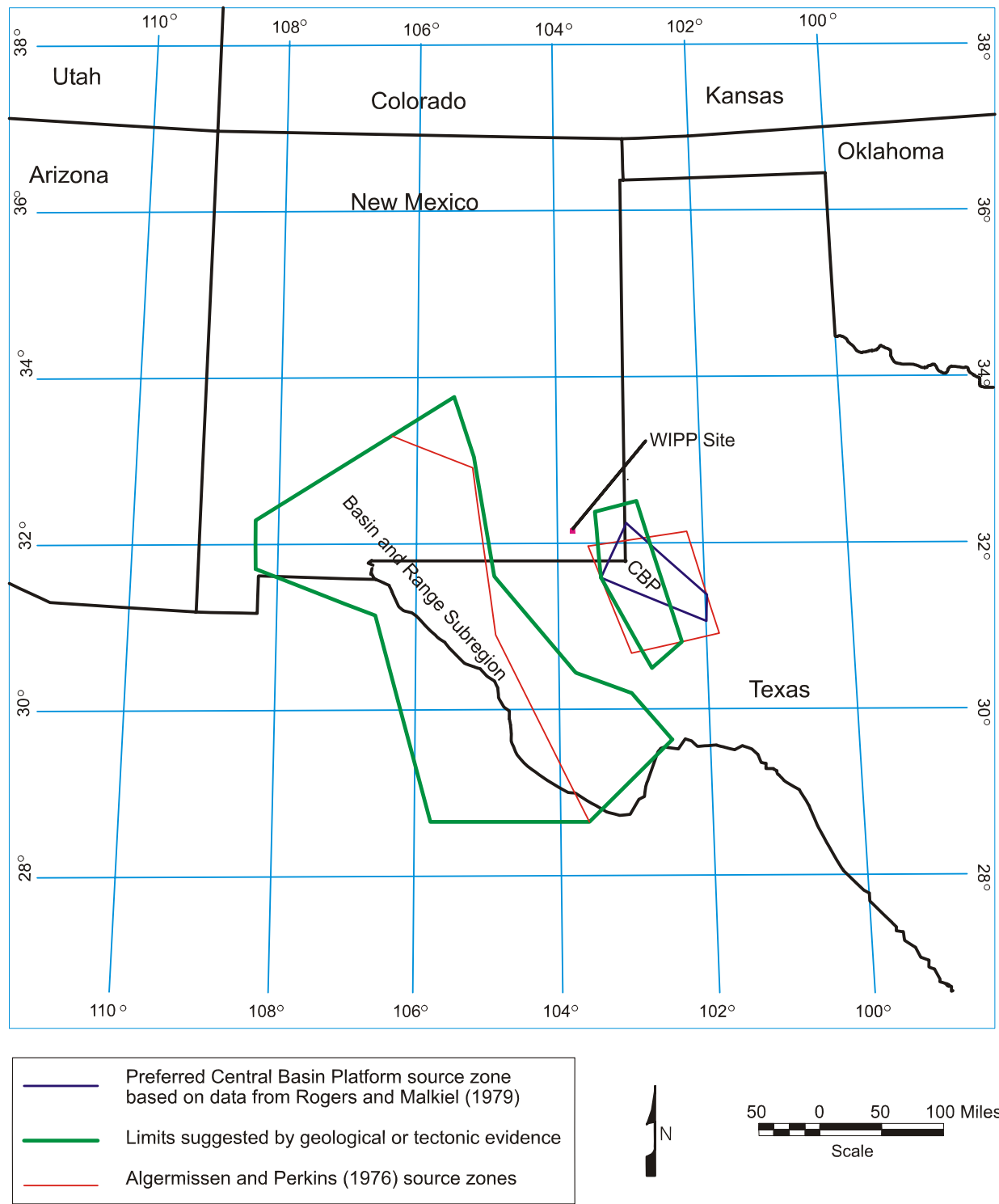


**Figure 2-59. Alternate Source Geometries**

1 The formulas have been determined to be

2     •  $\log N = 2.43 - M_{CORR}$  Site source zone (background) (2.5)

3     •  $\log N = 3.25 - M_{CORR}$  Basin and Range subregion (2.6)

4     •  $\log N = 3.19 - 0.9 M_{CORR}$  Central Basin Platform (2.7)

5 The rationale for their development and the relationship used to determine  $M_{CORR}$  can be found  
6 in CCA Appendix GCR, Section 5.3.

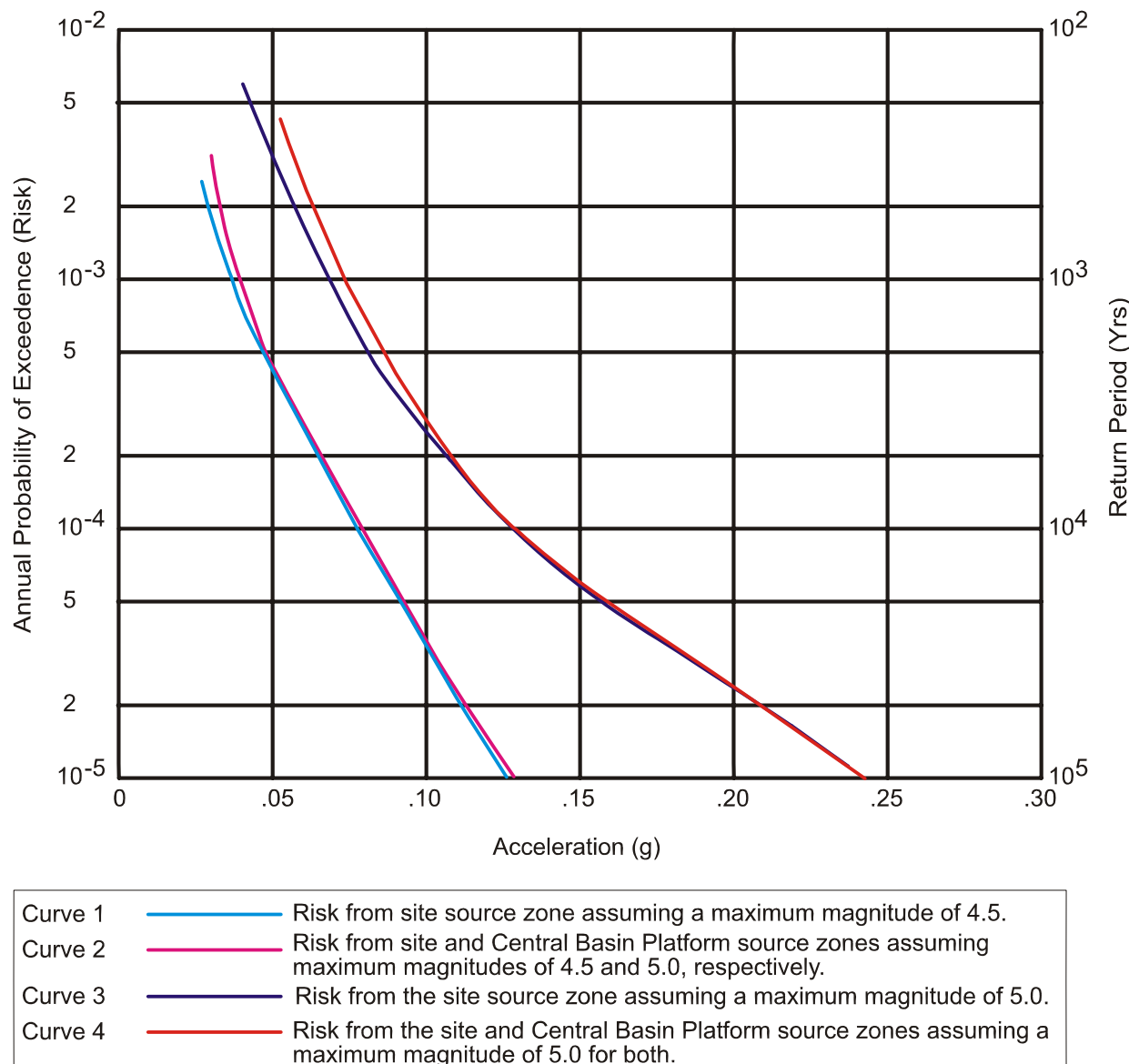
7 **2.6.2.4 Design Basis Earthquake**

8 The term Design Basis Earthquake (DBE) is used for the design of surface confinement  
9 structures and components at the WIPP facility. As used here, the DBE is equivalent to the  
10 design earthquake used in Regulatory Guide 3.24 (Nuclear Regulatory Commission [NRC]  
11 1974). That is, in view of the limited consequences of seismic events in excess of those used as  
12 the basis, the DBE is such that it produces ground motion at the WIPP facility with a recurrence  
13 interval of 1,000 years. In practice, the DBE is defined in terms of the 1,000-year acceleration  
14 and design response spectra.

15 The generation of curves expressing probability of occurrence or risk as a function of peak WIPP  
16 facility ground acceleration is discussed in detail in CCA Appendix GCR, Section 5.3, for a  
17 number of possible characterizations of WIPP facility region source zones and source zone  
18 earthquake parameters. The most conservative (and the least conservative) risk curves are shown  
19 in Figure 2-60.

20 From this figure, the most conservative calculated estimate of the 1,000-year acceleration at the  
21 WIPP facility is approximately 0.075 g. The geologic and seismic assumptions leading to this  
22 1,000-year peak acceleration include the consideration of a Richter magnitude 5.5 earthquake at  
23 the site, a 6.0 magnitude earthquake on the Central Basin Platform, and a 7.8 magnitude  
24 earthquake in the Basin and Range subregion. These values, especially the first two, are  
25 considered quite conservative, as are the other parameters used in the 0.075g derivation. For  
26 additional conservatism, a peak design acceleration of 0.1 g is selected for the WIPP facility  
27 DBE. The design response spectra for vertical and horizontal motions are taken from Regulatory  
28 Guide 1.60 (NRC 1973) with the high-frequency asymptote scaled to this 0.1g peak acceleration  
29 value.

30 This DBE and the risk analysis that serves an important role in its definition are directly  
31 applicable to surface confinement structures and components at the WIPP facility. Underground  
32 structures and components are not subject to DBE design requirements because according to  
33 Pratt et al. (1979), mine experience and studies on earthquake damage to underground facilities  
34 show that tunnels are not damaged at sites having peak surface accelerations below 0.2 g.



Note: Risk curves generated by using worst and best case assumption from the parameter variation considered for site region source zones. See Appendix GCR, Figure 5.3-7 for further details.

CCA-063-2

1  
2**Figure 2-60. Total WIPP Facility Risk Curve Extrema**

## REFERENCES

- 2 Adams, J.E. 1944. "Upper Permian Ochoa Series of the Delaware Basin, West Texas and  
3 Southeastern New Mexico." *American Association of Petroleum Geologists Bulletin*, Vol. 28,  
4 No. 11, 1596-1625.

5 Algermissen, S.T., and Perkins, D.M. 1976. *A Probabilistic Estimate of Maximum Ground*  
6 *Acceleration in the Contiguous United States*. Open-file Report 76-416, pp. 1 – 45. U.S.  
7 Geological Survey.

8 Anderson, R.Y. 1978. *Deep Dissolution of Salt, Northern Delaware Basin, New Mexico*.  
9 Report to Sandia National Laboratories, Albuquerque, NM. ERMS #229530.

10 Anderson, R.Y., and Kirkland, D.W. 1980. Dissolution of Salt Deposits by Brine Density Flow.  
11 *Geology*, Vol. 8, No. 2, pp. 66 – 69.

12 Anderson, R.Y. 1981. "Deep-Seated Salt Dissolution in the Delaware Basin, Texas and New  
13 Mexico." In *Environmental Geology and Hydrology in New Mexico*, S.G. Wells and W.  
14 Lambert, eds., Special Publication No. 10, pp. 133 - 145. New Mexico Geological Society.

15 Anderson, R.Y. 1993. "The Castile as a 'Nonmarine' Evaporite." In *Carlsbad Region, New*  
16 *Mexico and Texas, New Mexico Geological Society, Forty-Fourth Annual Field Conference,*  
17 *Carlsbad, NM, October 6-9, 1993*, D.W. Love et al., eds., pp. 12 - 13. New Mexico Geological  
18 Society, Socorro, NM.

19 Anderson, R.Y., Dean, W.E., Jr., Kirkland, D.W., and Snider, H. I. 1972. "Permian Castile  
20 Varved Evaporite Sequence, West Texas and New Mexico." *Geological Society of America*  
21 *Bulletin*, Vol. 83, No. 1, pp. 59 - 85.

22 Anderson, R.Y., and Powers, D.W. 1978. "Salt Anticlines in the Castile-Salado Evaporite  
23 Sequence, Northern Delaware Basin, New Mexico." In *Geology and Mineral Deposits of*  
24 *Ochoan Rocks in Delaware Basin and Adjacent Areas*, G.S. Austin, ed., Circular 159. pp. 79 -  
25 83. New Mexico Bureau of Mines and Mineral Resources, Socorro, NM.

26 Anderson, R.Y., Kietzke, K.K., and Rhodes, D.J. 1978. "Development of Dissolution Breccias,  
27 Northern Delaware Basin, New Mexico and Texas." In *Geology and Mineral Deposits of*  
28 *Ochoan Rocks in Delaware Basin and Adjacent Areas*, G.S. Austin, ed., Circular 159. New  
29 Mexico Bureau of Mines and Mineral Resources, Socorro, NM.

30 Bachman, G.O. 1973. *Surficial Features and Late Cenozoic History in Southeastern New*  
31 *Mexico*. Open-File Report 4339-8. U.S. Geological Survey, Reston, VA.

32 Bachman, G.O. 1974. *Geologic Processes and Cenozoic History Related to Salt Dissolution in*  
33 *Southeastern New Mexico*. Open-File Report 74-194. U.S. Geological Survey, Denver, CO.

34 Bachman, G.O. 1976. "Cenozoic Deposits of Southeastern New Mexico and an Outline of the  
35 History of Evaporite Dissolution." *Journal of Research*, Vol. 4, No. 2, pp. 135 - 149. U.S.  
36 Geological Survey.

- 1 Bachman, G.O. 1980. *Regional Geology and Cenozoic History of Pecos Region, Southeastern*  
2 *New Mexico*. Open-File Report 80-1099. U.S. Geological Survey, Denver, CO.
- 3 Bachman, G.O. 1981. *Geology of Nash Draw, Eddy County, New Mexico*. Open-File Report  
4 81-31. U.S. Geological Survey, Denver, CO.
- 5 Bachman, G.O. 1984. *Regional Geology of Ochoan Evaporites, Northern Part of Delaware*  
6 *Basin*. Circular 184, pp. 1 - 22. New Mexico Bureau of Mines and Mineral Resources, Socorro,  
7 NM.
- 8 Bachman, G.O. 1985. *Assessment of Near-Surface Dissolution at and Near the Waste Isolation*  
9 *Pilot Plant (WIPP), Southeastern New Mexico*. SAND84-7178. Sandia National Laboratories,  
10 Albuquerque, NM. ERMS #224609.
- 11 Barrows, L.J., Shaffer, S.E., Miller, W.B., and Fett, J.D. 1983. *Waste Isolation Pilot Plant*  
12 (*WIPP*) *Site Gravity Survey and Interpretation*. SAND82-2922. Sandia National Laboratories,  
13 Albuquerque, NM.
- 14 Beauheim, R.L., Hassinger, B.W., and Kleiber, J.A. 1983. *Basic Data Report for Borehole*  
15 *Cabin Baby-1 Deepening and Hydrologic Testing, Waste Isolation Pilot Plant (WIPP) Project,*  
16 *Southeastern New Mexico*. WTSD-TME-020. United States Department of Energy,  
17 Albuquerque, NM.
- 18 Beauheim, R.L. 1986. *Hydraulic-Test Interpretations for Well DOE-2 at the Waste Isolation*  
19 *Pilot Plant (WIPP) Site*. SAND86-1364. Sandia National Laboratories, Albuquerque, NM.  
20 ERMS #227656.
- 21 Beauheim, R.L. 1987a. *Interpretations of Single-Well Hydraulic Tests Conducted at and Near*  
22 *the Waste Isolation Pilot Plant (WIPP) Site, 1983–1987*. SAND87-0039. Sandia National  
23 Laboratories, Albuquerque, NM. ERMS #227679.
- 24 Beauheim, R.L. 1987b. *Analysis of Pumping Tests of the Culebra Dolomite Conducted at the*  
25 *H-3 Hydropad at the Waste Isolation Pilot Plant (WIPP) Site*. SAND86-2311. Sandia National  
26 Laboratories, Albuquerque, NM.
- 27 Beauheim, R.L. 1987c. *Interpretation of the WIPP-13 Multipad Pumping Test of the Culebra*  
28 *Dolomite at the Waste Isolation Pilot Plant (WIPP) Site*. SAND87-2456. Sandia National  
29 Laboratories, Albuquerque, NM.
- 30 Beauheim, R.L. 1989. *Interpretation of H-11b4 Hydraulic Tests and the H-11 Multipad*  
31 *Pumping Test of the Culebra Dolomite at the Waste Isolation Pilot Plant (WIPP) Site*. SAND89-  
32 0536. Sandia National Laboratories, Albuquerque, NM.
- 33 Beauheim, R.L. 2002. “*Analysis Plan for Evaluation of the Effects of Head Changes on*  
34 *Calibration of Culebra Transmissivity Fields, AP-088, Rev. 1*,” ERMS #524785. Carlsbad, NM:  
35 Sandia National Laboratories, WIPP Records Center.

- 1 Beauheim, R.L. 2000. "Appendix E, Summary of Hydraulic Tests Performed at Tracer-Test  
2 Sites," in *Interpretations of Tracer Tests Performed in the Culebra Dolomite at the Waste*  
3 *Isolation Pilot Plant Site*, Meigs, L.C., Beauheim, R.L., and Jones, T.L., eds. SAND97-3109.  
4 Albuquerque, NM: Sandia National Laboratories.
- 5 Beauheim, R.L., and Holt, R.M. 1990. "Hydrogeology of the WIPP Site." In *Geological and*  
6 *Hydrological Studies of Evaporites in the Northern Delaware Basin for the Waste Isolation Pilot*  
7 *Plant (WIPP), New Mexico, Geologic Society of America 1990 Annual Meeting Field Trip #14*  
8 *Guidebook*, pp. 131 -179. Dallas Geologic Society, Dallas, TX.
- 9 Beauheim, R.L., and Roberts, R.M. 2002. "Hydrology and Hydraulic Properties of a Bedded  
10 Evaporite Formation," *Journal of Hydrology*, v. 259, pp. 66-88.
- 11 Beauheim, R.L., and Ruskauff, G.J. 1998. *Analysis of Hydraulic Tests of the Culebra and*  
12 *Magenta Dolomites and Dewey Lake Redbeds Conducted at the Waste Isolation Pilot Plant Site*.  
13 SAND98-0049. Albuquerque, NM: Sandia National Laboratories.
- 14 Beauheim, R.L., Roberts, R.M., Dale, T.F., Fort, M.D., and Stensrud, W.A. 1993. *Hydraulic*  
15 *Testing of Salado Formation Evaporites at the Waste Isolation Pilot Plant Site: Second*  
16 *Interpretive Report*. SAND92-0533. Sandia National Laboratories, Albuquerque, NM. ERMS  
17 #223378.
- 18 Beauheim, R.L., Saulnier, G.J., Jr. and Avis, J.D. 1991a. *Interpretation of Brine-Permeability*  
19 *Tests of the Salado Formation at the Waste Isolation Pilot Plant Site: First Interim Report*.  
20 SAND90-0083. Sandia National Laboratories, Albuquerque, NM.
- 21 Beauheim, R.L., Dale, T.F., and Pickens, J.F. 1991b. Interpretations of Single-Well Hydraulic  
22 Tests of the Rustler Formation Conducted in the Vicinity of the Waste Isolation Pilot Plant Site,  
23 1988-1989. SAND89-0869. Sandia National Laboratories, Albuquerque, NM.
- 24 Beauheim, R.L., Meigs, L.C., Saulnier, G.J., Jr. and Stensrud, W.A. 1995. *Culebra Transport*  
25 *Program Test Plan: Tracer Testing of the Culebra Dolomite Member of the Rustler Formation*  
26 *at the H-19 and H-11 Hydropads on the WIPP Site*. ERMS #230156. Carlsbad, NM: Sandia  
27 National Laboratories, WIPP Records Center.
- 28 Bechtel National Inc. 1979. "Soils Design Report – Volume 1 Plant Site Near-Surface  
29 Structures," Doc. No. Dr-22-V-01. San Francisco, CA: Bechtel National Inc.
- 30 Becker, M.L., Rasbury, E.T., Meyers, W.J., and Hanson, G.N. 2002. U-Pb calcite age of the  
31 Late Permian Castile Formation, Delaware Basin: a constraint on the age of the Permian-Triassic  
32 boundary (?): *Earth and Planetary Science Letters*, v. 203, p. 681-689.
- 33 Blackwell, D.D., Steele, J.L., and Carter, L.S. 1991. "Heat-Flow Patterns of the North  
34 American Continent; A Discussion of the Geothermal Map of North America." In *Neotectonics*  
35 *of North America*, D.B. Slemmons, E.R. Engdahl, M.D. Zoback, and D.D. Blackwell, eds., pp.  
36 423 - 436. Geological Society of America, Boulder, CO.

- 1 Bodine, Jr., M.W. 1978. "Clay-Mineral Assemblages from Drill Core of Ochoan Evaporites,  
2 Eddy County, New Mexico." In *Geology and Mineral Deposits of Ochoan Rocks in Delaware*  
3 *Basin and Adjacent Areas*, G.S. Austin, ed., Circular 159. pp. 21 - 31. New Mexico Bureau of  
4 Mines and Mineral Resources, Socorro, NM.
- 5 Borns, D.J. 1987. *The Geologic Structures Observed in Drillhole DOE-2 and Their Possible*  
6 *Origins: Waste Isolation Pilot Plant*. SAND86-1495. Sandia National Laboratories,  
7 Albuquerque, NM.
- 8 Borns, D.J., Barrows, L.J., Powers, D.W., and Snyder, R.P. 1983. *Deformation of Evaporites*  
9 *Near the Waste Isolation Pilot Plant (WIPP) Site*. SAND82-1069. Sandia National  
10 Laboratories, Albuquerque, NM.
- 11 Borns, D.J. 1985. *Marker Bed 139: A study of Drillcore from a Systematic Array*. SAND85-  
12 0023. Sandia National Laboratories, Albuquerque, NM.
- 13 Borns, D.J., and Shaffer, S.E. 1985. *Regional Well-Log Correlation in the New Mexico Portion*  
14 *of the Delaware Basin*. SAND83-1798. Sandia National Laboratories, Albuquerque, NM.
- 15 Brausch, L.M., Kuhn, A.K., and Register, J.K. 1982. *Natural Resources Study, Waste Isolation*  
16 *Pilot Plant (WIPP) Project, Southeastern New Mexico*. TME 3156. Albuquerque, NM: U.S.  
17 Department of Energy, Waste Isolation Pilot Plant.
- 18 Brokaw, A.L., Jones, C.L., Cooley, M.E., and Hays, W.H. 1972. *Geology and Hydrology of the*  
19 *Carlsbad Potash Area, Eddy and Lea Counties, New Mexico*. Open-File Report 4339-1. U.S.  
20 Geological Survey, Denver, CO.
- 21 Brookins, D.G. 1980. "Polyhalite K-Ar Radiometric Ages from Southeastern New Mexico." In  
22 *Isochron/West*, No. 29, pp. 29 - 31.
- 23 Brookins, D.G. 1981. "Geochronologic Studies Near the WIPP Site, Southeastern New  
24 Mexico." In *Environmental Geology and Hydrology in New Mexico*, S.G. Wells, and  
25 W. Lambert, ed., Special Publication 10, pp. 147 - 152. New Mexico Geological Society.
- 26 Brookins, D.G., and Lambert, S.J. 1987. "Radiometric Dating of Ochoan (Permian) Evaporites,  
27 WIPP Site, Delaware Basin, New Mexico, USA." *Scientific Basis for Nuclear Waste*  
28 *Management X, Materials Research Society Symposia Proceedings, Boston, MA, December 1-4,*  
29 1986, J.K. Bates and W.B. Seefeldt, eds., Vol. 84, pp. 771 - 780, Materials Research Society,  
30 Pittsburgh, PA.
- 31 Brookins, D.G., Register, J.K., Jr., and Krueger, H.W. 1980. "Potassium-Argon Dating of  
32 Polyhalite in New Mexico." *Geochimica et Cosmochimica Acta*, Vol. 44, No. 5, pp. 635 - 637.
- 33 Butcher, B.M. 1997. *A Summary of the Sources of Input Parameter Values for the Waste*  
34 *Isolation Pilot Plant Final Porosity Surface Calculations*. SAND97-0796. Albuquerque, NM:  
35 Sandia National Laboratories.

- 1 Calzia, J.P., and Hiss, W.L. 1978. "Igneous Rocks in Northern Delaware Basin, New Mexico,  
2 and Texas." In *Geology and Mineral Deposits of Ochoan Rocks in Delaware Basin and*  
3 *Adjacent Areas*, G.S. Austin, ed., Circular 159, pp. 39 - 45. New Mexico Bureau of Mines and  
4 Mineral Resources, Socorro, NM.
- 5 Cartwright, Jr., L.D. 1930. Transverse Section of Permian Basin, West Texas and Southeastern  
6 New Mexico. *American Association of Petroleum Geologists Bulletin*, Vol. 14.
- 7 Casas, E., and Lowenstein, T.K. 1989. Diagenesis of Saline Pan Halite: Comparison of  
8 Petrographic Features of Modern, Quaternary and Permian Halites. *Journal of Sedimentary*  
9 *Petrology*, Vol. 59.
- 10 Chapman, J.B. 1986. *Stable Isotopes in the Southeastern New Mexico Groundwater:*  
11 *Implications for Dating Recharge in the WIPP Area*. EEG-35, DOE/AL/10752-35.  
12 Environmental Evaluation Group, Santa Fe, NM.
- 13 Chapman, J.B. 1988. *Chemical and Radiochemical Characteristics of Groundwater in the*  
14 *Culebra Dolomite, Southeastern NM*. EEG-39. Environmental Evaluation Group,  
15 Santa Fe, NM.
- 16 Chugg, J.C., Anderson, G.W., Kink, D.L., and Jones, L.H. 1952. *Soil Survey of Eddy Area, New*  
17 *Mexico*. U.S. Department of Agriculture.
- 18 Claiborne, H.C., and Gera, F. 1974. *Potential Containment Failure Mechanisms and Their*  
19 *Consequences at a Radioactive Waste Repository in Bedded Salt in New Mexico*. ORNL-TM  
20 4639. Oak Ridge National Laboratories, Oak Ridge, TN.
- 21 Corbet, T.F. and Knupp, P.M. 1996. *The Role of Regional Groundwater Flow in the*  
22 *Hydrogeology of the Culebra Member of the Rustler Formation at the Waste Isolation Pilot*  
23 *Plant (WIPP), Southeastern New Mexico*. SAND96-2133. Sandia National Laboratories:  
24 Albuquerque, NM.
- 25 Crawley, M.E., and Nagy, M. 1998. *Waste Isolation Pilot Plant RCRA Background*  
26 *Groundwater Quality Baseline Report*. DOE/WIPP 98-2285. Albuquerque, NM: IT  
27 Corporation for Westinghouse Electric Corporation.
- 28 Davies, P.B. 1984. "Deep-Seated Dissolution and Subsidence in Bedded Salt Deposits." Ph.D.  
29 Thesis. Stanford University, Palo Alto, CA.
- 30 Davies, P.B. 1989. *Variable-Density Ground-Water Flow and Paleohydrology in the Waste*  
31 *Isolation Pilot Plant (WIPP) Region, Southeastern New Mexico*. Open-File Report 88-490. U.S.  
32 Geological Survey, Albuquerque, NM.
- 33 Deal, D.E., and Case, J.B. 1987. *Brine Sampling and Evaluation Program Phase I Report*.  
34 DOE-WIPP 87-008. Westinghouse Electric Corporation, Carlsbad, NM.

- 1 Deal, D.E., Case, J.B., Deshler, R.M., Drez, P.E., Myers, J., and Tyburski, J.R. 1987. *Brine*  
2 *Sampling and Evaluation Program Phase II Report*. DOE-WIPP-87-010. Westinghouse  
3 Electric Corporation, Carlsbad, NM.
- 4 Deal, D.E., Abitz, R.J., Belski, D.S., Case, J.B., Crawley, M.E., Deshler, R.M., Drez, P.E.,  
5 Givens, C.A., King, R.B., Lauctes, B.A., Myers, J., Niou, S., Pietz, J.M., Roggenthen, W.M.,  
6 Tyburski, J.R., and Wallace, M.G. 1989. *Brine Sampling and Evaluation Program, 1988*  
7 *Report*. DOE-WIPP-89-015. Carlsbad, NM: Westinghouse Electric Corporation.
- 8 Deal, D.E., Abitz, R.J., Belski, D.S., Clark, J.B., Crawley, M.E., and Martin, M.L. 1991a. *Brine*  
9 *Sampling and Evaluation Program, 1989 Report*. DOE-WIPP-91-009. Carlsbad, NM:  
10 Westinghouse Electric Corporation.
- 11 Deal, D.E., Abitz, R.J., Myers, J. Case, J.B., Martin, M.L., Roggenthen, W.M., and Belski, D.S.  
12 1991b. *Brine Sampling and Evaluation Program, 1990 Report*. DOE-WIPP-91-036. Prepared  
13 for U.S. Department of Energy by IT Corporation and Westinghouse Electric Corporation.  
14 Westinghouse Electric Corporation, Waste Isolation Division, Carlsbad, NM.
- 15 Deal, D.E., Abitz, R.J., Myers, J., Martin, M.L., Milligan, D.J., Sobocinski, R.W., Lippner,  
16 P.P.J., and Belski, D.S. 1993. *Brine Sampling and Evaluation Program, 1991 Report*. DOE-  
17 WIPP-93-026. Carlsbad, NM: Westinghouse Electric Corporation.
- 18 Deal, D.E., Abitz, R.J. Belski, D.S., Case, J. B., Crawley, M.E., Givens, C. A., James Lippner,  
19 P.P.J., Milligan, D.J., Myers, J., Powers, D. W., and Valdivia, M. A. 1995. *Brine Sampling and*  
20 *Evaluation Program, 1992-1993 Report and Summary of BSEP Data Since 1982*, DOE-  
21 WIPP 94-011. Carlsbad, NM: Westinghouse Electric Corporation.
- 22 Domske, P.S., Upton, D.T., and Beauheim, R.L. 1996. *Hydraulic Testing Around Room Q:*  
23 *Evaluation of the Effects of Mining on the Hydraulic Properties of Salado Evaporites*. SAND96-  
24 0435. Sandia National Laboratories, Albuquerque, NM.
- 25 Duke Engineering and Services (DES). 1997. *Exhaust Shaft: Phase 2 Hydraulic Assessment*  
26 *Data Report Involving Drilling, Installation, Water-Quality Sampling, and Testing of*  
27 *Piezometers 1-12*. DOE/WIPP97-2278. Carlsbad, NM: Westinghouse Electric Corporation.
- 28 Eager, G.P. 1983. Core from the Lower Dewey Lake, Rustler, and Upper Salado Formation,  
29 Culberson County, Texas. In *Permian Basin Cores*, R.L. Shaw and B.J. Pollen, eds., P.B.S.-  
30 S.E.P.M. Core Workshop No. 2, pp. 273 - 283. Permian Basin Section, Society of Economic  
31 Paleontologists and Mineralogists, Midland, TX.
- 32 Earth Technology Corporation. 1988. *Final Report for Time Domain Electromagnetic (TDEM)*  
33 *Surveys at the WIPP Site*. SAND87-7144. Albuquerque, NM: Sandia National Laboratories.
- 34 Elliot Geophysical Company. 1976. *A Preliminary Geophysical Study of a Trachyte Dike in*  
35 *Close Proximity to the Proposed Los Medaños Nuclear Waste Disposal Site, Eddy and Lea*  
36 *Counties, New Mexico*. Elliot Geophysical Company, Tucson, AZ.

- 1 Environmental Science and Research Foundation (ESRF), Inc. 2000. *Waste Isolation Pilot*  
2 *Plant 1999 Site Environmental Report*. DOE/WIPP 00-2225, ESRF-039. Idaho Falls, ID:  
3 ESRF.
- 4 Environmental Science and Research Foundation (ESRF), Inc. 2001. *Waste Isolation Pilot*  
5 *Plant CY 2000 Site Environmental Report*. DOE/WIPP 01-2225, ESRF-045. Idaho Falls, ID:  
6 ESRF.
- 7 Environmental Science & Research Foundation (ESRF). 2002. *Waste Isolation Pilot Plant Site*  
8 *Environmental Report for Calendar Year 2001*, DOE/WIPP 02-2225, Carlsbad, NM.
- 9 Ewing, T.E. 1993. "Erosional Margins and Patterns of Subsidence in the Late Paleozoic West  
10 Texas Basin and Adjoining Basins of West Texas and New Mexico," *New Mexico Geological*  
11 *Society Guidebook*, 44th Field Conference, Carlsbad Region New Mexico and West Texas, D.W.  
12 Lowe et al., eds., pp. 155 - 166.
- 13 Foster, R.W. 1974. *Oil and Gas Potential of a Proposed Site for the Disposal of High-Level*  
14 *Radioactive Waste*. BNL/SUB-44231/1. Ridge National Laboratory, Oak Ridge, TN. Available  
15 from NTIS. NTIS Accession number: ORNL/SUB-4423-1.
- 16 Freeze, R.A., and Witherspoon, P.A. 1967. "Theoretical Analysis of Regional Groundwater  
17 Flow: 2. Effect of Water-Table Configuration and Subsurface Permeability Variation," *Water*  
18 *Resources Research*. Vol. 3, No. 2, pp. 623 - 634.
- 19 FWS (U.S. Fish and Wildlife Service). 1989. Letter from John C. Peterson, Field Supervisor,  
20 Albuquerque, NM, to Jack B. Tillman, Project Manager, U.S. DOE—Carlsbad, May 25, 1989.
- 21 Geohydrology Associates. 1978. *Ground-Water Study Related to Proposed Expansion of*  
22 *Potash Mining near Carlsbad, New Mexico*. Contractor Report to Bureau of Land Management,  
23 Denver, CO, Contract No. YA-512-CT7-217. Albuquerque, NM: Geohydrology Associates.
- 24 Hale, W.E., Hughes, L.S., and Cox, E.R. 1954. *Possible Improvement of Quality of Water of the*  
25 *Pecos River by Diversion of Brine at Malaga Bend, Eddy County, NM*. Pecos River Commission  
26 New Mexico and Texas, in cooperation with United States Department of the Interior,  
27 Geological Survey, Water Resources Division, Carlsbad, NM.
- 28 Harland, W.B., Armstrong, R.L., Cox, A.V., Craig, L.E., Smith, A.G., and Smith, D.G. 1989. A  
29 Geologic Time Scale 1989. *Cambridge Earth Science Series*. Cambridge University Press.
- 30 Harms, J.C., and Williamson, C.R. 1988. "Deep-Water Density Current Deposits of Delaware  
31 Mountain Group (Permian), Delaware Basin, Texas and New Mexico." *American Association of*  
32 *Petroleum Geologists Bulletin*, Vol. 72.
- 33 Haug, A., Kelley, V.A., LaVenue, A.M., and Pickens, J. F. 1987. *Modeling of Ground-Water*  
34 *Flow in the Culebra Dolomite at the Waste Isolation Pilot Plant (WIPP) Site: Interim Report*.  
35 SAND86-7167. Sandia National Laboratories, Albuquerque, NM.

- 1 Hawley, J.W. 1993. "The Ogallala and Gatuña Formations in the Southeastern New Mexico  
2 Region, a Progress Report." In *Carlsbad Region, New Mexico and West Texas, New Mexico*  
3 *Geological Society, Forty-Fourth Annual Field Conference, Carlsbad, NM, October 6-9, 1993*,  
4 D.W. Love et al., eds., pp. 261 - 269. New Mexico Geological Society, Socorro, NM.
- 5 Hayes, P.T., and Bachman, G.O. 1979. *Examination and Reevaluation of Evidence for the*  
6 *Barrera Fault, Guadalupe Mountains, New Mexico*. Open-File Report 79-1520. U.S.  
7 Geological Survey, Denver, CO.
- 8 Hazen, R.M., and Roedder, E. 2001. "How Old are Bacteria from the Permian Age?" *Nature*, v.  
9 411, p. 155.
- 10 Hills, J.M. 1984. Sedimentation, Tectonism, and Hydrocarbon Generation in Delaware Basin,  
11 West Texas and Southeastern New Mexico. *American Association of Petroleum Geologists*  
12 *Bulletin*, Vol. 68.
- 13 Hiss, W.L. 1975. "Stratigraphy and Ground-Water Hydrology of the Capitan Aquifer,  
14 Southeastern New Mexico and Western Texas." PhD dissertation. University of Colorado,  
15 Department of Geological Sciences, Boulder, CO.
- 16 Hiss, W.L. 1976. *Structure of the Premium Guadalupian Capitan Aquifer, Southeast New*  
17 *Mexico and West Texas*. Resource Map. New Mexico Bureau of Mines and Mineral Resources,  
18 Socorro, NM.
- 19 Holt, R.M. 1997. *Conceptual Model for Transport Processes in the Culebra Dolomite Member,*  
20 *Rustler Formation*. SAND97-0194. Albuquerque, NM: Sandia National Laboratories.
- 21 Holt, R.M., and Powers, D.W. 1984. *Geotechnical Activities in the Waste Handling Shaft Waste*  
22 *Isolation Pilot Plant (WIPP) Project Southeastern New Mexico*. WTSD-TME-038. U.S.  
23 Department of Energy, Carlsbad, NM.
- 24 Holt, R.M., and Powers, D.W. 1986. *Geotechnical Activities in the Exhaust Shaft*. DOE-WIPP-  
25 86-008. U.S. Department of Energy, Carlsbad, NM.
- 26 Holt, R.M., and Powers, D.W. 1988. *Facies Variability and Post-Depositional Alteration*  
27 *Within the Rustler Formation in the Vicinity of the Waste Isolation Pilot Plant, Southeastern*  
28 *New Mexico*. DOE/WIPP 88-004. U.S. Department of Energy, Carlsbad, NM. (CCA Appendix  
29 GCR.)
- 30 Holt, R.M., and Powers, D.W. 1990a. *Geologic Mapping of the Air Intake Shaft at the Waste*  
31 *Isolation Pilot Plant*. DOE/WIPP 90-051. U.S. Department of Energy, Carlsbad, NM.
- 32 Holt, R.M, and Powers, D.W. 1990b. "Halite Sequences within the Late Permian Salado  
33 Formation in the Vicinity of the Waste Isolation Pilot Plant," in Powers, D.W., Holt, R.M.,  
34 Beauheim, R.L., and Rempe, N., eds., *Geological and Hydrological Studies of Evaporites in the*  
35 *Northern Delaware Basin for the Waste Isolation Pilot Plant (WIPP): Guidebook 14*, *Geological*  
36 *Society of America* (Dallas Geological Society), pp. 45-78.

- 1 Holt, R.M., and Powers, D.W. 2002. "Impact of Salt Dissolution on the Transmissivity of the  
2 Culebra Dolomite Member or the Rustler Formation, Delaware Basin, Southeastern New  
3 Mexico" *Abstracts with Program*, v. 34, no. 6, p. 215.
- 4 Holt, R.M. and Yarbrough, L. 2002. *Analysis Report Task 2 of AP-088 – Estimating Base  
5 Transmissivity Field*. Sandia National Laboratories, WIPP Records Center. ERMS #523889.  
6 WIPP Records Center.
- 7 Howard, K.A., Aaron, J.M., Brabb, E.E., Brock, M.R., Gower, H.D., Hunt, S.J., Milton, D.J.,  
8 Muehlberger, W.R., Nakata, J.K., Plafker, G., Prowell, D.C., Wallace, R.E., and Witkind, I.J.  
9 1971 [reprinted 1991]. *Preliminary Map of Young Faults in the United States as a Guide to  
10 Possible Fault Activity*. Miscellaneous Field Studies Map MF-916, 1:5,000,000. 4 maps on  
11 2 sheets. U.S. Geological Survey, Denver, CO.
- 12 Hubbert, M.K. 1940. "The Theory of Ground-Water Motion," *The Journal of Geology*. Vol.  
13 48, no. 8, pt. 1., pp. 785 - 944.
- 14 Hunter, R.L. 1985. *A Regional Water Balance for the Waste Isolation Pilot Plant (WIPP) Site  
15 and Surrounding Area*. SAND84-2233. Sandia National Laboratories, Albuquerque, NM.
- 16 INTERA. 1997a. *Exhaust Shaft Hydraulic Assessment Data Report*. DOE-WIPP 97-2219.  
17 Carlsbad, NM: WIPP Management and Operating Contractor.
- 18 INTERA. 1997b. *Exhaust Shaft Data Report: 72-Hour Pumping Test on C-2506 and 24-Hour  
19 Pumping Test on C-2505*. Carlsbad, NM: Waste Isolation Pilot Plant.
- 20 IT Corporation. 2000. *Addendum 1, Waste Isolation Pilot Plant RCRA Background  
21 Groundwater Quality Baseline Update Report*. Prepared for Westinghouse Electric Corporation,  
22 Carlsbad, NM.
- 23 Izett, G.A., and Wilcox, R.E. 1982. *Map Showing Localities and Inferred Distribution of the  
24 Huckleberry Ridge, Mesa Falls, and Lava Creek Ash Beds in the Western United States and  
25 Southern Canada*. Misc. Investigations Map I-1325, scale 1:4,000,000. U.S. Geological Survey.
- 26 Jarolimek, L., Timmer, M.J., and McKinney, R.F. 1983. *Geotechnical Activities in the  
27 Exploratory Shaft—Selection of the Facility Interval, Waste Isolation Pilot Plant (WIPP)  
28 Project, Southeastern New Mexico*. TME 3178. U.S. Department of Energy, Albuquerque, NM.
- 29 Jones, C.L., Bowles, C.G., and Bell, K.G. 1960. *Experimental Drillhole Logging in Potash  
30 Deposits of the Carlsbad District, New Mexico*. Open-File Report. U.S. Geological Survey,  
31 Denver, CO.
- 32 Jones, C.L., Cooley, M.E., and Bachman, G.O. 1973. *Salt Deposits of Los Medaños Area, Eddy  
33 and Lea Counties, New Mexico*. Open-File Report 4339-7. U.S. Geological Survey, Denver,  
34 CO.

- 1 Jones, C.L. 1978. *Test Drilling for Potash Resources: Waste Isolation Pilot Plant Site, Eddy*  
2 *County, New Mexico.* Open-File Report 78-592. Vols. 1 and 2. U.S. Geological Survey,  
3 Denver, CO.
- 4 Jones, C.L. 1981. *Geologic Data for Borehole ERDA-6, Eddy County, New Mexico.* Open-File  
5 Report 81-468. U.S. Geological Survey, Denver, CO.
- 6 Jones, T.L., Kelley, V.A., Pickens, J.T., Upton, D.T., Beauheim, R.L., and Davies, P.B. 1992.  
7 *Integration of Interpretation Results of Tracer Tests Performed in the Culebra Dolomite at the*  
8 *Waste Isolation Pilot Plant Site.* SAND92-1579. Sandia National Laboratories, Albuquerque,  
9 NM.
- 10 Keesey, J. J. 1976. *Hydrocarbon Evaluation, Proposed Southeastern New Mexico Radioactive*  
11 *Material Storage Site, Eddy County, New Mexico.* SAND71-7033. Vols. I and II. Sipes,  
12 Williamson, and Aycock, Midland, TX.
- 13 Kehrman, R.F. 2002. *Compliance Recertification Application Monitoring Data, Volume Two.*  
14 Carlsbad, NM: Westinghouse TRU Solutions LLC. Copy on file in the Sandia WIPP Records  
15 Center under ERMS# 527193.
- 16 Kelley, V.A. 1971. *Geology of the Pecos Country, Southeastern New Mexico.* Memoir 24.  
17 New Mexico Bureau of Mines and Mineral Resources, Socorro, NM.
- 18 Kelley, V.A., and Saulnier, Jr., G.J. 1990. *Core Analyses for Selected Samples from the Culebra*  
19 *Dolomite at the Waste Isolation Pilot Plant Site.* SAND90-7011. Sandia National Laboratories,  
20 Albuquerque, NM.
- 21 King, P.B. 1948. *Geology of the Southern Guadalupe Mountains, Texas.* Professional Paper  
22 215. U.S. Geological Survey, Washington, D.C.
- 23 Krumhansl, J.L., Kimball, K.M. and Stein, C.L. 1991. *Intergranular Fluid Compositions from*  
24 *the Waste Isolation Pilot Plant (WIPP), Southeastern New Mexico.* SAND90-0584.  
25 Albuquerque, NM: Sandia National Laboratories.
- 26 Lambert, S.J. 1983a. *Dissolution of Evaporites in and around the Delaware Basin,*  
27 *Southeastern New Mexico and West Texas.* SAND82-0461. Sandia National Laboratories,  
28 Albuquerque, NM.
- 29 Lambert, S.J. 1983b. "Evaporite Dissolution Relevant to the WIPP Site, Northern Delaware  
30 Basin, Southeastern New Mexico." In *Scientific Basis for Nuclear Waste Management VI,*  
31 *Materials Research Society Symposia Proceedings, Boston, MA, November 1-4, 1982,* SAND82-  
32 1416C. D.G. Brookins, ed., pp. 291 - 298. Elsevier Science Publishing Company, New York,  
33 NY.
- 34 Lambert, S.J. 1987. *Feasibility Study: Applicability of Geochronologic Methods Involving*  
35 *Radiocarbon and other Nuclides to the Groundwater Hydrogeology of the Rustler Formation,*  
36 *Southeastern New Mexico.* SAND86-1054. Sandia National Laboratories, Albuquerque, NM.

- 1   Lambert, S.J. 1991. "Isotopic Constraints on the Rustler and Dewey Lake Groundwater  
2   Systems," in Siegel, M.D., Lambert, S.J., and Robinson, K.L., eds. *Hydrogeochemical Studies of  
3   the Rustler Formation and Related Rocks in the Waste Isolation Pilot Plant Area, Southeastern  
4   New Mexico.* SAND88-0196. Sandia National Laboratories, Albuquerque, NM.
- 5   Lambert, S.J., and Carter, J.A. 1987. *Uranium-Isotope Systematics in Groundwaters of the  
6   Rustler Formation, Northern Delaware Basin, Southeastern New Mexico. I. Principles and  
7   Preliminary Results.* SAND87-0388. Sandia National Laboratories, Albuquerque, NM.
- 8   Lambert, S.J., and Harvey, D.M. 1987. *Stable-Isotope Geochemistry of Groundwaters in the  
9   Delaware Basin of Southeastern New Mexico.* SAND87-0138. Sandia National Laboratories,  
10   Albuquerque, NM.
- 11   Lang, W.B. 1935. "Upper Permian Formation of Delaware Basin of Texas and New Mexico."  
12   *American Association of Petroleum Geologists Bulletin*, Vol. 19, pp. 262 - 276.
- 13   Lang, W.B. 1939. Salado Formation of the Permian Basin. *American Association of Petroleum  
14   Geologists Bulletin*, Vol. 23, pp. 1569 - 1572.
- 15   Lang, W.B. 1942. Basal Beds of Salado Formation in Fletcher Potash Core Test near Carlsbad,  
16   New Mexico. *American Association of Petroleum Geologists Bulletin*, Vol. 26.
- 17   Lang, W.B. 1947. "Occurrence of Comanche Rocks in Black River Valley, New Mexico,"  
18   *American Association of Petroleum Geologists Bulletin*, Vol. 31, pp. 1472 - 1478.
- 19   Lappin, A.R., Hunter, R.L., Garber, D.P., and Davies, P.B., eds, 1989. *Systems Analysis, Long -  
20   Term Radionuclide Transport, and Dose Assessments, Waste Isolation Pilot Plant (WIPP),  
21   Southeastern New Mexico; March 1989.* SAND89-0462. Sandia National Laboratories,  
22   Albuquerque, NM.
- 23   LaVenue, A.M., Haug, A., and Kelley, V.A. 1988. *Numerical Simulation of Ground-Water  
24   Flow in the Culebra Dolomite at the Waste Isolation Pilot Plant (WIPP) Site: Second Interim  
25   Report.* SAND88-7002. Sandia National Laboratories, Albuquerque, NM.
- 26   LaVenue, A.M., Cauffman, T.L., and Pickens, J.F. 1990. *Ground-Water Flow Modeling of the  
27   Culebra Dolomite.* Volume 1: Model Calibration. SAND89-7068/1. Sandia National  
28   Laboratories, Albuquerque, NM.
- 29   Lee, W.T. 1925. "Erosion by Solution and Fill." *In Contributions to Geography in the United  
30   States: USGS Bulletin*, 760-C.
- 31   Lord, K.J., and Reynolds, W.E., eds. 1985. *Archaeological Investigations of Three Sites within  
32   the WIPP Core Area.* Prepared for the U.S. Army Corps of Engineers (COE), Albuquerque  
33   District in NM. Eddy County, NM, Chambers Consultants and Planner, Albuquerque, NM.
- 34   Lowenstein, T.K. 1987. *Post Burial Alteration of the Permian Rustler Formation Evaporites,  
35   WIPP Site, New Mexico: Textural Stratigraphic and Chemical Evidence.* EEG-36, New Mexico  
36   Health and Environment Department, Santa Fe, New Mexico.

- 1 Lowenstein, T.K. 1988. "Origin of Depositional Cycles in a Permian Saline Giant: The Salado  
2 (McNutt Zone) Evaporites of New Mexico and Texas." *Geological Society of America Bulletin*,  
3 Vol. 100, No. 4, pp. 20 - 21, 592 - 608.
- 4 Lucas, S.G., and Anderson, O.J. 1993a. "Triassic Stratigraphy in Southeastern New Mexico and  
5 Southwestern Texas." In *Carlsbad Region, New Mexico and West Texas, New Mexico*  
6 *Geological Society, Forty-Fourth Annual Field Conference, Carlsbad, NM, October 6-9, 1993*.  
7 D.W. Love et al., eds., pp. 231 - 235. New Mexico Geological Society, Socorro, NM.
- 8 Lucas, S.G., and Anderson, O.J. 1993b. "Stratigraphy of the Permian-Triassic Boundary in  
9 Southeastern New Mexico and West Texas." In *Geology of the Carlsbad Region, New Mexico*  
10 *and West Texas*, D.W. Love et al., eds., Forty-Fourth Annual Field Conference Guidebook. New  
11 Mexico Geological Society, Socorro, NM.
- 12 Machette, M.N. 1985. "Calcic Soils of the Southwestern United States." In *Soils and*  
13 *Quaternary Geology of the Southwestern United States*, D.L. Weide and M.L. Faber, eds.,  
14 Special Paper Vol. 203, pp. 1 - 21. Geological Society of America, Denver, CO.
- 15 Madsen, B.M., and Raup, O.B. 1988. Characteristics of the Boundary between the Castile and  
16 Salado Formations near the Western Edge of the Delaware Basin, Southeastern New Mexico.  
17 *New Mexico Geology*, Vol. 10, No. 1.
- 18 Maley, V.C., and Huffington, R.M. 1953. "Cenozoic Fill and Evaporite Solution in the  
19 Delaware Basin, Texas and New Mexico." *Geological Society of America Bulletin*, Vol. 64.
- 20 McGowen, J.H., and Groat, C.G. 1971. *Van Horn Sandstone, West Texas: An Alluvial Fan*  
21 *Model for Mineral Exploration*. Report of Investigations No. 72. Bureau of Economic Geology,  
22 Austin, TX.
- 23 McGuire, R.K. 1976. *FORTRAN Computer Program for Seismic Risk Analysis*. Open-File  
24 Report No. 76-67, pp. 1 - 68. U.S. Geological Survey.
- 25 Meigs, L.C., and Beauheim, R.L. 2001. "Tracer Tests in a Fractured Dolomite, 1. Experimental  
26 Design and Observed Tracer Recoveries," *Water Resources Research*, Vol. 25, No. 5, pp. 1113-  
27 1128.
- 28 Meigs, L.C., Beauheim, R.L., and Jones, T.L. eds. 2000. *Interpretation of Tracer Tests*  
29 *Performed in the Culebra Dolomite at the Waste Isolation Pilot Plant*. SAND97-3109.  
30 Albuquerque, NM: Sandia National Laboratories.
- 31 Mercer, J.W. 1983. *Geohydrology of the Proposed Waste Isolation Pilot Site, Los*  
32 *Medaños Area, Southeastern New Mexico*. Water Resources Investigation Report 83-4016. U.S.  
33 Geological Survey, Albuquerque, NM. (CCA Appendix HYDRO.)
- 34 Mercer, J.W., Beauheim, R.L., Snyder, R.P., and Fairer, G.M. 1987. *Basic Data Report for*  
35 *Drilling and Hydrologic Testing of Drillhole DOE-2 at the Waste Isolation Pilot Plant (WIPP)*  
36 *Site*. SAND86-0611. Sandia National Laboratories, Albuquerque, NM.

- 1 Miller, D.N. 1955. *Petrology of the Pierce Canyon Formation, Delaware Basin, Texas and New*  
2 *Mexico* [Ph.D. Dissertation]. University of Texas, Austin.
- 3 Miller, D.N. 1966. Petrology of Pierce Canyon Redbeds, Delaware Basin, Texas and New  
4 Mexico. *American Association of Petroleum Geologists Bulletin*, Vol. 80.
- 5 Molecke, M.A. 1983. *A Comparison of Brines Relevant to Nuclear Waste Experimentation*.  
6 SAND83-0516. Albuquerque, NM: Sandia National Laboratories.
- 7 Muehlberger, W.R., Belcher, R.C., and Goetz, L.K. 1978. Quaternary Faulting on Trans-Pecos,  
8 Texas. *Geology*, Vol. 6, No. 6, pp. 337 - 340.
- 9 Neill, R.H., Channell, J.K., Chaturvedi, L., Little, M.S., Rehfeldt, K., and Spiegler, P. 1983.  
10 *Evaluation of the Suitability of the WIPP Site*. EEG-23. Environmental Evaluation Group, Santa  
11 Fe, NM.
- 12 New Mexico Bureau of Mines and Mineral Resources (NMBMMR). 1995. *Final Report*  
13 *Evaluation of Mineral Resources at the Waste Isolation Pilot Plant (WIPP) Site*. Vols. 1 to 4.
- 14 Nicholson, Jr., A., and Clebsch, Jr., A. 1961. *Geology and Ground-Water Conditions in*  
15 *Southern Lea County, New Mexico*. Ground-Water Report 6. New Mexico Bureau of Mines and  
16 Mineral Resources, Socorro, NM.
- 17 Nuttli, O.W. 1973. Design Earthquakes for the Central United States. Miscellaneous Paper S-  
18 73-1, pp. 1 - 45. U.S. Army Waterways Experiment Station, Vicksburg, MS.
- 19 Olive, W.W. 1957. "Solution-Subsidence Troughs, Castile Formation of Gypsum Plain, Texas  
20 and New Mexico." *Geological Society of America Bulletin*, Vol. 68.
- 21 O'Neill, J.R., Johnson, C.M., White, L.D., and Roedder, E. 1986. "The Origin of Fluid in the  
22 Salt Beds of the Delaware Basin, New Mexico and Texas," *Applied Geochemistry*, v. 1, pp. 265-  
23 271.
- 24 Palmer, A.R. 1983. "The Decade of North American Geology 1983 Geologic Time Scale."  
25 *Geology*, Vol. 11, No. 9, pp. 503 -504.
- 26 Piper, A.M. 1973. *Subrosion in and about the Four-Township Study Area near Carlsbad, New*  
27 *Mexico*. Report to Oak Ridge National Laboratories, Oak Ridge, TN.
- 28 Piper, A.M. 1974. *The Four-Township Study Area near Carlsbad, New Mexico: Vulnerability*  
29 *to Future Subrosion*. Report to Oak Ridge National Laboratories, Oak Ridge, TN.
- 30 Popielak, R.S., Beauheim, R.L., Black, S.B., Coons, W.E., Ellingson, C.T., and Olsen, R.L.  
31 1983. *Brine Reservoirs in the Castile Formation, Waste Isolation Pilot Plant (WIPP), Project*  
32 *Southeastern New Mexico*. TME-3153. Westinghouse Electric Corporation, Carlsbad, NM.

- 1 Powers, D.W. 1997. *Geology of Piezometer Holes to Investigate Shallow Water Sources under*  
2 *the Waste Isolation Pilot Plant, in INTERA, 1997, Exhaust Shaft Hydraulic Assessment Data*  
3 *Report*, DOE/WIPP 97-2219. Carlsbad, NM: US DOE
- 4 Powers, D.W. 2002a. *Analysis Report for Task 1 of AP-088 – Construction of Geologic*  
5 *Contour Maps*: ERMS #522086. Carlsbad, NM: Sandia National Laboratories, WIPP Records  
6 Center.
- 7 Powers, D.W. 2002b. “*Addendum to Analysis Report Task 1 of AP-088 Construction of*  
8 *Geologic Contour Maps*.” ERMS #523886. Carlsbad, NM: Sandia National Laboratories, WIPP  
9 Records Center.
- 10 Powers, D.W. 2002c. *Basic Data Report for Drillhole C-2737 (Waste Isolation Pilot Plant –*  
11 *WIPP)*: DOE/WIPP 01-3210. Carlsbad, NM: US DOE.
- 12 Powers, D.W. 2003a. *Addendum 2 to Analysis Reports Task 1 of AP-088, Construction of*  
13 *Geologic Contour Maps*. ERMS #525199. Carlsbad, NM: Sandia National Laboratories, WIPP  
14 Records Center.
- 15 Powers, D.W. 2003b. *Geohydrological conceptual model for the Dewey Lake Formation in the*  
16 *vicinity of the Waste Isolation Pilot Plant (WIPP)*. Test Plan TP02-05. ERMS# 526493.  
17 Carlsbad, NM: Sandia National Laboratories, WIPP Records Center.
- 18 Powers, D.W., and Hassinger, B.W. 1985. “Synsedimentary Dissolution Pits in Halite of the  
19 Permian Salado Formation, Southeastern New Mexico,” *Journal of Sedimentary Petrology*, Vol.  
20 55, pp. 769-773.
- 21 Powers, D.W. and Holt, R. 1990. *Sedimentology of the Rustler Formation Near the Waste*  
22 *Isolation Pilot Plant (WIPP) Site*. pp. 77 -106. GSA Field Trip #14. Geological Society of  
23 America 1990 Annual Meeting. October 29 - November 1, 1990. Dallas, TX.
- 24 Powers, D.W., and Holt, R.M. 1993. “The Upper Cenozoic Gatuña Formation of Southeastern  
25 New Mexico.” In *Carlsbad Region, New Mexico and West Texas, New Mexico Geological*  
26 *Society, Forty-Fourth Annual Field Conference, Carlsbad, NM, October 6-9, 1993*, D.W. Love  
27 et al., eds., pp. 271-282. New Mexico Geological Society, Roswell, NM.
- 28 Powers, D.W., and Holt, R.M. 1995. *Regional Geological Processes Affecting Rustler*  
29 *Hydrogeology*. Prepared for U.S. Department of Energy by IT Corporation, Albuquerque, NM.
- 30 Powers, D.W., and Holt, R.M. 1999. “The Los Medaños Member of the Permian Rustler  
31 Formation,” *New Mexico Geology*, Vol. 21, No. 4, pp. 97-103.
- 32 Powers, D. W., and R. M. Holt. 2000. “The Salt That Wasn’t There: Mudflat Facies  
33 Equivalents to Halite of the Permian Rustler Formation, Southeastern New Mexico,” *Journal of*  
34 *Sedimentary Research*, Vol. 70, No. 1, pp. 29-36.
- 35 Powers, D.W., and Stensrud, W.A. 2003. *Basic Data Report for Drillhole C-2811 (Waste*  
36 *Isolation Pilot Plant–WIPP)*. DOE/WIPP 02-3223. Carlsbad, NM: US DOE.

- 1 Powers, D.W., Lambert, S.J., Shaffer, S.E., Hill, L.R., and Weart, W.D., eds. 1978. *Geological*  
2 *Characterization Report for the Waste Isolation Pilot Plant (WIPP) Site, Southeastern New*  
3 *Mexico.* SAND78-1596, Vols. I and II. Sandia National Laboratories, Albuquerque, NM.  
4 (CCA Appendix GCR.)
- 5 Powers, D.W., Sigda, J.M., and Holt, R.M. 1996. "Probability of Intercepting a Pressurized  
6 Brine Reservoir Under the WIPP." ERMS #523414. Carlsbad, NM: Sandia National  
7 Laboratories. WIPP Records Center.
- 8 Powers, D.W., Vreeland, R.H., and Rosenzweig, W.D. 2001. "How Old are Bacteria from the  
9 Permian Age?" *Nature*, Vol. 411, pp. 155-156.
- 10 Powers, D.W., Holt, R.M., Beauheim, R.L., and McKenna, S.A. 2003. "Geological Factors  
11 Related to the Transmissivity of the Culebra Dolomite Member, Permian Rustler Formation,  
12 Delaware Basin, Southeastern New Mexico," in Johnson, K.S., and Neal, J.T., eds., *Evaporite*  
13 *karst and engineering/environmental problems in the United States: Oklahoma Geological*  
14 *Survey Circular* 109, pp. 211-218.
- 15 Pratt, H.R., Stephenson, D.E., Zandt, G., Bouchon, M., and Hustrulik, W.A. 1979. Earthquake  
16 Damage to Underground Facilities. *Proceedings of the 1979 RETC*, Vol. 1. AIME, Littleton,  
17 CO.
- 18 Ramey, D.S. 1985. *Chemistry of Rustler Fluids.* EEG-31. New Mexico Environmental  
19 Evaluation Group, Santa Fe, NM.
- 20 Rawson, D., Boardman, C., and Jaffe-Chazan, N. 1965. *The Environment Created by a Nuclear*  
21 *Explosion in Salt.* PNE-107F. U.S. Atomic Energy Commission Plowshare Program, Project  
22 Gnome, Carlsbad, NM.
- 23 Register, J.K. 1981. *Rubidium-Strontium and Related Studies of the Salado Formation,*  
24 *Southeastern New Mexico.* SAND81-7072. Sandia National Laboratories, Albuquerque, NM.
- 25 Register, J.K., and Brookins, D.G. 1980. "Rb-Sr Isochron Age of Evaporite Minerals from the  
26 Salado Formation (Late Permian), Southeastern New Mexico." *Isochron/West*, No. 29, pp. 39 -  
27 42.
- 28 Reiter, M., Barroll, M.W., and Minier, J. 1991. "An Overview of Heat Flow in Southwestern  
29 United States and Northern Chihuahua, Mexico." In *Neotectonics of North America*, D.B.  
30 Slemmons, E.R. Engdahl, M.D. Zoback, and D.D. Blackwell, eds., pp. 457 - 466. Geological  
31 Society of America, Boulder, CO.
- 32 Renne, P.R., Sharp, W.D. and Becker, T.A. 1998. " $^{40}\text{Ar}/^{39}\text{Ar}$  Dating of Langbeinite  $[\text{K}_2\text{Mg}_2(\text{SO}_4)_3]$  in Late Permian Evaporites of the Salado Formation, Southeastern New Mexico, USA,"  
33 *Mineralogy Magazine*, Vol. 62A, pp. 1253-1254

- 1 Renne, P.R., Steiner, M.B., Sharp, W.D., Ludwig, K.R., and Fanning, C.M. 1996. “ $^{40}\text{Ar}/^{39}\text{Ar}$  and U/Pb SHRIMP Dating of Latest Permian Tephra in the Midland Basin, Texas,” *Eos, Transactions, American Geophysical Union*, Vol. 77, p. 794.
- 4 Richardson, G.B. 1904. “Report of a Reconnaissance of Trans-Pecos Texas, North of the Texas  
5 and Pacific Railway.” *Texas University Bulletin* 23. Var Boeckmann-Jones Company, Austin,  
6 TX.
- 7 Richey, S.F. 1989. *Geologic and Hydrologic Data for the Rustler Formation Near the Waste  
8 Isolation Pilot Plant, Southeastern New Mexico*. Open-File Report 89-32. U.S. Geological  
9 Survey, Albuquerque, NM.
- 10 Richter, C.F. 1958. *Elementary Seismology*. W.H. Freeman & Co., San Francisco, CA.
- 11 Roberts, R.M., Beauheim, R.L., and Domski, P.S. 1999. *Hydraulic Testing of Salado  
12 Formation Evaporites at the Waste Isolation Pilot Plant Site: Final Report*. SAND98-2537.  
13 Sandia National Laboratories, Albuquerque, NM.
- 14 Robinson, T.W., and Lang, W.B. 1938. “Geology and Ground-Water Conditions of the Pecos  
15 River Valley in the Vicinity of Laguna Grande de la Sal, New Mexico, with Special Reference to  
16 the Salt Content of the River Water.” *Twelfth and Thirteenth Biennial Reports of the State  
17 Engineer of New Mexico for the 23rd, 24th, 25th, and 26th Fiscal Years, July 1, 1934 to July 30,  
18 1938*. State Engineer, Santa Fe, NM.
- 19 Robinson, J.Q., and Powers, D.W. 1987. “A Clastic Deposit within the Lower Castile  
20 Formation, Western Delaware Basin, New Mexico.” In *Geology of the Western Delaware Basin,  
21 West Texas and Southeastern New Mexico*, D.W. Powers, and W.C. James, eds., El Paso  
22 Geological Society Guidebook 18, pp. 66 -79. El Paso Geological Society, El Paso, TX.
- 23 Roedder, E. 1984. “The Fluids in Salt,” *American Mineralogist*, v. 69, pp. 413-439.
- 24 Rogers, A.M., and Malkiel, A. 1979. A Study of Earthquakes in the Permian Basin of Texas–  
25 New Mexico. *Bulletin of the Seismological Society of America*, Vol. 69, pp. 843 - 865.
- 26 Rosholt, J.N., and McKinney, C.R. 1980. *Uranium Series Disequilibrium Investigations  
27 Related to the WIPP Site, New Mexico (USA), Part II. Uranium Trend Dating of Surficial  
28 Deposits and Gypsum Spring Deposits Near WIPP Site, New Mexico*. Open-File Report 80-879.  
29 U.S. Geological Survey, Denver, CO.
- 30 Salvador, A. 1985. “Chronostratigraphic and Geochronometric Scales in Colorado SUNA  
31 Stratigraphic Correlation Charts of the United States.” *American Association of Petroleum  
32 Geologists Bulletin*, Vol. 69.
- 33 Sandia National Laboratories. 2000. “*Sandia National Laboratories Annual Compliance  
34 Monitoring Parameter Assessment, WBS 1.3.5.2.1.1, Pkg. No. 510062*.” ERMS #512733.  
35 Carlsbad, NM: Sandia National Laboratories, WIPP Records Center.
- 36

- 1 Sandia National Laboratories. 2001. "Sandia National Laboratories Annual Compliance  
2 Monitoring Parameter Assessment, WBS 1.3.5.3.1, Pkg. No. 510062, October 2001." ERMS  
3 #519620. Carlsbad, NM: Sandia National Laboratories, WIPP Records Center.
- 4 Sandia National Laboratories. 2002. "Sandia National Laboratories Annual Compliance  
5 Monitoring Parameter Assessment for 2002, WBS 1.3.5.3.1, Pkg. No. 510062, November 2002."  
6 ERMS #524449. Carlsbad, NM: Sandia National Laboratories, WIPP Records Center.
- 7 Sandia National Laboratories. 2003a. "Sandia National Laboratories Technical Baseline  
8 Reports, WBS 1.3.5.3, Compliance Monitoring; WBS 1.3.5.4, Repository Investigations,  
9 Milestone RI 03-210, January 31, 2003." ERMS #526049. Carlsbad, NM: Sandia National  
10 Laboratories, WIPP Records Center.
- 11 Sandia National Laboratories. 2003b. "Program Plan, WIPP Integrated Groundwater  
12 Hydrology Program, FY03-FY09, Revision 0, March 14, 2003." ERMS #526671. Carlsbad, NM:  
13 Sandia National Laboratories, WIPP Records Center.
- 14 Sanford, A.R., Jaksha, L.H., and Cash, D.J. 1991. "Seismicity of the Rio Grand Rift in New  
15 Mexico." In *Neotectonics of North America*, D.B. Slemmons, E.R. Engdahl, M.D. Zoback, and
- 16 Satterfield, C.L., Lowenstein, T.K., Vreeland, R., and Rosenzweig, W. 2002. "The Search for  
17 Microorganisms in Brine Inclusions in Halite: an Update," *Abstracts with Programs,*  
18 *Geological Society of America*, Annual Meeting, v. 34, no. 6, p. 19.
- 19 Schiel, K.A. 1988. "The Dewey Lake Formation: End Stage Deposit of a Peripheral Foreland  
20 Basin." Master's thesis. University of Texas at El Paso, El Paso, TX.
- 21 Schiel, K.A. 1994. "A New Look at the Age, Depositional Environment and Paleogeographic  
22 Setting of the Dewey Lake Formation (Late Permian)." *West Texas Geological Society Bulletin*,  
23 Vol. 33, No. 9, pp. 5 - 13.
- 24 Sergent, Hauskins & Beckwith, 1979. *Subsurface Exploration & Laboratory Testing. Plant  
25 Site: Waste Isolation Pilot Plant*. Vols I & II. Phoenix, AZ: Sergent, Hauskins & Beckwith  
26 (Copy on file at the U.S. Department of Energy, WIPP Information Center, Carlsbad, NM).
- 27 Sowards, T., Williams, M.L., and Keil, K. 1991. *Mineralogy of the Culebra Dolomite Member  
28 of the Rustler Formation*. SAND90-7008. Sandia National Laboratories, Albuquerque, NM.
- 29 Siegel, M.D., Lambert, S.J., and Robinson, K.L., eds. 1991. *Hydrogeochemical Studies of the  
30 Rustler Formation and Related Rocks in the Waste Isolation Pilot Plant Area, Southeastern New  
31 Mexico*. SAND88-0196. Sandia National Laboratories, Albuquerque, NM.
- 32 Silva, M.K. 1996. *Fluid Injection for Salt Water Disposal and Enhanced Oil Recovery as a  
33 Potential Problem for WIPP: Proceedings of a June 1995 Workshop and Analysis*. EEG-62.  
34 Albuquerque, NM: Environmental Evaluation Group.

- 1 Snider, H.I. 1966. "Stratigraphy and Associated Tectonics of the Upper Permian Castile-  
2 Salado-Rustler Evaporite Complex, Delaware Basin, West Texas and Southeast New Mexico."  
3 Ph.D. dissertation. University of New Mexico, Albuquerque, NM.
- 4 Snyder, R.P. 1985. *Dissolution of Halite and Gypsum, and Hydration of Anhydrite to Gypsum,*  
5 *Rustler Formation, in the Vicinity of the Waste Isolation Pilot Plant, Southeastern New Mexico.*  
6 Open-File Report 85-229. U.S. Geological Survey, Denver, CO.
- 7 Snyder, R.P., Gard, Jr., L.M., and Mercer, J.W. 1982. *Evaluation of Breccia Pipes in*  
8 *Southeastern New Mexico and Their Relation to the Waste Isolation Pilot Plant (WIPP) Site,*  
9 *with Section on Drill-Stem Tests.* Open-File Report 82-968. U.S. Geological Survey, Denver,  
10 CO.
- 11 Stein, C.L., and Krumhansl, J.L. 1988. "A Model for the Evolution of Brines in Salt from the  
12 Lower Salado Formation, Southeastern New Mexico," *Geochimica et Cosmochimica Acta*, v. 52,  
13 pp. 1037-1046.
- 14 Swift, P.N. 1992. *Long-Term Climate Variability at the Waste Isolation Pilot Plant,*  
15 *Southeastern New Mexico, USA.* SAND91-7055. Sandia National Laboratories, Albuquerque,  
16 NM. (CCA Appendix CLI.)
- 17 TerraTek, Inc. 1996. "Physical Property Characterization of Miscellaneous Rock Samples,  
18 Contract AA-2896." Contractor Report TR97-03 to Sandia National Laboratories. ERMS  
19 #238234. Salt Lake City, UT.
- 20 Thompson, G.A. and Zoback, M.L. 1979. Regional Geophysics of the Colorado Plateau.  
21 *Tectonophysics*, Vol. 61, Nos. 1 - 3, pp. 149 - 181.
- 22 Tóth, J., 1963. "A Theoretical Analysis of Groundwater Flow in Small Drainage Basins,"  
23 *Journal of Geophysical Research.* Vol. 68, No. 16, pp. 4795 - 4812.
- 24 UNM (University of New Mexico). 1984. *A Handbook of Rare and Endemic Plants of New*  
25 *Mexico.* New Mexico Native Plants Protection Advisory Committee, eds. University of New  
26 Mexico Press, Albuquerque, NM.
- 27 Urry, W.E. 1936. Post-Keweenawan Timescale. Exhibit 2, pp. 35 - 40. National Research  
28 Council, Report Committee on Measurement of Geologic Time 1935 -36.
- 29 U.S. Congress. 1992. *Waste Isolation Pilot Plant Land Withdrawal Act.* Public Law 102-579,  
30 October 1992. 102nd Congress, Washington, D.C.
- 31 U.S. Census Bureau. 2000. Census 2000 at <http://www.census.gov/main/www/access.html>.
- 32 U.S. Department of Commerce. 1990. *Census of Population, General Population*  
33 *Characteristics of New Mexico.* Bureau of the Census.

- 1 U.S. Department of Energy (DOE ). 1980. *Final Environmental Impact Statement, Waste*  
2 *Isolation Pilot Plant.* DOE/EIS-0026, Vols. 1 and 2. Office of Environmental Restoration and  
3 Waste Management, Washington, D.C.
- 4 U.S. Department of Energy (DOE). 1983. *Summary of the Results of the Evaluation of the*  
5 *WIPP Site and Preliminary Design Validation Program.* WIPP-DOE-161. Carlsbad, NM: Waste  
6 Isolation Pilot Plant.
- 7 U.S. Department of Energy (DOE). 1996. *Title 40 CFR Part 191 Compliance Certification*  
8 *Application for the Waste Isolation Pilot Plant,* DOE/CAO-1996-2184, October 1996, Carlsbad  
9 Field Office, Carlsbad, NM.
- 10 U.S. Department of Energy (DOE). 1999. *Exhaust Shaft: Phase III Hydraulic Assessment Data*  
11 *Report, October 1997 -- October 1998.* DOE-WIPP 99-2302. Carlsbad, NM: Waste Isolation  
12 Pilot Plant.
- 13 U.S. Department of Energy (DOE). 2002a. *Delaware Basin Monitoring Annual Report.*  
14 DOE/WIPP-99-2308, Rev. 03. Carlsbad, NM: Department of Energy.
- 15 U.S. Department of Energy (DOE). 2002b. *Geotechnical Analysis Report for July 2000 -June*  
16 *2001.* DOE/WIPP 02-3177, Vol. 1. Carlsbad, NM: Department of Energy.
- 17 U.S. Department of Energy (DOE). 2003. *Strategic Plan for Groundwater Monitoring at the*  
18 *Waste Isolation Pilot Plant.* DOE/WIPP-03-3220, United States Department of Energy.  
19 Carlsbad, NM: February 2003.
- 20 U.S. Environmental Protection Agency (EPA). 1988. "40 CFR Parts 124, 144, 146, and 148  
21 Underground Insertion Control Program: Hazardous Waste Disposal Injection Restrictions;  
22 Amendments to Technical Requirements for Class 1 Hazardous Waste Injection Wells, and  
23 Additional Monitoring Requirements Applicable to All Class 1 Wells." *Federal Register,*  
24 Vol. 53, 28188, July 26, 1988.
- 25 U.S. Environmental Protection Agency (EPA). 1993. 40 CFR Part 191 Environmental  
26 Radiation Protection Standards for the Management and Disposal of Spent Nuclear Fuel, High-  
27 Level and Transuranic Radioactive Wastes; Final Rule. *Federal Register,* Vol. 58, No. 242, pp.  
28 66398 - 66416, December 20, 1993. Office of Radiation and Indoor Air, Washington, D.C.
- 29 U.S. Environmental Protection Agency (EPA). 1996. 40 CFR Part 194: *Criteria for the*  
30 *Certification and Re-Certification of the Waste Isolation Pilot Plant's Compliance with the*  
31 *40 CFR Part 191 Disposal Regulations; Final Rule.* *Federal Register,* Vol. 61, No. 28,  
32 pp. 5224 - 5245, February 9, 1996. Office of Air and Radiation, Washington, D.C. In NWM  
33 Library as KF70.A35.C751.
- 34 U.S. Environmental Protection Agency (EPA). 1996. Docket A-93-02, Item II-I-01, Enclosure  
35 1, Letter from EPA to DOE, December 19, 1996 technical issues raised by EPA.
- 36 U.S. Nuclear Regulatory Commission (NRC). 1973. Design Spectra for Seismic Design of  
37 Nuclear Power Plants, Revision 1. *Regulatory Guide 1.60,* December 1973.

- 1   Vine, J.D. 1963. "Surface Geology of the Nash Draw Quadrangle, Eddy County, New Mexico."  
2   *U.S. Geological Survey Bulletin 1141-B*. U.S. Government Printing Office, Washington, DC.
- 3   Washington Regulatory & Environmental Services (WRES). 2003. *Waste Isolation Pilot Plant*  
4   *Site Environmental Report for Calendar Year 2002*, DOE/WIPP 03-2222, Carlsbad, NM.
- 5   Waste Isolation Pilot Plant Management and Operating Contractor (WIPP MOC). 1995. *Basic*  
6   *Data Report for WQSP 1, WQSP 2, WQSP 3, WQSP 4, WQSP 5, WQSP 6, WQSP 6a*,  
7   DOE/WIPP 95-2154. WIPP MOC, Carlsbad, NM.
- 8   Weart, W.D. 1983. *Summary Evaluation of the Waste Isolation Pilot Plant (WIPP) Site*  
9   *Suitability*. SAND83-0450. Albuquerque, NM: Sandia National Laboratories.
- 10   Westinghouse Electric Corporation (WEC). 1991a. *Waste Isolation Pilot Plant Groundwater*  
11   *Monitoring Program Plan and Procedures Manual*. WP02-1. Westinghouse Electric  
12   Corporation, Waste Isolation Division, Carlsbad, NM.
- 13   Westinghouse Electric Corporation (WEC). 1991b. *Waste Isolation Pilot Plant Site*  
14   *Environmental Report for Calendar Year 1990*. DOE/WIPP 91-008. Westinghouse Electric  
15   Corporation, Waste Isolation Division, Carlsbad, NM.
- 16   Westinghouse Electric Corporation (WEC). 1992. *Waste Isolation Pilot Plant Site*  
17   *Environmental Report for Calendar Year 1991*. DOE/WIPP 92-007. Westinghouse Electric  
18   Corporation, Waste Isolation Division, Carlsbad, NM.
- 19   Westinghouse Electric Corporation (WEC). 1993. *Waste Isolation Pilot Plant Site*  
20   *Environmental Report for Calendar Year 1992*. DOE/WIPP 93-017. Westinghouse Electric  
21   Corporation, Waste Isolation Division, Carlsbad, NM.
- 22   Westinghouse Electric Corporation (WEC). 1994. *Waste Isolation Pilot Plant Site*  
23   *Environmental Report for Calendar Year 1993*. DOE/WIPP 94-2003. Westinghouse Electric  
24   Corporation, Waste Isolation Division, Carlsbad, NM.
- 25   Westinghouse Electric Corporation (WEC). 1995. *Waste Isolation Pilot Plant Site*  
26   *Environmental Report for Calendar Year 1994*. DOE/WIPP 95-Draft-2094. Westinghouse  
27   Electric Corporation, Waste Isolation Division, Carlsbad, NM.
- 28   Westinghouse Electric Corporation (WEC). 1996. *Waste Isolation Pilot Plant Site*  
29   *Environmental Report for Calendar Year 1995*, DOE/WIPP 96-2182, Westinghouse Electric  
30   Corporation, Waste Isolation Division, Carlsbad, NM.
- 31   Westinghouse Electric Corporation (WEC). 1997. *Waste Isolation Pilot Plant Site*  
32   *Environmental Report for Calendar Year 1996*, DOE/WIPP 97-2225, Westinghouse Electric  
33   Corporation, Waste Isolation Division, Carlsbad, NM.
- 34   Westinghouse Electric Corporation (WEC). 1998. *Waste Isolation Pilot Plant Site*  
35   *Environmental Report for Calendar Year 1997*, DOE/WIPP 98-2225, Westinghouse Electric  
36   Corporation, Waste Isolation Division, Carlsbad, NM.

- 1 Westinghouse Government Environmental Services Company (WGESC), LLC. 1999. *Waste*  
2 *Isolation Pilot Plant Site Environmental Report for Calendar Year 1998*, DOE/WIPP 99-2225,  
3 Westinghouse Electric Corporation, Waste Isolation Division, Carlsbad, NM.
- 4 Wolfe, H.G., et al., eds. 1977. *An Environmental Baseline Study of the Los Medanos Waste*  
5 *Isolation Pilot Plant (WIPP) Project Area of New Mexico: A Progress Report*. SAND77-7017.  
6 Sandia National Laboratories, Albuquerque, NM.
- 7 Wood, B.J., Snow, R.E., Cosler, D.J., and Haji-Djafari, S. 1982. *Delaware Mountain Group*  
8 *(DMG) Hydrology—Salt Removal Potential, Waste Isolation Pilot Plant (WIPP) Project,*  
9 *Southeastern New Mexico*. TME 3166. U.S. Department of Energy, Albuquerque, NM.
- 10 Zoback, M.L., and Zoback, M.D. 1980. "State of Stress in the Conterminous United States." *Journal of Geophysical Research*, Vol. 85, No. B11, pp. 6113 - 6156.
- 11
- 12 Zoback, M.L., Zoback, M.D., Adams, J., Bell, S., Suter, M., Suarez, G., Estabrook, C., and  
13 Magee, M. 1991. *Stress Map of North America*. Continent Scale Map CSM-5, Scale  
14 1:5,000,000. Geological Society of America, Boulder, CO.
- 15 Zoback, M.D., and Zoback, M.L. 1991. "Tectonic Stress Field of North America and Relative  
16 Plate Motions." In *Neotectonics of North America*, D.B. Slemmons, E.R. Engdahl, M.D.  
17 Zoback, and D.D. Blackwell, eds., pp. 339 - 366. Geological Society of America, Boulder, CO.
- 18

1

**INDEX**

2	40 CFR Part 191.....	2-6
3	accessible environment .....	2-83, 2-85, 2-115
4	actinide	
5	Culebra.....	2-103
6	transport .....	2-103
7	advection.....	2-14, 2-45, 2-103, 2-108
8	analysis	
9	probabilistic.....	2-162, 2-166
10	anhydrite 2-24, 2-26, 2-31, 2-33, 2-34, 2-44, 2-45, 2-48, 2-51, 2-69, 2-74, 2-76, 2-83, 2-90, 2-93,	
11	2-97, 2-100, 2-107, 2-110, 2-115, 2-117, 2-119	
12	anthropogenic.....	2-120, 2-121, 2-122
13	archaeology .....	2-138, 2-143
14	area	
15	controlled .....	2-99, 2-134, 2-141
16	assurance requirements .....	2-83
17	barrier.....	2-13
18	engineered.....	2-7
19	natural .....	2-13
20	Bell Canyon 2-20, 2-23, 2-24, 2-26, 2-27, 2-28, 2-29, 2-71, 2-77, 2-80, 2-83, 2-89, 2-90, 2-91, 2-	
21	124	
22	borehole 2-7, 2-15, 2-16, 2-17, 2-26, 2-29, 2-37, 2-40, 2-47, 2-56, 2-65, 2-71, 2-73, 2-76, 2-78, 2-	
23	2-80, 2-82, 2-83, 2-89, 2-90, 2-93, 2-117, 2-119, 2-127, 2-133, 2-137	
24	boundary conditions.....	2-6, 2-108
25	breccia pipes.....	2-10, 2-74, 2-77, 2-80, 2-124
26	brine ..... 2-7, 2-29, 2-33, 2-35, 2-37, 2-73, 2-77, 2-80, 2-83, 2-88, 2-89, 2-91, 2-94, 2-96, 2-99, 2-	
27	127, 2-131, 2-133	
28	aquifer .....	2-35, 2-77, 2-125, 2-127
29	brine reservoirs.....	2-9, 2-30, 2-74, 2-89, 2-90, 2-91, 2-93
30	volume.....	2-90
31	calcite .....	2-30, 2-33
32	calibrate.....	2-115
33	Capitan Limestone ..... 2-24, 2-26, 2-31, 2-59, 2-71, 2-73, 2-78, 2-80, 2-83, 2-89, 2-122, 2-129	
34	carbonates .....	2-13, 2-23, 2-38, 2-40, 2-122
35	Castile 2-24, 2-26, 2-29, 2-30, 2-31, 2-33, 2-58, 2-71, 2-73, 2-74, 2-76, 2-77, 2-80, 2-83, 2-86, 2-	
36	88, 2-89, 2-90, 2-91, 2-93, 2-94, 2-95, 2-124, 2-133	
37	Cenozoic .....	2-50, 2-63, 2-68, 2-80
38	Central Basin Platform.....	2-19, 2-63, 2-69, 2-160, 2-163, 2-164, 2-166
39	channeling .....	2-35, 2-51, 2-95
40	Cherry Canyon .....	2-24
41	climate.....	2-97, 2-108, 2-133, 2-148
42	colloid .....	2-103
43	Compliance Certification Application (CCA) . 2-7, 2-12, 2-13, 2-14, 2-15, 2-19, 2-20, 2-23, 2-24,	
44	2-26, 2-29, 2-30, 2-31, 2-33, 2-34, 2-35, 2-37, 2-40, 2-42, 2-44, 2-45, 2-47, 2-48, 2-50, 2-57,	
45	2-58, 2-62, 2-69, 2-71, 2-73, 2-76, 2-78, 2-80, 2-83, 2-86, 2-87, 2-89, 2-91, 2-93, 2-95, 2-97,	
46	2-99, 2-101, 2-103, 2-104, 2-105, 2-108, 2-109, 2-110, 2-114, 2-115, 2-116, 2-117, 2-119, 2-	

1	120, 2-124, 2-125, 2-126, 2-127, 2-131, 2-133, 2-134, 2-137, 2-138, 2-143, 2-145, 2-160, 2-	
2	162, 2-163, 2-166	
3	computational model.....	2-7, 2-14
4	conceptual model ....2-6, 2-13, 2-14, 2-19, 2-30, 2-38, 2-44, 2-58, 2-78, 2-83, 2-91, 2-96, 2-99, 2-	
5	100, 2-101, 2-108, 2-116, 2-117, 2-125	
6	consequence analysis .....	2-58
7	controlled area.....	2-99, 2-134, 2-141
8	creep closure .....	2-38
9	Cretaceous.....	2-67
10	Culebra2-13, 2-15, 2-18, 2-20, 2-35, 2-38, 2-42, 2-44, 2-45, 2-46, 2-47, 2-48, 2-66, 2-67, 2-68, 2-	
11	74, 2-81, 2-83, 2-85, 2-86, 2-88, 2-99, 2-100, 2-101, 2-103, 2-104, 2-106, 2-110, 2-116, 2-119,	
12	2-120, 2-138	
13	model.....	2-101, 2-115
14	cuttings.....	2-48
15	data	
16	quality .....	2-15
17	deformation.....2-9, 2-13, 2-26, 2-29, 2-31, 2-34, 2-45, 2-51, 2-59, 2-65, 2-71, 2-74, 2-76, 2-90	
18	Delaware Basin 2-13, 2-16, 2-23, 2-24, 2-26, 2-29, 2-30, 2-31, 2-33, 2-34, 2-37, 2-38, 2-63, 2-65,	
19	2-69, 2-71, 2-76, 2-80, 2-83, 2-84, 2-85, 2-93, 2-96, 2-122, 2-124, 2-134, 2-137, 2-138, 2-145	
20	Delaware Mountain Group .....	2-20, 2-24
21	demographics .....	2-132, 2-138
22	Devonian.....	2-23
23	Dewey Lake 2-51, 2-52, 2-53, 2-55, 2-58, 2-66, 2-68, 2-69, 2-71, 2-83, 2-85, 2-86, 2-88, 2-89, 2-	
24	97, 2-119, 2-120, 2-121, 2-122	
25	diapirism .....	2-9
26	diffusion .....	2-45, 2-102
27	dike.....	2-37, 2-69, 2-72
28	discharge .....	2-11, 2-87, 2-89, 2-97, 2-100, 2-103, 2-109, 2-127, 2-129
29	disposal system	
30	performance .....	2-13, 2-38, 2-58, 2-110
31	dissolution... 2-10, 2-11, 2-12, 2-13, 2-16, 2-26, 2-29, 2-31, 2-34, 2-36, 2-40, 2-44, 2-48, 2-50, 2-	
32	59, 2-62, 2-69, 2-71, 2-74, 2-76, 2-78, 2-80, 2-88, 2-97, 2-100, 2-105, 2-114, 2-122, 2-124, 2-	
33	125, 2-133	
34	disturbed rock zone (DRZ) .....	2-7, 2-73, 2-85, 2-94, 2-96
35	Dockum Group.....	2-53, 2-66
36	double porosity.....	2-14
37	drainage.....	2-55, 2-59, 2-62, 2-82, 2-87, 2-97, 2-127, 2-131
38	drilling.. 2-14, 2-15, 2-23, 2-26, 2-44, 2-48, 2-53, 2-55, 2-69, 2-73, 2-74, 2-77, 2-83, 2-94, 2-105,	
39	2-122, 2-125, 2-132, 2-136, 2-141, 2-144	
40	engineered	
41	barriers .....	2-7
42	erosion.....2-11, 2-12, 2-16, 2-19, 2-51, 2-57, 2-58, 2-59, 2-62, 2-66, 2-81, 2-89, 2-105	
43	exposure pathways.....	2-145
44	facility design.....	2-7, 2-55
45	fault .....	2-9, 2-26, 2-62, 2-63, 2-73, 2-145, 2-150, 2-160, 2-161
46	fauna.....	2-12, 2-51, 2-145

1	features, events, and processes (FEPs) .....	2-6, 2-9, 2-15, 2-58, 2-134
2	natural .....	2-6, 2-9, 2-15
3	fluvial .....	2-11, 2-40, 2-51, 2-55, 2-146
4	Forty-niner .....	2-38, 2-40, 2-50, 2-86, 2-117
5	fractures....	2-9, 2-30, 2-34, 2-42, 2-45, 2-46, 2-51, 2-66, 2-77, 2-90, 2-95, 2-99, 2-102, 2-114, 2-
6	119, 2-127	
7	future events.....	2-162
8	Gatuña .....	2-50, 2-56, 2-59, 2-68, 2-71, 2-80, 2-146
9	glaciation.....	2-12, 2-146
10	groundwater	2-10, 2-11, 2-26, 2-34, 2-37, 2-45, 2-51, 2-58, 2-78, 2-89, 2-93, 2-97, 2-98, 2-99, 2-
11	101, 2-107, 2-115, 2-117, 2-119, 2-120, 2-121, 2-124, 2-125, 2-132, 2-138, 2-145	
12	monitoring.....	2-83, 2-89, 2-109, 2-115, 2-119, 2-120
13	Guadalupian Series .....	2-24
14	human intrusion .....	2-16, 2-82, 2-83
15	hummock.....	2-57, 2-59
16	hunting .....	2-141, 2-142
17	hydraulic	
18	potential.....	2-96
19	hydraulic conductivity .....	2-85, 2-88, 2-97, 2-100, 2-116, 2-121, 2-122, 2-124
20	hydraulic gradient .....	2-88, 2-89, 2-102, 2-110, 2-117, 2-124, 2-125
21	potential.....	2-96
22	hydrostatic.....	2-90, 2-95
23	independent review .....	2-15
24	infiltration .....	2-11, 2-51, 2-58, 2-82, 2-86, 2-87, 2-110, 2-120, 2-122, 2-124, 2-145
25	interbed .....	2-31, 2-38, 2-45, 2-95
26	inventory .....	2-144
27	karst.....	2-35, 2-59, 2-76, 2-78, 2-80, 2-99
28	Lamar limestone.....	2-24, 2-26
29	Land Withdrawal Act (LWA).....	2-141
30	land withdrawal area .....	2-141
31	Leonardian Series.....	2-24
32	lithofacies.....	2-55
33	Livingston Ridge.....	2-35, 2-62, 2-141
34	loading.....	2-62, 2-67, 2-114
35	Los Medaños.....	2-38, 2-40, 2-44, 2-86, 2-100
36	Magenta.....	2-13, 2-19, 2-20, 2-38, 2-48, 2-50, 2-83, 2-86, 2-99, 2-109, 2-116, 2-117
37	Malaga Bend .....	2-97, 2-125, 2-131
38	McNutt Potash Zone .....	2-31, 2-133
39	Mescalero Caliche.....	2-55, 2-57, 2-59, 2-146
40	metamorphic .....	2-10, 2-16
41	Mississippian.....	2-23
42	Mississippian Limestone.....	2-23
43	model	
44	computational.....	2-7, 2-14
45	conceptual .	2-6, 2-13, 2-14, 2-19, 2-30, 2-38, 2-44, 2-45, 2-47, 2-58, 2-78, 2-83, 2-91, 2-96, 2-
46	99, 2-100, 2-108, 2-116, 2-117, 2-125	

1	Culebra.....	2-101, 2-115
2	numerical.....	2-99
3	monitoring.....	2-15, 2-18, 2-19, 2-20, 2-83
4	environmental .....	2-121, 2-148
5	groundwater .....	2-89, 2-101, 2-108, 2-115, 2-116, 2-117, 2-119, 2-120
6	mudstone.....	2-34, 2-35, 2-48, 2-49, 2-100, 2-105, 2-115
7	Nash Draw .....	2-86, 2-97, 2-116, 2-121, 2-122, 2-125, 2-129, 2-146
8	natural barriers .....	2-13
9	numerical model.....	2-99
10	Ochoan.....	2-23, 2-26, 2-51, 2-63, 2-78
11	Ogallala Formation .....	2-55, 2-59, 2-62, 2-65, 2-68, 2-69, 2-76, 2-129
12	oil and gas .....	2-26, 2-69, 2-132, 2-137, 2-141, 2-142
13	Ordovician.....	2-23, 2-63
14	Paleozoic.....	2-20, 2-23, 2-62
15	parameter2-6, 2-13, 2-16, 2-20, 2-30, 2-38, 2-44, 2-62, 2-81, 2-95, 2-107, 2-116, 2-117, 2-121, 2-	2-137, 2-162, 2-166
16	value.....	2-7, 2-47, 2-48, 2-53, 2-91, 2-101, 2-103
17	Pecos River .....	2-55, 2-59, 2-62, 2-69, 2-82, 2-97, 2-124, 2-125, 2-127, 2-131, 2-142, 2-146
18	Pennsylvanian .....	2-23, 2-63
19	performance assessment (PA) 2-6, 2-7, 2-13, 2-14, 2-16, 2-38, 2-53, 2-83, 2-86, 2-91, 2-93, 2-95,	2-96, 2-97, 2-99, 2-102, 2-114, 2-134, 2-141
20	permafrost.....	2-12
21	permeability .....	2-85
22	Permian .....	2-23, 2-57
23	Basin .....	2-63, 2-64, 2-163, 2-164
24	Period .....	2-37, 2-63
25	plugging .....	2-137
26	polyhalite.....	2-31, 2-33, 2-34, 2-37, 2-71
27	possible futures .....	2-134
28	potash resources .....	2-14, 2-77
29	Precambrian .....	2-16, 2-23, 2-69
30	precipitation .....	2-12, 2-58, 2-81, 2-87, 2-121, 2-129, 2-131, 2-147, 2-148
31	Precipitation .....	2-151
32	pressure	
33	gradient .....	2-88
34	probabilistic analysis.....	2-162, 2-163, 2-166
35	probability .....	2-30, 2-58, 2-62, 2-73, 2-91, 2-122, 2-136, 2-162, 2-166
36	Project Gnome .....	2-145
37	quality assurance (QA) .....	2-14
38	Quaternary.....	2-57, 2-63, 2-69, 2-80
39	ranching.....	2-142
40	recharge.....	2-11, 2-78, 2-86, 2-87, 2-97, 2-108, 2-110, 2-119, 2-124
41	records packages .....	2-15
42	resources .....	2-7, 2-76, 2-141
43	potash .....	2-14, 2-77
44	Richter scale.....	2-150, 2-160

1	risk.....	2-132, 2-162, 2-163, 2-166
2	Rustler	2-13, 2-30, 2-33, 2-35, 2-38, 2-39, 2-40, 2-41, 2-42, 2-43, 2-44, 2-48, 2-49, 2-50, 2-53, 2-58, 2-69, 2-71, 2-73, 2-77, 2-78, 2-80, 2-83, 2-85, 2-86, 2-88, 2-97, 2-99, 2-100, 2-101, 2-105, 2-110, 2-119, 2-125, 2-127
3	Salado	2-12, 2-24, 2-26, 2-29, 2-32, 2-33, 2-35, 2-36, 2-37, 2-38, 2-42, 2-44, 2-58, 2-63, 2-71, 2-73, 2-74, 2-77, 2-78, 2-80, 2-81, 2-82, 2-83, 2-85, 2-86, 2-88, 2-89, 2-90, 2-93, 2-94, 2-95, 2-96, 2-97, 2-99, 2-100, 2-105, 2-106, 2-107, 2-110, 2-124, 2-125, 2-127, 2-133, 2-145
4	San Simon Sink.....	2-77
5	San Simon Swale .....	2-62
6	Santa Rosa.....	2-51, 2-54, 2-55, 2-68, 2-69, 2-86, 2-88, 2-97, 2-119, 2-120, 2-121, 2-124
7	scarp.....	2-59, 2-69
8	scenarios.....	2-6, 2-83, 2-133
9	seals.....	2-150
10	seismic.....	2-9, 2-10, 2-29, 2-62, 2-73, 2-144, 2-150, 2-160, 2-163, 2-166
11	shafts .....	2-38, 2-48, 2-74, 2-85, 2-105, 2-109, 2-119, 2-120
12	siliciclastic.....	2-34, 2-40, 2-44
13	siltstone .....	2-35, 2-48, 2-50, 2-100, 2-115, 2-117, 2-121
14	Silurian.....	2-23
15	Simpson.....	2-23
16	site	
17	characterization .....	2-6, 2-13, 2-15, 2-59, 2-120
18	sorption .....	2-103
19	stratigraphy .....	2-38, 2-39
20	subsidence .....	2-9, 2-59, 2-62, 2-63, 2-77, 2-80, 2-100
21	surface	
22	drainage.....	2-87, 2-127
23	structures.....	2-15, 2-86, 2-107, 2-120, 2-121, 2-122
24	water.....	2-11, 2-81, 2-87, 2-119, 2-145
25	sylvite .....	2-33, 2-34, 2-37, 2-133, 2-134
26	syndeposition .....	2-34, 2-37, 2-45, 2-48, 2-51, 2-74, 2-77
27	Tamarisk .....	2-38, 2-40, 2-47, 2-48, 2-78, 2-86, 2-101, 2-108, 2-115
28	tectonic .....	2-9, 2-58, 2-68, 2-69, 2-71, 2-78, 2-150, 2-161, 2-163
29	threshold pressure .....	2-95
30	time-domain electromagnetic (TDEM).....	2-91
31	transmissivity .....	2-14, 2-82, 2-85, 2-86, 2-88, 2-100, 2-114, 2-116, 2-117, 2-119, 2-125
32	Culebra.....	2-42, 2-101, 2-104, 2-106, 2-116
33	transport .....	2-12, 2-14, 2-40, 2-45, 2-50, 2-81, 2-85, 2-87, 2-93, 2-101, 2-108, 2-110, 2-115
34	transuranic (TRU) waste.....	2-80
35	Triassic.....	2-30, 2-51, 2-53, 2-66, 2-80
36	uncertainty.....	2-6, 2-42, 2-109, 2-115
37	underground .....	2-14, 2-150, 2-166
38	facilities.....	2-85, 2-150, 2-166
39	source of drinking water (USDW).....	2-86, 2-138
40	undisturbed performance (UP).....	2-82
41	unloading.....	2-62, 2-67, 2-114
42	unnamed lower member.....	2-31, 2-38, 2-44, 2-100

1	uplift.....	2-62, 2-63, 2-68, 2-69
2	Upper Devonian Woodford Shale.....	2-23
3	vug.....	2-44, 2-45, 2-102
4	Wolfcampian Series.....	2-23
5		